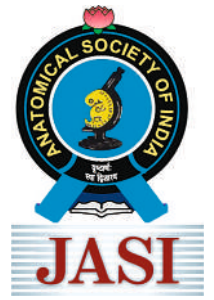


ISSN : 0003-2778

Scopus®

Indexed



# JOURNAL OF THE ANATOMICAL SOCIETY OF INDIA



An Official Publication of Anatomical Society of India

Full text online at <https://journals.lww.com/joi>  
Submit articles online at <https://review.jow.medknow.com/jasi>

*Editor-in-Chief*  
**Dr. Vishram Singh**

# JOURNAL OF THE ANATOMICAL SOCIETY OF INDIA

Print ISSN: 0003-2778

## GENERAL INFORMATION

### About the Journal

Journal of the Anatomical Society of India (ISSN: Print 0003-2778) is peer-reviewed journal. The journal is owned and run by Anatomical Society of India. The journal publishes research articles related to all aspects of Anatomy and allied medical/surgical sciences. Pre-Publication Peer Review and Post-Publication Peer Review Online Manuscript Submission System Selection of articles on the basis of MRS system Eminent academicians across the globe as the Editorial board members Electronic Table of Contents alerts Available in both online and print form. The journal is published quarterly in the months of January, April, July and October.

### Scope of the Journal

The aim of the *Journal of the Anatomical Society of India* is to enhance and upgrade the research work in the field of anatomy and allied clinical subjects. It provides an integrative forum for anatomists across the globe to exchange their knowledge and views. It also helps to promote communication among fellow academicians and researchers worldwide. The Journal is devoted to publish recent original research work and recent advances in the field of Anatomical Sciences and allied clinical subjects. It provides an opportunity to academicians to disseminate their knowledge that is directly relevant to all domains of health sciences.

The Editorial Board comprises of academicians across the globe.

JASI is indexed in Scopus, available in Science Direct.

### Abstracting and Indexing Information

The journal is registered with the following abstracting partners:

Baidu Scholar, CNKI (China National Knowledge Infrastructure), EBSCO Publishing's Electronic Databases, Ex Libris – Primo Central, Google Scholar, Hinari, Infotrieve, Netherlands ISSN center, ProQuest, TdNet, Wanfang Data

The journal is indexed with, or included in, the following:

SCOPUS, Science Citation Index Expanded, IndMed, MedInd, Scimago Journal Ranking, Emerging Sources Citation Index.

Impact Factor\* as reported in the 2022 Journal Citation Reports\* (Clarivate Analytics, 2023): 0.4

### Information for Authors

Article processing and publication charges will be communicated by the editorial office. All manuscripts must be submitted online at <https://review.jow.medknow.com/jasi>.

### Subscription Information

A subscription to JASI comprises 4 issues. Prices include postage. Annual Subscription Rate for non-members-

#### Rates of Membership (with effect from 1.1.2022)

|  | India     | International |
|--|-----------|---------------|
| Ordinary membership                                      | INR 1500  | US \$ 100     |
| Couple membership  | INR 2250  |               |
| Life membership  | INR 8000  | US \$ 900     |
| <b>Subscription Rates (till 31<sup>st</sup> August)</b>  |           |               |
| Individual   | INR 6000  | US \$ 650     |
| Library/Institutional                                    | INR 12000 | US \$ 1000    |
| Trade discount of 10% for agencies only                  |           |               |
| <b>Subscription Rates (after 31<sup>st</sup> August)</b> |           |               |
| Individual   | INR 6500  | US \$ 700     |
| Library/Institutional                                    | INR 12500 | US \$ 1050    |

The *Journal of Anatomical Society of India* (ISSN: 0003-2778) is published quarterly. Subscriptions are accepted on a prepaid basis only and are entered on a calendar year basis. Issues are sent by standard mail Priority rates are available upon request.

### Information to Members/Subscribers

All members and existing subscribers of the Anatomical Society of India are requested to send their membership/existing subscription fee for the current year to the Treasurer of the Society on the following address: Prof (Dr.) Punit Manik, Treasurer, ASI, Department of Anatomy, KGMU, Lucknow - 226003. Email: [punitamanik@yahoo.co.in](mailto:punitamanik@yahoo.co.in). All payments should be made through an account payee bank draft drawn in favor of the **Treasurer, Anatomical Society of India**, payable at **Lucknow** only, preferably for **Allahabad Bank, Medical College Branch, Lucknow**. Outstation cheques/drafts must include INR 70 extra as bank collection charges.

All complaints regarding non-receipt of journal issues should be addressed to the Editor-in-Chief, JASI at [editorjasi@gmail.com](mailto:editorjasi@gmail.com). The new subscribers may, please contact [wklrhpmedknow\\_subscriptions@wolterskluwer.com](mailto:wklrhpmedknow_subscriptions@wolterskluwer.com).

Requests of any general information like travel concession forms, venue of next annual

conference, etc. should be addressed to the General Secretary of the Anatomical Society of India.

For mode of payment and other details, please visit [www.medknow.com/subscribe.asp](http://www.medknow.com/subscribe.asp)

Claims for missing issues will be serviced at no charge if received within 60 days of the cover date for domestic subscribers, and 3 months for subscribers outside India. Duplicate copies cannot be sent to replace issues not delivered because of failure to notify publisher of change of address. The journal is published and distributed by Wolters Kluwer India Pvt. Ltd. Copies are sent to subscribers directly from the publisher's address. It is illegal to acquire copies from any other source. If a copy is received for personal use as a member of the association/society, one cannot resale or give-away the copy for commercial or library use.

The copies of the journal to the subscribers are sent by ordinary post. The editorial board, association or publisher will not be responsible for non receipt of copies. If any subscriber wishes to receive the copies by registered post or courier, kindly contact the publisher's office. If a copy returns due to incomplete, incorrect or changed address of a subscriber on two consecutive occasions, the names of such subscribers will be deleted from the mailing list of the journal. Providing complete, correct and up-to-date address is the responsibility of the subscriber.

**Nonmembers:** Please send change of address information to [subscriptions@medknow.com](mailto:subscriptions@medknow.com).

### Advertising Policies

The journal accepts display and classified advertising. Frequency discounts and special positions are available. Inquiries about advertising should be sent to Wolters Kluwer India Pvt. Ltd, [advertise@medknow.com](mailto:advertise@medknow.com).

The journal reserves the right to reject any advertisement considered unsuitable according to the set policies of the journal.

The appearance of advertising or product information in the various sections in the journal does not constitute an endorsement or approval by the journal and/or its publisher of the quality or value of the said product or of claims made for it by its manufacturer.

### Copyright

The entire contents of the JASI are protected under Indian and international copyrights. The Journal, however, grants to all users a free, irrevocable, worldwide, perpetual right of access to, and a license to copy, use, distribute, perform and display the work publicly and to make and distribute derivative works in any digital medium for any reasonable non-commercial purpose, subject to proper attribution of authorship and ownership of the rights. The journal also grants the right to make small numbers of printed copies for their personal non-commercial use.

### Permissions

For information on how to request permissions to reproduce articles/information from this journal, please visit <https://journals.lww.com/joi>.

### Disclaimer

The information and opinions presented in the Journal reflect the views of the authors and not of the Journal or its Editorial Board or the Publisher. Publication does not constitute endorsement by the journal. Neither the JASI nor its publishers nor anyone else involved in creating, producing or delivering the JASI or the materials contained therein, assumes any liability or responsibility for the accuracy, completeness, or usefulness of any information provided in the JASI, nor shall they be liable for any direct, indirect, incidental, special, consequential or punitive damages arising out of the use of the JASI. The JASI, nor its publishers, nor any other party involved in the preparation of material contained in the JASI represents or warrants that the information contained herein is in every respect accurate or complete, and they are not responsible for any errors or omissions or for the results obtained from the use of such material. Readers are encouraged to confirm the information contained herein with other sources.

### Addresses

#### Editorial Office

Dr. Vishram Singh, Editor-in-Chief, JASI  
B5/3 Hahnemann Enclave, Plot No. 40, Sector 6, Dwarka Phase – 2,  
New Delhi - 110 075, India.  
Email: [editorjasi@gmail.com](mailto:editorjasi@gmail.com)

#### Published by

Wolters Kluwer India Pvt. Ltd  
A-202, 2<sup>nd</sup> Floor, The Qube,  
C.T.S. No.1498A/2 Village Marol, Andheri (East),  
Mumbai - 400 059, India.  
Phone: 91-22-66491818  
Website: [www.medknow.com](http://www.medknow.com)

#### Printed at

Nikeda Art Printers Pvt. Ltd.,  
Building No. C/3 - 14,15,16, Shree Balaji Complex, Vehele Road,  
Village Bhatale, Taluka Bhiwandi, District Thane - 421302, India.

# JOURNAL OF THE ANATOMICAL SOCIETY OF INDIA

Print ISSN: 0003-2778

## EDITORIAL BOARD

### Editor-in-Chief

Dr. Vishram Singh, MBBS, MS, PhD (hc), FASI, FIMSA  
Adjunct Professor, Department of Anatomy, KMC, Mangalore, Manipal Academy of Higher Education, Manipal, Karnataka

### Joint-Editor

Dr. Murlimanju B.V.  
Associate Professor, Department of Anatomy, KMC, Mangalore, Manipal Academy of Higher Education, Manipal, Karnataka

### Managing Editor

Dr. C. S. Ramesh Babu  
Associate Professor, Department of Anatomy, Muzaffarnagar Medical College, Muzaffarnagar, Uttar Pradesh

### Associate Editor

Dr. D. Krishna Chaitanya Reddy  
Assistant Professor, Department of Anatomy, Kamini Academy of Medical Sciences and Research Center, Hyderabad

### Section Editors

#### Clinical Anatomy

Dr. Vishy Mahadevan, PhD, FRCS(Ed), FRCS  
Prof of Surgical Anatomy, The Royal College of Surgeons of England, London, UK

#### Histology

Dr. G.P. Pal, MS, DSc, Prof & Head, Department of Anatomy, MDC & RC, Indore, India

#### Gross and Imaging Anatomy

Dr. Srijit Das, Department of Human and Clinical Anatomy, College of Medicine and Health Sciences, Sultan Qaboos University, Muscat, Oman

#### Medical Education

Dr. Deepa Singh  
Professor, Department of Anatomy, HIMS, Swami Rama Himalayan University, Jolly Grant, Dehradun, Uttarakhand

#### Neuroanatomy

Dr. T.S. Roy, MD, PhD  
Prof & Head, Department of Anatomy, AIIMS, New Delhi

#### Embryology

Dr. Gayatri Rath, MS, FAMS  
Professor and Head, Department of Anatomy, NDMC Medical College, New Delhi

#### Genetics

Dr. Rima Dada, MD, PhD  
Prof, Department of Anatomy, AIIMS, New Delhi, India

#### Dental Sciences

Dr. Praveen B Kudva  
Professor and Head, Department of Periodontology, Jaipur Dental College, Jaipur, Rajasthan

### National Editorial Board

Dr. S.D. Joshi, Indore  
Dr. G.S. Longia, Jaipur  
Dr. A.K. Srivastava, Lucknow  
Dr. Daksha Dixit, Belgaum  
Dr. S.K. Jain, Moradabad  
Dr. P.K. Sharma, Lucknow  
Dr. S. Senthil Kumar, Chennai  
Dr. Daisy Sahani, Chandigarh  
Dr. N. Damayanti Devi, Imphal

Dr. Renu Chauhan, Delhi  
Dr. Ashok Sahai, Agra  
Dr. Ramesh Babu, Muzaffarnagar  
Dr. T.C. Singel, Ahmedabad  
Dr. P.K. Verma, Hyderabad  
Dr. S.L. Jethani, Dehradun  
Dr. Surajit Ghatak, Jodhpur  
Dr. Brijendra Singh, Rishikesh  
Dr. P. Vatsala Swamy, Pune

### International Editorial Board

Dr. Yun-Qing Li, China  
Dr. In-Sun Park, Korea  
Dr. K.B. Swamy, Malaysia  
Dr. Syed Javed Haider, Saudi Arabia  
Dr. Pasuk Mahakknaukrau, Thailand  
Dr. Tom Thomas R. Gest, USA

Dr. Chris Briggs, Australia  
Dr. Petru Matusz, Romania  
Dr. Min Suk Chung, South Korea  
Dr. Veronica Macchi, Italy  
Dr. Gopalakrishnakone, Singapore  
Dr. Sunil Upadhyay, UK



# JOURNAL OF THE ANATOMICAL SOCIETY OF INDIA

Volume 72 | Issue 4 | October-December 2023

## CONTENTS

### EDITORIAL

- Recent Advances in Speech Areas and Associated Neural Structures of the Brain**  
Vishram Singh, Rashi Singh, Gaurav Singh .....281

### ORIGINAL ARTICLES

- Analysis of Anterior Circulation Diameters According to Age, Gender, and Side Using Computed Tomography Angiography**  
Mustafa Yesilyurt, Recep Sade .....283
- A Microdissectional Study on Galen's Anastomosis: Anatomical Perspective with Clinical Emphasis**  
Isilsu Ezgi Uluisik, Deniz Sude Elbizim, Gursel Ortug .....290
- The Association of Vascular Loops of Anterior Inferior Cerebellar Artery and Vestibulocochlear Symptoms**  
Yeliz Dadali, Sercan Özkaçmaz, Mustafa Avcu, Muhammed Alpaslan, Cemil Göya, Mesut Özgökçe, Ilyas Dündar, Fatma Durmaz .....295
- Relationships of Matrix Metalloproteinase 3 Expression in Skeletal Muscle with Demographic Changes: Manual Microarray Study**  
Havva Erdem, Hacer Yasar Teke .....301
- Effects of 60-day Sodium Benzoate Exposure on the Ultramicroscopic Structure of Rat's Thyroid Gland Follicular Cells**  
Vitaliy Nikolaevich Morozov, Elena Nikolaevna Morozova, Aleksei Vladimirovich Tverskoi, Aleksei Vladimirovich Solin, Petr Mikhailovich Bykov .....307
- A Study of Morphometrical Analysis of the Human Malleus**  
Sanjay Prasad Sah, Naresh Chandra .....311
- An Introduction and Evaluation of Direct Observation with Checklist as a Teaching-Learning and Assessment Method in Anatomy**  
Jaikumar B. Contractor, Praveen Singh .....315
- Vascular Foramina of Talus in North Indian Population: A Dry Bone Study**  
Akriti Anand, Arvind Kumar Pankaj, Rintu Biswas, Rakesh Kumar Verma, Punita Manik, Garima Sehgal .....321
- Gender and Height Estimation from Hand and Handprint Sizes in the Turkish Population**  
Haci Keleş, Selim Çınaroğlu, Fatih Çiçek, Faruk Gazi Ceranoğlu, Mustafa Tekeli .....326
- Anatomical Study of Pterygoalar and Pterygospinous Bars/Foramina in West Anatolian Skulls**  
Funda Aksu, Selim Karabekir .....334
- Study of Neck-Shaft Angle in Plain Radiographs of Adult Kashmiri Population**  
Mohd Arif Makdoomi, Javed Ahmad Khan, Bhat Gulam Mohammad, Sajad A Bhat, Shahnawaz Hamid .....343
- Determination of the Foot Deformities that May Occur during the Coronavirus Disease 2019 Lockdown Process in Ballet Students**  
Ayse Gul Kabakci, Seda Ayvazoglu, Memduha Gulhal Bozkir .....349

*continued...*

**Pneumatized Crista Galli and its Correlation with Intraethmoidal Location of the Anterior Ethmoidal Artery**

Fulya Yaprak, Istemihan Coban, Mehmet Asim Ozer, Figen Govsa .....355

**Middle Mesenteric Artery: A Rare Vascular Anomaly**

C. S. Ramesh Babu, Arjun Kumar, Yashika Sharma, O. P. Gupta.....360

**INSTRUCTIONS TO AUTHOR** .....367

## Recent Advances in Speech Areas and Associated Neural Structures of the Brain

### Introduction

Speech is a communication or expression of one's thoughts through linguistic mode, i.e. through spoken or written words. The language is phonetic communication of well-articulated speech.

The human speech is comprehended, processed, planned, initiated, and controlled by the brain.

The neural structures that are responsible for speech consist of the Wernicke's area, Broca's area, arcuate fasciculus connecting these two areas, and motor cortex. All these structures are located in the left dominant cerebral hemisphere.<sup>[1]</sup>

The language is produced by the language production apparatus consisting of the lungs, larynx, oral cavity, and nasal cavity.

### Speech Areas of the Brain

There are two well-known cortical areas in the brain responsible for the production and comprehension of speech. These are Broca's motor speech area and Wernicke's sensory speech area.

#### Broca's Motor Speech Area (BA45 and BA44)

The Broca's motor speech area was discovered by a French Physician and Anatomist Pierre Paul Broca, in 1861. It is located in the inferior frontal gyrus (areas BA45 and BA44) of the left cerebral hemisphere.

Now, functional magnetic resonance imaging (fMRI) has shown that the processing of language production also involves the third part of the inferior frontal gyrus – the pars orbitalis (BA47). Therefore, these areas together form a larger speech area called Broca's region of speech.<sup>[2]</sup> In addition, there is a supplementary motor speech area in the lateral most part of the superior frontal gyrus. The Broca's speech area is connected with the supplementary motor area by the frontal aslant tract (FAT).<sup>[3]</sup>

The functions of Broca's speech area include:

- Production of expressive speech. It interacts with the flow of sensory information of speech from Wernicke's area and devises a plan for speaking and passing this plan to the motor cortex of the brain, which initiates and controls the action of muscles involved with the production of speech with the speech apparatus
- The speech production apparatus consists of the respiratory system, larynx, pharynx, oral cavity, palate, and nasal cavity.

#### Wernicke's Sensory Speech Area (BA22, BA40, and BA39)

Wernicke's sensory speech area was discovered by a German neurologist, Carl Wernicke, in 1874. It is located in the posterior part of the superior temporal gyrus (pSTG 22) and the posterior part of the parietal lobe (BA40 and BA39) of the left cerebral hemisphere. Recently, the BA37 located in the posterior part of the inferior temporal gyrus is involved in object naming and recognition memory.<sup>[4]</sup> Hence, Wernicke's speech area is now termed as Wernicke's sensory speech region.

The functions of Wernicke's speech area include:

- Comprehension of spoken and written language received by auditory, visual, and tactile input
- Is a source of constant availability of learned words.

#### Arcuate Fasciculus

It is an arched bundle of nerve fibers in the left cerebral hemisphere which connects Wernicke's area with the Broca's area.

Now, with the help of a diffusion tensor imaging tractography (DTIT) of the association fibers of a left cerebral hemisphere, it is found that the Wernicke's sensory speech area is connected with Broca's speech area by two distinct fasciculi as under:

1. Superior longitudinal fasciculus associated with phonological processing of language
2. Inferior-fronto-occipital fasciculus associated with semantic processing of language.

#### Neuronal Circuitry of Speech Production

Areas 22, 39, and 40 receive input from hearing, vision, touch, and proprioception. After comprehension of input the information is sent through arcuate fasciculus to Broca's area [Figure1].<sup>[5]</sup>

#### Applied Aspects

The lesions of the brain involving neural structures involved in speech production lead to aphasia. These are cerebral stroke, head injury, brain tumor, infections, and Alzheimer's disease.

Aphasia is a language disorder in which a person fails to communicate spoken and written words properly.

These are commonly classified into four types as follows:

- Broca's aphasia (nonfluent aphasia/expressive aphasia): In this, the person has:
  - Difficulty in speaking fluently, hence also called as

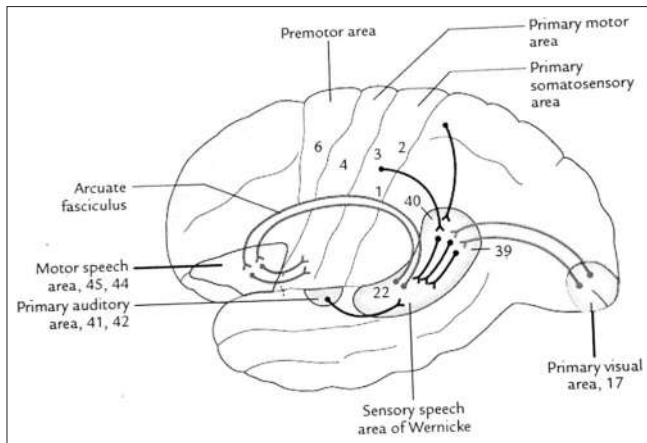


Figure 1: Neuronal circuitry of speech production

nonfluent aphasia

- He is able to understand what is being said to him but is not able to choose the correct words to express it.
- Wernicke's aphasia (fluent aphasia): In this, the person has:
  - Impaired language comprehension, i.e. loss of ability to understand spoken and written words, but he is himself able to speak fluently but incoherently
  - He is not able to read (alexia), write (agraphia), compute (acalculia), and recognize the names of known objects (anomia)
  - Intrusion of irrelevant words in severe cases
  - Impaired reading and writing.

### Conduction Aphasia (Associative Aphasia)

People with conduction aphasia have inability to repeat the words or sentences that have spoken to them when asked by an examining doctor.

### Global Aphasia

It occurs due to extensive damage of the brain involving both Broca's and Wernicke's areas. It impacts both ability to speak and ability to comprehend the speech.

### Treatment of Aphasia

- Speech and language therapy (SLT) by different techniques
- Certain drugs are being used for aphasia. These drugs either improve the blood flow in the region involved or help replace the depleted neurotransmitters in the brain
- Brain stimulation either by transcranial magnetic

stimulation or by transcranial direct current stimulation. This is aimed to stimulate damaged nerve cells of the brain.

### Vishram Singh, Rashi Singh<sup>1</sup>, Gaurav Singh<sup>2</sup>

Department of Anatomy, Kasturba Medical College, Mangalore, Manipal Academy of Higher Education, Manipal, Karnataka, <sup>1</sup>Department of Pediatric and Preventive Dentistry, Santosh Dental College and Hospital, Ghaziabad, <sup>2</sup>Clinical Editor, British Medical Journal, Noida, Uttar Pradesh, India

Address for correspondence: Prof. Vishram Singh, B5/3 Hahnemann Enclave, Plot No. 40, Sector 6, Dwarka Phase - 2, New Delhi - 110 075, India.  
E-mail: drvishramsingh@gmail.com

### References

1. Ferpozzi V. The Neural Network Underlying Speech in Humans: Intraoperative Investigation of Motor Control of Speech in Broca, Ventral Pre-Motor and Primary Motor Cortices. 2017.
2. Hickok G, Venezia J, Teghipco A. Beyond Broca: Neural architecture and evolution of a dual motor speech coordination system. *Brain* 2023;146:1775-90.
3. Gallet C, Clavreul A, Bernard F, Menei P, Lemée JM. Frontal aslant tract in the non-dominant hemisphere: A systematic review of anatomy, functions, and surgical applications. *Front Neuroanat* 2022;16:1025866.
4. Giampiccolo D, Duffau H. Controversy over the temporal cortical terminations of the left arcuate fasciculus: A reappraisal. *Brain* 2022;145:1242-56.
5. Barbeau EB, Kousaie S, Brass K, Descoteaux M, Petrides M, Klein D. The importance of the dorsal branch of the arcuate fasciculus in phonological working memory. *Cereb Cortex* 2023;33:9554-65.

This is an open access journal, and articles are distributed under the terms of the Creative Commons Attribution-NonCommercial-ShareAlike 4.0 License, which allows others to remix, tweak, and build upon the work non-commercially, as long as appropriate credit is given and the new creations are licensed under the identical terms.

#### Article Info

Received: 28 November 2023

Accepted: 28 November 2023

Available online: 30 December 2023

| Access this article online   |  |
|--|--|
| Quick Response Code:   | Website: <a href="https://journals.lww.com/joai">https://journals.lww.com/joai</a> |
|  | DOI: 10.4103/jasi.jasi_124_23  |

**How to cite this article:** Singh V, Singh R, Singh G. Recent advances in speech areas and associated neural structures of the brain. *J Anat Soc India* 2023;72:281-2.

# Analysis of Anterior Circulation Diameters According to Age, Gender, and Side Using Computed Tomography Angiography

## Abstract

**Background:** The anterior circulation is the blood supply to the anterior portion of the brain. Computed tomography angiography (CTA) is a noninvasive and effective anatomic evaluation method. **Objective:** The objective of the study was to investigate the relationship between the diameters of the anterior circulation arteries and age, gender, and side using CTA. **Materials and Methods:** In this single-center cross-sectional study, 200 cases that presented to the hospital between January 2019 and January 2022 were retrospectively examined using CTA. The diameters of the anterior circulation arteries (common carotid artery [CCA], internal carotid artery [ICA], anterior cerebral artery [ACA], medial cerebral artery [MCA], posterior communicating artery [PcomA], and anterior communicating artery [AcomA]) were measured and recorded by two radiologists. The mean diameters of CCA, ICA, ACA, AcomA, and PcomA were analyzed and compared based on age, gender, and side. **Results:** The mean diameters of the right CCA, ICA, MCA, and ACA and the left CCA, ICA, and MCA were statistically significantly greater in the elderly ( $P < 0.001$ ,  $P < 0.001$ ,  $P = 0.01$ ,  $P = 0.024$ ,  $P < 0.001$ ,  $P < 0.001$ , and  $P = 0.024$ , respectively). There was no statistically significant difference between the right and left vascular structures in CCA, ICA proximal, ICA distal, PcomA, MCA, and AcomA ( $P = 0.16$ ,  $P = 0.48$ ,  $P = 0.07$ ,  $P = 0.62$ ,  $P = 0.27$ , and  $P = 0.09$ , respectively). A statistically significant difference was observed between the right and left ACA in the whole cohort ( $P = 0.05$ ). The mean diameters of the right CCA, ICA proximal, ICA distal, MCA, and ACA and the left CCA, ICA proximal, ICA distal, and MCA were statistically significantly higher in men than in women ( $P < 0.001$ ,  $P < 0.001$ ,  $P = 0.002$ ,  $P < 0.001$ ,  $P = 0.038$ ,  $P < 0.001$ ,  $P < 0.001$ ,  $P = 0.002$ , and  $P < 0.001$ , respectively). **Conclusion:** CTA is a valuable modality for vascular evaluation. It revealed statistically significant differences in anterior circulation based on age, gender, and side.

**Keywords:** Anatomic variations, anterior circulation, computed tomography angiography

## Introduction

The anterior circulation is the blood supply to the anterior portion of the brain, including most supratentorial structures excluding the occipital lobes. Anterior cerebral circulation consists of the anterior cerebral artery (ACA) and middle cerebral artery forming the circle of Willis, as well as their branches. It is very variable and sometimes complex. The perfusion area of the ACA extends medially through all the frontal and parietal lobes, septum, and basal forebrain structures, such as the hypothalamus, pituitary, and optic chiasma. The ACA also supplies blood to the rostrum, genu, and trunk of the corpus callosum. Knowing the distinct and precise anatomy, pathological variations, and possible pathological consequences of the

This is an open access journal, and articles are distributed under the terms of the Creative Commons Attribution-NonCommercial-ShareAlike 4.0 License, which allows others to remix, tweak, and build upon the work non-commercially, as long as appropriate credit is given and the new creations are licensed under the identical terms.

For reprints contact: WKHLRPMedknow\_reprints@wolterskluwer.com

anterior cerebral circulation is essential for surgical interventions and postoperative follow-up. Although digital subtraction angiography (DSA) is the gold standard in vascular imaging, it has been shown that computed tomography angiography (CTA) has become as effective as DSA with the advances in technology.<sup>[1]</sup> A brain CTA examination is a noninvasive evaluation method. There are several morphologic studies which evaluate the brain arterial system.<sup>[1-4]</sup> There are several studies investigating variations in the anterior circulatory system; however, the number of those involving the measurement of arterial diameter is limited. To our knowledge, this is the first study in the English language literature to simultaneously investigate the relationship between the diameters of the anterior circulation arteries and age, gender, and side.

**How to cite this article:** Yesilyurt M, Sade R. Analysis of anterior circulation diameters according to age, gender, and side using computed tomography angiography. *J Anat Soc India* 2023;72:283-9.

Mustafa Yesilyurt<sup>1,2</sup>,  
Recep Sade<sup>1,2</sup>

<sup>1</sup>Department of Radiology,  
Faculty of Medicine, Ataturk  
University, Erzurum, <sup>2</sup>Radiology  
Clinic, Patnos State Hospital,  
Agri, Turkey

## Article Info

Received: 16 June 2022

Revised: 27 November 2022

Accepted: 10 November 2023

Available online: 30 December 2023

## Address for correspondence:

Dr. Recep Sade,

Department of Radiology,  
Faculty of Medicine, Ataturk  
University, Erzurum 25040,  
Turkey.

E-mail: [receptsade@yahoo.com](mailto:receptsade@yahoo.com)

## Access this article online

Website: <https://journals.lww.com/joai>

DOI:  
10.4103/jasi.jasi\_90\_22

## Quick Response Code:



## Materials and Methods

This retrospective study included data obtained from the patient files stored in the local image archiving and communication systems for the period between January 2019 and January 2022. A total of 269 patients were evaluated. CTA examinations were performed using a 320-row detector computed tomography (Aquilion ONE Vision; Toshiba Medical Systems Corporation, Otawara, Japan) or a 256-row detector (Somatom® Definition Flash, Siemens Healthcare, Forchheim, Germany) device. The CT acquisition protocol was also performed with the following parameters: 0.5 s gantry rotation time, 0.5 mm slice thickness, 128 mm × 0.6 mm or 192 mm × 0.6 mm collimation, z-flying focal point, 200 mAs tube current, and 120 kVp tube voltage. For optimum intraluminal contrast enhancement, the delay time between the start of contrast agent administration and the start of scanning was determined for each patient individually using the bolus tracking technique. A total of 60–75 mL of iopromide (Ultravist 370 mg/mL, Bayer Schering Pharma, Berlin, Germany) was administered through the 18G intravenous route placed in the right antecubital vein over 15 s at a rate of 4–5 mL/s using an automatic injector (MCT Plus; Medrad, Pittsburgh, PA, USA). Immediately after the iodinated contrast injection, 50 mL of saline was infused with the same syringe through the same route. Cases with trauma, tumor, or vascular pathology, pediatric patients, and repeated examinations were excluded [Figure 1]. As a result, a total of 200 brain CTA examinations on axial, coronal, or sagittal images were evaluated by two radiologists with 3 and 13 years of neuroradiology experience.

The diameters of the common carotid artery (CCA) were measured from the 1-cm area below the bifurcation, those of the internal carotid artery (ICA) from the C1 and C7 segment, those of the ACA from the A1 segment, those of

the medial cerebral artery (MCA) from the M1 segment, those of the anterior communicating artery (AcomA) from the mid portion, and those of the posterior communicating artery (PcomA) from the first 1-cm segment of the artery. Each measurement was performed for both the right (R) and left (L) sides. The measurements and patients' demographic data were recorded [Figure 4].

## Statistical analysis

Statistical analyses were performed using SPSS version 22.0 (SPSS Inc., Chicago IL, USA). The suitability of the data to the normal distribution was evaluated with the one-sample Kolmogorov–Smirnov test. The Levene statistics were used for the homogeneity analysis of the group variances. The independent samples *t*-test was used to determine differences between the male and female biometric measurements, and the paired samples *t*-test was conducted to determine differences between the left and right measurements of men and women. *P* < 0.05 was accepted as the significance level.

## Results

Of the patients, 102 (51%) were female. The mean age of the male patients was 48.58 ± 15.84 (range: 18–82) years and that of the female patients was 48.47 ± 15.48 (range: 18–91) years.

The mean diameters were calculated as 6.74 ± 0.92 (range: 4.07–8.91) mm for R-CCA, 6.63 ± 0.92 (range: 4.62–8.91) mm for L-CCA, 4.51 ± 0.67 (range: 3.08–6.67) mm for R-ICA proximal, 4.48 ± 0.59 (range: 2.77–6.75) mm for L-ICA proximal, 3.24 ± 0.6 (range: 1.65–5.15) mm for the R-ICA distal, 3.3 ± 0.64 (range: 1.78–5.1) mm for L-ICA distal, 1.2 ± 0.13 (range: 0.15–1.55) mm for AcomA, 1.28 ± 0.64 (range: 0.42–2.77) mm for R-PcomA, 1.24 ± 0.6 (range: 0.13–2.8) mm for L-PcomA, 2.41 ± 0.47 (range: 1.28–4.21) mm for R-MCA, 2.39 ± 0.45 (range: 1.33–4.1) mm for L-MCA, 1.72 ± 0.44 (range: 0.44–2.93) mm for

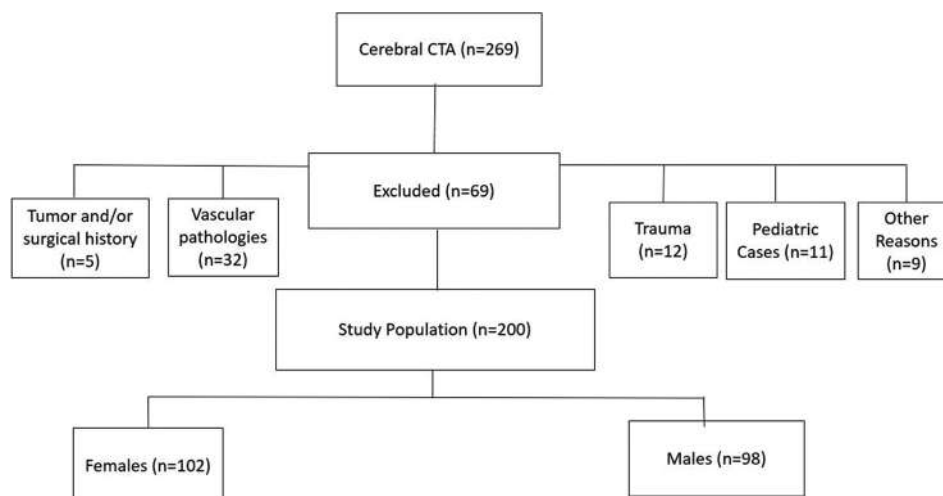


Figure 1: Patient selection diagram. CTA: Computed tomography angiography

R-ACA, and  $1.85 \pm 0.45$  (range: 0.6–3.21) mm for L-ACA. No statistically significant difference was found between the right and left vascular structures in CCA, ICA proximal, ICA distal, PcomA, MCA, and AcomA ( $P = 0.16$ ,  $P = 0.48$ ,  $P = 0.07$ ,  $P = 0.62$ ,  $P = 0.27$ , and  $P = 0.09$ , respectively).

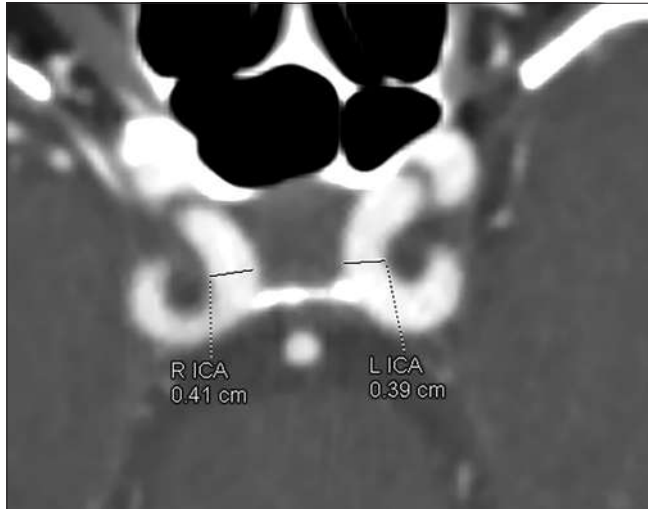


Figure 2: Axial computed tomography image of a 34-year-old male patient showing the measurement of the left and right internal carotid arteries. R-ICA: Right internal carotid artery, L-ICA: Left internal carotid artery

The only statistically significant difference between the right and left sides was observed in relation to the ACA measurements in the whole cohort ( $P = 0.05$ ).

The measurements were evaluated separately for the male and female patients [Figures 2 and 3]. In the male patients, the mean diameters of the arteries were calculated as  $7.16 \pm 0.88$  (range: 5.42–8.91) mm for R-CCA, 7.03

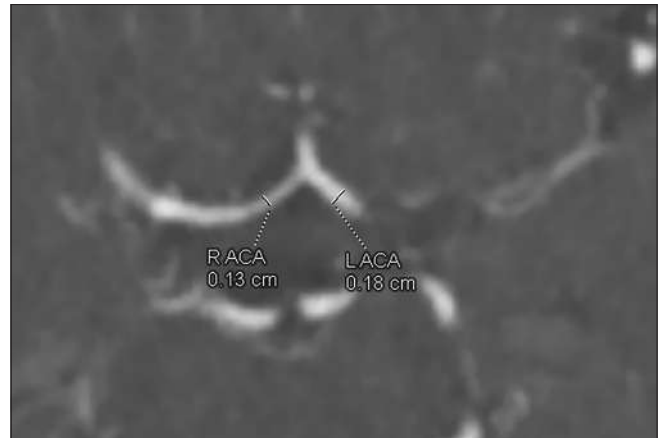


Figure 3: Axial computed tomography image of a 55-year-old female patient showing the measurement of the left and right anterior cerebral arteries. R-ACA: Right anterior cerebral artery, L-ACA: Left anterior cerebral artery

Table 1: Intergroup comparison of the anterior circulation artery measurements by gender

| Artery             | Gender | n   | Mean±SD (minimum–maximum) | P     |
|--------------------|--------|-----|---------------------------|-------|
| Right-CCA          | Male   | 36  | 7.16±0.88 (5.42–8.91)     | 0.00  |
|                    | Female | 43  | 6.39±0.81 (4.07–8.09)     |       |
| Right-ICA proximal | Male   | 95  | 4.71±0.71 (3.08–6.67)     | 0.00  |
|                    | Female | 105 | 4.33±0.56 (3.2–6.62)      |       |
| Right-ICA distal   | Male   | 95  | 3.38±0.64 (1.65–5.15)     | 0.00  |
|                    | Female | 105 | 3.11±0.53 (1.7–4.53)      |       |
| Right-PcomA        | Male   | 49  | 1.34±0.67 (0.43–2.7)      | 0.429 |
|                    | Female | 59  | 1.24±0.62 (0.42–2.77)     |       |
| Right-MCA          | Male   | 95  | 2.58±0.47 (1.68–4.21)     | 0.000 |
|                    | Female | 105 | 2.26±0.41 (1.28–3.4)      |       |
| Right-ACA          | Male   | 93  | 1.79±0.43 (0.44–2.93)     | 0.038 |
|                    | Female | 102 | 1.66±0.44 (0.8–2.85)      |       |
| Left-CCA           | Male   | 36  | 7.03±0.87 (5.73–8.91)     | 0.000 |
|                    | Female | 43  | 6.29±0.84 (4.62–8.41)     |       |
| Left-ICA proximal  | Male   | 95  | 4.64±0.62 (3.4–6.75)      | 0.000 |
|                    | Female | 105 | 4.34±0.54 (2.77–5.75)     |       |
| Left-ICA distal    | Male   | 95  | 3.44±0.64 (2.08–5.09)     | 0.002 |
|                    | Female | 105 | 3.16±0.62 (1.78–5.1)      |       |
| Left-PcomA         | Male   | 46  | 1.25±0.60 (0.46–2.86)     | 0.863 |
|                    | Female | 55  | 1.23±0.60 (0.13–2.66)     |       |
| Left-MCA           | Male   | 95  | 2.57±0.46 (1.76–4.1)      | 0.000 |
|                    | Female | 105 | 2.23±0.39 (1.33–3.35)     |       |
| Left-ACA           | Male   | 94  | 1.91±0.47 (0.6–2.86)      | 0.092 |
|                    | Female | 102 | 1.8±0.44 (0.94–3.21)      |       |
| AcomA              | Male   | 77  | 1.33±0.15 (0.25–1.55)     | 0.155 |
|                    | Female | 91  | 1.14±0.24 (0.15–1.42)     |       |

ACA: Anterior cerebral artery, ICA: Internal carotid artery, MCA: Medial cerebral artery, CCA: Common carotid artery, PcomA: Posterior communicating artery, AcomA: Anterior communicating artery, SD: Standard deviation

± 0.87 (range: 5.73–8.91) mm for L-CCA, 4.71 ± 0.71 (range: 3.08–6.67) mm for R-ICA proximal, 4.64 ± 0.61 (range: 3.4–6.75) mm for L-ICA proximal, 3.38 ± 0.64 (range: 1.65–5.15) mm for R-ICA distal, 3.44 ± 0.64 (range: 2.08–5.09) mm for L-ICA distal, 1.33 ± 0.15 (range: 0.25–1.55) mm for AcomA, 1.34 ± 0.67 (range: 0.43–2.7) mm for R-PcomA, 1.25 ± 0.6 (range: 0.46–2.86) mm for L-PcomA, 2.58 ± 0.47 (range: 1.68–4.21) mm for R-MCA, 2.57 ± 0.45 (range: 1.76–4.1) mm for L-MCA, 1.79 ± 0.43 (range: 0.44–2.93) mm for R-ACA, and 1.91 ± 0.47 (range: 0.6–2.86) mm for L-ACA.

In the female patients, the mean diameters of the arteries were calculated as 6.39 ± 0.81 (range: 4.07–8.09) mm for R-CCA, 6.29 ± 0.83 (range: 4.62–8.41) mm for L-CCA, 4.32 ± 0.56 (range: 3.2–6.62) mm for R-ICA proximal, 4.34 ± 0.54 (range: 2.77–5.75) mm for L-ICA proximal, 3.11 ± 0.53 (range: 1.7–4.53) mm for R-ICA distal, 3.16 ± 0.62 (range: 1.78–5.1) mm for L-ICA distal, 1.14 ± 0.24 (range: 0.15–1.42) mm for AcomA, 1.24 ± 0.62 (range: 0.42–2.77) mm for R-PcomA, 1.23 ± 0.6 (range: 0.13–2.66) mm for L-PcomA, 2.26 ± 0.41 (range: 1.28–3.4) mm for R-MCA, 2.23 ± 0.39 (range: 1.33–3.35) mm for L-MCA, 1.66 ± 0.44 (range: 0.8–2.85) mm for R-ACA, and 1.8 ± 0.43 (range: 0.94–3.21) mm for L-ACA.

The mean diameters of R-CCA, R-ICA proximal, R-ICA distal, R-MCA, R-ACA, L-CCA, L-ICA proximal, L-ICA distal, and L-MCA were statistically significantly higher in men than in women ( $P < 0.001$ ,  $P < 0.001$ ,  $P = 0.002$ ,  $P < 0.001$ ,  $P = 0.038$ ,  $P < 0.001$ ,  $P < 0.001$ ,  $P = 0.002$ , and  $P < 0.001$ , respectively).

Among the female patients, the only difference between the right and left side measurements was observed in relation to the ACA diameters ( $P = 0.025$ ). The left ACA diameter

was larger than the right in both groups, but this was not significant in men. No statistically significant difference was found in the measurement of any of the arteries in the male patients [Table 1].

In the whole cohort, the mean diameters of R-CCA, R-ICA distal, R-MCA, R-ACA, L-CCA, L-ICA distal, and L-MCA were statistically significantly greater in the elderly (aged 50 years and older) ( $P < 0.001$ ,  $P < 0.001$ ,  $P = 0.01$ ,  $P = 0.024$ ,  $P < 0.001$ ,  $P < 0.001$ , and  $P = 0.024$ , respectively) [Table 2].

In the male patients aged 50 years and older, the mean diameters of R-CCA, R-ICA distal, L-CCA, and L-ICA distal were statistically significantly greater compared to the nonelderly male patients ( $P = 0.003$ ,  $P = 0.012$ ,  $P = 0.034$ , and  $P = 0.017$ , respectively) [Table 3].

In the female patients aged 50 years and older, the mean diameters of R-CCA, R-ICA proximal, R-ICA distal, R-PcomA, R-MCA, R-ACA, L-CCA, L-ICA proximal, L-ICA distal, and L-MCA were statistically significantly greater compared to the nonelderly female patients ( $P = 0.004$ ,  $P = 0.003$ ,  $P < 0.001$ ,  $P = 0.003$ ,

**Table 2: Intergroup comparison of the anterior circulation artery measurements by age**

|                    | Age (years) | n   | Mean±SD   | P     |
|--------------------|-------------|-----|-----------|-------|
| Right-CCA          | ≥50         | 37  | 7.15±0.87 | 0.000 |
|                    | <50         | 42  | 6.39±0.83 |       |
| Right-ICA proximal | ≥50         | 93  | 4.58±0.63 | 0.154 |
|                    | <50         | 107 | 4.45±0.70 |       |
| Right-ICA distal   | ≥50         | 93  | 3.45±0.50 | 0.000 |
|                    | <50         | 107 | 3.06±0.63 |       |
| Right-PcomA        | ≥50         | 49  | 1.42±0.71 | 0.071 |
|                    | <50         | 59  | 1.19±0.57 |       |
| Right-MCA          | ≥50         | 93  | 2.51±0.45 | 0.01  |
|                    | <50         | 107 | 2.34±0.48 |       |
| Right-ACA          | ≥50         | 90  | 1.80±0.43 | 0.024 |
|                    | <50         | 105 | 1.66±0.44 |       |
| Left-CCA           | ≥50         | 37  | 7.01±0.90 | 0.000 |
|                    | <50         | 42  | 6.29±0.82 |       |
| Left-ICA proximal  | ≥50         | 93  | 4.57±0.61 | 0.064 |
|                    | <50         | 107 | 4.41±0.58 |       |
| Left-ICA distal    | ≥50         | 93  | 3.50±0.64 | 0.000 |
|                    | <50         | 107 | 3.13±0.60 |       |
| Left-PcomA         | ≥50         | 44  | 1.34±0.65 | 0.165 |
|                    | <50         | 57  | 1.17±0.55 |       |
| Left-MCA           | ≥50         | 93  | 2.48±0.46 | 0.024 |
|                    | <50         | 107 | 2.33±0.45 |       |
| Left-ACA           | ≥50         | 92  | 1.88±0.45 | 0.5   |
|                    | <50         | 104 | 1.83±0.47 |       |
| AcomA              | ≥50         | 80  | 1.06±0.55 | 0.095 |
|                    | <50         | 88  | 1.23±0.51 |       |

ACA: Anterior cerebral artery, ICA: Internal carotid artery, MCA: Medial cerebral artery, CCA: Common carotid artery, PcomA: Posterior communicating artery, AcomA: Anterior communicating artery, SD: Standard deviation



**Figure 4: Three-dimensional volume-rendered image of a 42-year-old female patient showing the anterior circulation and right anterior cerebral artery fenestration (arrows). R-ICA: Right internal carotid artery, L-ICA: Left internal carotid artery, R-MCA: Right medial cerebral artery, L-MCA: Left medial cerebral artery, R-ACA: Right anterior cerebral artery, L-ACA: Left anterior cerebral artery**

**Table 3: Intergroup comparison of the anterior circulation artery measurements in the male patients by age**

|                    | Age (years) | n  | Mean±SD   | P     |
|--------------------|-------------|----|-----------|-------|
| Right-CCA          | ≥50         | 17 | 7.61±0.78 | 0.003 |
|                    | <50         | 19 | 6.77±0.78 |       |
| Right-ICA proximal | ≥50         | 45 | 4.66±0.66 | 0.515 |
|                    | <50         | 50 | 4.76±0.77 |       |
| Right-ICA distal   | ≥50         | 45 | 3.55±0.50 | 0.012 |
|                    | <50         | 50 | 3.23±0.73 |       |
| Right-PcomA        | ≥50         | 23 | 1.28±0.68 | 0.572 |
|                    | <50         | 26 | 1.39±0.68 |       |
| Right-MCA          | ≥50         | 45 | 2.64±0.47 | 0.252 |
|                    | <50         | 50 | 2.53±0.47 |       |
| Right-ACA          | ≥50         | 43 | 1.85±0.34 | 0.267 |
|                    | <50         | 50 | 1.75±0.49 |       |
| Left-CCA           | ≥50         | 17 | 7.36±0.90 | 0.034 |
|                    | <50         | 19 | 6.74±0.76 |       |
| Left-ICA proximal  | ≥50         | 45 | 4.61±0.63 | 0.620 |
|                    | <50         | 50 | 4.67±0.61 |       |
| Left-ICA distal    | ≥50         | 45 | 3.61±0.64 | 0.017 |
|                    | <50         | 50 | 3.30±0.61 |       |
| Left-PcomA         | ≥50         | 18 | 1.29±0.66 | 0.779 |
|                    | <50         | 28 | 1.23±0.58 |       |
| Left-MCA           | ≥50         | 45 | 2.61±0.48 | 0.494 |
|                    | <50         | 50 | 2.55±0.45 |       |
| Left-ACA           | ≥50         | 45 | 1.90±0.47 | 0.815 |
|                    | <50         | 49 | 1.92±0.49 |       |
| AcomA              | ≥50         | 37 | 1.03±0.55 | 0.080 |
|                    | <50         | 40 | 1.26±0.51 |       |

ACA: Anterior cerebral artery, ICA: Internal carotid artery, MCA: Medial cerebral artery, CCA: Common carotid artery, PcomA: Posterior communicating artery, AcomA: Anterior communicating artery, SD: Standard deviation

$P = 0.008$ ,  $P = 0.043$ ,  $P = 0.002$ ,  $P = 0.001$ ,  $P < 0.001$ , and  $P = 0.006$ , respectively) [Table 4].

CCA entered the imaging area in 79 patients, and therefore, the evaluation of CCA could only be made in these patients. R-PcomA could not be visualized in 46 male and 46 female patients, L-PcomA in 47 male and 51 female patients, and AcomA in 18 male and 14 female patients. This was considered to be secondary to agenesis. Finally, R-ACA could not be visualized in two male and three female patients and L-ACA in one male and three female patients. Data shown in Tables 2-4.

### Discussion

CTA can reveal various pathologies and variations, including carotid system stenosis, aneurysms, vasospasm, arteriovenous malformations, dissections, and venous thrombus. Although CTA is a rapid and noninvasive imaging method, it has disadvantages, such as the need for contrast material, exposure to radiation, long data processing times, and difficulties in evaluating the arteries at the base of the skull due to bone structures.

The knowledge of cerebrovascular dimensions is an integral part of neurovascular procedures. These procedures may require the placement of an endoluminal device, and therefore, knowing the diameter of these structures can assist in device selection and modification, potentially making them more compatible with arterial anatomy. In this study, we used CTA due to its noninvasive and ubiquitous nature. The role and accuracy of CTA in the imaging of the cerebral vasculature are well established, and this modality is increasingly used for screening and investigating neurovascular pathologies.<sup>[5]</sup>

In this study, the diameters of R-CCA and L-CCA were similar to the measurement ranges reported in the literature (6.74 mm vs. 6.5–8.03 mm and 6.63 mm vs. 6.4–8.5 mm, respectively).<sup>[6,7]</sup> The reported diameter of the ICA terminal ranges from 3.7 mm to 4.57 mm,<sup>[8,9]</sup> depending on the distance from the terminal where these measurements are taken. Rai *et al.* found the mean R-ICA distal and L-ICA distal diameters to be  $3.6 \pm 0.4$  and  $3.7 \pm 0.3$ , respectively.<sup>[10]</sup> In the current study, the diameters of R-ICA proximal, R-ICA distal, L-ICA proximal, and L-ICA distal were similar to the ranges given in previous studies.

In the literature, the MCA diameter varies between 2.5 mm and 3.82 mm, again depending on its proximity to the measurement point and MCA source.<sup>[8,9]</sup> Rai *et al.* found the mean R-MCA M1 and L-MCA M1 diameters to be  $3.1 \pm 0.4$  and  $3 \pm 0.3$ , respectively.<sup>[10]</sup> However, in our study, the bilateral MCA diameter was lower compared to the literature range (R-MCA:  $2.41 \pm 0.47$  mm; L-MCA:  $2.39 \pm 0.45$  mm). This may be related to the differences in the methods (cadaver vs. CTA), imaging protocol (1 mm vs. 0.5 mm slice thickness), or patient selection (inclusion and exclusion criteria).

In our study, we discussed the diameters of the anterior cerebral arteries, which provide blood supply to important cerebral areas. The presence of only a few studies in the literature in this area encouraged us to conduct this study.<sup>[11]</sup> Karatas *et al.* found the PcomA diameter to be  $1.30 \pm 0.50$  mm on the right side and  $1.27 \pm 0.55$  mm on the left side using CTA.<sup>[11]</sup> In a cadaveric study, the right and left PcomA diameters were determined to be  $0.90 \pm 0.39$  mm and  $0.90 \pm 0.36$  mm, respectively.<sup>[12]</sup> Yeniçeri *et al.* reported the PcomA diameter as 1.12 mm using three-dimensional time of flight magnetic resonance angiography (3D-TOF-MRA).<sup>[13]</sup> In our study, we obtained similar results to the literature.

In a previous CTA study, the ACA A1 diameter was measured as  $2.15 \pm 0.63$  mm on the right and  $2.26 \pm 0.61$  mm on the left.<sup>[11]</sup> Shatri *et al.* found the ACA A1 diameter to be  $2.04 \pm 0.28$  mm for the right side and  $2.06 \pm 0.26$  mm for the left side using 3D-TOF-MRA.<sup>[14]</sup> In another 3D-TOF-MRA study, Yeniçeri *et al.* measured the right and left ACA A1 diameters as 1.58 mm and

**Table 4: Intergroup comparison of the anterior circulation artery measurements in the female patients by age**

|                    | Age (years) | n  | Mean±SD   | P     |
|--------------------|-------------|----|-----------|-------|
| Right-CCA          | ≥50         | 20 | 6.76±0.76 | 0.004 |
|                    | <50         | 23 | 6.08±0.73 |       |
| Right-ICA proximal | ≥50         | 48 | 4.51±0.59 | 0.003 |
|                    | <50         | 57 | 4.18±0.50 |       |
| Right-ICA distal   | ≥50         | 48 | 3.35±0.49 | 0.000 |
|                    | <50         | 57 | 2.91±0.49 |       |
| Right-PcomA        | ≥50         | 26 | 1.53±0.73 | 0.003 |
|                    | <50         | 33 | 1.02±0.41 |       |
| Right-MCA          | ≥50         | 48 | 2.38±0.39 | 0.008 |
|                    | <50         | 57 | 2.17±0.42 |       |
| Right-ACA          | ≥50         | 47 | 1.76±0.49 | 0.043 |
|                    | <50         | 55 | 1.58±0.38 |       |
| Left-CCA           | ≥50         | 20 | 6.72±0.81 | 0.002 |
|                    | <50         | 23 | 5.93±0.69 |       |
| Left-ICA proximal  | ≥50         | 48 | 4.53±0.59 | 0.001 |
|                    | <50         | 57 | 4.18±0.45 |       |
| Left-ICA distal    | ≥50         | 48 | 3.40±0.62 | 0.000 |
|                    | <50         | 57 | 2.97±0.56 |       |
| Left-PcomA         | ≥50         | 26 | 1.38±0.66 | 0.101 |
|                    | <50         | 29 | 1.10±0.52 |       |
| Left-MCA           | ≥50         | 48 | 2.34±0.40 | 0.006 |
|                    | <50         | 57 | 2.13±0.36 |       |
| Left-ACA           | ≥50         | 47 | 1.86±0.40 | 0.239 |
|                    | <50         | 55 | 1.75±0.36 |       |
| AcomA              | ≥50         | 47 | 1.05±0.56 | 0.580 |
|                    | <50         | 44 | 1.20±0.48 |       |

ACA: Anterior cerebral artery, ICA: Internal carotid artery, MCA: Medial cerebral artery, CCA: Common carotid artery, PcomA: Posterior communicating artery, AcomA: Anterior communicating artery, SD: Standard deviation

1.6 mm, respectively.<sup>[13]</sup> In cadavers, the right and left ACA A1 diameters were determined as 1.87 ± 0.48 mm and 1.96 ± 0.49 mm, respectively.<sup>[12]</sup> Our results (R-ACA A1: 1.72 ± 0.44 mm; L-ACA A1: 1.85 ± 0.45 mm) were consistent with the literature.

A transcranial color Doppler ultrasonography study of 120 patients showed that the arteries on the left side were larger than those on the right.<sup>[15]</sup> However, according to a study by Rai *et al.*, there was no significant relationship between arterial diameter and gender or measurement side.<sup>[10]</sup> In our study, L-ACA A1 was found to be greater than R-ACA in the whole cohort and in the female patients. There was no statistically significant difference between the diameters of the right and left arteries in the male patients.

Krabbe-Hartkamp *et al.* showed that the diameters of the main arteries forming the circle of Willis, such as CCA and ICA, increased with advancing age.<sup>[16]</sup> In our study, the mean diameters of CCA and ICA were even higher in individuals older than 50 years of age. We associated this condition with atherosclerosis, compensatory dilatation of

the arteries as a result of a decrease in cardiac output, and a decrease in vascular elasticity in the elderly population. These factors can also explain the lower rate of blood flow in the arteries of older individuals. Therefore, in TOF-MRA studies, the arterial diameters forming the circle of Willis were reported to decrease with increasing age.<sup>[16,17]</sup>

In the current study, the mean diameters of R-CCA, R-ICA proximal, R-ICA distal, R-MCA, R-ACA, L-CCA, L-ICA proximal, L-ICA distal, and L-MCA were statistically significantly higher in men than in women. Similarly, in a study by Krabbe-Hartkamp *et al.*, the mean vessel diameter tended to be larger in male patients.<sup>[16]</sup>

The most common circle of Willis variations in our study were similar to those reported in the literature. In several radiological studies, the most common variation was determined to be the absence of bilateral PcomA or the absence of unilateral PcomA.<sup>[16-19]</sup> This was followed by the absence of AcomA, P1, and the ACA at decreasing frequency.

**Limitations**

This study has several limitations. First, a CTA study cannot provide as comprehensive data as a cadaveric study. Second, we used a 0.5-mm slice thickness; therefore, we could not evaluate arteries smaller than 0.5 mm in diameter; however, 0.5 mm is the lowest available section thickness of CTA devices in current medical use. Another limitation concerns the small sample size. Finally, we excluded patients with vascular diseases, which may have affected our age-related assessment.

**Conclusion**

CTA is a valuable modality for vascular evaluation. In our study, the mean diameters of R-CCA, R-ICA proximal, R-ICA distal, R-MCA, R-ACA, L-CCA, L-ICA proximal, L-ICA distal, and L-MCA were statistically significantly higher in men than in women. We also found that most arteries tended to increase in diameter with increasing age. In our study, the most common variations were the absence of PcomA, AcomA, and ACA A1 in order of frequency.

**Financial support and sponsorship**

Nil.

**Conflicts of interest**

There are no conflicts of interest.

**References**

- Han A, Yoon DY, Chang SK, Lim KJ, Cho BM, Shin YC, *et al.* Accuracy of CT angiography in the assessment of the circle of Willis: Comparison of volume-rendered images and digital subtraction angiography. *Acta Radiol* 2011;52:889-93.
- Li Q, Li J, Lv F, Li K, Luo T, Xie P. A multidetector CT angiography study of variations in the circle of Willis in a Chinese population. *J Clin Neurosci* 2011;18:379-83.

3. Rai AT, Rodgers D, Williams EA, Hogg JP. Dimensions of the posterior cerebral circulation: An analysis based on advanced non-invasive imaging. *J Neurointerv Surg* 2013;5:597-600.
4. Vitosevic F, Rasulic L, Medenica SM. Morphological characteristics of the posterior cerebral circulation: An analysis based on non-invasive imaging. *Turk Neurosurg* 2019;29:625-30.
5. Saba L, Sanfilippo R, Montisci R, Mallarini G. Assessment of intracranial arterial stenosis with multidetector row CT angiography: A postprocessing techniques comparison. *AJNR Am J Neuroradiol* 2010;31:874-9.
6. Ozgur Z, Govsa F, Ozgur T. Anatomic evaluation of the carotid artery bifurcation in cadavers: Implications for open and endovascular therapy. *Surg Radiol Anat* 2008;30:475-80.
7. Choudhry FA, Grantham JT, Rai AT, Hogg JP. Vascular geometry of the extracranial carotid arteries: An analysis of length, diameter, and tortuosity. *J Neurointerv Surg* 2016;8:536-40.
8. Wollschlaeger PB, Wollschlaeger G. Anterior cerebral-internal carotid artery and middle cerebral-internal carotid artery ratios. *Acta Radiol Diagn (Stockh)* 1966;5:615-20.
9. Müller HR, Brunhölzl C, Radü EW, Buser M. Sex and side differences of cerebral arterial caliber. *Neuroradiology* 1991;33:212-6.
10. Rai AT, Hogg JP, Cline B, Hobbs G. Cerebrovascular geometry in the anterior circulation: An analysis of diameter, length and the vessel taper. *J Neurointerv Surg* 2013;5:371-5.
11. Karatas A, Coban G, Cinar C, Oran I, Uz A. Assessment of the circle of Willis with cranial tomography angiography. *Med Sci Monit* 2015;21:2647-52.
12. Karatas A, Yilmaz H, Coban G, Koker M, Uz A. The anatomy of circulus arteriosus cerebri (circle of Willis): A study in Turkish population. *Turk Neurosurg* 2016;26:54-61.
13. Yeniçeri İÖ, Çullu N, Deveer M, Yeniçeri EN. Circle of Willis variations and artery diameter measurements in the Turkish population. *Folia Morphol (Warsz)* 2017;76:420-5.
14. Shatri J, Cerkezi S, Ademi V, Reci V, Bexheti S. Anatomical variations and dimensions of arteries in the anterior part of the circle of Willis. *Folia Morphol (Warsz)* 2019;78:259-66.
15. Macchi C, Catini C. The measurement of the calibers and blood-flow velocities of the arteries of the circle of Willis: A statistical investigation of 120 living subjects using transcranial color-Doppler ultrasonography. *Ital J Anat Embryol* 1994;99:9-16.
16. Krabbe-Hartkamp MJ, van der Grond J, de Leeuw FE, de Groot JC, Algra A, Hillen B, *et al.* Circle of Willis: Morphologic variation on three-dimensional time-of-flight MR angiograms. *Radiology* 1998;207:103-11.
17. Horikoshi T, Akiyama I, Yamagata Z, Sugita M, Nukui H. Magnetic resonance angiographic evidence of sex-linked variations in the circle of Willis and the occurrence of cerebral aneurysms. *J Neurosurg* 2002;96:697-703.
18. Papantchev V, Stoinova V, Aleksandrov A, Todorova-Papantcheva D, Hristov S, Petkov D, *et al.* The role of Willis circle variations during unilateral selective cerebral perfusion: A study of 500 circles. *Eur J Cardiothorac Surg* 2013;44:743-53.
19. Zaninovich OA, Ramey WL, Walter CM, Dumont TM. Completion of the circle of Willis varies by gender, age, and indication for computed tomography angiography. *World Neurosurg* 2017;106:953-63.

# A Microdissectional Study on Galen's Anastomosis: Anatomical Perspective with Clinical Emphasis

## Abstract

**Purpose:** Galen's anastomosis, which is placed over the dorsal surface of the posterior cricoarytenoid muscle, is formed by the internal branch of the superior laryngeal nerve and the dorsal branch of the recurrent laryngeal nerve (RLN). This study aims to contribute literature about the prevalence of Galen's anastomosis which is still a controversial issue and indicates the prevalence of this type of anastomosis in both sides of the larynx and indicate the importance of this anastomosis in different neck surgeries and procedures. **Subjects and Methods:** Twenty-two adult formalin-fixed hemilaryngeal (11 larynx) specimens' anatomical micro-dissection were performed on both sides (right-left) posteriorly. Every specimen consisted of larynx, trachea, epiglottis, and hyoid bone. Internal laryngeal nerve, recurrent laryngeal nerve, and inferior thyroid artery were freed up connective tissue to better analyze their relationship and to find their exact course with termination point. **Results:** In our current study, total Galen's anastomosis prevalence was found %54.53 with %27.27 right single trunk, %18.18 left single trunk, 4.54 left plexus formation, and 4.54 left double trunk. There has not been any anastomotic structure in %22.72 of the left side and in %22.72 of the right side microdissection of laryngeal specimens. **Conclusion:** During laryngeal or thyroid surgery, observation of an unknown intralaryngeal branching pattern may lead to confusion and may increase the risk of iatrogenic nerve injury, thus it is crucial to contribute to the literature about microanatomy and prevalence of Galen's anastomosis.

**Keywords:** Galen's anastomosis, larynx, microdissection, recurrent laryngeal nerve, superior laryngeal nerve

**Isilsu Ezgi Uluisik,  
Deniz Sude Elbizim,  
Gursel Ortug**

Department of Anatomy,  
School of Anatomy, Bahcesehir  
University, Istanbul, Turkey

## Introduction

Gladius Galen (129–200 AD), also known as “Second Hypocrates,” was the first to describe recurrent laryngeal nerve (RLN) and its function. He depicted RLN as the nerve of most of the laryngeal muscles and emphasized its importance about voice.<sup>[1]</sup> It's been shown that RLN provides innervation to all intrinsic muscles of the larynx except the cricothyroid muscle.<sup>[2]</sup> Superior laryngeal nerve (SLN) on the other hand contributes to the innervation of larynx by its two branches – internal branch of the SLN (ibSLN) and external branch of the SLN (ebSLN). Whilst ibSLN is responsible for the sensory innervation of the supraglottis and vocal cords,<sup>[3]</sup> ebSLN innervates cricothyroid muscle, it increases tension in ipsilateral vocal cords.<sup>[4]</sup>

The origin of the two mentioned nerves (SLN and RLN) is important to better understand their relationship with surrounding anatomical structures. The SLN, before medially

following its course toward the thyrohyoid membrane, arises from the inferior vagal ganglion and it gives off internal and external branches at the level of C2.<sup>[5]</sup> The right RLN branches off RLN ahead of the subclavian artery when the left RLN arises on the left side of the aortic arch.<sup>[6]</sup>

Sañudo *et al.*<sup>[7]</sup> classified different relationships between ibSLN and RLN, between ebSLN and RLN, and between ebSLN and ibSLN. Nerve connections between ibSLN and RLN have been frequently studied and four different anastomosis of ibSLN and RLN has been defined which are Galen's anastomosis, arytenoid plexus, cricoid anastomosis, and thyroarytenoid anastomosis.<sup>[7]</sup>

Galen's anastomosis was first described by May in 1968 in the book edited and translated from Galen's work in Greek (*Peri chreias moriōn*). May reported: “*At the larynx itself these recurrent nerves with which this whole discussion of mine has been concerned are mingled to some extent with the nerves (n. laryngeal superior)*

## Article Info

Received: 15 August 2023

Accepted: 24 November 2023

Available online: 30 December 2023

## Address for correspondence:

Prof. Dr. Gursel Ortug,  
Department of Anatomy,  
School of Medicine, Bahcesehir  
University, Istanbul, Turkey.  
E-mail: gurselortug@gmail.com

## Access this article online

Website: <https://journals.lww.com/joai>

DOI:  
10.4103/jasi.jasi\_86\_23

## Quick Response Code:



**How to cite this article:** Uluisik IE, Elbizim DS, Ortug G. A microdissectional study on Galen's anastomosis: Anatomical perspective with clinical emphasis. *J Anat Soc India* 2023;72:290-4.

This is an open access journal, and articles are distributed under the terms of the Creative Commons Attribution-NonCommercial-ShareAlike 4.0 License, which allows others to remix, tweak, and build upon the work non-commercially, as long as appropriate credit is given and the new creations are licensed under the identical terms.

For reprints contact: WKHLRPMedknow\_reprints@wolterskluwer.com

which grow off from the sixth pair and go to the depths of the larynx."<sup>[8]</sup>

Galen's anastomosis is formed by the dorsal branch of ibSLN and the dorsal branch of RLN.<sup>[7]</sup> The anastomosis is placed over the dorsal surface of the posticus, transverse interarytenoid, and oblique interarytenoid muscles also under the mucosa of hypopharynx.

Temporary and permanent palsy of ibSLN and RLN after thyroid surgery and anterior cervical spine surgery have been a subject for literature. Since RLN injury is more noticeable postoperatively compared to ibSLN, it has been studied more than ibSLN injuries. Damage to the RLN can cause many morbidities, including dysphagia and hoarseness due to vocal cord damage.<sup>[9,10]</sup> Voice damage due to RLN injury is particularly important for patients since it results with difficulties in communication and causes social-, psychological-, and work-related problems.<sup>[11]</sup> SLN injury, on the other hand, may lead to aspiration and pneumonitis since the nerve has a role in initiating protective reflexes.<sup>[12]</sup>

This study aims to contribute literature about the prevalence of Galen's anastomosis (GA) which is still a controversial issue and indicates the prevalence of the type of anastomosis in both sides of larynx and to indicate importance of this anastomosis in different neck surgeries and procedures.

## Subjects and Methods

### Specimens and ethical approval

Twenty-two adult hemilaryngeal specimens' (11 larynx-both sides) anatomical micro-dissection were performed posteriorly. Every specimen consisted of larynx, trachea, epiglottis, and hyoid bone. The specimens were fixed in 10% formalin and preserved in ethyl alcohol. These specimens were provided by our universities' department of anatomy. This study has been approved by the local institutional ethics committee in conformity with the 1964 Helsinki Declaration and its later amendments or comparable ethical standards. (Protocol number: E-22481095-020-91, Approval date: January 07, 2022).

### Dissections

Specimens were microdissected cautiously under the Leica M320 microscope. Internal laryngeal nerve, RLN, and inferior thyroid artery were freed up connective tissue to better analyze their relationship and to find their exact course and the termination point. Then, they were pursued through their path until they connected. The type of anastomoses (single, double, or plexus) were determined. All specimens were photographed immediately after dissection [Figures 1-3]. Prevalence of Galen's anastomosis and type of anastomoses were documented on both sides separately [Figure 4].

## Results

In this study, the connecting branch(s) between ibSLN and RLN were classified according to whether they

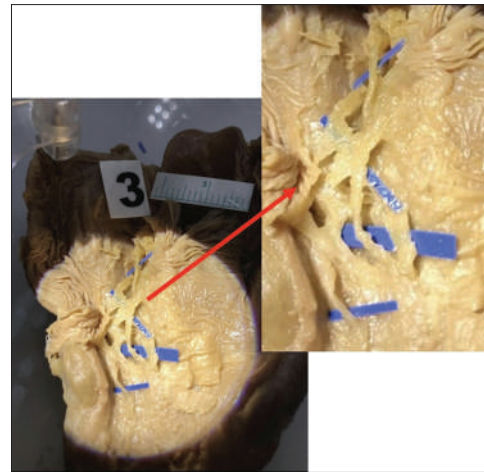


Figure 1: Plexus type of Galen's Anastomosis. The connection between the internal branch of the superior laryngeal nerve and the recurrent laryngeal nerve in the left half of the 3<sup>rd</sup> specimen is highlighted with blue markings and enlarged at the right upper side. Red arrow indicates the plexus

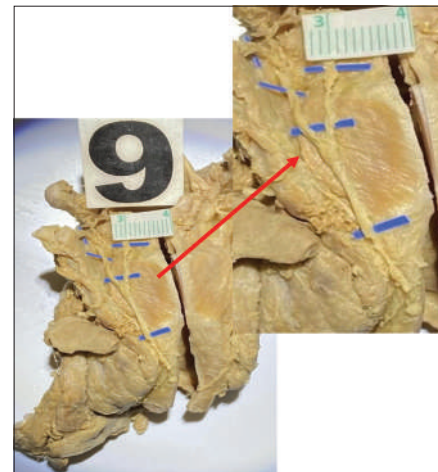


Figure 2: Single trunk type of Galen's anastomosis. The connection between internal branch of the superior laryngeal nerve and recurrent laryngeal nerve in the left half of the 9<sup>th</sup> specimen is highlighted with blue markings and enlarged at the right upper side. Red arrow indicates the trunk

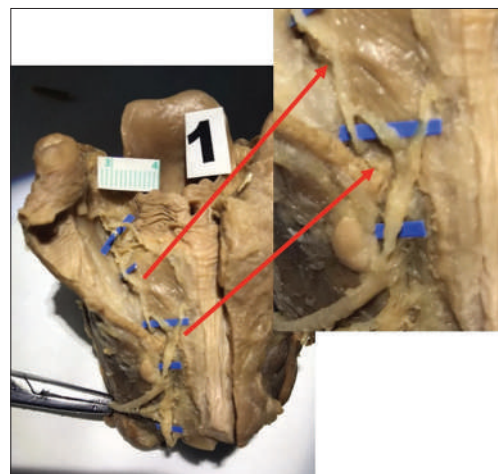


Figure 3: Double trunk type of Galen's anastomosis. The connection between superior laryngeal nerve and recurrent laryngeal nerve in the left half of the 1<sup>st</sup> specimen is highlighted with blue markings. The arrows indicate the double trunks

were single trunk, double trunk, or plexus [Figure 4]. In our study, 22 hemilarynxes were dissected from 11 adult larynx in total. Galen Anastomosis was not found in 10 of 22 half-larynxes (45.45%). In terms of single trunk formation, 6 right-sided (27.27%) and 4 left-sided (18.18%) Galen Anastomosis were observed. As for the double trunk formation, a single left-sided double trunk formation (4.54%) is observed. Finally, 1 plexus formation (4.54%) was dissected in one left half-larynx.

The connection between the ibSLN and the RLN in the left half of the 3<sup>rd</sup>, 9<sup>th</sup>, and 1<sup>st</sup> specimens was given as an example of the plexus, single trunk, and double trunk, respectively, in Figures 1-3.

## Discussion

### Anatomical prevalence in literature

In this study, the morphology of the connection between the dorsal branch of ibSLN and the dorsal branch of RLN has been described as a single trunk, double trunk,

and plexus, and Galen anastomosis prevalence was found %54.53 [Table 1]. According to the reviewed literature, Galen anastomosis varies between %15.8 and %100.<sup>[13]</sup>

Our results showed that Galen anastomosis can appear in all three forms which are single trunk, double trunk, and plexus as mentioned in the past literature. According to Henry *et al.*, the single trunk is the most seen variation with a prevalence of 92.3%, followed by a double trunk with a prevalence of %4.2, and the least common variation is the plexus with a prevalence of %3.5.<sup>[2]</sup> We found similar results as in this study single trunk was the most seen variation, followed by double trunk and plexus formation.

Furthermore, as the prevalence of the single trunk of Galen anastomosis is the most common variation, they suggested considering the single trunk subtype as normal anatomy, whereas other studies have different varieties of prevalences about the subtypes. We think it is difficult to say, considering the most seen variation of Galen's anastomosis as a part of typical anatomy, even when the existence of Galen's anastomosis and the prevalence of subtypes are still unclear. Even with the limitations of this study, many studies<sup>[14]</sup> show that the prevalence of subtypes may differ with sex and geography, which supports the difficulty of what to consider a typical result.

Naidu *et al.* suggest that the internal laryngeal nerve can have a greater contribution to anastomosis due to its greater diameter if it is compared with RLN.<sup>[13]</sup> This information differs with authors, for instance, according to Dilworth Galen's Anastomosis can be considered as the continuation of the internal laryngeal nerve upwards.<sup>[15]</sup> As shown in the reviewed literature and also in our current study, the RLN has an important contribution to the Galen's anastomosis.

According to Song *et al.* 2009, Galen's anastomosis was thought of as sensory nature initially, 3 years later with the study from Naidu *et al.*, it is shown that 13% of branches of Galen anastomosis supply posterior cricoarytenoid

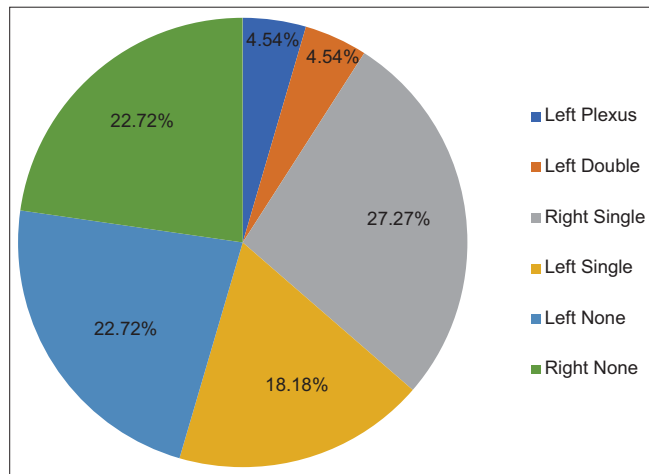


Figure 4: Percentage and types of anastomosis found in our current study and their distribution as a percentage

Table 1: Comparison of the prevalence of Galen's anastomosis

| Author                       | Number of dissections | Material                           | Magnification power  | Prevalence (%) |
|------------------------------|-----------------------|------------------------------------|----------------------|----------------|
| Berlin and Lahey (1929)      | 12                    | ND                                 | ND                   | 25             |
| Norland (1930)               | 19                    | ND                                 | ND                   | 15.8           |
| Lemere (1932)                | 10                    | ND                                 | ND                   | Nonconstant    |
| Williams (1951)              | 60                    | ND                                 | ND                   | 75             |
| Pichler and Gisel (1957)     | 100                   | ND                                 | Binocular microscope | 100            |
| Rueger (1972)                | 19                    | Fresh cadavers                     | 6                    | 89.5           |
| Souza <i>et al.</i> (1981)   | 150                   | Fixed cadavers                     | 10                   | 42             |
| Migueis <i>et al.</i> (1989) | 47                    | Fresh cadavers                     | 6                    | 88             |
| Schweizer and Dörfel (1996)  | 32                    | Fixed cadavers                     | Operative microscope | 84.4           |
| Sanudo <i>et al.</i> (1999)  | 180                   | Fixed cadavers                     | 6                    | 100            |
| Liebermann-Meffert (1999)    | 6                     | Fixed cadavers                     | ND                   | 33.3           |
| Furlan <i>et al.</i> (2001)  | 100                   | Fresh cadavers                     | 2,5                  | 87             |
| Naidu <i>et al.</i> (2012)   | 100                   | En bloc laryngeal specimens        | 4 light microscope   | 81             |
| Current study                | 22                    | Formalin-fixed laryngeal specimens | 2.5                  | 54.53          |

The table was adapted from Naidu *et al.*<sup>[13]</sup> with permission from Copyright 2014 by Wiley.

muscle.<sup>[13,16]</sup> As this study was purely anatomical, it is hard to contribute to the function of Galen's anastomosis.

### Clinical importance

It is very important to identify the RLN during thyroidectomy procedures. According to Pironi *et al.*, good identification of RLN can reduce the risk of nerve damage by up to 6.6%.<sup>[17]</sup> RLNs have many variations in terms of size, shape, and path. It enters the larynx through the berry ligament and provides stimulation of the intrinsic laryngeal muscles, with the exception of the cricothyroid muscle.<sup>[18]</sup> Inferior and superior thyroid poles are one of the places where RLN variations are frequently seen.<sup>[18]</sup> New-onset hoarseness, changes in vocal pitch, or noisy breathing which start in the patient after thyroid surgery or intubation should make us think of RLN damage. It is vital for surgeons to have knowledge of Galen's anastomosis and its types to minimize nerve damage.

As for the ibSLN, which is the other component of anastomosis, it is reported that injury to this branch disrupts the laryngeal cough reflex, which can cause aspiration pneumonia and other respiratory system diseases.<sup>[19]</sup> The ibSLN can also be used for therapeutic purposes. According to Zhipeng *et al.*, ultrasound-guided ibSLN blocks are used to reduce the risk of perioperative stress during intubation before surgeries.<sup>[20]</sup> In addition to preventing surgical complications, it is necessary to have good knowledge of the location of Galen's anastomosis to obtain maximum therapeutic efficiency.

### Limitations

Certain limitations of our study deserve mention. We had a limited number of specimens (11 larynx) due to difficulties in obtaining cadavers. In addition to that, it was difficult to measure sensitively the diameters of the fibers which contribute to Galen's anastomosis because of the lack of measurement equipment.

### Conclusion

From the laryngeal surgery perspective, because of the complexity and variety of the anatomical structures in this region, elaborative knowledge about the communication type of nerves is crucial. During laryngeal or thyroid surgery, observing an unknown intralaryngeal branching pattern may lead to confusion and an increased risk of iatrogenic nerve injury.

### Acknowledgement

The authors sincerely thank those who donated their bodies to science so that anatomical research could be performed. The results from such research can potentially increase humanity's overall knowledge that can then improve patient care. Therefore, these donors and their families deserve our highest gratitude.

### Financial support and sponsorship

Nil.

### Conflicts of interest

The authors declare that the article content was composed in the absence of any commercial or financial relationships that could be construed as a potential conflict of interest.

### References

1. Furlan JC, Brandão LG, Ferraz AR. Prevalence of Galen's anastomosis: An anatomical and comparative study. *J Laryngol Otol* 2002;116:823-5.
2. Henry BM, Peçkala PA, Sanna B, Vikse J, Sanna S, Saganiak K, *et al.* The anastomoses of the recurrent laryngeal nerve in the larynx: A meta-analysis and systematic review. *J Voice* 2017;31:495-503.
3. Wasserman JM, Sundaram K, Alfonso AE, Rosenfeld RM, Har-El G. Determination of the function of the internal branch of the superior laryngeal nerve after thyroidectomy. *Head Neck* 2008;30:21-7.
4. Cheruiyot I, Kipkorir V, Henry BM, Munguti J, Cirocchi R, Odula P, *et al.* Surgical anatomy of the external branch of the superior laryngeal nerve: A systematic review and meta-analysis. *Langenbecks Arch Surg* 2018;403:811-23.
5. Monfared A, Kim D, Jaikumar S, Gorti G, Kam A. Microsurgical anatomy of the superior and recurrent laryngeal nerves. *Neurosurgery* 2001;49:925-32.
6. Barral JP, Croibier A. *Manual Therapy for the Cranial Nerves*. London, UK: Churchill Livingstone; 2008.
7. Sañudo JR, Marañillo E, León X, Mirapeix RM, Orús C, Quer M. An anatomical study of anastomoses between the laryngeal nerves. *Laryngoscope* 1999;109:983-7.
8. May MT. *Galen on the usefulness of the parts of the body (Peri Chreias Morion. De usu partium)*, Ithaca, N.Y.:Cornell University Press; 1968.
9. Gunn A, Oyekunle T, Stang M, Kazaure H, Scheri R. Recurrent laryngeal nerve injury after thyroid surgery: An analysis of 11,370 patients. *J Surg Res* 2020;255:42-9.
10. Monfared A, Gorti G, Kim D. Microsurgical anatomy of the laryngeal nerves as related to thyroid surgery. *Laryngoscope* 2002;112:386-92.
11. Dralle H, Sekulla C, Lorenz K, Brauckhoff M, Machens A, German IONM Study Group. Intraoperative monitoring of the recurrent laryngeal nerve in thyroid surgery. *World J Surg* 2008;32:1358-66.
12. Melamed H, Harris MB, Awasthi D. Anatomic considerations of superior laryngeal nerve during anterior cervical spine procedures. *Spine (Phila Pa 1976)* 2002;27:E83-6.
13. Naidu L, Ramsaroop L, Partab P, Satyapal KS. Galen's "anastomosis" revisited. *Clin Anat* 2012;25:722-8.
14. Liebermann-Meffert DM, Walbrun B, Hiebert CA, Siewert JR. Recurrent and superior laryngeal nerves: A new look with implications for the esophageal surgeon. *Ann Thorac Surg* 1999;67:217-23.
15. Dilworth TF. The nerves of the human larynx. *J Anat* 1921;56:48-52.
16. Song P, Schwartz JS, Gacek RR, Malmgren LT, Blitzer A. Peripheral laryngeal motor innervation. In: *Neurologic Disorders of the Larynx*. New York: Thieme; 2009.
17. Pironi D, Pontone S, Vendettuoli M, Podzemny V, Mascagni D, Arcieri S, *et al.* Prevention of complications during reoperative thyroid surgery. *Clin Ter* 2014;165:e285-90.

18. Stefanou CK, Papathanakos G, Stefanou SK, Tepelenis K, Kitsouli A, Barbouti A, *et al.* Surgical tips and techniques to avoid complications of thyroid surgery. *Innov Surg Sci* 2022;7:115-23.
19. Shin DU, Sung JK, Nam KH, Cho DC. Bilateral internal superior laryngeal nerve palsy of traumatic cervical injury patient who presented as loss of cough reflex after anterior cervical discectomy with fusion. *J Korean Neurosurg Soc* 2012;52:264-6.
20. Zhipeng L, Meiyi H, Meirong W, Qunmeng J, Zhenhua J, Yuezhen H, *et al.* Ultrasound-guided internal branch of superior laryngeal nerve block on postoperative sore throat: A randomized controlled trial. *PLoS One* 2020;15:e0241834.

# The Association of Vascular Loops of Anterior Inferior Cerebellar Artery and Vestibulocochlear Symptoms

## Abstract

**Aim:** The association of vascular loops of anterior inferior cerebellar artery (AICA) with vestibulocochlear symptoms including hear loss, tinnitus, and vertigo is controversial. We aimed to investigate the relationship between vestibulocochlear symptoms and AICA vascular loop syndrome on magnetic resonance imaging (MRI). **Materials and Methods:** The patients underwent a posterior fossa MRI examination were reviewed regarding the presence of hear loss, tinnitus, and vertigo by an experienced ear-nose-throat specialists' physical examinations. The incidences of these lesions in the patients with and without AICA vascular loop syndromes were compared. Furthermore, the correlation between the AICA vascular loop syndrome subtypes (grade 1–3) and the incidence of the symptoms were analyzed. **Results:** A total of 502 patients (1004 ears) were included in this study. Vascular loops were demonstrated in 150 ears (14.9%). Subtype 1 was observed in 97 (9.7%), subtype 2 in 40 (4.0%) and subtype 3 in 13 (1.3%) ears. The incidences of tinnitus, hear loss, and tinnitus + hear loss were statistically significantly higher in the patients with vascular loops than without vascular loops ( $p: 0.000042$ ,  $p: 0.0446906$ ,  $p: 0.028106$ , respectively). However, there was not a significant correlation between the incidence of the symptoms and the grade of the vascular loop formation ( $p>0.05$ ). Vertigo incidence was very similar among the patients with no, with one-sided and with both-sided AICA vascular loops (41.5%, 39.8% and 46.2%, respectively) with no statistical difference ( $p>0.05$ ). **Conclusion:** The AICA vascular loop is associated with either tinnitus or hear loss but there is no correlation with the degree of the vascular loops. There is no relationship between AICA vascular loops and vertigo.

**Keywords:** Anterior inferior cerebellar artery vascular loop, hear loss, tinnitus, vertigo, vestibulocochlear symptoms

Yeliz Dadali,  
Sercan Özkaçmaz<sup>1</sup>,  
Mustafa Avcu<sup>2</sup>,  
Muhammed  
Alpaslan,  
Cemil Göya<sup>1</sup>,  
Mesut Özgökçe<sup>1</sup>,  
Ilyas Dündar<sup>1</sup>,  
Fatma Durmaz<sup>1</sup>

Departments of Radiology and  
<sup>2</sup>Otorhinolaryngology, Kırşehir  
Ahi Evran University Faculty of  
Medicine, Kırşehir, <sup>1</sup>Department  
of Radiology, Yüzüncü Yıl  
University Faculty of Medicine,  
Van, Turkey

## Introduction

Tinnitus, hearing loss, and vertigo are the most common vestibulocochlear symptoms. The incidence of tinnitus was found to be 22%, hearing loss 9%, and vertigo 42% in general population which increase with age.<sup>[1-3]</sup>

The contrast-enhanced magnetic resonance imaging (MRI) of the posterior fossa is essential for the detailed examination of posterior fossa, internal acoustic canal, and cerebellopontine angle (CPA) structures which can be associated with vestibulocochlear symptoms.<sup>[4]</sup> Although otological symptoms including tinnitus, hearing loss, and vertigo reported to occur secondary to malignant (acoustic schwannoma, etc.) and vascular conditions (vascular loop syndromes,) in CPA and internal acoustic canal, these symptoms can be seen also in asymptomatic individuals.<sup>[5]</sup>

This is an open access journal, and articles are distributed under the terms of the Creative Commons Attribution-NonCommercial-ShareAlike 4.0 License, which allows others to remix, tweak, and build upon the work non-commercially, as long as appropriate credit is given and the new creations are licensed under the identical terms.

For reprints contact: WKHLRPMedknow\_reprints@wolterskluwer.com

Vascular compression loop syndrome was first described by McKenzie but the association of this syndrome with otological syndromes is still controversial.<sup>[6,7]</sup> In this study, we aimed to examine the possible association of Vascular loops of the anterior inferior cerebellar artery (AICA) and vestibulocochlear symptoms including tinnitus, hearing loss and vertigo.

## Materials and Methods

### Patients

The data of the patients who underwent an MRI of posterior fossa 1 week within the admission of the otorhinolaryngology department because of various complaints between January 2016 and January 2018 were collected from the hospital and clinic database. Demographic features, results of physical examination regarding having vestibulocochlear findings, and radiological images were obtained. This retrospective

**How to cite this article:** Dadali Y, Özkaçmaz S, Avcu M, Alpaslan M, Göya C, Özgökçe M, *et al.* The association of vascular loops of anterior inferior cerebellar artery and vestibulocochlear symptoms. *J Anat Soc India* 2023;72:295-300.

### Article Info

Received: 04 June 2022

Accepted: 25 November 2023

Available online: 30 December 2023

### Address for correspondence:

Dr. Sercan Özkaçmaz,  
Department of Radiology,  
Yüzüncü Yıl University Faculty  
of Medicine, Van, Turkey.  
E-mail: sercanozkacmaz@  
hotmail.com

### Access this article online

Website: <https://journals.lww.com/joi>

DOI:  
10.4103/jasi.jasi\_85\_22

### Quick Response Code:



study was approved by a university ethics committee on September 18, 2018 with a number of 2018-18/155.

### Magnetic resonance imaging

MRI examinations were performed using a 1.5 Tesla MRI system (GE Signa Excite) with an 8-channel neurovascular head coil. The imaging protocol of posterior fossa consisted of axial T2-weighted images (TR/TE, 4000/100 ms; NEX, 4; section thickness, 5 mm; intersection spacing, 1.5 mm; matrix size, 256 × 160), axial T1-weighted images before and after the administration of intravenous contrast material (TR/TE, 540/8 ms; NEX, 4; section thickness, 5 mm; intersection spacing, 1.5 mm; matrix size, 288 × 192) and 3D-FIESTA images (TR/TE, 4/1.28 ms; flip angle, 60°, FOV, 19; matrix size, 352 × 224; section thickness, 1 mm).

All the images were transferred to a workstation and interpreted by a radiologist with 10 years' experience on neuroradiology who was blinded to the otological examination results of the patients.

### Anterior inferior cerebellar artery vascular loop compression syndrome

The AICA supplies the ventral-inferior parts of cerebellum and lateral lower portions of pons which originates from the lateral wall of the caudal third of the basilar artery. After AICA usually arises from the basilar artery as a single trunk, it courses laterally and posteriorly [Figure 1], frequently bifurcating into the superior and inferior trunk at the pontomedullary junction close to where the facial and vestibulocochlear nerves exit the brain stem and enter to internal auditory canal.<sup>[8]</sup>

AICA vascular loop refers to an anatomic variation in that AICA locates close to 7–8 cranial nerves in CPA or internal auditory canal. The classification of the vascular loop of AICA is based on the anatomical location of AICA as in type 1 AICA lies in the CPA but does not enter to internal auditory canal [Figure 2], in type 2 enters the CPA and extends less than half of length of internal auditory canal [Figure 3] and in type 3 enters the CPA and extends more than half of the length of internal auditory canal [Figures 4 and 5].<sup>[9]</sup>

### Assessment of hearing loss

Audiological evaluation hearing test examinations were made by an ear–nose–throat specialist with the assistance of an audiometrist. A resonance A R37A audiometer (Italy) device was used to perform the audiometric evaluation with a pure-tone audiometer inside a sound-proof cabin. Pure-tone thresholds were examined at 0.25, 0.5, 1, 2, 3, 4, and 8 kHz.<sup>[10]</sup> The patients with a value >15 were accepted as with hearing loss.

### Assessment of tinnitus

The patients completed the tinnitus handicap inventory questionnaire during the first examination. When the score

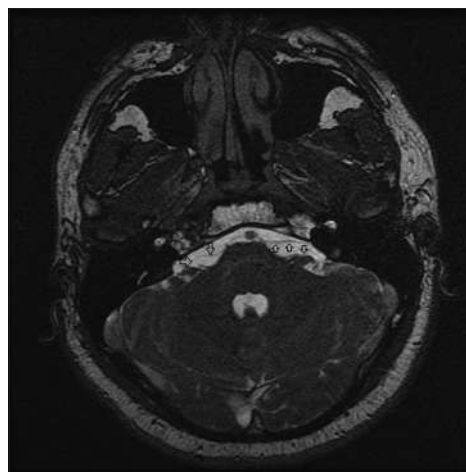


Figure 1: Normal location of bilateral anterior inferior cerebellar artery (arrows) as they are far from internal auditory canals

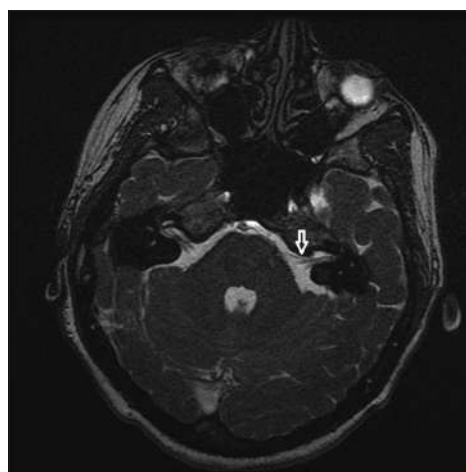


Figure 2: Type 1 anterior inferior cerebellar artery (AICA) loop syndrome in left side as the AICA lying close to the internal auditory canal but is not entering (arrow)

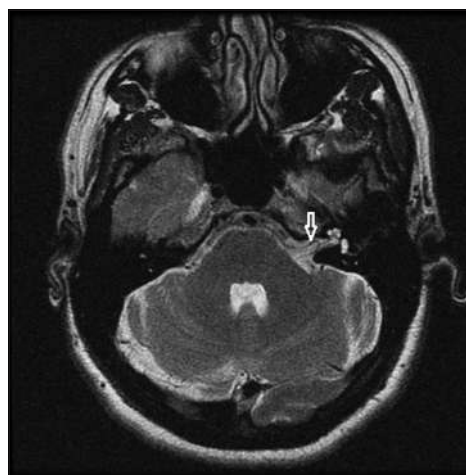
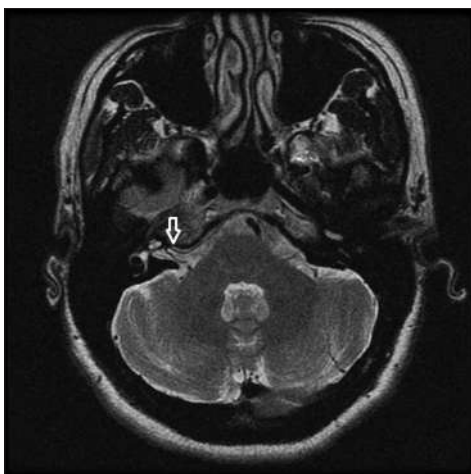


Figure 3: Type 2 anterior inferior cerebellar artery (AICA) vascular loop syndrome in left side as the AICA is entering less than half of internal auditory canal (arrow)

in this questionnaire, 0–16 it was defined as slight tinnitus, 18–36 mild tinnitus, 38–56 moderate, tinnitus, and 58–76



**Figure 4:** Type 3 anterior inferior cerebellar artery (AICA) vascular loop syndrome in right side as the AICA is entering more than half of internal auditory canal (arrow)

severe tinnitus. The patients with a score  $>1$  were accepted as with tinnitus.<sup>[11]</sup>

### Assessment of vertigo

The patients who had no identified cause including cardiovascular, hematological, metabolic and endocrine disorders, admitted with complaints of dizziness and imbalance were accepted as having vertigo.

### Groups

Patients were classified into 4 groups as group N (with no AICA vascular loop syndrome), group 1 (patients with type 1 AICA vascular loop syndrome), group 2 (patients with type 2 AICA vascular loop syndrome), and group 3 (patients with type 3 AICA vascular loop syndrome) and group 4 (patients with all types [group 1 + 2 + 3] of AICA vascular loop syndrome). For all these 5 groups, the presence of only tinnitus, only hearing loss, and tinnitus + hear loss in the same ear were analyzed and compared with each other. Also in the groups, a comparison of the presence of otological symptoms was performed between males and females.

In addition, patients were classified into three other groups according to the side location of AICA vascular loop syndrome as group N (the patients with no AICA vascular loop compression syndrome in any ear), group S (the patients with AICA loop vascular loop syndrome in only one ear) and group D (the patients with AICA vascular loop syndrome in both ears). The frequency of presence of vertigo was compared between these three groups. In each group, comparison of the presence of vertigo was performed also between males and females.

### Statistical analysis

Categorical variables were presented as frequency (n) and percentage (%); numerical variables were expressed as mean  $\pm$  standard deviation, minimum and maximum. A Chi-square test was used for the comparison of

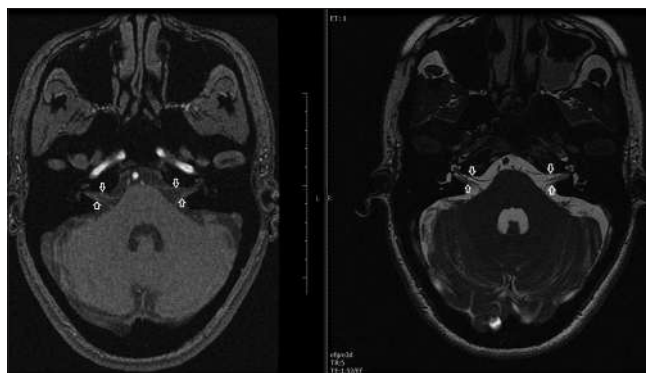


**Figure 5:** Type 2 (left side) and type 3 (right side) anterior inferior cerebellar artery vascular loops (arrows)

categorical variables. A  $P < 0.05$  was considered statistically significant. All the statistical analyses were made by an SPSS 20 software program (IBM Corporation, Armonk, NY, USA).

### Results

Among 596 patients, 29 ones with previous intracranial or ear surgery anamnesis, 21 with posterior fossa or internal auditory canal lesions, 3 with inner ear anatomical variations were excluded from the study. Detailed medical records of 41 patients were not available. Finally, a total of 502 patients (1004 ears) were included in this study.

Male/female ratio was 1.02 (253/249) and the mean age was  $43.4 \pm 19.1$  (18–79) years. The mean age of the groups was similar with no significant differences.

The control group was consisted of 854 ears (429 males and 425 females), group 1 of 97 ears (38 males and 59 females), group 2 of 40 ears (24 males and 16 females), group 3 of 13 ears (7 males and 6 females), and group 4 of 150 ears (69 males and 81 females) [Table 1].

Only tinnitus frequency was statistically significantly higher in group 1 (30.9% 30/97) than in group N (14.5% 124/854) ( $p:0.000032$ ). The difference between group 2 (27.5% 11/40) and group N (14.5% 124/854) was significant ( $p:0.025034$ ). The difference between group 3 (7.7% 1/13) and group N (14.5% 124/854) was nonsignificant ( $p:0.486718$ ). The difference between group 4 (28.0% 42/150) and group N (14.5% 124/854) was significant ( $p:0.000042$ ). The difference between group 1 and 2 ( $p:0.69037$ ), 1 and 3 ( $p:0.080345$ , and 2 and 3 ( $p:0.138211$ ) were all nonsignificant [Table 1]. Only hear loss frequency was nonsignificantly higher in group 1 (17.5% 17/97) than group N (12.6% 108/854) ( $p:0.177721$ ). The difference between group 2 (20.0% 8/40) and group N (12.6% 108/854), between group 3 (33.3% 3/10) and group N (12.6% 108/854), between group 2 (20.0% 8/40) and group 1 (17.5% 17/97), between group 3 (33.3% 3/10) and group 1 (17.5% 17/97), and between group 3 (33.3% 3/10) and group 2 (20.0%

**Table 1: Groups and the incidences of tinnitus, hear loss and tinnitus+hear loss**

|                      | Group N (Grade 0) |            | Group 1 (grade 1) |           | Group 2 (grade 2) |           | Group 3 (grade 3) |           | Group 4 (group 1+2 + 3) |           | Total     |           |              |
|----------------------|-------------------|------------|-------------------|-----------|-------------------|-----------|-------------------|-----------|-------------------------|-----------|-----------|-----------|--------------|
|                      | Male              | Female     | Male              | Female    | Male              | Female    | Male              | Female    | Male                    | Female    | Male      | Female    | Total        |
| No finding           | 303 (49.4)        | 310 (50.6) | 17 (35.4)         | 31 (64.6) | 9 (47.4)          | 10 (52.6) | 4 (1.9)           | 4 (50.0)  | 8 (0.8)                 | 30 (40.0) | 45 (60.0) | 75 (7.5)  | 333 (48.4)   |
| Tinnitus             | 64 (54.6)         | 60 (48.4)  | 16 (53.3)         | 14 (46.7) | 7 (63.6)          | 4 (36.4)  | 11 (1.1)          | 1 (100)   | 1 (0.1)                 | 23 (54.8) | 19 (45.2) | 42 (4.2)  | 87 (52.4)    |
| Hear loss            | 59 (54.6)         | 49 (45.4)  | 5 (29.4)          | 12 (70.6) | 6 (75.0)          | 2 (25.0)  | 8 (0.8)           | 2 (66.7)  | 1 (33.3)                | 3 (0.3)   | 13 (46.4) | 15 (53.6) | 28 (2.8)     |
| Tinnitus + hear loss | 3 (33.3)          | 6 (66.7)   | 0 (100.0)         | 2 (0.2)   | 2 (100.0)         | 0 (0.0)   | 2 (0.2)           | 1 (100.0) | 0 (0.0)                 | 3 (60.0)  | 2 (40.0)  | 5 (5.0)   | 6 (42.9)     |
| Total                | 429 (50.2)        | 425 (49.8) | 38 (39.2)         | 59 (60.8) | 24 (60.0)         | 16 (40.0) | 40 (4.0)          | 7 (53.8)  | 6 (46.2)                | 13 (1.3)  | 69 (46.0) | 81 (54.0) | 150 (14.9)   |
|                      |                   |            |                   |           |                   |           |                   |           |                         |           |           |           | 498 (50.4)   |
|                      |                   |            |                   |           |                   |           |                   |           |                         |           |           |           | 506 (50.4)   |
|                      |                   |            |                   |           |                   |           |                   |           |                         |           |           |           | 1004 (100.0) |

8/40) were all nonsignificant ( $p:0.176142$ ,  $p:0.263948$ ,  $p:0.733173$ ,  $p:0.626042$ ,  $p:0.812154$ , respectively). However, the frequency of only hearing loss was statistically significantly higher in group 4 (18.7% 28/150) than group N (12.6% 108/854) ( $p:0.046906$ ) [Table 1].

Tinnitus + hear loss frequency of group N (1.1% 9/854) was statistically lower than group 2 (5.0% 2/40) ( $p: 0.026918$ ), group 4 (3.0% 5/150) ( $p: 0.028106$ ) and group 3 (7.7% 1/13) ( $p: 0.026096$ ). The difference between group N and group 1 (2.1%) was nonsignificant ( $p:0.378948$ ). The difference between group 1 and 2, group 1 and 3, and group 2 and 3 was all nonsignificant ( $p:0.35025$ ,  $p:0.214829$ ,  $p:0.71558$ , respectively) [Table 1].

Vertigo was recorded in 41.5% (160/386) of the patients with group N (no involvement in ears), 39.8% (35/88) of in group S (single ear involvement) and 46.2% (13/28) in group D (Double ear involvement). The difference of the vertigo frequency between group N and group S ( $p:0.77283$ ), group N and group D ( $p:0.60683$ ) and group S and group D ( $p:0.533389$ ) was all non-significant [Table 2].

### Discussion

AICA usually arises from the lateral wall of the proximal segment of basilar artery (98%) at the level of CPA or from rarely vertebral artery (2%) as a single (92%) or duplicate (8%) branch.<sup>[12]</sup> AICA gives three branches as an internal auditory branch (passes into internal acoustic meatus), lateral branch (supplies superior/inferior semilunar lobules), and medial branch (supplies biventral lobule).<sup>[13]</sup>

Vertigo or tinnitus not only results from inner ear or cranial nerve lesions but also from vascular compression syndromes in the pontocerebellar angle. Various vascular compression syndromes may lead to hemifacial spasm, trigeminal neuralgia, and glossopharyngeal neuralgia.<sup>[14,15]</sup> Compression or close neighborhood of the vestibulocochlear nerve by vascular structures is associated with vertigo and hearing loss. The pathomechanism of this condition is suggested as edema and gliosis followed by demyelination, fibrosis, and subsequently axonal degeneration of the nerve by chronic compression.<sup>[16,17]</sup> Besides AICA, PICA, and petrosal arteries may lead to vascular compression syndromes.<sup>[18,19]</sup>

Contrast-enhanced temporal MRI is an excellent modality to discriminate inflammatory processes such as labyrinthitis or mastoiditis and neoplastic conditions such as acoustic schwannoma and meningioma. Furthermore, it provides the best view to detect and grade the vascular loop syndrome in pontocerebellar angle and internal acoustic canal. MRI is superior to computed tomography as it can differentiate soft tissues from fluids and also shows inner ear structures very clear in especially patients with sensorineural hearing loss.<sup>[20,21]</sup> Fast spin echo T2-weighted images have been widely used for the examination of posterior fossa and CPA, currently CISS sequence is very useful for evaluating

**Table 2: Groups and the incidences of vertigo**

|             | Group N (normal) no involvement of ear |            |            | Group S (single) involvement of one ear |           |           | Group D (double) involvement of two ear |           |           | Total      |            |             |
|-------------|--|------------|------------|---|-----------|-----------|---|-----------|-----------|------------|------------|-------------|
|             | Male                                   | Female     | Total      | Male                                    | Female    | Total     | Male                                    | Female    | Total     | Male       | Female     | Total       |
| Vertigo (-) | 117 (51.8)                             | 109 (48.2) | 226 (45.0) | 29 (54.7)                               | 24 (45.3) | 53 (10.6) | 7 (46.7)                                | 8 (53.3)  | 15 (29.9) | 153 (52.0) | 141 (48.0) | 294 (58.6)  |
| Vertigo (+) | 79 (49.4)                              | 81 (50.6)  | 160 (31.9) | 13 (37.1)                               | 22 (62.9) | 35 (7.0)  | 4 (30.8)                                | 9 (69.2)  | 13 (2.6)  | 96 (46.2)  | 112 (53.8) | 208 (41.4)  |
| Total       | 196 (508)                              | 190 (49.2) | 386 (76.9) | 42 (47.7)                               | 46 (52.3) | 88 (17.5) | 11 (39.3)                               | 17 (60.7) | 28 (5.6)  | 249 (49.6) | 253 (50.4) | 502 (100.0) |

the course of cranial nerves and the association of vascular structures with them in the internal acoustic canal and CPA.<sup>[22]</sup>

In literature, there are some inconsistent data about the association between vestibulocochlear symptoms and AICA vascular loop syndrome.<sup>[7]</sup> Various studies did not show a marked association<sup>[10,23-27]</sup> between AICA compression syndrome and tinnitus while some reported significant<sup>[28-32]</sup> results. In our study, we found statistically significantly higher tinnitus rates among the patients with AICA vascular loop syndrome (group 4) than ones without AICA vascular loop syndrome (group N) ( $P$ : 0.000042). However, we did not detect any correlation between the grade of AICA loop syndrome and tinnitus rate as the difference between group 3 (type 3) and the control group was nonsignificant while the difference was higher when compared group 1 and controls. Furthermore, differences between all AICA syndrome groups (group 1–4) were nonsignificant.

Similarly, the data about the association of hear loss and AICA vascular loop syndrome are very inconsistent. Most of the studies did not report a significant<sup>[24,25,32-34]</sup> association between hear loss and AICA loop syndrome since a few studies suggested significant results.<sup>[28,35]</sup> We also found statistically significant higher hear loss rates in the patients with AICA vascular loops than in controls. This rate was highest in group 3 followed by group 2, group 1, group N, but the differences between these groups were nonsignificant. As the result, we detected a significant difference on hear loss rate between patients with and without AICA vascular loops but not a significant correlation with the AICA vascular loop grades.

In literature, we did not find any study about the association between AICA vascular loop syndrome and the presence of either hear loss and tinnitus in the same side. We found statistically significant higher rates of either hear loss + tinnitus in the same ear in the patients with AICA loop syndrome when compared with ones without AICA loop syndrome. In all groups with AICA vascular loops (groups 2, 3, and 4) except from group 1, the rates of hear loss + tinnitus were statistically significantly higher than controls.

Almost all previous studies did not suggest a significant association<sup>[23,24,27,32]</sup> between AICA vascular loop syndrome and vertigo while only one study<sup>[31]</sup> reported a significant relationship. In our study, the vertigo incidence in controls was slightly higher than the patient with AICA in only

one ear and slightly lower than with AICA in both ears. Hence, there was no significant association between vertigo incidence and AICA loop syndrome in this study.

The major limitations of this study are retrospective design and relatively small sample size. We also could not evaluate the patients regarding hemifacial spasm, nystagmus, and otalgia.

## Conclusion

We found that individuals with AICA loop syndrome have significantly higher incidence of only tinnitus, only hearing loss and either tinnitus + hear loss while the incidence of these symptoms does not correlate with the degree of the vascular loop formation. However, there was not such association between vertigo and AICA loop syndromes.

## Financial support and sponsorship

Nil.

## Conflicts of interest

There are no conflicts of interest.

## References

- Oiticica J, Bittar RS. Tinnitus prevalence in the city of São Paulo. *Braz J Otorhinolaryngol* 2015;81:167-76.
- Lockwood AH, Salvi RJ, Burkard RF. Tinnitus. *N Engl J Med* 2002;347:904-10.
- Nondahl DM, Cruickshanks KJ, Wiley TL, Klein R, Klein BE, Tweed TS. Prevalence and 5-year incidence of tinnitus among older adults: The epidemiology of hearing loss study. *J Am Acad Audiol* 2002;13:323-31.
- Rinaldo FC, Paul RL. Tinnitus. In: *The Ear: Comprehensive Otolaryngology*. Philadelphia: LWW; 2000. p. 565.
- Lunsford LD, Niranjana A, Flickinger JC, Maitz A, Kondziolka D. Radiosurgery of vestibular schwannomas: Summary of experience in 829 cases. *J Neurosurg* 2005;102:195-9.
- Markowski J, Gierak T, Kluczevska E, Witkowska M. Assessment of vestibulocochlear organ function in patients meeting radiologic criteria of vascular compression syndrome of vestibulocochlear nerve – Diagnosis of disabling positional vertigo. *Med Sci Monit* 2011;17:R169-73.
- Papadopoulou AM, Bakoyiannis N, Sofokleous V, Skrapari I, Bakoyiannis C. The impact of vascular loops in the cerebellopontine angle on audio-vestibular symptoms: A systematic review. *Audiol Neurootol* 2022;27:200-7.
- Fogwe DT, Mesfin FB. Neuroanatomy, Anterior inferior cerebellar arteries. In: *StatPearls*. Treasure Island (FL): StatPearls Publishing; 2019. Available from: <https://www.ncbi.nlm.nih.gov/books/NBK448167/>. [Last updated on 2019 Mar 26].

9. Gultekin S, Celik H, Akpek S, Oner Y, Gumus T, Tokgoz N. Vascular loops at the cerebellopontine angle: Is there a correlation with tinnitus? *AJNR Am J Neuroradiol* 2008;29:1746-9.
10. Clark JG. Uses and abuses of hearing loss classification. *ASHA* 1981;23:493-500.
11. Newman CW, Jacobson GP, Spitzer JB. Development of the tinnitus handicap inventory. *Arch Otolaryngol Head Neck Surg* 1996;122:143-8.
12. Kim HN, Kim YH, Park IY, Kim GR, Chung IH. Variability of the surgical anatomy of the neurovascular complex of the cerebellopontine angle. *Ann Otol Rhinol Laryngol* 1990;99:288-96.
13. Balansard CH, Meller R, Bruzzo M, Chays A, Girard N, Magnan J. Trigeminal neuralgia: Results of microsurgical and endoscopic-assisted vascular decompression. *Ann Otolaryngol Chir Cervicofac* 2003;120:330-7.
14. Sindou M, Leston J, Decullier E, Chapuis F. Microvascular decompression for primary trigeminal neuralgia: Long-term effectiveness and prognostic factors in a series of 362 consecutive patients with clear-cut neurovascular conflicts who underwent pure decompression. *J Neurosurg* 2007;107:1144-53.
15. Naraghi R, Tanrikulu L, Troeschler-Weber R, Bischoff B, Hecht M, Buchfelder M, *et al.* Classification of neurovascular compression in typical hemifacial spasm: Three-dimensional visualization of the facial and the vestibulocochlear nerves. *J Neurosurg* 2007;107:1154-63.
16. Mailer MB. Results of microvascular decompression of the eighth nerve as a treatment for disabling positional vertigo. *Ann Otol Rhinol Laryngol* 1990;99:724-9.
17. Schwaber MK, Whetsell WO. Cochleovestibular nerve compression syndrome. II. Vestibular nerve histopathology and theory of pathophysiology. *Laryngoscope* 1992;102:1030-6.
18. Fukuda H, Ishikawa M, Okumura R. Demonstration of neurovascular compression in trigeminal neuralgia and hemifacial spasm with magnetic resonance imaging: Comparison with surgical findings in 60 consecutive cases. *Surg Neurol* 2003;59:93-9.
19. Jung NY, Moon WJ, Lee MH, Chung EC. Magnetic resonance cisternography: Comparison between 3-dimensional driven equilibrium with sensitivity encoding and 3-dimensional balanced fast-field echo sequences with sensitivity encoding. *J Comput Assist Tomogr* 2007;31:588-91.
20. Naganawa S, Yamakawa K, Fukatsu H, Ishigaki T, Nakashima T, Sugimoto H, *et al.* High-resolution T2-weighted MR imaging of the inner ear using a long echo-train-length 3D fast spin-echo sequence. *Eur Radiol* 1996;6:369-74.
21. Stuckey SL, Harris AJ, Mannolini SM. Detection of acoustic schwannoma: Use of constructive interference in the steady state three-dimensional MR. *AJNR Am J Neuroradiol* 1996;17:1219-25.
22. Czerny C, Rand T, Gstoettner W, Woelfl G, Imhof H, Trattinig S. MR imaging of the inner ear and cerebellopontine angle: Comparison of three-dimensional and two-dimensional sequences. *AJR Am J Roentgenol* 1998;170:791-6.
23. Sirikci A, Bayazit Y, Ozer E, Ozkur A, Adaletli I, Cüce MA, *et al.* Magnetic resonance imaging based classification of anatomic relationship between the cochleovestibular nerve and anterior inferior cerebellar artery in patients with non-specific neuro-otologic symptoms. *Surg Radiol Anat* 2005;27:531-5.
24. Hoekstra CE, Pijls VF, van Zanten GA. Diagnostic yield of a routine magnetic resonance imaging in tinnitus and clinical relevance of the anterior inferior cerebellar artery loops. *Otol Neurotol* 2015;36:359-65.
25. de Abreu Junior L, Kuniyoshi CH, Wolosker AB, Borri ML, Antunes A, Ota VK, *et al.* Vascular loops in the anterior inferior cerebellar artery, as identified by magnetic resonance imaging, and their relationship with otologic symptoms. *Radiol Bras* 2016;49:300-4.
26. Ensari N, Gür ÖE, Selçuk ÖT, Renda L, Osma Ü, Eyigör H, *et al.* Is presence of vascular loop in magnetic resonance imaging always related to tinnitus? *J Craniofac Surg* 2017;28:e295-8.
27. Beyazal Celiker F, Dursun E, Celiker M, Durakoglugil T, Beyazal M, Inecikli MF, *et al.* Evaluation of vascular variations at cerebellopontine angle by 3D T2WI magnetic-resonance imaging in patients with vertigo. *J Vestib Res* 2017;27:147-53.
28. Gorrie A, Warren FM 3<sup>rd</sup>, de la Garza AN, Shelton C, Wiggins RH 3<sup>rd</sup>. Is there a correlation between vascular loops in the cerebellopontine angle and unexplained unilateral hearing loss? *Otol Neurotol* 2010;31:48-52.
29. Cho YH, Lee SH, Park C, Min HJ, Choi EJ, Oh J, *et al.* The association of anterior inferior cerebellar artery in IAC with tinnitus and hearing loss. *Otolaryngol Head Neck Surg* 2012;147:222-3.
30. Bae YJ, Jeon YJ, Choi BS, Koo JW, Song JJ. The role of MRI in diagnosing neurovascular compression of the cochlear nerve resulting in typewriter tinnitus. *AJNR Am J Neuroradiol* 2017;38:1212-7.
31. Di Stadio A, Dipietro L, Ralli M, Faralli M, Della Volpe A, Ricci G, *et al.* Loop characteristics and audio-vestibular symptoms or hemifacial spasm: Is there a correlation? A multiplanar MRI study. *Eur Radiol* 2020;30:99-109.
32. Mejía-Quiñones V, Valderrama-Chaparro JA, Paredes-Padilla S, Orejuela-Zapata JF, Granados-Sánchez AM. Vascular loop in the cerebellopontine angle: clinical-radiological correlation. *Correlación clínico-radiológica del asa vascular del ángulo pontocerebeloso. Radiologia (Engl Ed)* 2020. [doi:10.1016/j.rx.2020.06.005].
33. van der Steenstraten F, de Ru JA, Witkamp TD. Is microvascular compression of the vestibulocochlear nerve a cause of unilateral hearing loss? *Ann Otol Rhinol Laryngol* 2007;116:248-52.
34. Loader B, Linauer I, Korkesch S, Krammer-Effenberger I, Zielinski V, Schibany N, *et al.* A connection between neurovascular conflicts within the cerebellopontine angle and vestibular neuritis, a case controlled cohort study. *Acta Otorhinolaryngol Ital* 2016;36:421-7.
35. Ezerarslan H, Sanhal EO, Kurukahvecioğlu S, Ataç GK, Kocatürk S. Presence of vascular loops entering internal acoustic channel may increase risk of sudden sensorineural hearing loss and reduce recovery of these patients. *Laryngoscope* 2017;127:210-5.

# Relationships of Matrix Metalloproteinase 3 Expression in Skeletal Muscle with Demographic Changes: Manual Microarray Study

## Abstract

**Background:** Skeletal muscle enzymes in the matrix metalloproteinase (MMP) family play a key role in myogenesis, tissue remodeling, and muscle regeneration. It is an extensive family of enzymes that are active in both the physiological and pathological processes of many tissues. This study aimed to investigate the differences of MMP-3 along with different age groups, histopathological changes, and other clinical data. **Materials and Methods:** Samples from 34 intercostal space muscles were used in this study. Samples were preferred to be taken from young and elderly. Paraffin blocks were prepared with a manual microarray method. They were also immunohistochemically stained with MMP-3. They were rated and scored as no staining, weak, moderate, and strong. The results were evaluated in terms of age, gender, histopathological changes, and chronic disease. Then, they were statistically analyzed. **Results:** In statistical evaluation, substance use was statistically significantly higher in the group aged 65 years and older than in the younger group ( $P = 0.02$ ). Although there was no statistically significant difference between the young and old groups in histopathological evaluations, it was observed that the staining rate of MMP-3 was significantly higher in the older group ( $P < 0.01$ ). It was understood that there was a statistical relationship between MMP-3 staining and chronic obstructive pulmonary disease ( $H = 4.23, P = 0.04$ ); this relationship was understood to be due to the relationship between weak staining and strong staining groups ( $Z = -2.05, P = 0.04$ ). **Conclusion:** Although MMP-3 expression prevalence increases in the elderly, its degree decreases. This variability can be useful in terms of tracking the degree of aging and degeneration.

**Keywords:** Demographic data, histopathology, matrix metalloproteinase-3, skeletal muscle

## Introduction

Aging is a complex and multifactor process characterized by a loss of muscle mass and impaired physiological functions and damaging changes in multisystems.<sup>[1]</sup> These changes include an increase in collagen concentration and the appearance of cross-bonds between collagen fibers in the extracellular matrix (ECM).<sup>[2,3]</sup> ECM, which surrounds the skeletal muscle fibers, provides structural support, protection, and maintenance of the functional integrity of the skeletal muscle through various mechanisms.<sup>[4]</sup> The modulation of the function is controlled by matrix metalloproteinases (MMPs). MMPs are a family of zinc- and calcium-dependent enzymes that support the breakdown and synthesis of ECM components such as collagen, proteoglycans, and glycoproteins during normal and pathological tissue remodeling.<sup>[5]</sup> These enzymes stimulate

the release of local growth factors in skeletal muscles.<sup>[6]</sup> In addition, MMPs are related to the modulation of inflammatory processes at various levels, for example, they regulate the bioavailability and activity of inflammatory cytokines, as well as the survival and escape of inflammatory cells.<sup>[7,8]</sup> It has even been shown that MMPs can regulate the transmigration of inflammatory cells.<sup>[7,8]</sup>

In collagen degradation, MMP-3 activates MMP-1, which acts as an important role in the degradation of collagen I.<sup>[9,10]</sup> MMP-3 digests components of the ECM can activate hidden forms of MMPs, and induce apoptosis.<sup>[11]</sup> MMP-3 plays an important role in the physiological process of tissue remodeling, but its improper expression can lead to the progression of cancer and facilitate the formation of invasion and metastasis.<sup>[12,13]</sup>

This study aimed to reveal the relationship of MMP-3 expression degree in striated muscle with age, clinical data as well as morphological changes.

**How to cite this article:** Erdem H, Teke HY. Relationships of matrix metalloproteinase 3 expression in skeletal muscle with demographic changes: Manual microarray study. *J Anat Soc India* 2023;72:301-6.

Havva Erdem,  
Hacer Yasar Teke<sup>1</sup>

Departments of Pathology  
and <sup>1</sup>Forensic Medicine, Ordu  
University of Medical Faculty,  
Ordu, Turkey

## Article Info

Received: 22 April 2022

Revised: 05 September 2023

Accepted: 10 November 2023

Available online: 30 December 2023

## Address for correspondence:

Dr. Havva Erdem,  
Department of Pathology, Ordu  
University of Medical Faculty,  
Ordu, Turkey.

E-mail: drhavvaerdem@gmail.  
com, haker.hgulderen2004@  
gmail.com

## Access this article online

Website: <https://journals.lww.com/joai>

DOI:  
10.4103/jasi.jasi\_65\_22

## Quick Response Code:



This is an open access journal, and articles are distributed under the terms of the Creative Commons Attribution-NonCommercial-ShareAlike 4.0 License, which allows others to remix, tweak, and build upon the work non-commercially, as long as appropriate credit is given and the new creations are licensed under the identical terms.

For reprints contact: WKHLRPMedknow\_reprints@wolterskluwer.com

## Materials and Methods

This study was deemed ethically appropriate by the Clinical Research Ethics Committee of Ordu University (240/2018). In addition, official permissions have been obtained from the judicial authorities. In this study, samples were taken from cases that were autopsied for different reasons between 2018 and 2019. Samples of these cases were divided into two groups according to their age to make comparisons. In the study, the elderly group (EG) was considered to be over 65 years old, and the younger group (YG) was considered to be under 50 years of age. The age range was grouped by the age distribution of the cases and the number of cases.

The fourth intercostal space muscle sample was used as a skeletal muscle sample. Paraffin blocks were prepared with the manual microarray method from the existing samples. Sections with a thickness of 5  $\mu\text{m}$  were taken from these muscle samples. Sections were stained with H and E. Parameters such as acidophilic sarcoplasm, prominence in striation, nucleus placement, vacuolization, deterioration in fibers, disruption, cellular infiltration, lipofuscin pigment accumulation, and acidophilic fluid accumulation were assessed under a light microscope [Figures 1-3].

### Immunohistochemical analysis

During the immunohistochemical study stages, the Leica Bond-Max IHC staining device (VisionBiosystems, Melbourne, Australia) was employed, and an MMP3 antibody was used. The MMP-3 antibody

(100  $\mu\text{g}$ , GTX103647) was diluted in a ratio of 1:200. Immunohistochemical findings were evaluated on the basis of staining frequency and intensity. The staining intensity was rated from 0 to 3. The staining was 0 (negative), 1 (weak), 2 (medium), and 3 (strong). The staining intensity was rated between 0 and 4. Rating 0 showed <3% staining; rating 1: 3%–25%; rating 2: 26%–50%; rating 3: 51%–75%; and rating 4: >75% staining. The score was calculated by multiplying the intensity and diffusiveness scores. Results were shown in order: score 0 = 0; score 1 = 1–2; score 2 = 3–5; and score 3 = 6–7.<sup>[14,15]</sup>

Immunohistochemical staining scores were evaluated in terms of age, gender, chronic disease, and histopathological changes.

### Statistical analysis

The data were analyzed statistically using computer software. The Shapiro–Wilk test was performed to investigate the distribution of data. The Chi-square testing, as well as descriptive statistics, was used in the classification of categorical data. Kruskal–Wallis test and Bonferroni corrected Mann–Whitney *U*-test from *post hoc* tests were performed in the investigation of the relationship between MMP-3 staining and other parameters.  $P < 0.05$  was taken for statistical significance.

## Results

The average age of 34 patients participating in the study was  $63.08 \pm 17.77$ , the youngest was 35 years old and the

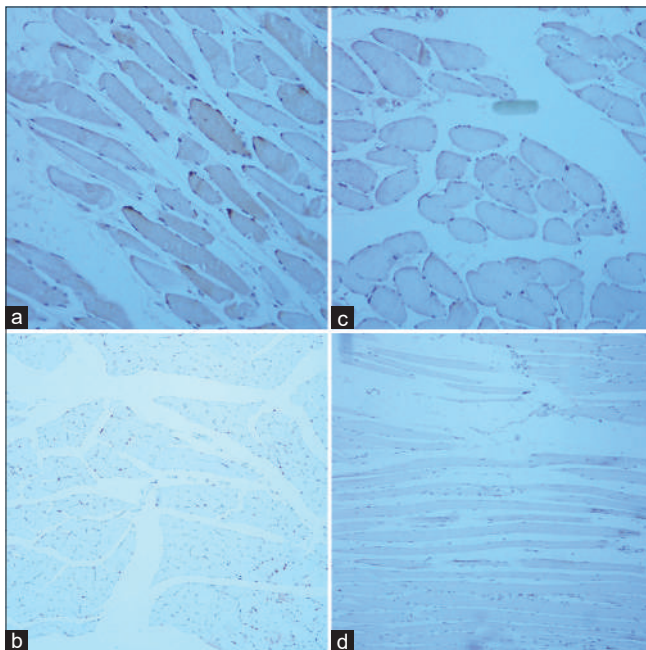


**Figure 1:** (a) Mild staining with matrix metalloproteinase (MMP)-3 in a striated muscle tissue (MMP3  $\times 200$ ), (b) no staining with MMP-3 in muscle tissue (MMP3  $\times 100$ ), (c) mild staining with MMP-3 in striated muscle tissue (MMP-3  $\times 200$ ), (d) no staining with MMP-3 was observed in striated muscle tissue (MMP-3  $\times 100$ )

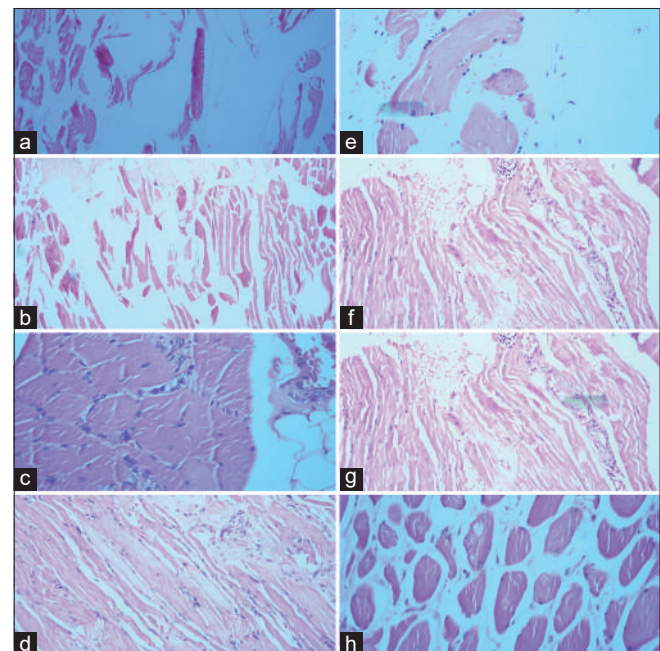


**Figure 2:** (a) Mild degree acidophilic sarcoplasm in muscle fibers (H and E  $\times 200$ ), (b) mild degree fiber deterioration in muscle fibers (H and E  $\times 100$ ), (c) moderate increase in cellularity in muscle fibers (H and E  $\times 400$ ), (d) mild degree striation of muscle fibers (H and E  $\times 40$ ), (e) deposition of lipofuscin in muscle fibers (H and E  $\times 40$ ), (f) moderate cellularity in muscle fibers (H and E  $\times 200$ ), (g) moderate cellularity in muscle fibers (H and E  $\times 200$ ), (h) moderate cellularity in muscle fibers (H and E  $\times 400$ )

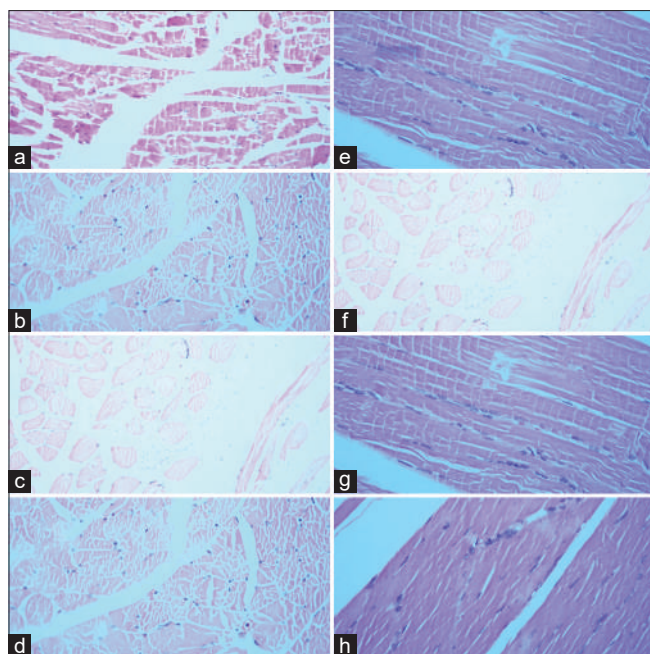


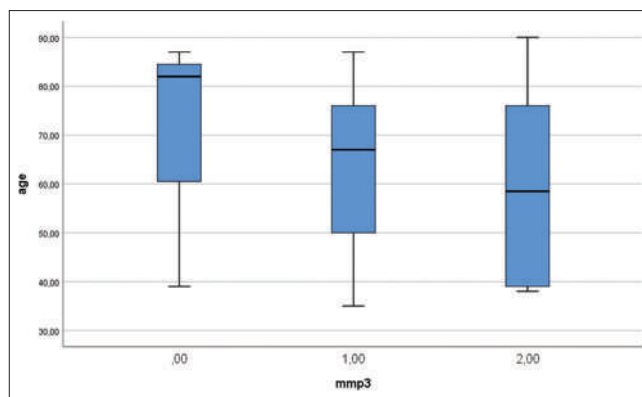
**Figure 3:** (a) Mild degree acidophilic sarcoplasm in muscle fibers (H and E  $\times 200$ ), (b) mild fragmentation of muscle fibers (H and E  $\times 100$ ), (c) multinucleation in muscle cell (H and E  $\times 200$ ), (d) mild degree streaking in muscle cell (H and E  $\times 40$ ), (e) moderate streaking in muscle cell (H and E  $\times 200$ ), (f) multinucleation in muscle cell (H and E  $\times 200$ ), (g) mild degree streaking in muscle cell (H and E  $\times 40$ ), (h) moderate vacuolization of muscle fibers (H and E  $\times 40$ )

oldest was 90 years old. Of the cases, 94.1% ( $n = 32$ ) were male and 5.9% ( $n = 2$ ) were female. The mean body mass index (BMI) of the cases was  $25.22 \pm 4.87$ , the lowest BMI was 17.04, and the highest BMI was 36.24.

Of the cases, 73.5% ( $n = 25$ ) were found to smoke, 8.8% ( $n = 3$ ) smoked and had alcohol use, 2.9% ( $n = 1$ ) had only alcohol use, and 14.7% ( $n = 5$ ) had no substance use in the story. Furthermore, 55.9% had a history of atherosclerotic heart disease ( $n = 19$ ) and 17.6% ( $n = 6$ ) had a chronic obstructive pulmonary disease (COPD). Substance use in the group aged 65 years and older was statistically significantly higher than in the young group ( $P = 0.02$ ). The distribution of sociodemographic characteristics of the young group aged 50 years and under and the older group aged 65 years and over was presented in Table 1.

In the histopathological examination, acidophilic fluid accumulation was not observed in both groups. Although there were no statistically significant differences between the two groups in histopathological assessments, staining with MMP-3 was statistically significantly higher in the EG ( $P < 0.01$ ), Graph 1. Histopathological characteristics of Group 1 and Group 2 were compared in Table 2. In addition, the correlation analysis showed a statistically significant relationship between MMP3 staining and histopathological disruption ( $P < 0.05$ ,  $r = -0.35$ ).

No significant differences were found between Group 1 and Group 2 in terms of staining with MMP-3 ( $H = 1.32$ ,



**Graph 1:** Distribution of matrix metalloproteinase-3 staining levels by age. MMP3: Matrix metalloproteinase-3

$P = 0.24$ ). In the Kruskal–Wallis test, it was understood that there was a statistical relationship between MMP3-staining and COPD ( $H = 4.23$ ,  $P = 0.04$ ), and in the *post hoc* test, this relationship was understood to be due to the relationship between weak staining and strong staining groups ( $Z = -2.05$ ,  $P = 0.04$ ) (strong staining was observed in all COPD patients). Data representation in Tables 1 and 2.

## Discussion

Chronic muscle degeneration is quite common in the elderly, and the molecular mechanisms affected in chronic conditions have not been fully understood.<sup>[16]</sup>

Here, we present a study that reveals changes in MMP-3 expression and histopathological changes through the intercostal muscle sample.

MMP-3 belongs to the MMP family and is additionally induced during development, wound repair, inflammation, and cancer.<sup>[17-20]</sup> With the increasing knowledge of MMP function and its effect on physiological and pathological processes, interest in MMP substrates has increased further.<sup>[20]</sup>

MMP-3 also plays a role in many inflammatory diseases such as ultraviolet-B irradiation and photo-aging, arthritis, lung damage, vascular disease, and inflammation of the intestine. In studies, MMP-3-silenced mouse have been found to show decreased inflammatory responses to various stimuli and decreased cutaneous wound contraction.<sup>[21-23]</sup>

In addition, numerous bone pathologies, including arthritis, osteoporosis, osteonecrosis, periodontitis, sinonasal osteitis, degenerated lumbar disc tissues, and bone cancer metastasis, were reported to contribute to MMP activity and were associated with various stimuli and reduced cutaneous wound contraction.<sup>[17-19]</sup>

As for wound healing and inflammation, Çıraklı *et al.* found that MMP-3 expression was higher in the tenotomy group than in the treatment group, which was associated with inflammation.<sup>[15]</sup>

In this study, although the number of cases showing expression of MMP-3 in EG is higher than in YG, its

**Table 1: Distribution of sociodemographic data of the groups**

|                                       | Group 1 |            | Group 2 |            | P     |
|---------------------------------------|---------|------------|---------|------------|-------|
|                                       | n       | SD (%)     | n       | SD (%)     |       |
| Age                                   | 13      | 42.53±4.89 | 21      | 75.80±7.91 | <0.01 |
| BMI                                   | 13      | 25.86±4.08 | 21      | 24.83±5.36 | 0.55  |
| Gender                                | 13      | 13/0       | 21      | 19/2       | 0.02  |
| Substance use                         |         |            |         |            |       |
| Smoking                               | 6       | 17.64      | 19      | 55.8       | 0.02  |
| Smoking and alcohol                   | 3       | 8.82       | -       | -          |       |
| Alcohol                               | 1       | 2.94       | -       | -          |       |
| No substance use                      | 3       | 8.82       | 2       | 5.88       |       |
| Atherosclerotic heart disease         |         |            |         |            |       |
| There is                              | 11      | 32.35      | 4       | 11.76      | <0.01 |
| None                                  | 2       | 5.88       | 17      | 50.00      |       |
| Chronic obstructive pulmonary disease |         |            |         |            |       |
| There is                              | 11      | 32.35      | 16      | 47.05      | 0.23  |
| None                                  | 1       | 2.94       | 5       | 14.70      |       |

BMI: Body mass index, SD: Standard deviation

**Table 2: Histopathological properties of Group 1 and Group 2 and staining status of matrix metalloproteinase 3**

|                         | Group 1 | Group 2 | P                           |
|-------------------------|---------|---------|-----------------------------|
|                         | n       | n       |                             |
| Acidophilic sarcoplasm  |         |         |                             |
| None                    | 5       | 10      | $\chi^2=0.27;$<br>$P=0.60$  |
| There is                | 8       | 11      |                             |
| Prominence in striation |         |         |                             |
| None                    | 10      | 15      | $\chi^2=0.12;$<br>$P=0.72$  |
| There is                | 3       | 6       |                             |
| Nucleus placement       |         |         |                             |
| 0                       | 9       | 14      | $\chi^2=4.21;$<br>$P=0.12$  |
| 1                       | 2       | 7       |                             |
| 2                       | 2       | 0       |                             |
| Vacuolization           |         |         |                             |
| None                    | 13      | 19      | $\chi^2=1.31;$<br>$P=0.25$  |
| There is                | 0       | 2       |                             |
| Deterioration in fibers |         |         |                             |
| None                    | 7       | 12      | $\chi^2=1.31;$<br>$P=0.25$  |
| There is                | 6       | 9       |                             |
| Disruption              |         |         |                             |
| None                    | 7       | 9       | $\chi^2=0.38;$<br>$P=0.53$  |
| There is                | 6       | 12      |                             |
| Cellular infiltration   |         |         |                             |
| None                    | 13      | 17      | $\chi^2=2.80;$<br>$P=0.09$  |
| There is                | 0       | 4       |                             |
| Lipofuscin accumulation |         |         |                             |
| None                    | 7       | 11      | $\chi^2=2.80;$<br>$P=0.09$  |
| There is                | 6       | 10      |                             |
| MMP3                    |         |         |                             |
| 0                       | 1       | 0       | $\chi^2=10.65;$<br>$P<0.01$ |
| 1                       | 5       | 19      |                             |
| 2                       | 7       | 2       |                             |

MMP: Matrix metalloproteinase

intensity is weak. It was observed that the degree of MMP-3 expression decreased in cases with the fragmentation of muscle fibers in terms of striated muscle degeneration. In a study on muscle degeneration that confirms this result, it was reported that MMP-3 levels decreased in the degenerated group compared to the healthy group.<sup>[19]</sup>

Lakemeier stated that while an increase in MMP-9 and 1 was monitored, a decrease in MMP-3 was observed, and it was responsible for regulating MMP-1 and 9.<sup>[19]</sup>

When these patients were examined, it was seen that COPD patients were mostly in the EG. However, this relationship was thought to be independent of age and staining score and was associated with inflammation.

An increase in muscle fiber fragmentation is noted in the EG. While the expression of MMP-3 is (weak degree) increased, the degree of intensity is weak compared to the EG. This weak MMP-3 elevation may be due to the effect of inflammatory cytokines in the inflammatory-aging mechanism.<sup>[24]</sup>

As a result of pronounced inflammation after infarction rupture in men, especially the interstitial collagen network activated by MMP-9 shows greater damage.<sup>[25]</sup> MMP-9 was not studied in this research. However, MMP-3 can be associated with the regulation of MMP-9.

In this study, the increase in expression intensity in people with COPD led to the conclusion that it may be related to the effect of cytokines released in the inflammatory response.

In a study involving morphological changes in normal skeletal muscle by age group, it was reported that the cell nucleus shrank in the EG compared to the young and child group; sarcoplasm was irregular and there was

ballooning and degeneration in mitochondrial clusters.<sup>[26]</sup> In this study, parameters such as acidophilic sarcoplasm, prominence in striation, nucleus placement, vacuolization, deterioration in fibers, disruption, cellular infiltration, lipofuscin pigment accumulation, and acidophilic fluid accumulation were assessed according to age groups. It was observed that the disruption of muscle fibers was more common in the older group than in the YG, but this difference was not statistically significant. However, it is thought that differences in MMP-3 staining may be related to this disruption. The absence of other MMPs such as MMP-1 and MMP-9, which were claimed to increase in degeneration by many publications and could illuminate this relationship, is one of the parameters that limit our work.

Data obtained by Si-Tayeb *et al.* show that nuclear MMP-3 is associated with the beginning of apoptosis. In the study, cells expressing the nuclear form of MMP-3 contained a higher proportion of apoptotic cell fraction than control cells. Furthermore, evidence suggests that MMP-3 is directly effective in apoptosis induction.<sup>[27]</sup> In addition, considering the relationship between smoking and apoptosis, Zhang *et al.* found that apoptosis activation is related to smoking and contributes to the pathogenesis of muscular atrophy.<sup>[28]</sup>

As seen in the literature, apoptosis is induced by smoking. This is also associated with an increase in MMP-3. In this study, the weak degree increase in MMP-3 expression in EG compared to YG may also be associated with smoking and apoptosis activation. Studying apoptotic markers in this group can be enlightening in terms of apoptosis.

### Limitations of the study

Causes of death such as drowning or gas poisoning were not included in this study. Again, those with color changes on the body were not included in the study. The sampled muscles were selected from hidden areas so as not to disturb body integrity. In addition, MMP-9, MMP-1, inflammatory markers, and apoptosis markers were not investigated. These reasons are the limitations of the study.

### Conclusion

MMP-3 expression increases with age and its intensity decreases. In addition to inflammatory conditions that affect this variability, the parameters that cause degeneration and aging affect the expression level. The degree and expression of MMP-3 may be indicative of the aging process. It will be illuminating to reveal this relationship with more case groups. In addition, we also believe that MMP-3 follow-up may be beneficial in terms of tracking the degree of aging and degeneration.

### Financial support and sponsorship

Nil.

### Conflicts of interest

There are no conflicts of interest.

### References

- Joanisse S, Nederveen JP, Snijders T, McKay BR, Parise G. Skeletal muscle regeneration, repair and remodelling in aging: The importance of muscle stem cells and vascularization. *Gerontology* 2017;63:91-100.
- Kragstrup TW, Kjaer M, Mackey AL. Structural, biochemical, cellular, and functional changes in skeletal muscle extracellular matrix with aging. *Scand J Med Sci Sports* 2011;21:749-57.
- Doria E, Buonocore D, Focarelli A, Marzatico F. Relationship between human aging muscle and oxidative system pathway. *Oxid Med Cell Longev* 2012;2012:830257.
- Carmeli E, Moas M, Reznick AZ, Coleman R. Matrix metalloproteinases and skeletal muscle: A brief review. *Muscle Nerve* 2004;29:191-7.
- Marqueti RC, Prestes J, Stotzer US, Paschoal M, Leite RD, Perez SE, *et al.* MMP-2, jumping exercise and nandrolone in skeletal muscle. *Int J Sports Med* 2008;29:559-63.
- Heinemeier KM, Olesen JL, Haddad F, Schjerling P, Baldwin KM, Kjaer M. Effect of unloading followed by reloading on expression of collagen and related growth factors in rat tendon and muscle. *J Appl Physiol* (1985) 2009;106:178-86.
- Nissinen L, Kähäri VM. Matrix metalloproteinases in inflammation. *Biochim Biophys Acta* 2014;1840:2571-80.
- Parks WC, Wilson CL, López-Boado YS. Matrix metalloproteinases as modulators of inflammation and innate immunity. *Nat Rev Immunol* 2004;4:617-29.
- Alge-Priglinger CS, Kreutzer T, Obholzer K, Wolf A, Mempel M, Kernt M, *et al.* Oxidative stress-mediated induction of MMP-1 and MMP-3 in human RPE cells. *Invest Ophthalmol Vis Sci* 2009;50:5495-503.
- Murphy G, Nagase H. Progress in matrix metalloproteinase research. *Mol Aspects Med* 2008;29:290-308.
- Visse R, Nagase H. Matrix metalloproteinases and tissue inhibitors of metalloproteinases: Structure, function, and biochemistry. *Circ Res* 2003;92:827-39.
- Sternlicht MD, Bissell MJ, Werb Z. The matrix metalloproteinase stromelysin-1 acts as a natural mammary tumor promoter. *Oncogene* 2000;19:1102-13.
- Pijnenborg R, Anthony J, Davey DA, Rees A, Tiltman A, Vercruyse L, *et al.* Placental bed spiral arteries in the hypertensive disorders of pregnancy. *Br J Obstet Gynaecol* 1991;98:648-55.
- Erdem H, Yasar Teke H, Sahin Y. Evaluation of fibrosis and histopathological changes in the psoas muscle with E-cadherin, claudin-5 expression and demographic data: An autopsy study. *Med Bull Haseki* 2021;59:280-5.
- Çıraklı A, Gürgör PN, Uzun E, Erdem H, Şahin AA, Baş O. Tranexamic acid has positive effect in early period of tendon healing by stimulating the tumor necrosis factor-alpha and matrix metalloproteinase-3 expression levels. *Jt Dis Relat Surg* 2020;31:463-9.
- Raz Y, Henseler JF, Kolk A, Tatum Z, Groosjohan NK, Verwey NE, *et al.* Molecular signatures of age-associated chronic degeneration of shoulder muscles. *Oncotarget* 2016;7:8513-23.
- Nerusu KC, Warner RL, Bhagavathula N, McClintock SD, Johnson KJ, Varani J. Matrix metalloproteinase-3 (stromelysin-1) in acute inflammatory tissue injury. *Exp Mol Pathol* 2007;83:169-76.
- Mirastchijski U, Lupše B, Maedler K, Sarma B, Radtke A,

- Belge G, *et al.* Matrix metalloproteinase-3 is key effector of TNF- $\alpha$ -induced collagen degradation in skin. *Int J Mol Sci* 2019;20:5234.
19. Lakemeier S, Schwuchow SA, Peterlein CD, Foelsch C, Fuchs-Winkelmann S, Archontidou-Aprin E, *et al.* Expression of matrix metalloproteinases 1, 3, and 9 in degenerated long head biceps tendon in the presence of rotator cuff tears: An immunohistological study. *BMC Musculoskelet Disord* 2010;11:271.
  20. Witty JP, Wright JH, Matrisian LM. Matrix metalloproteinases are expressed during ductal and alveolar mammary morphogenesis, and misregulation of stromelysin-1 in transgenic mice induces unscheduled alveolar development. *Mol Biol Cell* 1995;6:1287-303.
  21. Brenneisen P, Sies H, Scharffetter-Kochanek K. Ultraviolet-B irradiation and matrix metalloproteinases: From induction via signaling to initial events. *Ann N Y Acad Sci* 2002;973:31-43.
  22. Kurz B, Lemke AK, Fay J, Pufe T, Grodzinsky AJ, Schünke M. Pathomechanisms of cartilage destruction by mechanical injury. *Ann Anat* 2005;187:473-85.
  23. Yoo J, Rodriguez Perez CE, Nie W, Sinnott-Smith J, Rozengurt E. Protein kinase D1 mediates synergistic MMP-3 expression induced by TNF- $\alpha$  and bradykinin in human colonic myofibroblasts. *Biochem Biophys Res Commun* 2011;413:30-5.
  24. Franceschi C, Campisi J. Chronic inflammation (inflammaging) and its potential contribution to age-associated diseases. *J Gerontol A Biol Sci Med Sci* 2014;69 Suppl 1:S4-9.
  25. Fang L, Gao XM, Moore XL, Kiriazis H, Su Y, Ming Z, *et al.* Differences in inflammation, MMP activation and collagen damage account for gender difference in murine cardiac rupture following myocardial infarction. *J Mol Cell Cardiol* 2007;43:535-44.
  26. Mohamed RA, El Aasar HM, Mohamed LA, Abbas AM. Morphological features of normal human skeletal muscle in different age groups: A histological and ultrastructural study. *J Med Sci* 2007;7:161-9.
  27. Si-Tayeb K, Monvoisin A, Mazzocco C, Lepreux S, Decossas M, Cubel G, *et al.* Matrix metalloproteinase 3 is present in the cell nucleus and is involved in apoptosis. *Am J Pathol* 2006;169:1390-401.
  28. Zhang Y, Gao J, Luo Y. The effect of various durations of cigarette smoke exposure on muscle fibre remodeling in rat diaphragms. *Biomed Pharmacother* 2019;117:109053.

## Effects of 60-day Sodium Benzoate Exposure on the Ultramicroscopic Structure of Rat's Thyroid Gland Follicular Cells

### Abstract

**Background:** The sodium benzoate is widely used as a preservative in the food and pharmaceutical industries. There is information about the ability of this food additive to cause hepato- and nephrotoxicity, gonadotoxicity by initiating oxidative stress in cells. However, information on the effect of long-term exposure to sodium benzoate on the ultrastructure of endocrine cells, particularly of those thyroid follicular cells is completely absent. **Aim:** The aim of the study was to investigate electron microscopic changes in thyroid gland follicular cells in mature rats after 60 days of sodium benzoate administration. **Materials and Methods:** The first group consisted of rats injected daily with 1 ml sodium benzoate solution at a dosage of 1000 mg/kg of body weight through a feeding tube for 60 calendar days. The second group consisted of control animals injected with 0.9% saline solution under the same conditions. Thyroid gland pieces were processed according to the standard protocol for electron microscopy. **Results:** Microscopic examination of the thyroid gland of experimental animals showed that the follicular cells had a cubic or flattened shape. The apical surface of these cells contained a small number of low microvilli. The rough endoplasmic reticulum (rER) of most thyrocytes was enlarged and its cisterns contained homogeneous material, but some had abnormal electron dense deposits. In most cells, the nuclei were often irregular in shape with irregular contours, compared to the control. Heterochromatin occupied almost the entire periphery of the karyoplasm. The mitochondrial matrix was electron dense. Lysosomes were evenly distributed in the cytoplasm. A small number of small pinocytic vesicles with colloids were located in the apical part of most thyrocytes. A wide electron light pericapillary space was observed between the basal part of the latter and fenestrated capillaries. **Conclusion:** The 60 day administration of sodium benzoate to rats causes adverse ultrastructural changes in thyroid follicular cells. The rER undergoes the greatest morphological changes.

**Keywords:** Follicular cells, rats, sodium benzoate, thyroid gland, ultrastructure

Vitaliy Nikolaevich  
Morozov,  
Elena Nikolaevna  
Morozova,  
Alekssei  
Vladimirovich  
Tverskoi,  
Alekssei  
Vladimirovich Solin,  
Petr Mikhailovich  
Bykov

*Department of Human Anatomy  
and Histology, Federal State  
Autonomous Educational  
Institution of Higher Education,  
Belgorod National Research  
University, Belgorod, Russia*

### Introduction

At present, sodium benzoate is widely used as a preservative for food and beverages, in the pharmaceutical industry. It can be found as part of canned food, dairy and meat products, seasonings, and semi-finished products, as well as in the outer shell of drugs and personal hygiene products.<sup>[1]</sup> However, concerns remain about its complete safety for human health. The experimental and clinical studies show ambiguous results in this regard.

Thus, there is experimental evidence that the introduction of sodium benzoate causes chromosomal aberrations in cultured human lymphocytes;<sup>[2]</sup> induces the development of oxidative stress, reduces the activity of enzymes of the antioxidant system, increases the level of liver biochemical

markers (alanine aminotransferase and aspartate aminotransferase) and pro-inflammatory cytokines (interleukin 6, tumor necrosis factor-alpha) in cells.<sup>[3]</sup>

According to other sources, sodium benzoate has no mutagenic and teratogenic effects<sup>[4]</sup> and is also used in clinical practice in the therapy of resistant forms of schizophrenia, dementia, chronic liver diseases, and Parkinson's disease.<sup>[5-8]</sup>

The endocrine system, together with the nervous system, ensures the regulation and coordination of body functions and is one of the first to be exposed to adverse factors of both the external and internal environment.<sup>[9]</sup>

Physical and emotional health requires the normal functioning of the thyroid gland, which regulates the body's executive systems, metabolic rate, behavior, and cognitive function. The earliest

This is an open access journal, and articles are distributed under the terms of the Creative Commons Attribution-NonCommercial-ShareAlike 4.0 License, which allows others to remix, tweak, and build upon the work non-commercially, as long as appropriate credit is given and the new creations are licensed under the identical terms.

For reprints contact: WKHLRPMedknow\_reprints@wolterskluwer.com

**How to cite this article:** Morozov VN, Morozova EN, Tverskoi AV, Solin AV, Bykov PM. Effects of 60-day sodium benzoate exposure on the ultramicroscopic structure of rat's thyroid gland follicular cells. *J Anat Soc India* 2023;72:307-10.

### Article Info

Received: 12 April 2022

Revised: 07 August 2023

Accepted: 10 November 2023

Available online: 30 December 2023

### Address for correspondence:

*Prof. Alekssei Vladimirovich  
Solin,  
85, Pobeda St, Belgorod  
308015, Russia.  
E-mail: medps@yandex.ru*

### Access this article online

Website: <https://journals.lww.com/joi>

DOI:  
10.4103/jasi.jasi\_62\_22

### Quick Response Code:



morphological changes under the influence of unfavorable factors are found at the subcellular and cellular levels of the organization of matter. The aim of the study was to investigate electron microscopic changes in thyroid gland follicular cells in mature rats after 60 days of administration of sodium benzoate.

## Subjects and Methods

For the experiment, 12 white male mature rats weighing 200–250 g were selected. The animals were divided into two groups of six individuals each. The first group consisted of rats injected daily with 1 ml sodium benzoate solution at a dosage of 1000 mg/kg of body weight through a feeding tube for 60 calendar days. The second group consisted of control animals injected with 0.9% saline solution under the same conditions.

The animals were kept and manipulated in accordance with the rules for keeping experimental animals established by EU Directive 2010/63/EU of the European Parliament and the Council of September 22, 2010.<sup>[10]</sup> All procedures were approved by the bioethics committee of the State Establishment “Saint Luka Lugansk State Medical University,” Lugansk, People’s Republic of Lugansk (protocol number 2 dated March 25, 2022). The animals were removed from the experiment by the decapitation method. Immediately after removal, the thyroid gland was divided into pieces of 1 mm<sup>3</sup> sizes, then fixed in 2.5% glutaraldehyde solution, followed by treatment in 1% osmium tetroxide, according to Palade.<sup>[11]</sup> After dehydration in increasing concentration of ethanol and absolute acetone, the material was poured with a mixture of epoxy resins (epon-araldite). Polymerization was carried out for 36 h at 60°C. Ultrathin sections were made on a UMTP-4 ultramicrotome of the Sumy PO Electron, contrasted in a solution of uranyl acetate and lead citrate according to Reynolds<sup>[12]</sup> and studied under an EM-125 electron microscope with further photography.

## Results

The results of the study showed that in the animals of the control group, the thyroid gland consisted of typical follicles filled with colloids. Follicular cells are closely opposed to each other, had a predominantly cubic or columnar shape, and their apical surfaces are characterized by numerous irregularly spaced microvilli. Typical tight junctions or interdigitations are found between neighboring cells.

The nucleus of the follicular cell is predominantly oval or round in shape, located in the central or basal part of the cell, had slightly sinuous contours. Heterochromatin is located in a narrow, discontinuous rim under the nuclear membrane. The nucleolus is visualized in the peripheral part of the karyoplasm and had a different electron density. The rough endoplasmic reticulum (rER) of the

follicular cell is distributed throughout the cytoplasm, and its cisterns are expanded toward the base of the cell. The cytoplasm contained single free ribosomes, numerous typical elongated mitochondria with a homogeneous, and fine-grained matrix. A moderate number of electron-dense lysosomes are distributed mainly in the apical part of cells. A noticeable zone is visualized near the nucleus, containing the Golgi complex, consisting of a group of cisterns with densely packed vacuoles and small vesicles. The apical part of the cytoplasm contained several small bubbles and typical large colloidal droplets with a substance having a similar electron density to the colloid.

The bases of the epithelial cells of the follicles are adjacent to the fenestrated capillaries, in the lumen of which electron-dense blood cells are determined.

The stroma in the thyroid gland of the control animals is moderately developed [Figure 1].

Electron microscopic examination of the thyroid gland of experimental animals revealed that the follicular cells had a cuboidal shape, less often flat. The apical surface of these cells contained a small number of low microvilli. The rER of most thyrocytes was enlarged. In general, the rER tubules contained homogeneous material, but some had abnormal electron-dense deposits. In some cases, the assembly in the tubules progressed to well-defined clusters of wavy structures of various sizes with a circular orientation, located loosely relative to each other.

In most cells, the nuclei were often irregular in shape with irregular contours, compared to the control. Heterochromatin occupied almost the entire periphery of the karyoplasm. The mitochondrial matrix was electron-dense. Lysosomes were evenly distributed in the cytoplasm. A small number

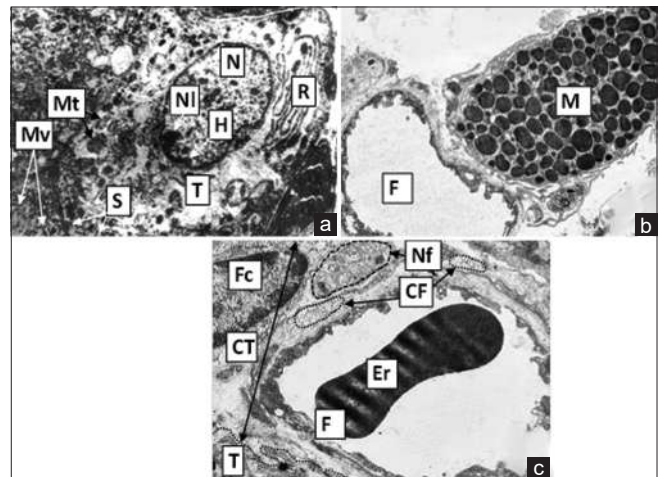


Figure 1: The piece of the thyroid gland of control mature rats ([a] piece of the thyroid gland with thyrocyte, [b] piece of thyroid gland with mast cell, [c] piece of the thyroid gland with connective tissue between follicles). T: Thyrocyte, N: Nucleus, NI: Nucleolus, H: Heterochromatin, R: Rough endoplasmic reticulum, Mt: Mitochondria, M: Mast cell, S: Secretory granules, Mv: Microvillus, F: Fenestrated capillary, Er: Erythrocyte, CT: Connective tissue between follicles, Fc: Fibrocyte, CF: Collagen fibers (cross-section), Nf: Nerve fiber ( $\times 8000$ )

of small pinocytic vesicles with colloids were located in the apical part of most thyrocytes. A wide electron-light pericapillary space was observed between the basal part of the latter and fenestrated capillaries [Figures 2 and 3].

## Discussion

Thus, ultramicroscopic examination showed that the thyroid gland of mature male rats contains thyrocytes of typical structure. Follicular cells delimit the colloid cavity and form the follicles. The stroma is moderately developed. A similar ultramicroscopic structure of thyroid follicular cells is confirmed by the data obtained by other researchers:

- In control, male mature outbred rats, thyrocytes of columnar shape contain interdigitations on the lateral surfaces, microvilli – on the apical surface and tight junctions on apicolateral borders. The nucleus is located in the basal part of the cell. Nucleolus of different electronic density occupies the area under the nuclear membrane. The rER is well developed, and mitochondria were randomly spread in the cytoplasm. The Golgi apparatus is located near the nucleus<sup>[13]</sup>
- In control male mature African giant rats, the thyroid gland is enclosed by a thin connective tissue capsule. The parenchyma consists of round, oval, or sometimes irregularly shaped follicles of variable sizes. The peripheral part of the thyroid gland contains large follicles lined with cuboidal or squamous follicular cells, while the central part – small- and medium-sized follicles lined with columnar or cuboidal cells. The apical surface of the thyrocyte has microvilli, apicolateral borders, tight junctions, and the base of the cell rests on the basement membrane. The nucleus was oval-shaped in the cuboidal or columnar follicular cells and flattened in squamous cells. In general, the nucleus occupies the central or basal part of the cell. The cisterns of rER and round- or rod-shaped mitochondria were distributed throughout the cytoplasm. Golgi apparatus is well developed and situated close to the nucleus<sup>[14]</sup>
- In control male mature Wistar rats, the thyrocytes contain a prominent nucleus, well developed rER, and small dense lysosomes. The Golgi complex is placed near the nucleus of the cell. The numerous long, regular

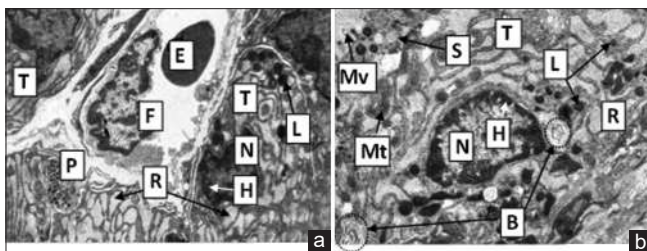


Figure 2: The piece of the thyroid gland of experimental mature rats ([a and b] pieces of thyroid gland with thyrocytes). T: Thyrocyte, N: Nucleus, H: Heterochromatin, R: Rough endoplasmic reticulum, B: Fibrous deposits in the cisterns of the rough endoplasmic reticulum, Mt: Mitochondria, L: Lysosomes, S: Secretory granules, Mv: Microvillus, F: Fenestrated capillary, E: Erythrocyte, P: Parafollicular cell ( $\times 8000$ )

microvilli projecting into the follicular lumen are situated on the apical surface of thyrocytes.<sup>[15]</sup>

In the experimental group, in comparison with the control, a small number of microvilli and small secretory granules in the apical part of thyrocytes were visualized on electronograms. Lysosomes were evenly distributed in the cytoplasm. Follicular cells were found to be cuboidal, less often flat in shape. Similar structural changes in thyrocytes were observed with exogenous administration of thyroid hormones into the body of rats, which, as shown by the study, reduced the level of endogenous thyroxine.<sup>[15]</sup> The systematic intake or high concentration of sodium benzoate in mice, reduces the synthesis of leptin by adipocytes.<sup>[16]</sup> The decrease in leptin, acting through the arcuate nucleus of the hypothalamus, leads to a decrease in the production of thyroliberin, and, consequently, reduces the production of thyrotropine.<sup>[17]</sup> The latter acts on the follicular cells of the thyroid gland and reduces the synthesis of thyroxine.

It should be noted that in the cytoplasm of the follicular cells of the thyroid gland of experimental animals, dilated cisterns of the rER are observed, in which there are single wavy structures of various sizes with a circular orientation, located loosely to each other. On the periphery of the nucleus, there are significant accumulations of heterochromatin, the mitochondrial matrix is electron-dense. The high doses of sodium benzoate cause DNA damage not only to the nuclei of rat liver epithelial cells but also to mitochondria.<sup>[18]</sup> DNA mutations can lead to impaired protein synthesis and a slowdown in its transport from the rER.<sup>[19,20]</sup> These studies can explain the changes revealed in the electronograms of the experimental group of rats.

## Conclusion

In animals of the control group, the thyroid gland follicular cells had a typical structure. The 60-day administration

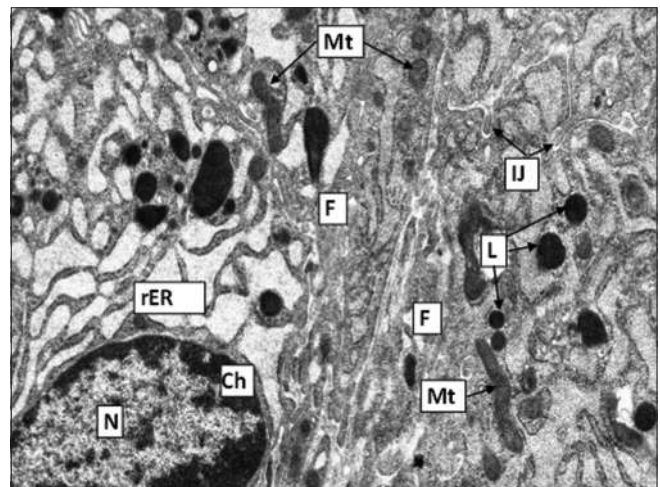


Figure 3: The area of the thyroid gland of mature rats (experimental group). F: Follicular cells, N: Nucleus, Ch: Chromatin, rER: Rough endoplasmic reticulum, Mt: Mitochondria, L: Lysosomes, IJ: Intercellular junctions (interdigitations) ( $\times 16,000$ )

of sodium benzoate to rats causes adverse ultrastructural changes in thyroid follicular cells. The rER undergoes the greatest morphological changes. The above-mentioned ultrastructural changes can be explained by the direct effect of the sodium benzoate on the DNA of the nucleus and mitochondria of thyrocytes or indirectly through a decrease in the level of leptin and, as a consequence, the effect on the hypothalamic–pituitary–thyroid axis.

#### Financial support and sponsorship

Nil.

#### Conflicts of interest

There are no conflicts of interest.

#### References

- Linke BG, Casagrande TA, Cardoso LA. Food additives and their health effects: A review on preservative sodium benzoate. *Afr J Biotechnol* 2018;17:306-10.
- Pongsavee M. Effect of sodium benzoate preservative on micronucleus induction, chromosome break, and Ala40Thr superoxide dismutase gene mutation in lymphocytes. *Biomed Res Int* 2015;2015:103512.
- Khan IS, Dar KB, Ganie SA, Ali MN. Toxicological impact of sodium benzoate on inflammatory cytokines, oxidative stress and biochemical markers in male Wistar rats. *Drug Chem Toxicol* 2022;45:1345-54.
- Emon ST, Orakdogan M, Uslu S, Somay H. Effects of the popular food additive sodium benzoate on neural tube development in the chicken embryo. *Turk Neurosurg* 2015;25:294-7.
- Seetharam JC, Maiti R, Mishra A, Mishra BR. Efficacy and safety of add-on sodium benzoate, a D-amino acid oxidase inhibitor, in treatment of schizophrenia: A systematic review and meta-analysis. *Asian J Psychiatr* 2022;68:102947.
- Lin CH, Chen PK, Wang SH, Lane HY. Effect of sodium benzoate on cognitive function among patients with behavioral and psychological symptoms of dementia: Secondary analysis of a randomized clinical trial. *JAMA Netw Open* 2021;4:e216156.
- Snehavardhan P, Lal BB, Sood V, Khanna R, Alam S. efficacy and safety of sodium benzoate in the management of hyperammonemia in decompensated chronic liver disease of the childhood-a double-blind randomized controlled trial. *J Pediatr Gastroenterol Nutr* 2020;70:165-70.
- Rangasamy SB, Dasarathi S, Nutakki A, Mukherjee S, Nellivalasa R, Pahan K. Stimulation of dopamine production by sodium benzoate, a metabolite of cinnamon and a food additive. *J Alzheimers Dis Rep* 2021;5:295-310.
- Koubassov RV. Hormonal changes in response to extreme environment factors]. *Vestn Ross Akad Med Nauk* 2014;69:102-9.
- Directive 2010/63/EU of the European Parliament and of the Council of 22 September 2010 on the protection of animals used for scientific purposes. *Official Journal of the European Union*; L276, vol. 53: 33-79.
- Palade GE. A study of fixation for electron microscopy. *J Exp Med* 1952;95:285-98.
- Reynolds ES. The use of lead citrate at high pH as an electron-opaque stain in electron microscopy. *J Cell Biol* 1963;17:208-12.
- Kuvneva ON, Radionov SN. Morphological changes in the thyroid gland under the influence of ionizing radiation. *Tavrisheskiy Mediko-Biologicheskiy Vestnik* 2013;16:124-6.
- Igbokwe CO, Ezeasor DN. Light and electron microscopic study of thyroid gland in the African giant rat, *Cricetomys gambianus*, Waterhouse. *Pak J Zool* 2014;46:1223-30.
- Ali Rajab NM, Ukropina M, Cacic-Milosevic M. Histological and ultrastructural alterations of rat thyroid gland after short-term treatment with high doses of thyroid hormones. *Saudi J Biol Sci* 2017;24:1117-25.
- Piper JD, Piper PW. Benzoate and sorbate salts: A systematic review of the potential hazards of these invaluable preservatives and the expanding spectrum of clinical uses for sodium benzoate. *Compr Rev Food Sci Food Saf* 2017;16:868-80.
- Ramos CF, Zamoner A. Thyroid hormone and leptin in the testis. *Front Endocrinol (Lausanne)* 2014;5:198.
- Saatcia C, Erdemb Y, Bayramova R, Akalina H, Tascioglu N, Ozkul Y. effect of sodium benzoate on DNA breakage, micronucleus formation and mitotic index in peripheral blood of pregnant rats and their newborns. *Biotechnol Biotechnol Equip* 2016;30:1179-83.
- Shapiro F, Mulhern H, Weis MA, Eyre D. Rough endoplasmic reticulum abnormalities in a patient with spondyloepimetaphyseal dysplasia with scoliosis, joint laxity, and finger deformities. *Ultrastruct Pathol* 2006;30:393-400.
- Abdul-Hamid M, Salah M. Lycopene reduces deltamethrin effects induced thyroid toxicity and DNA damage in albino rats. *J Basic Appl Zool* 2013;66:155-63.

## A Study of Morphometrical Analysis of the Human Malleus

### Abstract

**Introduction:** Malleus is one of the three ear ossicles which are the largest among all. It is present in the middle ear cavity and is responsible for the conduction of sound waves from external to inner ear. The malleus has a head, neck, manubrium, and anterior and lateral processes. The aim of this study was to study the morphometry of human malleus and to determine the normal range of the various measurements of malleus. **Materials and Methods:** A total of 120 dry adult human malleus were used in this study. Malleus bones were collected during the routine dissection of cadavers by the MBBS students of first professional in the dissection hall of anatomy department of various medical colleges of Uttar Pradesh. These dimensions of malleus bone were taken with the help of digital Vernier caliper which has an accuracy of 0.01 mm. **Results:** The mean value of total length of malleus was found 7.915 mm, mean value of length of handle was found 4.74 mm, and mean value of total width of head was found 2.63 mm. **Discussion and Conclusion:** No statistical significant difference was found when compared with the morphometric parameters of malleus of the right and left sides.

**Keywords:** Ear ossicles, malleus, middle ear, ossiculoplasty, prosthesis

### Introduction

The auditory ossicles malleus, incus, and stapes are the smallest bones in the human body and are structurally and functionally most complicated.<sup>[1,2]</sup> The presence of malleus was noted by Alessandro Achillini (1463–1513) for the first time in 15<sup>th</sup> century.<sup>[3]</sup> The malleus is derived from Meckel's cartilage of the first pharyngeal arch and ossification begins in the 4<sup>th</sup> month of intrauterine life and is completed by the 8 month.<sup>[1,2]</sup> Malleus assumes adult size at birth.<sup>[4]</sup> The malleus is the largest ear ossicles.<sup>[5]</sup> It is 8–9 mm long.<sup>[6]</sup> Malleus does not have periosteum and cannot be regenerated.<sup>[1,2]</sup> The malleus has a head, neck, manubrium (handle), and anterior and lateral processes.<sup>[5]</sup> The head is the larger upper end of the malleus and is situated in the epitympanic recess. It is ovoid in shape and articulates posteriorly with the body of the incus.<sup>[2]</sup> To form the incudomalleolar joint, this is a saddle type of synovial joint.<sup>[7]</sup> The neck is the narrowed part below the head and proceeds inferiorly as handle of the malleus.<sup>[5]</sup> The handle is directed downward, medially, and backward. The size of the handle decreases toward its free

end, which is curved slightly forward and is flattened transversely. The anterior process is a delicate bony spicule, which is directed forward from the enlargement below the neck. In fetal life, anterior process is the longest process of the malleus and is continuous in front with Meckel's cartilage.<sup>[6]</sup> The lateral process is a conical projection from the root of the handle of the malleus and is directed laterally.<sup>[2]</sup> This study is designed to find the morphometry of the human malleus and to determine the normal range of the various measurements of it.

### Materials and Methods

In the present study, 120 dry adult malleus bones were used. Malleus bones were collected during the routine dissection of cadavers by the MBBS students of the first professional in the Dissection Hall of Anatomy Department of various Medical Colleges of Uttar Pradesh, India. Out of total 120 malleus bones used, 60 were retrieved from the male cadavers (30 from right side and 30 from left side) and 60 were retrieved from the female cadavers (30 from right side and 30 from left side). Malleus was cleaned, dried and finally kept into the plastic satchel bags with zip locking mechanism. These pouches were assigned the serial number, age, date, side, and sex.

This is an open access journal, and articles are distributed under the terms of the Creative Commons Attribution-NonCommercial-ShareAlike 4.0 License, which allows others to remix, tweak, and build upon the work non-commercially, as long as appropriate credit is given and the new creations are licensed under the identical terms.

For reprints contact: WKHLRPMedknow\_reprints@wolterskluwer.com

**How to cite this article:** Sah SP, Chandra N. A study of morphometrical analysis of the human malleus. *J Anat Soc India* 2023;72:311-4.

**Sanjay Prasad Sah,  
Naresh Chandra**

*Department of Anatomy, Hind  
Institute of Medical Sciences,  
Barabanki, Uttar Pradesh, India*

### Article Info

**Received:** 13 March 2021

**Accepted:** 08 November 2023

**Available online:** 30 December 2023

### Address for correspondence:

*Dr. Sanjay Prasad Sah,  
Department of Anatomy, Hind  
Institute of Medical Sciences,  
Safedabad, Barabanki,  
Uttar Pradesh, India.  
E-mail: sanjayprasad3939@  
gmail.com*

### Access this article online

**Website:** <https://journals.lww.com/joai>

**DOI:**  
10.4103/jasi.jasi\_55\_21

### Quick Response Code:



**Table 1: Side comparison and statistical significance of malleus**

| Parameters                          | Side  | n  | Range (minimum–maximum) | Mean±SD    | Mean±SD     | P     |
|-------------------------------------|-------|----|-------------------------|------------|-------------|-------|
| Total length of malleus (mm)        | Right | 60 | 7.40–8.55               | 7.95±0.347 | 7.603–8.297 | 0.122 |
|                                     | Left  | 60 | 7.20–8.50               | 7.88±0.314 | 7.566–8.194 |       |
| Length of handle (mm)               | Right | 60 | 4.40–5.46               | 4.77±0.234 | 4.536–5.004 | 0.095 |
|                                     | Left  | 60 | 4.19–5.00               | 4.71±0.238 | 4.472–4.948 |       |
| Total width of head of malleus (mm) | Right | 60 | 2.20–3.16               | 2.62±0.284 | 2.336–2.904 | 0.341 |
|                                     | Left  | 60 | 2.06–3.35               | 2.64±0.320 | 2.32–2.96   |       |

$P < 0.05$  mm was regarded as statistically significant. n: Number of bones taken, SD: Standard deviation

**Table 2: Morphometric data of the human malleus**

| Parameters                          | Mean±SD     |
|-------------------------------------|-------------|
| Total length of malleus (mm)        | 7.915±0.330 |
| Length of handle (mm)               | 4.74±0.236  |
| Total width of head of malleus (mm) | 2.63±0.302  |

SD: Standard deviation

Pathological and fractured mallei were excluded from the study. Only fully ossified malleus was included in this study. The dimensions of malleus bones were studied from selected points as depicted in Figure 2. These dimensions of malleus bone were taken with the help of digital Vernier caliper which has an accuracy of 0.01 mm. The parameters of the malleus bones are studied [Figures 1 and 2]:

1. Total length of malleus (mm): Total length of malleus was measured as the maximum straight distance between the top of the head and the end of the handle of the Malleus (A-B)
2. Length of handle of malleus (mm): Length of handle of malleus was measured as the maximum straight distance between the end of the lateral process and the end of the handle of the Malleus (C-A)
3. Total width of head of malleus (mm): Maximum width of the head of malleus (D-E).

To avoid intraobserver variation, each measurement was done by the principal investigator at three different times and mean of all these three readings was taken as the final reading [Table 1]. For abovementioned measurements, mean value, standard deviation (SD), and mean  $\pm$  SD were calculated. Independent sample “t”-test was applied, and “P” value was calculated at 95% confidence interval using advance Excel/SPSS (Statistical Package for the Social Sciences) software version 26 [Table 2].

## Results

In the present study, no statistically significant difference was found when we compared morphometric parameters of malleus of the right and left sides when analyzed collectively from both the sexes as shown in Table 1.

## Discussion

Variations occur in the morphometric data of human malleus might be due to regional population or racial difference, and also variations occur in the dimension

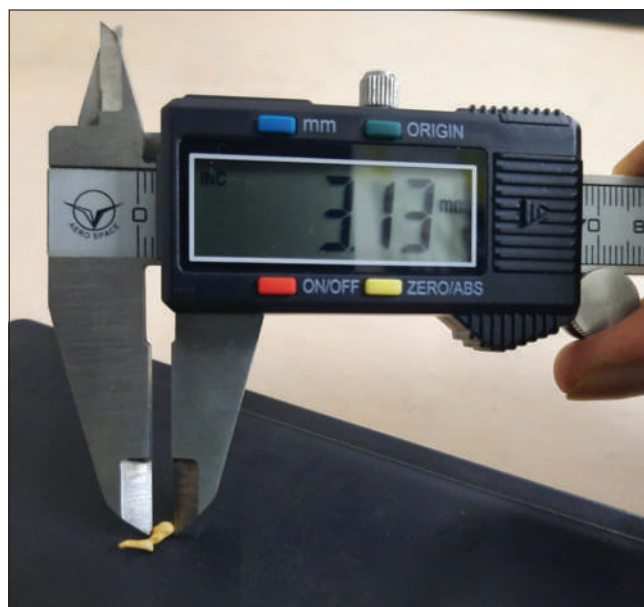


Figure 1: Method of measuring malleus

of malleus might be due to various types of instruments used for measurement; methods used for measurement of malleus or interobserver error by other researchers. Ear ossicles play an important role in hearing. Malleus provides 1.3 time mechanical advantage due to lever ratio, hence potentiates sound energy by that ratio. Morphometric analysis of ear ossicles has been the subject of interest since mid-15<sup>th</sup> century.<sup>[3]</sup> Malleus bones obtain full adult size during fetal life but continue to undergo changes throughout life, so the variations of the size of malleus bones are expected.<sup>[8]</sup> In present study, P values for all the parameters were more than 0.05 mm, which suggest that there is no statistically significant difference for these parameters of malleus between the right and left sides.

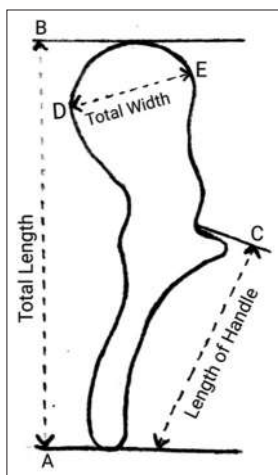
### Total length of malleus (mm)

In the present study (2021), the mean value of the total length of malleus was 7.915 mm which is similar to the study reported by Nadeem<sup>[9]</sup> (8 mm), Rathava *et al.*<sup>[10]</sup> (7.81 mm) and Sodhi *et al.*<sup>[11]</sup> (7.83 mm).

In the present study (2021), the mean value of total length of malleus was higher than the study reported by Vinaychandra<sup>[12]</sup> (7.45 mm) and Radha<sup>[13]</sup> (7.4 mm).

**Table 3: Comparison of morphometric data of malleus between present and previous studies**

| Researcher                            | Side  | Total length of malleus (mm) | Length of handle (mm) | Total width of head of malleus (mm) |
|---------------------------------------|-------|------------------------------|-----------------------|-------------------------------------|
| Singh <i>et al.</i> <sup>[19]</sup>   | Right | 7.94±0.41                    | 4.76±0.45             | -                                   |
|                                       | Left  | 7.94±0.40                    | 4.72±0.37             | -                                   |
| Makhija <i>et al.</i> <sup>[20]</sup> | Right | 7.59±0.36                    | 4.64±0.30             | 2.34±0.19                           |
|                                       | Left  | 7.62±0.14                    | 4.49±0.32             | 2.54±0.20                           |
| Sodhi <i>et al.</i> <sup>[21]</sup>   | Right | 7.68±0.51                    | 4.35±0.42             | -                                   |
|                                       | Left  | 7.79±0.47                    | 4.42±0.51             | -                                   |
| Present study                         | Right | 7.603–8.297                  | 4.536–5.004           | 2.336–2.904                         |
|                                       | Left  | 7.566–8.194                  | 4.472–4.948           | 2.32–2.96                           |

**Figure 2: Various measurements of Malleus bone. Total length (A-B), Length of handle (C-A), Total width of head (D-E)**

In the present study (2021), the mean value of the total length of malleus was lower than the study reported by Ramirez and Ballesteros<sup>[14]</sup> (8.18 mm), Mogra *et al.*<sup>[15]</sup> (8.53 mm) and Kumar *et al.*<sup>[16]</sup> (8.23 mm) [Table 3].

#### Length of handle (mm)

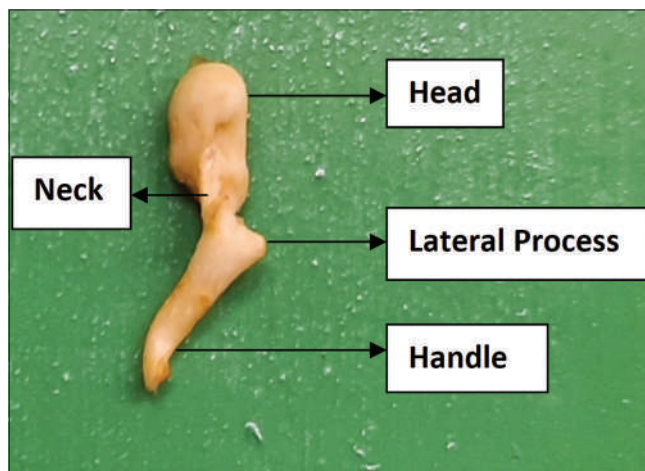
In the present study (2021), the mean value of length of handle (4.74 mm) was almost similar to the study reported by Bhatnagar *et al.*<sup>[17]</sup> (4.65 mm) and Unur *et al.*<sup>[18]</sup> (4.7 mm).

In the present study (2021), the mean value of length of handle was higher than the study reported by Nadeem G (2012-13)<sup>[9]</sup> (4.58 mm), Rathava *et al.*<sup>[10]</sup> (4.59 mm), Radha<sup>[13]</sup> (4.2 mm), Sodhi *et al.*<sup>[11]</sup> (4.44 mm), and Kumar *et al.*<sup>[16]</sup> (4.17 mm).

In the present study (2021), the mean value of length of handle was lower than the study reported by Ramirez and Ballesteros<sup>[14]</sup> (4.91 mm) and Mogra *et al.*<sup>[15]</sup> (5.2 mm).

#### Total width of the head of malleus (mm)

In the present study (2021), the mean value of total width of the head of malleus (2.63 mm) was almost similar to the study reported by Kumar *et al.*<sup>[16]</sup> (2.56 mm).

**Figure 3: Malleus bone**

## Conclusion

In the present study, we determined the normal range of the values of the various measurements of the human malleus [Figure 3]. The mean value of total length of malleus was found to be 7.915 mm, mean value of length of handle was 4.74 mm, and mean value of total width of head was 2.63 mm. No statistically significant difference was found when compared with the morphometric parameters of malleus of the right and left sides. The detailed knowledge of the morphometric data of various dimensions of the human malleus will help the otologist during reconstructive surgery and provide necessary information for the prosthesis designer for designing the prosthesis more appropriately suited for North Indian population. Human malleus can be used as homograft ossicles which are available in the regional tissue banks. This study will also give a basis for teaching the medical students about the human malleus.

#### Financial support and sponsorship

Nil.

#### Conflicts of interest

There are no conflicts of interest.

## References

1. Krogman WM. The Human Skeleton in Forensic Medicine. USA: Charles C Thomas, Springfield, Illinois; 1962.

2. Veeramani R, Holla SJ, (eds). Gray's Anatomy For Students: Second South Asia Edition E-Book. Elsevier Health Sciences; 2019.
3. Arensburg B, Harell M, Nathan H. The human middle ear ossicles: Morphometry and taxonomic implications. *J Hum Evol* 1981;10:199-205.
4. Andson BJ, Donaldson JA. Surgical Anatomy of the Temporal Bone and Ear. Vol. 37. Philadelphia: WB Saunders; 1973. p. 238-52.
5. Standring S. Gray's Anatomy: The Anatomical Basis of Clinical Practice, Expert Consult. Aubrey Durkin; 2009.
6. Javia M, Saravanan P. Morphometric analysis of various measurements of malleus on the basis of sexual dimorphism. *Indian J Anat Surg Head Neck Brain* 2018;4:94-101.
7. Kulkarni, Neeta V. Clinical anatomy (a problem solving approach). JP Medical Ltd, 2011.
8. Harmeja NK, Chaturvedi RP. A study of human ear ossicles. *Indian J Otol* 1973;25:154-60.
9. Nadeem G. Can fetal ossicles be used as prosthesis in adults? A morphometric study. *Anatomy* 2013;7:52-7.
10. Rathava J, Trivedi P, Kukadiya U. Morphometric study of malleus in Gujarati population. *Int J Adv Res* 2015;3:306310.
11. Sodhi S, Singh Z, Lal J. Morphometric dimensions of human ear ossicles of males. *Natl J Med Res* 2017;7:47-51.
12. Vinaychandra PH. Morphometry and variations of malleus with clinical correlation. *Int J Anat Res* 2014;2:191-4.
13. Radha K. Morphological and morphometric study of malleus in South Indian population. *Int J Anat Res* 2016;4:2342-4.
14. Ramirez LM, Ballesteros LE. Anthropometry of the malleus in humans: A direct anatomic study. *Int J Morphol* 2013;31:177-83.
15. Mogra K, Gupta S, Chauhan S. Morphological and morphometrical variations of malleus in human cadavers. *Int J Health Biomed Res* 2014;2:186-92.
16. Kumar DV, Chaitanya DK, Singh V, Reddy DS. A morphometric study of human middle ear ossicles in cadaveric temporal bones of Indian population and a comparative analysis. *J Anat Soc India* 2018;67:12-7.
17. Bhatnagar DP, Singal P, Thapar SP. Anatomy of malleus- a human ear ossicle. *Anthropologists* 2001;3:139-41.
18. Unur E, Ulger H, Ekinci N. Morphometrical and morphological variations in the middle ear ossicles in the newborn. *Erciyes Med J* 2002;24:57-63.
19. Singh K, Chhabra S, Sirohiwal BL, Yadav SP. Morphometry of malleus a possible tool in sex determination. *J Forensic Res* 2012;3:1-3.
20. Makhija K, Jain A, Mehra S, Asthana S. Malleus and its anatomical variations. *Int J Sci Appl Res* 2016;3:21-5.
21. Sodhi S, Singh Z, Davessar JL. Morphometry of human ear ossicles in females of North India. *Hum Biol Rev* 2018;7:172-82.

# An Introduction and Evaluation of Direct Observation with Checklist as a Teaching–Learning and Assessment Method in Anatomy

## Abstract

**Background:** Surface anatomy, which correlates with clinically relevant structural outlines and palpable features, is a core clinical skill that forms an essential component of physical examination. The teaching methodologies used currently lack clarity and adequacy of content as well as the assessment methods are ambiguous. With curricular reforms in India, there is a need for a student-centric teaching that integrates the principles of active and collaborative learning, feedback, and student autonomy. **Methodology:** The current study introduced and evaluated a new methodology, i.e. “Direct Observation with Checklist” for surface anatomy in 1<sup>st</sup>-year MBBS undergraduate students to gather their perception and gauge any improvement in learning. Students were taught and observed during their performance of a particular surface marking with the checklists and relevant improvements in their performances were suggested. At the end of the month, an examination was arranged and each student was individually assessed by two separate examiners during his/her performance. This was followed by an anonymous feedback to gather the student as well as faculty perception using a five-point Likert scale. **Results:** Z-test computation revealed a significant difference between the scores obtained through direct observation with checklist and without checklist. The faculty and student feedback provided encouraging results and suggestions in the implementation of direct observation with checklist. **Conclusion:** Direct observation with checklist is a novel teaching–learning and assessment method implemented for the first time in anatomy for teaching psychomotor skills of surface anatomy and can be explored further to educate and empower students.

**Keywords:** Competency-based medical education, direct observation of procedural skills, medical education, objectively structured clinical examination, surface anatomy

## Introduction

Historically, anatomy has been considered the foundation stone for medical education and continues to be so.<sup>[1]</sup> Even today, despite the technological advances in medicine, anatomical knowledge is not only essential for surgeons but also for anyone who performs a physical examination of a patient, examines radiological imaging, interprets any diagnostic tests, carries out emergency procedures, or explains a procedure to a patient.<sup>[2]</sup>

Surface anatomy, in particular, correlates with palpable surface features such as bony protuberances, tendons, and clinically relevant structural outlines that form an essential component of physical examination and interventional procedures.<sup>[3]</sup> A core clinical skill for the vast majority of general practitioners,

interventionists, anaesthetists, and surgeons, surface anatomy provides ample opportunities to assess structures under the skin, recognize their palpable characteristics demonstrate the techniques of physical examination and familiarize oneself in a safe environment before the clinical practice.<sup>[4]</sup> In spite of the clearly evident need for a solid foundation in surface anatomy, anatomy textbooks, barring a few, devote very less learning resources and time to it. The teaching methodologies being used currently are vaguely defined and lack clarity, quality as well as adequacy of content.<sup>[5]</sup> Moreover, living and surface anatomy has been designated as a skill that can be better assessed at the “Shows How” level of Miller’s pyramid with ambiguous assessment methods in the form of “skill assessment.”<sup>[6]</sup>

To top this, with the worldwide reforms in medical education in the 21<sup>st</sup> century, anatomy education has also entered into

## Jaikumar B. Contractor, Praveen Singh<sup>1</sup>

Department of Anatomy,  
GMERS Medical College,  
Panchmahal, Godhra,  
<sup>1</sup>Department of Anatomy,  
Pramukhswami Medical  
College, Bhaikaka University,  
Karamsad, Gujarat, India

## Article Info

Received: 16 May 2023

Revised: 10 September 2023

Accepted: 23 November 2023

Available online: 30 December 2023

## Address for correspondence:

Dr. Jaikumar B. Contractor,  
Associate Professor, GMERS  
Medical College, Panchmahal,  
Godhra, Gujarat, India.  
E-mail: jaicontractor02@gmail.  
com

## Access this article online

Website: <https://journals.lww.com/joai>

DOI:  
10.4103/jasi.jasi\_45\_23

## Quick Response Code:



**How to cite this article:** Contractor JB, Singh P. An introduction and evaluation of direct observation with checklist as a teaching–learning and assessment method in anatomy. *J Anat Soc India* 2023;72:315-20.

This is an open access journal, and articles are distributed under the terms of the Creative Commons Attribution-NonCommercial-ShareAlike 4.0 License, which allows others to remix, tweak, and build upon the work non-commercially, as long as appropriate credit is given and the new creations are licensed under the identical terms.

For reprints contact: WKHLRPMedknow\_reprints@wolterskluwer.com

a renaissance to move toward a student-centered teaching framework that is not only functionally and clinically relevant but also integrates the principles of active and collaborative learning, feedback, and student autonomy.<sup>[7]</sup> However, designing a pedagogical framework alone will not address the challenges of anatomy education. The designed teaching approach needs to be implemented through pertinent teaching–learning and assessment methods in the delivery of anatomy education and then evaluated.<sup>[8]</sup> Taking these into consideration, the present study was designed to introduce and evaluate direct observation with checklist as teaching–learning and assessment method in surface anatomy for undergraduate students and gather the perception of students and faculties for its implementation.

## Methodology

The present interventional study was conducted on Phase I MBBS students during the academic year 2019–2020. After obtaining necessary permissions from the Institutional Ethics Committee and concerned authorities, clinically relevant surface anatomy topics were identified by the principal investigator for the lower limb region of gross anatomy from Volume I of the Medical Council of India booklet for competency-based undergraduate curriculum for Indian medical graduate [Table 1].

These topics representing the desired competencies were further analyzed into specific learning objectives and the expected outcomes. Based on the guidelines provided by Degani and Wiener<sup>[9]</sup> and Stufflebeam,<sup>[10]</sup> 18 individual checklists, one for each identified topic, were developed

using the reference textbooks and through performance of surface marking on mummified cadavers by the principal investigator. Each individual topic checklist consisted of specific and sequentially arranged observable checkpoints. The checkpoints, in turn, comprised statements with brief descriptors in the form of criteria to be met by the students. Reference material was cited at the end of the checklist for the purpose of explanation of the descriptors. Each individual checkpoint was taught and assessed on a Yes or No Scale during student demonstration of a particular surface marking. Each checklist weighed 5 marks with each checkpoint scored individually from a minimum of 0.25 to 1.5 maximum based on the significance of that particular checkpoint in the expected outcome of the checklist. Each checklist also incorporated a space for open-ended suggestions from the assessor. The initial version of all the checklists was forwarded to subject experts both internally and externally (see acknowledgments) for their critical review in terms of clarity and applicability of the content, usability, effectiveness, and feasibility. The review comments and suggestions from subject experts were incorporated and the marking scheme of each checklist was prevalidated and finalized unanimously [Table 2].

First-year MBBS students and faculties of the anatomy department were sensitized and trained about the checklists and using direct observation with checklist as a teaching–learning and assessment method. Over the next month, the final version of the checklists along with their marking schemes was printed on A4 sheet and hard copies of appropriate topics were distributed to the students in small groups during routine dissection classes for surface marking of that particular topic. Students were observed during their performance of a particular surface marking with the checklists and relevant improvements in their performance were suggested.

At the end of the month, an examination for surface marking of the lower limb was arranged, where each student was individually assessed during his/her performance of surface marking. A single performance of an individual student was simultaneously assessed by two separate examiners, one through direct observation with checklist and another with direct observation without checklist. A total of 150 students were divided into 3 batches of 50 each and each batch (50 students) was assessed by two examiners, one with direct observation with checklist and another with direct observation without checklist. Both simultaneous assessments were scored out of 5 and the best score obtained by the student irrespective of the method of assessment was considered for summative assessment.

Informed written consent was procured from students before pooling the data and filling feedback forms. Students not willing to participate in the study or failing to provide informed written consent were excluded from the sample without any bias. The assessment scores of the

**Table 1: List of identified topics for checklist**

|   |
|---|
| Front of thigh                              |
| Saphenous opening                           |
| Great saphenous vein                        |
| Small saphenous vein                        |
| Femoral opening                             |
| Femoral artery                              |
| Femoral vein                                |
| Femoral nerve                               |
| Profunda femoris artery                     |
| Popliteal fossa                             |
| Popliteal artery                            |
| Tibial nerve                                |
| Common peroneal nerve                       |
| Back of thigh                               |
| Sciatic nerve                               |
| Front, lateral, and medial sides of the leg |
| Superior extensor retinaculum               |
| Anterior tibial artery                      |
| Deep peroneal nerve                         |
| Dorsalis pedis artery                       |
| Superficial peroneal nerve                  |
| Back of leg                                 |
| Posterior tibial artery                     |

**Table 2: Sample checklist**

| Surface marking – great saphenous vein   |     |    |       |
|--|-----|----|-------|
| Points to assess   | Yes | No | Marks |
| Uses appropriate color chalk for marking   |     |    | 0.5   |
| Correctly palpates and marks point 1 at the proximal end of 1st metatarsal bone  |     |    | 0.5   |
| Correctly palpates medial malleolus  |     |    | 0.25  |
| Marks point 2 at the anterior surface of the medial malleolus  |     |    | 0.25  |
| Correctly palpates the medial border of the tibia  |     |    | 0.25  |
| Marks point 3 approximately at the junction of the upper 2/3 <sup>rd</sup> and lower 1/3 <sup>rd</sup> on the medial border of the tibia |     |    | 0.25  |
| Correctly palpates and marks adductor tubercle as point 4  |     |    | 0.5   |
| Correctly palpates pubic tubercle  |     |    | 0.5   |
| Marks point 5 approximately 5 cm below and lateral to pubic tubercle   |     |    | 0.5   |
| Draws a line joining all the above-mentioned 5 points  |     |    | 1     |
| Handles the cadaver/mummy respectfully (wipes the marking with cloth)  |     |    | 0.5   |
| Total=( ___ /5)  |     |    |       |

students marked by direct observation with checklist and direct observation without checklist were computed using descriptive statistics such as mean, median, mode, and relational statistics Z-test for analyzing significance. An anonymous feedback using a five-point Likert scale was obtained through a Google Forms questionnaire to gather the student's perception and their level of satisfaction with both the assessment methods as well as faculty perceptions regarding teaching-learning and assessment techniques using direct observation with checklist. The questionnaire also included open-ended statements and suggestions for improvement from the students as well as faculties.

## Results

### Student feedback

The impact of direct observation with checklist as a teaching and assessment method was evaluated at level 1 (reaction) and level 2 (learning) using the four levels of evaluation by Kirkpatrick. Figure 1 shows the results of the Student's feedback ( $n = 110$ ), where majority of the students agreed that the method was simple, clear, and easy to understand as well as helps them learn and perform better in examinations. The students perceived that it increases objectivity in the assessment, provides timely feedback, and reduces their stress in terms of any ambiguity with the assessment. Similarly, all faculty ( $n = 6$ ) agreed that direct observation as a teaching-learning and assessment method is simple, clear, and easy to implement (6/6) and that it helps to teach more effectively (6/6) and give timely feedback (6/6). As an assessment method, it reduces bias (4/6) and should be frequently used in other examinations as well (5/6).

### Student scores

As for level 2, while it was difficult to comment on the direct observation with checklist as a teaching method through acquisition of knowledge and skills, there is a definite improvement in the scores of the students. Pooled data of the scores obtained by students ( $n = 148$ ) revealed a significant difference in the assessment conducted through direct observation with checklist and direct observation without checklist. The mean and median values of the corresponding scores are mentioned in Figure 2. Z-test computation to test the difference between the scores obtained through direct observation with checklist and without checklist revealed sufficient evidence that there exists a significant difference between the scores obtained through direct observation with checklist and without checklist [Table 3].

### Faculty scores

Additionally, an insight into the mean of scores given by individual faculties in pairs for 3 separate batches through direct observation revealed that while using checklist for assessment a higher score can be achieved by the students as compared to the method wherein the checklist is not used [Figure 3].

## Discussion

We found that there was a significant improvement in the scores obtained by the students through direct observation with checklist and the method was well received by the students and faculties alike because it was easy and clear to understand as well as helped the students to learn and perform better in examinations. It enabled a timely feedback and increased the objectivity in assessment which encouraged further frequent use in other examinations.

As for the scores, there is enough evidence to suggest that educational interventions with attention to teaching methods are one of the foremost parameters for improvement of academic performance.<sup>[11]</sup> In particular, topics of clinical relevance garner more attention from students especially when presented through newer and innovative methods.<sup>[12]</sup> Furthermore, apart from student feedback, high academic performance of the students is also a reliable parameter to ensure effective teaching.<sup>[13]</sup> These could indicate the improvement in scores obtained by the students through the newer teaching method we implemented.

Moreover, direct observation and corrective feedback are the cornerstones of teaching clinical skills since they guide learners to potential improvement by providing particulars about their performance.<sup>[14,15]</sup> In a prospective observational study by Benenson and Pollack<sup>[16]</sup> in emergency trainee performance for actual death notifications, constructive feedback by supervising doctors on unsatisfactory performance after direct observation led to improved

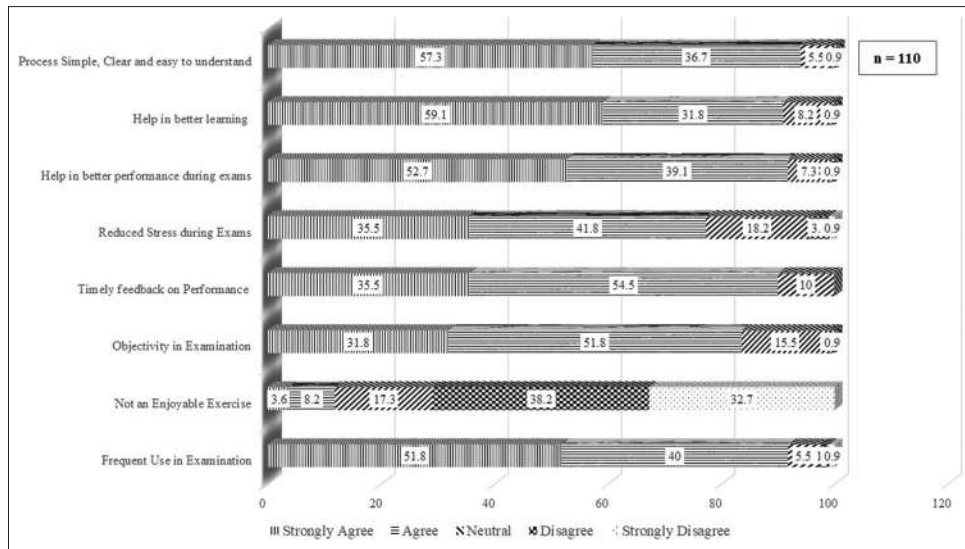


Figure 1: Student's feedback on direct observation with checklist

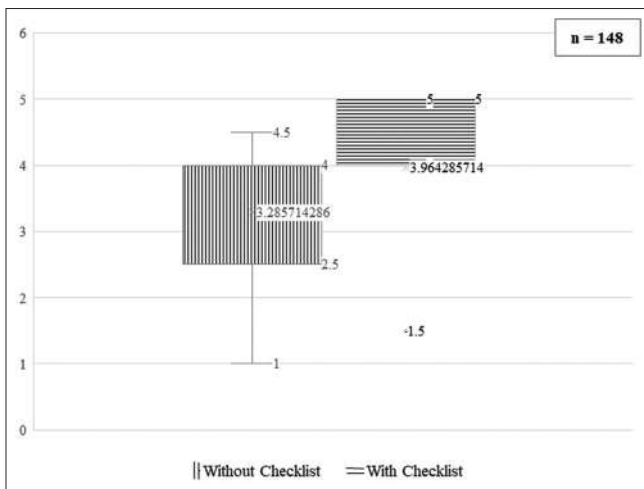


Figure 2: Differences in scores obtained for direct observation with checklist and without checklist

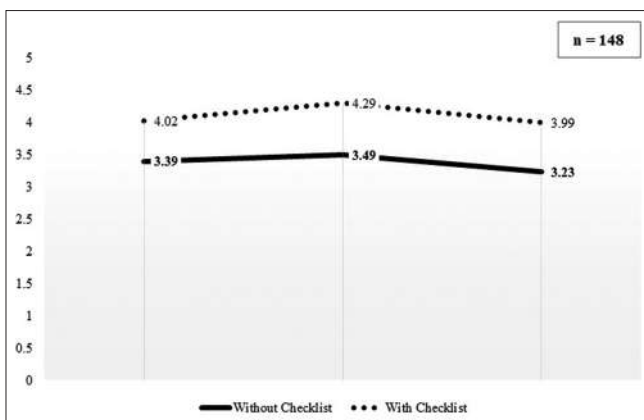


Figure 3: Differences in faculty scoring for direct observation with checklist and without checklist

performance in those initially assessed as unsatisfactory. Dorfsman and Wolfson<sup>[17]</sup> also reported improved efficiency

Table 3: Z-test analysis for scores obtained through both methods

| Scores obtained through direct observation | Mean scores | SE   | Z    |
|--|-------------|------|------|
| With checklist                             | 4.11        | 0.12 | 6.18 |
| Without checklist                          | 3.37        |      |      |

SE: Standard error

of emergency medicine residents in physical examination skills after receiving observer feedback. Furthermore, in the absence of direct observation and feedback, learners might acquire incorrect techniques.<sup>[18]</sup> In this context, specific feedback through checklists can be highly effective in terms of explaining the learners on what they need to do differently.<sup>[19]</sup> Similar feedback was shared by the students through their open-ended statements that a checklist gives them the “exact and necessary steps,” “makes learning very simple and structured,” “increases transparency as well as reduces the stress of vagueness” and “helps them improve on their performance through corrective measures.”

Another important factor to explore is the peer feedback. Since the checklists were distributed in small groups ( $n = 17$ ) and students practiced the surface marking on mummified cadavers in small groups, observing their peers could have played a substantial role in better learning.<sup>[20]</sup> Similar improvements have been reported by Zaidi *et al.*<sup>[21]</sup> where skills practice with positively deviant peers led to a better clinical skill performance of participating students.

While literature search did not yield direct observation with checklist as a teaching–learning or assessment method being implemented in various subjects or colleges, methods such as direct observation of procedural skills (DOPS) and objective structured clinical examination (OSCE) closely resemble the pattern we implemented with minor

differences. In effect in both these methods too, students are assessed by multiple assessors on multiple encounters aimed at improving performance and hence they serve the twin purpose of assessment as well as learning by direct observation of the trainee at the workplace.<sup>[22,23]</sup>

Similar to the feedback of our study for direct observation with checklist, Singh *et al.*<sup>[24]</sup> in their study to evaluate the feasibility, acceptability, and utility of DOPS for undergraduate dental students stated that DOPS had good acceptability among faculty and students in spite of no exposure to DOPS earlier. Students felt that this helps them in better skills learning and should cover other areas of the curriculum. The faculty, on the other hand, felt that training in observation and providing feedback would improve their effectiveness as assessors. Hoseini *et al.*<sup>[25]</sup> also reported high satisfaction scores with DOPS as compared to logbook documentation for practicing skills in midwifery students at University Hospitals Affiliated to Mashhad University of Medical Sciences, Iran. Similarly, Lagoo and Joshi<sup>[26]</sup> recently reported positive perceptions of postgraduate students as well as faculties in the Anaesthesia Department at St John's Medical College, Karnataka, regarding DOPS as an effective assessment and teaching-learning tool.

As for OSCE, Majumder *et al.*<sup>[27]</sup> in their study on students and examiners who participated for the MBBS exit OSCE held at the Cave Hill Campus, UWI, observed OSCE to be covering a wide range of clinical skills and knowledge as well as being a standardized examination for all students. Previously, Pierre *et al.*<sup>[28]</sup> in their cross-sectional survey on students during evaluation of child health clerkship received overwhelming response to OSCE as a fair and objective assessment method. Moreover, nursing students and lecturers at University of Hertfordshire perceive that principles of OSCE can also be used in a formative way to enhance skill acquisition.<sup>[29]</sup>

Pertaining to acquisition of knowledge and skills, Tsui *et al.*<sup>[30]</sup> concluded that clinicians can enhance clinical skills education in certain circumstances with strategic incorporation of tools like DOPS into medical student training programs. Similarly, randomized controlled trials carried out by Hengameh *et al.*<sup>[31]</sup> and Roghieh *et al.*<sup>[32]</sup> on undergraduate nursing trainees' performance reported a high educational impact of formative DOPS against routine assessment methods like subjective judgment of the assessor and logbook assessment. Even for OSCE, Lien *et al.*<sup>[33]</sup> and Pell *et al.*<sup>[34]</sup> reported a gradual but observable increase in the mean learning curve.

### Limitations

The method, direct observation with checklist, was used for the first time as a teaching method in the Department of Anatomy and it was not possible to have control group in order to avoid ethical issues or to prevent sharing of checklists amongst the students. A focused group

discussion is planned with the students to further explore the perceptions and views shared in this article.

### Conclusion

Direct observation with checklist is a method suitable for psychomotor skills in surface marking of anatomy. It can also be used as a teaching learning and assessment method to educate and empower students.

### Acknowledgments

The authors wish to thank Dr. Shital Patel, Assistant Professor, Department of Anatomy, Baroda Medical College, The Maharaja Sayajirao University, Vadodara, Gujarat, and Dr. Sumati, Professor and Head, Department of Anatomy, Pramukhswami Medical College, Bhaikaka University, Karamsad, Gujarat, for their review and valuable inputs in the validation of the Checklists.

### Financial support and sponsorship

Nil.

### Conflicts of interest

There are no conflicts of interest.

### References

1. Louw G, Eizenberg N, Carmichael SW. The place of anatomy in medical education: AMEE guide no 41. *Med Teach* 2009;31:373-86.
2. Sbayeh A, Qaedi Choo MA, Quane KA, Finucane P, McGrath D, O'Flynn S, *et al.* Relevance of anatomy to medical education and clinical practice: Perspectives of medical students, clinicians, and educators. *Perspect Med Educ* 2016;5:338-46.
3. Sugand K, Abrahams P, Khurana A. The anatomy of anatomy: A review for its modernization. *Anat Sci Educ* 2010;3:83-93.
4. Standring S. Evidence-based surface anatomy. *Clin Anat* 2012;25:813-5.
5. Azer SA. The place of surface anatomy in the medical literature and undergraduate anatomy textbooks. *Anat Sci Educ* 2013;6:415-32.
6. Medical Council of India. Competency based Undergraduate Curriculum for the Indian Medical Graduate. Vol. I. Dwarka, New Delhi: Medical Council of India; Available from: <https://www.nmc.org.in/wp-content/uploads/2020/01/UG-Curriculum-Vol-I.pdf>. [Last accessed on 2019 Mar 24].
7. Papa V, Vaccarezza M. Teaching anatomy in the XXI century: New aspects and pitfalls. *ScientificWorldJournal* 2013;2013:310348.
8. Naidoo N, Akhras A, Banerjee Y. Confronting the challenges of anatomy education in a competency-based medical curriculum during normal and unprecedented times (COVID-19 pandemic): Pedagogical framework development and implementation. *JMIR Med Educ* 2020;6:e21701.
9. Degani A, Wiener EL. Cockpit checklists: Concepts, design, and use. *Hum Factors* 1993;35:345-59.
10. Stufflebeam DL. Guidelines for Developing Evaluation Checklists: The Checklists Development Checklist (CDC). Available from: [https://wmich.edu/sites/default/files/attachments/u350/2014/guidelines\\_cdc.pdf](https://wmich.edu/sites/default/files/attachments/u350/2014/guidelines_cdc.pdf). [Last accessed on 2019 May 05].

11. Ahmady S, Khajeali N, Sharifi F, Mirmoghtadaei Z. Educational intervention to improve preclinical academic performance: A systematic review. *J Educ Health Promot* 2019;8:83.
12. Ismail S, Rahman NI, Mohamad N, Jusoh NM, Hood AI, Arif LA. Preference of teaching and learning methods in a new medical school of Malaysia. *J Appl Pharm Sci* 2014;4:48-55.
13. Archibong IA, Nja ME. Towards improved teaching effectiveness in Nigerian public universities: Instrument design and validation. *High Educ Stud* 2011;1:78-91.
14. Telio S, Ajjawi R, Regehr G. The “educational alliance” as a framework for reconceptualizing feedback in medical education. *Acad Med* 2015;90:609-14.
15. Weinstein DF. Feedback in clinical education: Untying the Gordian knot. *Acad Med* 2015;90:559-61.
16. Benenson RS, Pollack ML. Evaluation of emergency medicine resident death notification skills by direct observation. *Acad Emerg Med* 2003;10:219-23.
17. Dorfsman ML, Wolfson AB. Direct observation of residents in the emergency department: A structured educational program. *Acad Emerg Med* 2009;16:343-51.
18. Fischer T, Chenot JF, Simmenroth-Nayda A, Heinemann S, Kochen MM, Himmel W. Learning core clinical skills – A survey at 3 time points during medical education. *Med Teach* 2007;29:397-9.
19. Fitzgerald M, Mallory M, Mittiga M, Schubert C, Schwartz H, Gonzalez J, *et al*. Experience-based guidance for implementing a direct observation checklist in a pediatric emergency department setting. *J Grad Med Educ* 2012;4:521-4.
20. Martineau B, Mamede S, St-Onge C, Rikers RM, Schmidt HG. To observe or not to observe peers when learning physical examination skills; that is the question. *BMC Med Educ* 2013;13:55.
21. Zaidi Z, Jaffery T, Shahid A, Moin S, Gilani A, Burdick W. Change in action: Using positive deviance to improve student clinical performance. *Adv Health Sci Educ Theory Pract* 2012;17:95-105.
22. Kundra S, Singh T. Feasibility and acceptability of direct observation of procedural skills to improve procedural skills. *Indian Pediatr* 2014;51:59-60.
23. Brazeau C, Boyd L, Crosson J. Changing an existing OSCE to a teaching tool: The making of a teaching OSCE. *Acad Med* 2002;77:932.
24. Singh G, Kaur R, Mahajan A, Thomas AM, Singh T. Piloting direct observation of procedural skills in dental education in India. *Int J Appl Basic Med Res* 2017;7:239-42.
25. Hoseini BL, Mazloum SR, Jafarnejad F, Foroughipour M. Comparison of midwifery students’ satisfaction with direct observation of procedural skills and current methods in evaluation of procedural skills in Mashhad nursing and midwifery school. *Iran J Nurs Midwifery Res* 2013;18:94-100.
26. Lagoo JY, Joshi SB. Introduction of direct observation of procedural skills (DOPS) as a formative assessment tool during postgraduate training in anaesthesiology: Exploration of perceptions. *Indian J Anaesth* 2021;65:202-9.
27. Majumder MA, Kumar A, Krishnamurthy K, Ojeh N, Adams OP, Sa B. An evaluative study of objective structured clinical examination (OSCE): Students and examiners perspectives. *Adv Med Educ Pract* 2019;10:387-97.
28. Pierre RB, Wierenga A, Barton M, Branday JM, Christie CD. Student evaluation of an OSCE in paediatrics at the University of the West Indies, Jamaica. *BMC Med Educ* 2004;4:22.
29. Alinier G. Nursing students’ and lecturers’ perspectives of objective structured clinical examination incorporating simulation. *Nurse Educ Today* 2003;23:419-26.
30. Tsui K, Liu C, Lui J, Lee S, Tan R, Chang P. Direct observation of procedural skills to improve validity of students’ measurement of prostate volume in predicting treatment outcomes. *Urol Sci* 2013;24:84-8.
31. Hengameh H, Afsaneh R, Morteza K, Hosein M, Marjan SM, Abbas E. The effect of applying direct observation of procedural skills (DOPS) on nursing students’ clinical skills: A randomized clinical trial. *Glob J Health Sci* 2015;7:17-21.
32. Roghieh N, Fateme H, Hamid S, Hamid H. The effect of formative evaluation using “direct observation of procedural skills” (DOPS) method on the extent of learning practical skills among nursing students in the ICU. *Iran J Nurs Midwifery Res* 2013;18:290-3.
33. Lien HH, Hsu SF, Chen SC, Yeh JH. Can teaching hospitals use serial formative OSCEs to improve student performance? *BMC Res Notes* 2016;9:464.
34. Pell G, Fuller R, Homer M, Roberts T. Advancing the objective structured clinical examination: Sequential testing in theory and practice. *Med Educ* 2013;47:569-77.

# Vascular Foramina of Talus in North Indian Population: A Dry Bone Study

## Abstract

**Background:** The talus, which serves as a bony connection between the leg and foot, is the foundation of the medial longitudinal arch. Its main role is to stabilize the ankle joint through ligaments without any muscular attachments. Hence, the vessels are closely related to bony surfaces for the blood supply. The late consequence of talus fracture led to avascular necrosis (AVN). Knowing the vascular foramina can assist one in better comprehending the vascularity of the various talus surfaces. Hence, the knowledge of the distribution of nutrient foramina in the talus is helpful in assessing the jeopardy of damage to vessels during surgical interventions and the likelihood of AVN. **Aim and Objective:** The aim of this study was to describe the dispersion of foramina for vessels on the talus. In every aspect of the body and neck surfaces of the talus, the distribution of nutritional foramina was counted and macroscopically analyzed. **Materials and Methods:** A total of 600 human tali dry bone from the Anatomy Department's Osteology Laboratory at King George's Medical University in Lucknow, Uttar Pradesh served as the study's subject. By inserting a k wire of 0.5 mm diameter through each surface of the talus' neck and body and using a hand lens, the number and size of foramina for vessels on each surface were examined. **Results:** Medial, superior, lateral, and inferior surfaces of the talus' neck had vascular foramina. On observing the talus body, its medial, lateral, and posterior surfaces had foramina for vessels. In our research, we noted that most of the foramina for vessels were located on the inferior surface of the neck with a range of 2–24, which is more as compared to its lateral surface, and the majority were located on the medial surface of the body range of 1–15 which are more as compared to the lateral surface of the talus bone. Foramina of more than 0.5 mm in size accounted for 72.83%, with foramina indices ranging from 39.04% to 69.99% of the inferior surface of tali. **Conclusion:** The orthopedic, vascular, and podiatric surgeons must be aware of the location of vascular foramina while performing procedures on the hindfoot. Because there is less vascular foramina on the lateral approach compared to other surfaces, we believe this method would be more beneficial for surgical procedures on the talus.

**Keywords:** Avascular necrosis, neck and body of talus, talus, vascular foramina

**Akriti Anand,  
Arvind Kumar  
Pankaj,  
Rintu Biswas,  
Rakesh Kumar  
Verma,  
Punita Manik,  
Garima Sehgal**

*Department of Anatomy, King George's Medical University, Lucknow, Uttar Pradesh, India*

## Introduction

The talus is a tarsal bone (second biggest tarsal) in the human foot, which has a head, neck, and body. The articular surface present on the body and head of the talus articulates with the tibia, fibula, navicular, and calcaneus bones to form the supratalar, pretalar, and subtalar joints, respectively.<sup>[1]</sup> The blood supply of the talus is provided by multiple branches of extraosseous arteries, including the anterior tibial or dorsalis pedis, posterior tibial, and perforating fibular arteries that anastomose to form slings around the talus to form the periosteal network and intraosseous vasculature of the talus.<sup>[2]</sup> The sinus tarsi, which is situated on the plantar aspect of the talus neck and lies in anterior relation to

the posterior facets as well as posterior to the middle facet of the subtalar joint. The tarsal canal is a continuation in the medial aspect of the sinus tarsi, which allows the tarsal canal artery branch of the posterior tibial artery to pass through it.<sup>[3]</sup> The intraosseous blood supply of the talus gets its nourishment through several vascular foramina present on its different surfaces, which give pathways to the dorsalis pedis artery branches, the artery of the tarsal sinus for the head, and the anastomotic artery of the tarsal canal for the body.<sup>[4]</sup> The basic understanding of the presence of foramina for vascular supply on different surfaces of the talus provides arterial topography and may aid in risk assessment in talus surgical techniques and talar neck fractures like avascular necrosis (AVN), which is a more common complication.<sup>[5]</sup> The extent of involvement of the talus by

This is an open access journal, and articles are distributed under the terms of the Creative Commons Attribution-NonCommercial-ShareAlike 4.0 License, which allows others to remix, tweak, and build upon the work non-commercially, as long as appropriate credit is given and the new creations are licensed under the identical terms.

For reprints contact: WKHLRPMedknow\_reprints@wolterskluwer.com

**How to cite this article:** Anand A, Pankaj AK, Biswas R, Verma RK, Manik P, Sehgal G. Vascular foramina of talus in North Indian population: A dry bone study. *J Anat Soc India* 2023;72:321-5.

## Article Info

**Received:** 19 April 2023  
**Revised:** 03 December 2023  
**Accepted:** 11 December 2023  
**Available online:** 30 December 2023

## Address for correspondence:

*Prof. Arvind Kumar Pankaj,  
Department of Anatomy, King George's Medical University,  
Lucknow, Uttar Pradesh, India.  
E-mail: drarvindpankajcsmmu@yahoo.com*

## Access this article online

**Website:** <https://journals.lww.com/joi>

**DOI:** 10.4103/jasi.jasi\_40\_23

## Quick Response Code:



osteonecrosis is directly related to the degree of vascular disruption.<sup>[5,6]</sup> Determining the foramina for vessels may aid in the estimation of its dispersion over the various surfaces, as well as assessing the threat of vascular injury during surgical approaches and the possibility of talus AVN. Reference data pertaining to the distribution of talus vascular foramina in the North Indian population will be available in the present study.

## Materials and Methods

The present observational study of 600 human tali (right = 249 and left = 351) of unknown age and sex was carried out in the Department of Anatomy at King George Medical University, Lucknow, from April 2022 to September 2022. Ethical Clearance was obtained from the Institutional Ethics Committee, King George Medical University, Lucknow, through (Ref.code: 121 ECMIIA/P3). As far as could be ascertained, samples were free of physical and pathological changes or anomalies. All the 600 tali were numbered and photographed.

The presence of vessel impressions leading to foramina was identified as vascular foramina of the talus [Figure 1a]. Kruschner wire (k wire = 0.5 mm diameter) and hand lens were used to confirm the foramina patency, size, location, and number. The nonarticulating and articulating surfaces of the talus, including the body, head, and neck, were examined for vascular foramen. Vascular foramina is classified as either >0.5 mm or <0.5 mm in size by passing k wire.

The total length, farthest foramina, and nearest foramina of the talus were measured from the posterolateral tubercle on the inferior surface of the talus [Figure 1b]. The Lf1 was the nearest foramen distance measured from the posterolateral tubercle. Lf2 was the farthest foramen distance measured from the posterolateral tubercle, and Tol was the total length of the talus from the posterolateral tubercle to the head. The evaluation of the foraminal index was done by implying the formula  $Lf/Tol \times 100$ , where Lf is the foraminal distance measured from the posterolateral tubercle in each talus, i.e., Lf1 and Lf2. The foraminal index

of the farthest and nearest foramina represented Ff and Fn, respectively. The digital Vernier caliper was used for the measurements with a precision of 0.02 mm. Using SPSS version 26, the data were analyzed. Descriptive statistics were presented in the form of means, and frequencies were depicted as bar charts. The Wilcoxon rank-sum test was used to evaluate the number of foraminal openings on different surfaces of the talus and to compare the number of distributions with one another. Thereafter, interpretations were drawn from the analyzed data.  $P = 0.05$  demonstrated the statistical significance.

## Results

All over the nonarticular surfaces of 600 tali vascular foramina were examined. The articulating surfaces of the talus, for example, head and trochlear surface, were devoid of vascular foramina [Figure 1]. The nonarticulating aspect of the body of talus foramina was present on the posterior [Figure 2e and f], lateral, and medial [Figure 3g and i] surfaces. The talus's nonarticulating surface had foramina on the inferior, superior [Figure 1], lateral, and medial surfaces [Figure 3]. The count of foramina for vessels on the inferior side of the neck varied from 2 to 24, with a mean of 13.67, whereas the vascular foramina on the medial surface of the body ranged from 1 to 15, with a mean of 3.64. Calculating the total count of foramina in 600 tali revealed 8203 (52.49%) foramina on the inferior surface of the talus and 659 (4.21%) foramina on the lateral surface of the talus's neck [Table 1]. In 21.33% of cases, the lateral aspect of the talar neck was totally devoid of foramina for vessels.

The Wilcoxon rank-sum test was used to evaluate and compare the count of foramina present overall on the talar neck surfaces, which revealed that the inferior surface had significantly more than the superior ( $U = 87,094$ ;  $P = 0.001$ ), medial ( $U = 25,634$ ;  $P = 0.001$ ), and lateral ( $U = 4352$ ,  $P = 0.001$ ) surfaces [Table 1].

The minimum (least) and maximum (highest) numbers of foramina were present on the lateral and medial surfaces of the body, respectively. The total count of vascular

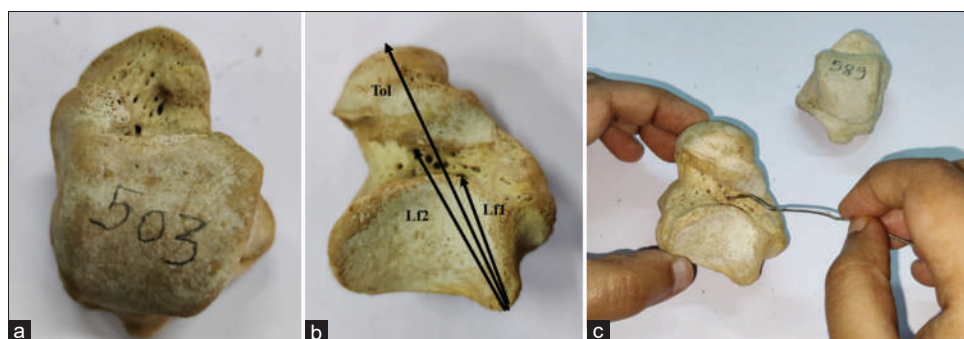


**Figure 1:** Illustrative images displaying the presence of foramina for vessels on different surfaces of the talus with (a), the neck's superior surface. (b), the measurements of: Lf1 – distance between the posterior tubercle and the nearby vascular foramina, Lf2 – distance between the posterior tubercle and the furthest foramina for vessels, Tol – total length of bony talus at the inferior surface of the right talus. (c), neck's inferior surface



**Figure 2:** Posterior surface (e and f) of the body of the talus with vascular foramina

foramina was 2185 (54.42%) and ranged from 1 to 15 on the medial surface of the talar body, with a mean of 3.64 showing a greater number as compared to the lateral (621) and posterior (1209) surfaces [Table 1]. Foramina were completely absent on the lateral and posterior surfaces of the talar body in 21.5% and 3.33% of bones, respectively. The total count of foramina found on the medial surface of the talar body was significantly greater than the number noted on the lateral ( $U = 20,294; P = 0.001$ ) and posterior ( $U = 73,937; P = 0.001$ ) surfaces [Table 1]. The superior and medial surfaces of the left-sided tali neck had the greatest count of foramina, with a mean of 7.54 and 4.36, respectively, compared to the right-sided tali, with a mean of 6.87 and 3.51 of the superior and medial aspects, respectively [Figure 4]. However, the Wilcoxon rank-sum test revealed a statistically significant difference in the aggregated count of foramina on the superior and medial surfaces of the neck among the right and left tali ( $U = 38,158.5, P = 0.008$  and  $U = 33,441.0, P = 0.001$ ). The lateral surface of the left-sided talus body had the highest count of foramina, with a mean of 0.9 as compared to the right talus with a mean of 1.23 [Table 2]. However, the Wilcoxon rank-sum test revealed a statistically significant difference in the foramina's total number on the lateral surface of the body between the right and left tali ( $U = 32,117.0, P = 0.001$ ).

Right and left tali had mean total lengths of  $55.57 \pm 29$  mm and  $56.45 \pm 3.99$  mm, respectively. Table 3 provides a summary of the foraminal indices measurements made on the inferior surface of the tali neck [Figure 1]. The mean Fn for left-sided tali was  $39.04\% \pm 6.3\%$ , whereas it was  $40.25\% \pm 6.55\%$  for right-sided tali, yet 351 (50%) left-sided tali had indices that range from 18.41% to 75.38%. The mean Ff for left-sided tali was  $66.34\% \pm 8.69\%$ , compared to  $69.99\% \pm 8.97\%$  for right-sided tali, whereas the majority of left-sided tali had an index ranging from 41.6% to 99.8%. The measurements of the distances and foraminal indices of the foramina for vessels between the right and left tali are listed in Table 3. There was no statistically significant difference between the left and right

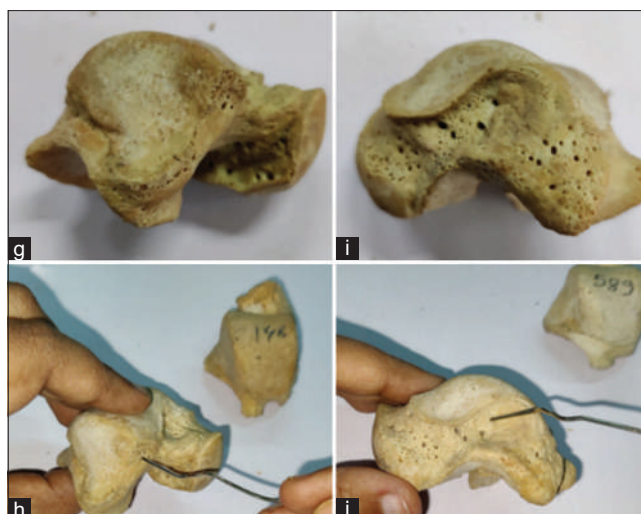


**Figure 3:** Illustrative images displaying vascular foramina on surfaces of talus with (g and h) lateral surface of body and neck. (i and j) Medial surface of body and neck

**Table 1: Dispersion of foramina for vessels on the body and neck surfaces of tali (n=600)**

|      |           | Vascular Foramina count |                   |       |                |
|------|-----------|-------------------------|-------------------|-------|----------------|
|      | Surface   | Minimum (least)         | Maximum (highest) | Mean  | Total (%)      |
| Neck | Superior  | 1                       | 18                | 7.27  | 4359 (27.89)*  |
|      | Inferior  | 2                       | 24                | 13.67 | 8203 (52.49)   |
|      | Medial    | 0                       | 12                | 4.01  | 2405 (15.39)** |
|      | Lateral   | 0                       | 5                 | 1.1   | 659 (4.21)***  |
| Body | Medial    | 1                       | 15                | 3.64  | 2185 (54.42)   |
|      | Lateral   | 0                       | 5                 | 1.04  | 621 (15.46)>   |
|      | Posterior | 0                       | 6                 | 2.02  | 1209 (30.11)>  |

\*Test of Wilcoxon Rank Sum  $U=87,094; P=0.001$  implies that there were statistically significantly more foramina on the neck's inferior surface than its superior surface, \*\*Test of Wilcoxon Rank Sum  $U=25,634; P=0.001$  implies that there were statistically significantly more foramina on the neck's inferior surface than its medial surface, \*\*\*Test of Wilcoxon Rank Sum  $U=4352, P=0.001$  implies that there were statistically significantly more foramina on the neck's inferior surface than its lateral surface, >Test of Wilcoxon Rank Sum  $U=20,294; P=0.001$  implies that there were statistically significantly more foramina on the body's medial surface than its lateral surface, >Test of Wilcoxon Rank Sum  $U=73,937; P=0.001$  implies that there were statistically significantly more foramina on the body's medial surface than its posterior surface

tali. There were 19,641 numbers of vascular foramina; out of the majority, 14,304 (72.83%) and 5337 (27.17%) foramina were more than 0.5 mm and <0.5 mm in size, respectively, on the body and neck of the talus.

## Discussion

The injury or fracture of the talus, which leads to AVN, has been a longtime concern for orthopedics.<sup>[7]</sup> In our study, the nonarticular surfaces of the talus had vascular foramina

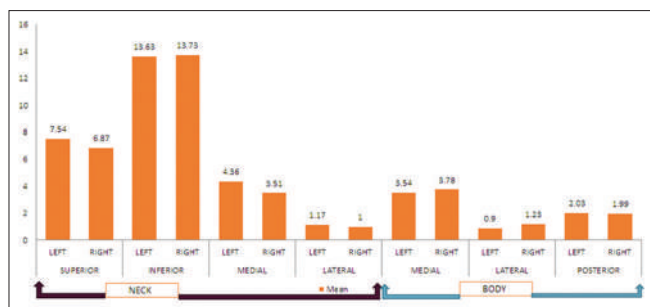


Figure 4: Bar graph showing mean value of the number of foramina present on neck and body based on laterality

with the impression of a groove for entering vessels, which was reported by Giebel *et al.*<sup>[8]</sup> and Vani *et al.* (2020)<sup>[9]</sup> in their studies.

Giebel *et al.*<sup>[8]</sup> reported the entering of vessels from the superior, inferior, medial, and lateral surfaces of the neck of the talus as well as the medial, lateral, and posterior surfaces of the body, which was also reported by Vani *et al.* (2020),<sup>[9]</sup> who observed the number of foramina on 56 talus bones. In the present study, we also observed a number of foramina on the nonarticulating surface of the neck and body of 600 talus. In this study, the mean distribution of the number of foramina for vessels on nonarticular surfaces of the neck, like the superior aspect, was 7.27 (range 1–18), inferiorly, 13.67 (range 2–24), medially, 4.01 (0–12), and laterally, 1.1 (range 0–5), which was slightly higher than those reported by Vani *et al.* (2020).<sup>[9]</sup>

The mean count of foramina for vessels on the medial surface of the body of the talus was 6 (range 2–16), reported by Vani *et al.* (2020),<sup>[9]</sup> which was greater than the present study, i.e., 3.64 (range 1–15), whereas the mean count of foramina on other surfaces in the present observations was 1.04 (range 0–5) on the lateral surface and 2.02 (range 0–6) on the medial surface, which were similar to those reported by Vani *et al.* (2020)<sup>[9]</sup> as 1 (0–7) for the lateral and 2 (0–7) for the medial surfaces.

Based on laterality Vani *et al.* (2020)<sup>[9]</sup> reported that the difference between the number of foramina on the right tali and the left tali was statistically relevant, which was found to be different in the present study. As we observed, the mean count of the number of foramina for vessels on the left talus of its superior surface was 7.54 (1–18) and the medial surface was 4.36 (0–12) greater than the right-sided talus of its superior surface, which was 6.87 (1–12) and the medial surface was 3.51 (0–9). Hence, according to laterality, there was statistical significance with  $P = 0.008$  and  $P < 0.001$  for the superior and medial surfaces of the talus neck, respectively.

In the previous study of Vani *et al.* (2020),<sup>[9]</sup> it was reported that within 56 dry tali, the foramina was absent on the medial aspect of the neck in 5.36% of bones and that 19.66%, 26.79%, and 30.36% of tali lacked foramina on

Table 2: Dispersion of foramina for vessels on the neck and body surface between left ( $n1=351$ ) and right ( $n2=249$ ) tali

| Vascular foramina count |           |                 |                   |      |                     |                     |
|-------------------------|-----------|-----------------|-------------------|------|---------------------|---------------------|
| Surface                 | Side      | Minimum (least) | Maximum (highest) | Mean | <i>P</i>            |                     |
| Neck                    | Superior  | Left            | 1                 | 18   | 7.54                | 0.008 <sup>^</sup>  |
|                         |           | Right           | 1                 | 12   | 6.87                |                     |
|                         | Inferior  | Left            | 2                 | 24   | 13.63               | 0.838               |
|                         |           | Right           | 2                 | 23   | 13.73               |                     |
| Medial                  | Left      | 0               | 12                | 4.36 | <0.001 <sup>^</sup> |                     |
|                         | Right     | 0               | 9                 | 3.51 |                     |                     |
| Lateral                 | Left      | 0               | 6                 | 1.17 | 0.092               |                     |
|                         | Right     | 0               | 5                 | 1    |                     |                     |
| Body                    | Medial    | Left            | 1                 | 12   | 3.54                | 0.476               |
|                         |           | Right           | 1                 | 15   | 3.78                |                     |
|                         | Lateral   | Left            | 0                 | 5    | 0.9                 | <0.001 <sup>^</sup> |
|                         |           | Right           | 0                 | 4    | 1.23                |                     |
|                         | Posterior | Left            | 0                 | 6    | 2.03                | 0.411               |
|                         |           | Right           | 0                 | 5    | 1.99                |                     |

<sup>^</sup>The Wilcoxon rank-sum test ( $P=0.008$ ,  $U=38,158.5$  and  $P=0.001$ ,  $U=33,441.0$ ) implies a statistically significant variation between the number of foramina on the superior and medial surface of the neck between the right and left tali, <sup>^</sup>The Wilcoxon rank-sum test ( $P=0.001$ ,  $U=32,117.0$ ) implies a statistically significant variation between the number of foramina on the body's lateral surface on the right and left tali. The disparities in rest among the right and left tali did not significantly vary

Table 3: Foramina for vessels on the inferior surface and their respective distances and foraminal indices of the left ( $n1=351$ ) and right ( $n2=249$ ) tali

|                       | Side  | Minimum (least) | Maximum (highest) | Mean±SD    | <i>P</i> |
|-----------------------|-------|-----------------|-------------------|------------|----------|
| Total length (mm)     | Left  | 40.2            | 64.9              | 56.45±3.99 | <0.001   |
|                       | Right | 48.3            | 63.4              | 55.57±2.9  |          |
| Neck-inferior surface |       |                 |                   |            |          |
| Lf1 (mm)              | Left  | 11.1            | 34.9              | 21.93±3.18 | 0.095    |
|                       | Right | 11.1            | 39.8              | 22.3±3.38  |          |
| Lf2 (mm)              | Left  | 24.5            | 51.3              | 37.29±4.35 | <0.001   |
|                       | Right | 22.6            | 48.9              | 38.74±4.09 |          |
| Fn (%)                | Left  | 18.41           | 75.38             | 39.04±6.3  | 0.017    |
|                       | Right | 18.41           | 73.98             | 40.25±6.55 |          |
| Ff (%)                | Left  | 41.6            | 95.49             | 66.34±8.69 | <0.001   |
|                       | Right | 42.01           | 99.8              | 69.99±8.97 |          |

SD: Standard deviation

the lateral surface of the body, the neck, and the posterior tubercle, respectively, which was slightly different in the present study. We observed the absence of foramina on the lateral surface of the neck in 21.33% and the lateral surface of the body in 21.5% of 600 dry tali. The present study depicted the absence of foramina on the medial surface of the neck in a very small number of bones (<0.008%) and on the posterior surface of the body in 3.33% of

bones. In our study, 72.83% of the total number of foramina were  $\geq 0.5$  mm, which was approximately similar to the previous study reported by Vani *et al.* (2020),<sup>[9]</sup> for orthopedic surgeons it is necessary information while performing bone graft preparation, congenital pseudoarthrosis, tumor resections, instrumentation, and fixation described by Haris (2021).<sup>[10]</sup> The previous study suggests that the arterial branches that give major blood supply to the talus come from posterior tibial vessels, including deltoid vessels, and tarsal canal vessels may be catastrophically damaged by the anteromedial or medial approach due to the existence of foramina on the superior and inferior surface necks, as well as on the medial surface of the talar body, as reported by Giebel *et al.*<sup>[8]</sup> The present study confirms that the absence of foramina on the lateral surface of the neck, lateral surface of the body, and posterior surface in 21.335%, 21.5%, and 3.33% implies that any surgical intervention through the lateral, anterolateral, and sometimes posterolateral aspects of the talus might cause a smaller degree of vascular injury. Hence, a lateral approach should be more preferable than a medial approach for talar surgeries, as reported by Giebel *et al.*<sup>[8]</sup>

We observed that the talus length mean was 56.45 mm and 55.57 mm on the left and right sides, respectively. This observation was similar to earlier research on the Indian population conducted by Motagi *et al.*,<sup>[11]</sup> Prasad and Rajasekhar,<sup>[12]</sup> and Vani *et al.* (2020).<sup>[9]</sup> The data gathered on the mean length could improve the design of the tools employed for invasive talus intervention or realignment. On the inferior aspect of the bone's neck, the nearest foramina of the left and right-sided tali had mean foraminal indices of 39.04%  $\pm$  6.3% and 40.25%  $\pm$  6.5%, respectively. The mean foraminal indices of the Ff on the inferior surface of the neck of the left and right tali were 66.34%  $\pm$  8.7% and 69.99%  $\pm$  8.97%, respectively, which was less than the previous study reported by Vani *et al.* (2020).<sup>[9]</sup> The measurement of the closest and farthest nutrient foramen from the proximal end is valuable for determining the overall length of the bone, which is significant in medicolegal and anthropological investigations. In addition, the foraminal index may be used to predict the prognosis of grafts, tumors, and bone fractures.<sup>[13]</sup> Understanding vascular foramina distribution and their foraminal indices could facilitate the development of surgical strategies to decrease the likelihood of iatrogenic causes of vascular damage.<sup>[12]</sup> According to Ibrahim,<sup>[14]</sup> there were many surgical techniques utilized to deal with fractures of the neck of the talus, including osteotomy from the anterior approach, either medial or lateral, whereas the present study was more in favor of proceeding from the lateral aspect of the talus bone. The gender-related gap and age were not taken into consideration, which is one of the study's limitations. The results of the current study may be useful for orthopedic, podiatric, and vascular surgeons doing procedures on the hindfoot.

## Conclusion

- The orthopedic, vascular, and podiatric surgeons must be aware of the location of foramina for vessels while performing procedures on the hindfoot because the incidence of AVN is usually associated with trauma to the neck and body of the talus
- During talus fixation or procedure, it was assumed that the surgeon should proceed with the talus by giving more priority to its lateral aspect of the body as well as the neck due to the lesser number of foramina noted after comparing it with other surfaces foramina for vascular supply.

## Financial support and sponsorship

Nil.

## Conflicts of interest

There are no conflicts of interest.

## References

1. Anthony VD, Tubbs RS. Ankle and foot. In: Strandring SG, editor. Gray's Anatomy: The Anatomical Basis of Clinical Practice. Vol. 41. Edinburgh: Elsevier Limited; 2016. p. 1423-4.
2. Mulfinger GL, Trueta J. The blood supply of the talus. *J Bone Joint Surg Br* 1970;52:160-7.
3. Prasam ML, Miller AN, Dyke JP, Helfet DL, Lorich DG. Arterial anatomy of the talus: A cadaver and gadolinium-enhanced MRI study. *Foot Ankle Int* 2010;31:987-93.
4. Bali N, Theivendran K, Prem H. Computed tomography review of tarsal canal anatomy with reference to the fitting of sinus tarsi implants in the tarsal canal. *J Foot Ankle Surg* 2013;52:714-6.
5. Cunningham M. The leg and foot. In: Cunningham's Manual of Practical Anatomy, Upper and Lower Limbs. Vol. 16. Oxford: Oxford University Press; 2017. p. 221.
6. Gelberman RH, Mortensen WW. The arterial anatomy of the talus. *Foot Ankle* 1983;4:64-72.
7. Fortin PT, Balazsy JE. Talus fractures: Evaluation and treatment. *J Am Acad Orthop Surg* 2001;9:114-27.
8. Giebel GD, Meyer C, Koebke J, Giebel G. The arterial supply of the ankle joint and its importance for the operative fracture treatment. *Surg Radiol Anat* 1997;19:231-5.
9. Vani PC, Arthi G, Jessy JP, Rani N, Jhahria SK. Vascular foramina of talus: An anatomical study with reference to surgical dissection. *Surg Radiol Anat* 2020;42:685-90.
10. Haris M, Baseer N, Haris S, Wazir NU, Deebea F. Topographic anatomy and clinical impact of vascular foramen on the trochlear groove of adult human dry femora. *Cureus* 2021;13:e19732.
11. Motagi M, Kottapurath S, Dharwadkar K. Morphometric analyses of human dry Tali of South Indian origin. *Int J Med Sci Public Health* 2014;4:237.
12. Prasad SA, Rajasekhar SS. Morphometric analysis of talus and calcaneus. *Surg Radiol Anat* 2019;41:9-24.
13. Ambekar SA, Sukre SB. Diaphyseal nutrient foramen of lower limb long bones: Variations and importance. *Int J Anat Res* 2016;4:2684-8.
14. Rao SP, Ibrahim MS, Chahal G, Crow R, Ramos J. Talar neck fractures: an overview. *J Nov Physiother Phys Rehabil* 2014;1:013-8.

# Gender and Height Estimation from Hand and Handprint Sizes in the Turkish Population

## Abstract

**Introduction:** In forensic medicine, it becomes impossible to identify corpses in events that affect a large part of the population, such as natural disasters, accidents, and wars. The aim of this study is to determine the height and gender of the Turkish population with hand and handprint morphometric measurements. **Materials and Methods:** The sample size of the study consists of 600 Turkish population aged between 18 and 58 years (mean  $\pm$  standard deviation:  $22.18 \pm 5.43$ ) living in Middle Anatolia. In the morphometric measurements of the hand, 21 anthropometric measurements were taken from each volunteer. **Results:** It was determined that men had higher values than women in all hand and handprint measurements and were statistically significant. When the correlation between hand and handprint measurements and stature was examined, it was determined that hand length and handprint length had the highest correlation with height in both genders (male:  $r: 0.57$ ,  $r: 0.62$ ; female:  $r: 0.49$ ,  $r: 0.50$ ). When comparing the bilateral asymmetry of the right and left hands of both sexes, it was observed that there was a statistically significant difference between the lengths of the thumb distal phalanx, little finger proximal, and middle phalanx in men and between the lengths of the index finger distal phalanx, middle finger middle and distal phalanx, and ring finger distal phalanx in women ( $P < 0.05$ ). **Conclusion:** As a result, it was seen that the use of hand and handprint measurements to determine height and gender in the Turkish population gave high results.

**Keywords:** Forensic medicine, hand and handprints, sex estimation, height estimation, Turkish population

## Introduction

In disasters that affect the whole society such as natural disasters, terrorist incidents, accidents, and war, the identification, which is the most comprehensive subject of forensic medicine, and the usage of related techniques are increasing and becoming more significant.<sup>[1]</sup> Cases such as dismemberment or incineration of a dead body make it impossible to identify the body. It is, therefore, important to develop methods to accurately estimate the physical characteristics and gender of individuals. Height can be determined by combinations of the skull, vertebrae, pelvis, lower limbs, hand, and each part of the body. In cases where gender and height cannot be determined, it can be analyzed by morphometric measurements of reference anatomical structures on bodies with intact anatomical structures.<sup>[2,3]</sup>

When the literature is examined, it is observed that morphometric measurements

This is an open access journal, and articles are distributed under the terms of the Creative Commons Attribution-NonCommercial-ShareAlike 4.0 License, which allows others to remix, tweak, and build upon the work non-commercially, as long as appropriate credit is given and the new creations are licensed under the identical terms.

For reprints contact: WKHLRPMedknow\_reprints@wolterskluwer.com

of the hands and feet were used to determine gender in a number of studies from the 19<sup>th</sup> century to the 21<sup>st</sup> century.<sup>[2,4-6]</sup> The related earliest studies were conducted by Ecker in 1875. In his studies, Ecker revealed that the 2<sup>nd</sup> and 4<sup>th</sup> finger length ratio of the hand varies according to gender.<sup>[7]</sup> In 1952, Phelps revealed that there was some similarity in finger ratios between the genders, but he also noted that there were differences between men and women. In this regard, he found that while the ratio of the length of the 2<sup>nd</sup> finger to the length of the 4<sup>th</sup> finger was approximately 1.00 in women, this ratio was considerably lower in men.<sup>[8]</sup> In addition, Case and Ross stated in 2007 that phalanx lengths give better outcomes than ossa metatarsi and ossa metacarpi lengths in gender determination from hand and foot bones.<sup>[5]</sup>

Ishak *et al.* have recently addressed the lack of research examining the accuracy of gender and height determination using hand size.<sup>[9]</sup>

Since anthropometric hand measurements in forensic anthropology are a newer method

**How to cite this article:** Keleş H, Çınaroğlu S, Çiçek F, Ceranoğlu FG, Tekeli M. Gender and height estimation from hand and handprint sizes in the Turkish population. *J Anat Soc India* 2023;72:326-33.

Haci Keleş,  
Selim Çınaroğlu,  
Fatih Çiçek,  
Faruk Gazi Ceranoğlu,  
Mustafa Tekeli

Department of Anatomy, Faculty of Medicine, Niğde Ömer Halisdemir University, Niğde, Türkiye

## Article Info

Received: 16 November 2022

Revised: 11 August 2023

Accepted: 26 November 2023

Available online: 30 December 2023

## Address for correspondence:

Dr. Haci Keleş,  
Department of Anatomy, Faculty of Medicine, Niğde Ömer Halisdemir University, Central Campus, On Bor Road, 51240 Center, Niğde, Türkiye.  
E-mail: hacikeles@ohu.edu.tr

## Access this article online

Website: <https://journals.lww.com/joai>

DOI:  
10.4103/jasi.jasi\_159\_22

## Quick Response Code:



for determining gender estimation, it is essential to make measurements using statistical methods in the population to be implemented to prove reliability and accuracy. Previous studies have revealed that morphometric characteristics of body measurements have distinctive features according to race due to the influence of genetic and environmental factors. For this reason, the morphometric values of any measurements derived for one race cannot be used for different races.<sup>[3,10]</sup>

Therefore, the aim of this study is to evaluate the hand and handprint morphometric measurements and to determine the gender and height of the Middle Anatolia Turkish population, which are not available in the existing literature.

## Materials and Methods

### The design of the study

This study was approved by the Ethics Committee of Niğde Ömer Halisdemir University Non-Interventional Clinical Research Ethics Committee with decision number 2021/87. The sample size of the study consisted of 600 Turkish individuals aged between 18 and 58 years (mean  $\pm$  standard deviation: 22.18  $\pm$  5.43) living in Middle Anatolia. Exclusion criteria for this study included pregnancy and the presence of any injury that would affect the morphometric properties of the hand and neck, disease, and developmental disorder. The volunteers participating in the study were informed before the measurement and asked to sign a consent form. The volunteers were not pressured to participate in the study by any means. All data were annihilated at the end of the study to ensure the confidentiality of the data obtained.

### Morphometric measurements of height and hand

In the study, the height of each volunteer was measured in cm with a stadiometer while the volunteers were standing upright with their heels joined together and their arms next to their thighs. In hand morphometric measurements, 21 anthropometric measurements were obtained from each

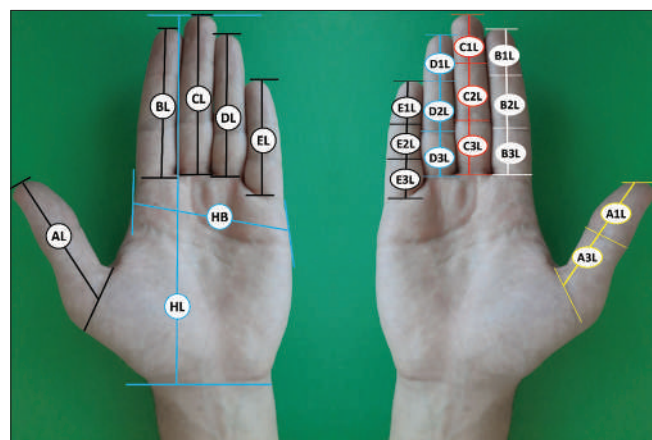


Figure 1: Hand morphometric measurements. HL: Hand length, HB: Hand breadth, AL: 1<sup>st</sup> finger length, BL: 2<sup>nd</sup> finger length, CL: 3<sup>rd</sup> finger length, DL: 4<sup>th</sup> finger length, EL: 5<sup>th</sup> finger length

volunteer [Table 1 and Figure 1]. Measurements were made bilaterally using calipers and a ruler when necessary. For handprint anthropometric measurements, a disposable plain acetate paper was used for each volunteer. Black finger paint, which washes off quickly when washed in water, was implemented evenly on the acetate paper with a paint roller. The volunteer was then instructed to place his/her hands on the finger-painted acetate paper and then place his/her hands on a plain white A4 paper. Two anthropometric measurements were carried out on the handprints obtained: handprint length (HPL) and handprint width [Figure 2]. At the end of the measurement, the papers with handprints were destroyed. All measurements were performed between 11:00 and 17:00 as a standard since height and hand morphometric characteristics change during the day and after sleep.

### Statistical analysis

The data obtained in the study were analyzed with the SPSS (software version 23.0, IBM, SPSS Inc, Chicago, IL, USA) statistical data package program (SPSS 23.0 evaluation version for Windows, Trial Version). Descriptive statistical values of all parameters were revealed. A paired sample *t*-test was performed to compare the differences between bilateral asymmetry and hand and handprints, and an independent samples *t*-test was performed to compare the measurements between male and female individuals. The Pearson correlation test was employed to examine the correlation between height and hand and handprint measurements. Discrimination analysis was carried out to evaluate gender estimation from hand and handprint measurements.

## Results

### Descriptive statistics, bilateral asymmetry, and comparison of measurements between hand and handprint

When the findings of the study were analyzed, it was observed that it was statistically significant ( $P < 0.05$ )

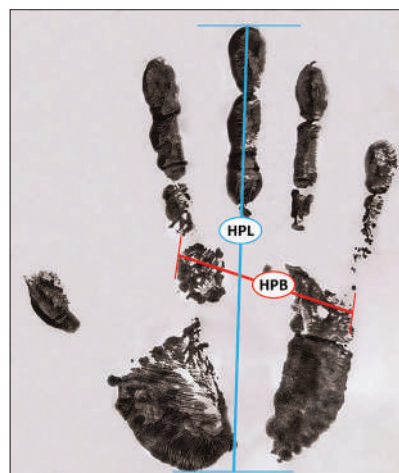


Figure 2: Handprint length and breadth measurement. HPL: Handprint length, HPB: Handprint breadth

that the height of males (mean  $\pm$  standard deviation: 178.10  $\pm$  5.12) was longer than the height of females (mean  $\pm$  standard deviation: 163.37  $\pm$  5.98). The results of hand and handprint measurements for both genders for both right and left hands are presented in Table 2. In Table 2, it was statistically significant ( $P < 0.05$ ) that all values of hand and handprint measurements for both sides were larger in the male gender than in the female gender [Table 2]. The relationship between height and

hand and handprint measurements is presented in Table 3. Table 3 indicates that there are statistically significant correlations between hand and handprint measurements and height ( $P < 0.05$ ) [Table 3]. When the correlation coefficient values were examined, it was noticed that the highest correlation with height was observed between hand length (HL) ( $r: 0.57, r: 0.62$ ) and HPL ( $r: 0.49, r: 0.50$ ) in men and women [Table 3]. The comparison of right and left hands in terms of bilateral asymmetry in both genders

**Table 1: Hand and handprint measurements and explanations**

| Measurement   | Explanations   |
|---|--|
| HL  | The most distal point of the 3 <sup>rd</sup> finger and the distal wrist line (measured in cm)   |
| HB  | The most lateral point of the 2 <sup>nd</sup> metacarpal bone and the most medial point of the 5 <sup>th</sup> metacarpal bone (measured in cm)  |
| AL, BL, CL, DL, EL (finger lengths)                             | The distance between the proximal flexion folds of the fingers and their most distal points (measured in mm)   |
| A1L, B1L, C1L, D1L, E1L (distal phalanx lengths of the fingers) | The distance between the most distal points of the fingers and the distalis fold of the interphalangeal joint (measured in mm)   |
| B2L, C2L, D2L, E2L (middle phalanx lengths of fingers)          | The distance between the distal interphalangeal joint fold and the proximal interphalangeal joint fold (measured in mm)  |
| A3L, B3L, C3L, D3L, E3L (proximal phalanx lengths of fingers)   | The distance between the proximal interphalangeal joint fold and the metacarpophalangeal joint fold (measured in mm)   |
| HPL   | The distance between the most proximal border of the palm and the most distal point of the 3 <sup>rd</sup> finger in the handprint (measured in mm)  |
| HPB   | The distance between the trace of the most lateral point of the extremitas distalis of the os metacarpale II and the most medial point of the extremitas distalis of the os metacarpale V (measured in mm) |

HL: Hand length, HB: Hand breadth, HPL: Handprint length, HPB: Handprint breadth

**Table 2: Comparison of right and left hand and handprint measurements for both genders**

| Measurement | Right hand, mean $\pm$ SD |                  | P      | Left hand, mean $\pm$ SD |                  | P      |
|-------------|---------------------------|------------------|--------|--------------------------|------------------|--------|
|             | Male (n=260)              | Female (n=340)   |        | Male (n=260)             | Female (n=340)   |        |
| HL          | 18.93 $\pm$ 0.98          | 17.19 $\pm$ 0.83 | <0.001 | 18.96 $\pm$ 0.95         | 17.23 $\pm$ 0.87 | <0.001 |
| HB          | 8.62 $\pm$ 0.60           | 7.55 $\pm$ 0.37  | <0.001 | 9.03 $\pm$ 5.84          | 7.90 $\pm$ 4.74  | <0.001 |
| AL          | 67.94 $\pm$ 5.40          | 61.17 $\pm$ 5.15 | <0.001 | 67.50 $\pm$ 5.32         | 61.11 $\pm$ 4.98 | <0.001 |
| A1L         | 33.49 $\pm$ 3.33          | 29.40 $\pm$ 2.77 | <0.001 | 32.83 $\pm$ 3.13         | 29.06 $\pm$ 2.64 | <0.001 |
| A3L         | 34.11 $\pm$ 5.31          | 31.79 $\pm$ 4.56 | <0.001 | 34.72 $\pm$ 5.22         | 32.28 $\pm$ 4.42 | <0.001 |
| BL          | 71.74 $\pm$ 5.32          | 66.92 $\pm$ 4.43 | <0.001 | 72.26 $\pm$ 5.13         | 67.23 $\pm$ 4.64 | <0.001 |
| B1L         | 25.72 $\pm$ 2.17          | 24.02 $\pm$ 1.98 | <0.001 | 25.74 $\pm$ 2.22         | 23.62 $\pm$ 1.88 | <0.001 |
| B2L         | 22.91 $\pm$ 2.26          | 21.34 $\pm$ 2.21 | <0.001 | 22.62 $\pm$ 2.29         | 21.18 $\pm$ 2.33 | <0.001 |
| B3L         | 23.85 $\pm$ 2.82          | 22.54 $\pm$ 2.29 | <0.001 | 23.95 $\pm$ 2.89         | 22.52 $\pm$ 2.44 | <0.001 |
| CL          | 78.28 $\pm$ 5.17          | 72.28 $\pm$ 4.59 | <0.001 | 78.08 $\pm$ 5.40         | 72.47 $\pm$ 4.27 | <0.001 |
| C1L         | 26.39 $\pm$ 2.58          | 24.38 $\pm$ 1.96 | <0.001 | 26.57 $\pm$ 2.50         | 24.02 $\pm$ 2.23 | <0.001 |
| C2L         | 25.43 $\pm$ 2.74          | 23.84 $\pm$ 2.16 | <0.001 | 25.91 $\pm$ 3.62         | 23.37 $\pm$ 2.49 | <0.001 |
| C3L         | 25.73 $\pm$ 2.72          | 24.34 $\pm$ 2.79 | <0.001 | 25.47 $\pm$ 2.93         | 24.08 $\pm$ 2.72 | <0.001 |
| DL          | 71.81 $\pm$ 5.37          | 66.07 $\pm$ 4.44 | <0.001 | 72.04 $\pm$ 5.00         | 66.44 $\pm$ 4.42 | <0.001 |
| D1L         | 26.22 $\pm$ 2.42          | 24.27 $\pm$ 2.01 | <0.001 | 26.09 $\pm$ 2.46         | 23.59 $\pm$ 2.17 | <0.001 |
| D2L         | 23.58 $\pm$ 2.60          | 22.08 $\pm$ 2.41 | <0.001 | 23.52 $\pm$ 2.26         | 21.84 $\pm$ 2.26 | <0.001 |
| D3L         | 22.23 $\pm$ 2.59          | 21.13 $\pm$ 2.45 | <0.001 | 22.41 $\pm$ 2.67         | 21.11 $\pm$ 2.71 | <0.001 |
| EL          | 59.38 $\pm$ 4.61          | 55 $\pm$ 4.51    | <0.001 | 59.44 $\pm$ 4.44         | 54.68 $\pm$ 3.87 | <0.001 |
| E1L         | 23.68 $\pm$ 2.38          | 21.98 $\pm$ 1.94 | <0.001 | 23.40 $\pm$ 2.26         | 21.86 $\pm$ 2.04 | <0.001 |
| E2L         | 17.64 $\pm$ 2.46          | 16.47 $\pm$ 2.38 | <0.001 | 18.19 $\pm$ 2.46         | 16.45 $\pm$ 2.27 | <0.001 |
| E3L         | 18.44 $\pm$ 2.75          | 17.11 $\pm$ 2.13 | <0.001 | 17.74 $\pm$ 2.54         | 16.86 $\pm$ 2.37 | <0.001 |
| HPL         | 17.35 $\pm$ 0.93          | 15.80 $\pm$ 0.92 | <0.001 | 17.32 $\pm$ 0.92         | 15.84 $\pm$ 0.89 | <0.001 |
| HPB         | 7.05 $\pm$ 0.58           | 6.41 $\pm$ 0.46  | <0.001 | 7.02 $\pm$ 0.53          | 6.37 $\pm$ 0.49  | <0.001 |

SD: Standard deviation, HL: Hand length, HB: Hand breadth, HPL: Handprint length, HPB: Handprint breadth

**Table 3: Correlation between stature and hand and handprint measurements**

| Measurement | Male (n=260) |      |      |            |      |      | Female (n=340) |      |      |            |      |      |
|-------------|--------------|------|------|------------|------|------|----------------|------|------|------------|------|------|
|             | Right        |      |      | Left       |      |      | Right          |      |      | Left       |      |      |
|             | Mean±SD      | r    | P    | Mean±SD    | r    | P    | Mean±SD        | r    | P    | Mean±SD    | r    | P    |
| HL          | 18.93±0.98   | 0.57 | 0.00 | 18.96±0.95 | 0.55 | 0.00 | 17.19±0.83     | 0.57 | 0.00 | 17.23±0.87 | 0.62 | 0.00 |
| HB          | 8.62±0.60    | 0.33 | 0.00 | 9.03±5.84  | 0.01 | 0.86 | 7.55±0.37      | 0.30 | 0.00 | 7.90±4.74  | 0.11 | 0.41 |
| AL          | 67.94±5.40   | 0.22 | 0.00 | 67.50±5.32 | 0.33 | 0.00 | 61.17±5.15     | 0.20 | 0.00 | 61.11±4.98 | 0.24 | 0.00 |
| A1L         | 33.49±3.33   | 0.29 | 0.00 | 32.83±3.13 | 0.13 | 0.26 | 29.40±2.77     | 0.29 | 0.00 | 29.06±2.64 | 0.28 | 0.00 |
| A3L         | 34.11±5.31   | 0.24 | 0.00 | 34.72±5.22 | 0.20 | 0.01 | 31.79±4.56     | 0.05 | 0.29 | 32.28±4.42 | 0.07 | 0.20 |
| BL          | 71.74±5.32   | 0.39 | 0.00 | 72.26±5.13 | 0.35 | 0.00 | 66.92±4.43     | 0.41 | 0.00 | 67.23±4.64 | 0.35 | 0.00 |
| B1L         | 25.72±2.17   | 0.30 | 0.00 | 25.74±2.22 | 0.25 | 0.00 | 24.02±1.98     | 0.25 | 0.00 | 23.62±1.88 | 0.26 | 0.00 |
| B2L         | 22.91±2.26   | 0.31 | 0.00 | 22.62±2.29 | 0.19 | 0.01 | 21.34±2.21     | 0.20 | 0.00 | 21.18±2.33 | 0.30 | 0.00 |
| B3L         | 23.85±2.82   | 0.27 | 0.00 | 23.95±2.89 | 0.18 | 0.03 | 22.54±2.29     | 0.17 | 0.02 | 22.52±2.44 | 0.24 | 0.00 |
| CL          | 78.28±5.17   | 0.47 | 0.00 | 78.08±5.40 | 0.30 | 0.00 | 72.28±4.59     | 0.45 | 0.00 | 72.47±4.27 | 0.48 | 0.00 |
| C1L         | 26.39±2.58   | 0.30 | 0.00 | 26.57±2.50 | 0.27 | 0.00 | 24.38±1.96     | 0.29 | 0.00 | 24.02±2.23 | 0.36 | 0.00 |
| C2L         | 25.43±2.74   | 0.31 | 0.00 | 25.91±3.62 | 0.23 | 0.00 | 23.84±2.16     | 0.22 | 0.00 | 23.37±2.49 | 0.20 | 0.00 |
| C3L         | 25.73±2.72   | 0.31 | 0.00 | 25.47±2.93 | 0.10 | 0.81 | 24.34±2.79     | 0.24 | 0.00 | 24.08±2.72 | 0.16 | 0.02 |
| DL          | 71.81±5.37   | 0.38 | 0.00 | 72.04±5.00 | 0.31 | 0.00 | 66.07±4.44     | 0.40 | 0.00 | 66.44±4.42 | 0.35 | 0.00 |
| D1L         | 26.22±2.42   | 0.28 | 0.00 | 26.09±2.46 | 0.34 | 0.00 | 24.27±2.01     | 0.26 | 0.00 | 23.59±2.17 | 0.24 | 0.00 |
| D2L         | 23.58±2.60   | 0.27 | 0.00 | 23.52±2.26 | 0.21 | 0.00 | 22.08±2.41     | 0.29 | 0.00 | 21.84±2.26 | 0.31 | 0.00 |
| D3L         | 22.23±2.59   | 0.26 | 0.00 | 22.41±2.67 | 0.19 | 0.02 | 21.13±2.45     | 0.24 | 0.00 | 21.11±2.71 | 0.29 | 0.00 |
| EL          | 59.38±4.61   | 0.36 | 0.00 | 59.44±4.44 | 0.35 | 0.00 | 55±4.51        | 0.26 | 0.00 | 54.68±3.87 | 0.30 | 0.00 |
| E1L         | 23.68±2.38   | 0.23 | 0.00 | 23.40±2.26 | 0.14 | 0.16 | 21.98±1.94     | 0.22 | 0.00 | 21.86±2.04 | 0.15 | 0.05 |
| E2L         | 17.64±2.46   | 0.35 | 0.00 | 18.19±2.46 | 0.30 | 0.00 | 16.47±2.38     | 0.34 | 0.00 | 16.45±2.27 | 0.23 | 0.00 |
| E3L         | 18.44±2.75   | 0.24 | 0.00 | 17.74±2.54 | 0.29 | 0.00 | 17.11±2.13     | 0.27 | 0.00 | 16.86±2.37 | 0.24 | 0.00 |
| HPL         | 17.35±0.93   | 0.41 | 0.00 | 17.32±0.92 | 0.49 | 0.00 | 15.80±0.92     | 0.50 | 0.00 | 15.84±0.89 | 0.48 | 0.00 |
| HPB         | 7.05±0.58    | 0.31 | 0.00 | 7.02±0.53  | 0.34 | 0.00 | 6.41±0.46      | 0.25 | 0.00 | 6.37±0.49  | 0.24 | 0.00 |

SD: Standard deviation, HL: Hand length, HB: Hand breadth, HPL: Handprint length, HPB: Handprint breadth

**Table 4: Comparison of hand and handprint measurements in terms of bilateral asymmetry in both genders**

| Measurement | Male (n=260), mean±SD |            | P     | Female (n=340), mean±SD |            | P       |
|-------------|-----------------------|------------|-------|-------------------------|------------|---------|
|             | Right hand            | Left hand  |       | Right hand              | Left hand  |         |
| HL          | 18.93±0.98            | 18.96±0.95 | 0.742 | 17.19±0.83              | 17.23±0.87 | 0.543   |
| HB          | 8.62±0.60             | 9.03±5.84  | 0.256 | 7.55±0.37               | 7.90±4.74  | 0.184   |
| AL          | 67.94±5.40            | 67.50±5.32 | 0.352 | 61.17±5.15              | 61.11±4.98 | 0.893   |
| A1L         | 33.49±3.33            | 32.83±3.13 | 0.022 | 29.40±2.77              | 29.06±2.64 | 0.096   |
| A3L         | 34.11±5.31            | 34.72±5.22 | 0.186 | 31.79±4.56              | 32.28±4.42 | 0.155   |
| BL          | 71.74±5.32            | 72.26±5.13 | 0.251 | 66.92±4.43              | 67.23±4.64 | 0.365   |
| B1L         | 25.70±2.17            | 25.74±2.22 | 0.861 | 24.02±1.98              | 23.62±1.88 | 0.008   |
| B2L         | 22.91±2.26            | 22.62±2.29 | 0.150 | 21.34±2.21              | 21.18±2.33 | 0.364   |
| B3L         | 28.85±2.82            | 23.95±2.89 | 0.683 | 22.54±2.29              | 22.52±2.44 | 0.919   |
| CL          | 78.28±5.17            | 78.08±5.40 | 0.660 | 72.28±4.59              | 72.47±4.27 | 0.572   |
| C1L         | 26.39±2.58            | 26.57±2.50 | 0.404 | 24.38±1.96              | 24.02±2.23 | 0.026   |
| C2L         | 25.43±2.74            | 25.91±3.62 | 0.086 | 23.84±2.16              | 23.37±2.49 | 0.009   |
| C3L         | 25.73±2.72            | 25.47±2.93 | 0.290 | 24.34±2.79              | 24.08±2.72 | 0.224   |
| DL          | 71.81±5.37            | 72.04±5    | 0.615 | 66.07±4.44              | 66.44±4.42 | 0.284   |
| D1L         | 26.22±2.42            | 26.09±2.46 | 0.535 | 24.27±2.01              | 23.59±2.17 | P<0.001 |
| D2L         | 23.58±2.60            | 23.52±2.26 | 0.782 | 22.08±2.41              | 21.84±2.26 | 0.186   |
| D3L         | 22.23±2.59            | 22.41±2.67 | 0.458 | 21.13±2.45              | 21.11±2.71 | 0.916   |
| EL          | 59.38±4.61            | 59.44±4.44 | 0.876 | 55±4.51                 | 54.68±3.87 | 0.319   |
| E1L         | 23.68±2.38            | 23.40±2.26 | 0.178 | 21.98±1.94              | 21.86±2.04 | 0.444   |
| E2L         | 17.64±2.46            | 18.19±2.46 | 0.011 | 16.47±2.38              | 16.45±2.27 | 0.921   |
| E3L         | 18.44±2.75            | 17.74±2.54 | 0.003 | 17.11±2.13              | 16.86±2.37 | 0.154   |
| HPL         | 17.35±0.93            | 17.32±0.92 | 0.721 | 15.80±0.92              | 15.84±0.89 | 0.613   |
| HPB         | 7.05±0.58             | 7.02±0.53  | 0.446 | 6.41±0.46               | 6.37±0.49  | 0.316   |

SD: Standard deviation, HL: Hand length, HB: Hand breadth, HPL: Handprint length, HPB: Handprint breadth

is demonstrated in Table 4. Table 4 reveals that there is a statistically significant difference between the lengths of the distal phalanges of the thumb and the proximal and middle phalanges of the pinkie finger in males and between the distal phalanges of the index finger, middle and distal phalanges of the middle finger, and the distal phalanges of the ring finger in females ( $P < 0.05$ ) [Table 4]. There was no statistically significant difference between the length and width of the handprint between the right and left hands in both genders ( $P > 0.05$ ) [Table 4]. The comparison of the length and width values between the right and left hand and handprint for both genders is listed in Table 5. Table 5 shows that there was a significant difference between hand and HPL in terms of HL on both the right and left sides in males ( $P < 0.05$ ), while there was a significant difference in hand and handprint width on the right side in terms of hand width ( $P < 0.05$ ), while there was no significant difference on the left side ( $P > 0.05$ ) [Table 5]. In women, a statistically significant difference was observed between hand and HPL and width in terms of HL and hand width on both the right and left sides ( $P < 0.05$ ).

### Simple linear regression

The standard error of estimate (SEE) and linear regression formulas for height estimation from hand and handprint measurements are presented in Table 6. When Table 6 is evaluated, the standard error of prediction for both left and right hand and handprint measurements was higher in females than in males (Left-hand male: 4.26–5.12; left-hand female: 4.64–5.92; right-hand male: 4.21–5.01; right-hand female: 4.90–6.04) [Table 6].

### Discrimination analysis

The metrics useful for gender estimation and their demarcation values are provided in Table 7. Demarking point values are calculated using the average of the relevant measurements for both males and females and represent the range above which an individual is classified as male and below which an individual is classified as female. Table 7 illustrates that height (92.7%), HL (83%), and HPL (80.2%) are the measurements that give the highest accuracy of gender classification.

## Discussion

Gender is the most important factor in identifying the body. Many physical characteristics such as height and weight depend on gender. Studies have found that the morphometric characteristics of body measurements have distinctive features according to race under the influence of genetic and environmental factors. In general, the morphometric value of anybody measurement derived for one race is not applied to different races. Therefore, in this study, it was aimed to estimate gender and height from hand and handprint dimensions in the Turkish population. When the results of the study were evaluated, it was statistically significant that males had higher values than females in all hand and handprint measurements. When the correlation between hand and handprint measurements and height was analyzed, it was determined that HL and HPL had the highest correlation with height in both genders (male:  $r: 0.57$ ,  $r: 0.62$ ; female:  $r: 0.49$ ,  $r: 0.50$ ). In the comparison of the right and left hand in terms of bilateral asymmetry in both genders, there was a statistically significant difference between the lengths of the distal phalanx of the thumb, proximal and middle phalanx of the little finger in males, and between the distal phalanx of the index finger, middle and distal phalanx of the middle finger, and distal phalanx of the ring finger in females ( $P < 0.05$ ). When the discrimination analysis for gender prediction from hand and handprint dimensions was analyzed, it was concluded that the measurements that gave the highest accuracy of gender classification were height (92.7%), HL (83%), and HPL (80.2%).

When the studies conducted on different populations in the literature were examined, it was observed that there was a significant difference in hand and handprint measurements on both right and left sides in both genders<sup>[11-13]</sup> and that hand and handprint measurements were higher in men than in women.<sup>[9,12,14-18]</sup> In the results of our study [Table 1], a significant difference was detected in all hand and handprint measurements between men and women, and it was statistically significant that all measurements were higher in men than in women ( $P < 0.05$ ).

When bilateral asymmetry in hand and handprint measurements in both genders is examined, it was observed that some studies in the literature did not

**Table 5: Comparison of hand and handprint measurements in both genders in terms of right and left sides**

| Measurement    | Right hand, mean±SD |           | P      | r    | Left hand, mean±SD |        | P      | r    |
|----------------|---------------------|-----------|--------|------|--------------------|--------|--------|------|
|                | Hand                | Handprint |        |      | El                 | El izi |        |      |
| Male (n=260)   |                     |           |        |      |                    |        |        |      |
| HL             | 18.93               | 17.35     | <0.001 | 0.58 | 18.96              | 17.32  | <0.001 | 0.72 |
| HB             | 8.62                | 7.05      | <0.001 | 0.35 | 9.03               | 7.02   | 0.879  | 0.00 |
| Female (n=340) |                     |           |        |      |                    |        |        |      |
| HL             | 17.19               | 15.80     | <0.001 | 0.61 | 17.23              | 15.84  | <0.001 | 0.67 |
| HB             | 7.55                | 6.41      | <0.001 | 0.28 | 7.90               | 6.37   | <0.001 | 0.21 |

SD: Standard deviation, HL: Hand length, HB: Hand breadth

**Table 6: Standard estimation error and regression formulas for height estimation from hand and handprint measurements**

| Male (n=260)           |      |      | Female (n=340)         |      |      |
|------------------------|------|------|------------------------|------|------|
| Formula                | SEE  | r    | Formula                | SEE  | r    |
| <b>Left hand</b>       |      |      |                        |      |      |
| 121.78 + (HL × 2.966)  | 4.26 | 0.55 | 90.603 + (HL × 4.222)  | 4.64 | 0.62 |
| 177.94 + (HB × 0.009)  | 5.12 | 0.01 | 162.49 + (HB × 0.138)  | 5.90 | 0.11 |
| 156.25 + (A × 0.323)   | 4.82 | 0.33 | 145.43 + (AL × 0.293)  | 5.75 | 0.24 |
| 170.61 + (A1L × 0.226) | 5.07 | 0.13 | 144.96 + (A1L × 0.632) | 5.69 | 0.28 |
| 171.18 + (A3L × 0.197) | 5.02 | 0.20 | 160.32 + (A3L × 0.093) | 5.92 | 0.07 |
| 152.23 + (BL × 0.357)  | 4.78 | 0.35 | 132.56 + (BL × 0.458)  | 5.54 | 0.35 |
| 162.97 + (B1L × 0.585) | 4.95 | 0.25 | 143.58 + (B1L × 0.836) | 5.72 | 0.26 |
| 168.13 + (B2L × 0.438) | 5.02 | 0.19 | 147.05 + (B2L × 0.769) | 5.65 | 0.30 |
| 170.27 + (B3L × 0.324) | 5.04 | 0.18 | 150.18 + (B3L × 0.584) | 5.76 | 0.24 |
| 155.42 + (CL × 0.289)  | 4.88 | 0.30 | 114.40 + (CL × 0.675)  | 5.18 | 0.48 |
| 162.99 + (C1L × 0.566) | 4.92 | 0.27 | 140.22 + (C1L × 0.962) | 5.53 | 0.36 |
| 169.37 + (C2L × 0.334) | 4.98 | 0.23 | 152.06 + (C2L × 0.482) | 5.81 | 0.20 |
| 173.21 + (C3L × 0.189) | 5.09 | 0.10 | 154.56 + (C3L × 0.365) | 5.85 | 0.16 |
| 154.66 + (DL × 0.324)  | 4.86 | 0.31 | 131.62 + (DL × 0.477)  | 5.54 | 0.35 |
| 159.13 + (D1L × 0.724) | 4.80 | 0.34 | 147.81 + (D1L × 0.658) | 5.76 | 0.24 |
| 166.51 + (D2L × 0.490) | 5.00 | 0.21 | 145.28 + (D2L × 0.826) | 5.63 | 0.31 |
| 169.62 + (D3L × 0.375) | 5.02 | 0.19 | 149.86 + (D3L × 0.638) | 5.68 | 0.29 |
| 153.43 + (EL × 0.414)  | 4.78 | 0.35 | 137.91 + (EL × 0.465)  | 5.65 | 0.30 |
| 170.13 + (E1L × 0.337) | 5.07 | 0.14 | 153.65 + (E1L × 0.443) | 5.86 | 0.15 |
| 166.51 + (E2L × 0.633) | 4.88 | 0.30 | 153.20 + (E2L × 0.616) | 5.76 | 0.23 |
| 167.49 + (E3L × 0.594) | 4.89 | 0.29 | 153.15 + (E3L × 0.604) | 5.76 | 0.24 |
| 130.68 + (HPL × 2.733) | 4.45 | 0.49 | 112.77 + (HPL × 3.192) | 5.19 | 0.48 |
| 154.78 + (HPB × 3.331) | 4.80 | 0.34 | 145.00 + (HPB × 2.877) | 5.76 | 0.24 |
| <b>Right hand</b>      |      |      |                        |      |      |
| 121.17 + (HL × 3.010)  | 4.21 | 0.57 | 92.45 + (HL × 4.128)   | 4.90 | 0.57 |
| 153.40 + (HB × 2.871)  | 4.84 | 0.33 | 125.72 + (HB × 4.984)  | 5.75 | 0.30 |
| 163.61 + (AL × 0.214)  | 5.01 | 0.22 | 148.94 + (AL × 0.236)  | 5.92 | 0.20 |
| 162.92 + (A1L × 0.455) | 4.92 | 0.29 | 144.79 + (A1L × 0.633) | 5.79 | 0.29 |
| 170.01 + (A3L × 0.239) | 4.99 | 0.24 | 161.01 + (A3L × 0.075) | 6.04 | 0.05 |
| 157.61 + (BL × 0.383)  | 4.72 | 0.39 | 125.84 + (BL × 0.561)  | 5.51 | 0.41 |
| 159.54 + (B1L × 0.724) | 4.90 | 0.30 | 144.51 + (B1L × 0.768) | 5.84 | 0.25 |
| 161.64 + (B2L × 0.721) | 4.88 | 0.31 | 151.91 + (B2L × 0.558) | 5.92 | 0.20 |
| 166.40 + (B3L × 0.493) | 4.95 | 0.27 | 153.32 + (B3L × 0.447) | 5.96 | 0.17 |
| 141.40 + (CL × 0.470)  | 4.54 | 0.47 | 119.93 + (CL × 0.601)  | 5.38 | 0.45 |
| 162.36 + (C1L × 0.599) | 4.91 | 0.30 | 141.24 + (C1L × 0.908) | 5.78 | 0.29 |
| 163.32 + (C2L × 0.584) | 4.89 | 0.31 | 148.38 + (C2L × 0.630) | 5.89 | 0.22 |
| 163.18 + (C3L × 0.585) | 4.89 | 0.21 | 150.70 + (C3L × 0.522) | 5.87 | 0.24 |
| 151.79 + (DL × 0.367)  | 4.75 | 0.38 | 126.66 + (DL × 0.556)  | 5.52 | 0.40 |
| 162.34 + (D1L × 0.603) | 4.93 | 0.28 | 143.84 + (D1L × 0.805) | 5.83 | 0.26 |
| 165.58 + (D2L × 0.534) | 4.95 | 0.27 | 146.99 + (D2L × 0.743) | 5.78 | 0.29 |
| 166.29 + (D3L × 0.534) | 4.96 | 0.26 | 150.83 + (D3L × 0.595) | 5.87 | 0.24 |
| 153.97 + (EL × 0.407)  | 4.79 | 0.36 | 143.62 + (EL × 0.359)  | 5.83 | 0.26 |
| 165.98 + (E1L × 0.515) | 5.00 | 0.23 | 147.84 + (E1L × 0.708) | 5.89 | 0.22 |
| 165.28 + (E2L × 0.730) | 4.82 | 0.35 | 148.94 + (E2L × 0.878) | 5.67 | 0.34 |
| 169.82 + (E3L × 0.452) | 4.99 | 0.24 | 150.15 + (E3L × 0.774) | 5.82 | 0.27 |
| 138.50 + (HPL × 2.285) | 4.68 | 0.41 | 110.95 + (HPL × 3.318) | 5.22 | 0.50 |
| 158.55 + (HPB × 2.779) | 4.88 | 0.31 | 142.22 + (HPB × 3.304) | 5.85 | 0.25 |

SEE: Standart estimation error, HL: Hand length, HB: Hand breadth

evaluate bilateral asymmetry because they were conducted unilaterally.<sup>[17,19-21]</sup> When bilateral studies are examined, Abdel-Malek *et al.*<sup>[11]</sup> and Ishak *et al.*<sup>[9]</sup>

suggest that there is a bilateral difference only in hand width measurement in both men and women. In some bilateral studies, there was no bilateral difference in

**Table 7: Estimation rates of hand and handprint measurements in determining gender**

| Measurement | Demarking points          | Estimation rate (%) | Sex bias (%) |
|-------------|---------------------------|---------------------|--------------|
| Function 1  | Height (cm) ♀ <170.73 < ♂ | 92.7                | 0.1          |
| Function 2  | HL (cm) ♀ <18.07 < ♂      | 83                  | -10.7        |
| Function 3  | HPL (cm) ♀ <16.58 < ♂     | 80.2                | -16.6        |
| Function 4  | HB (cm) ♀ <8.28 < ♂       | 56.5                | -99.0        |
| Function 5  | HBP (cm) ♀ <13.43 < ♂     | 75.5                | -19.2        |
| Function 6  | AL (mm) ♀ <64.43 < ♂      | 73.5                | -14.3        |
| Function 7  | A1L (mm) ♀ <31.19 < ♂     | 77.7                | -13.5        |
| Function 8  | A3L (mm) ♀ <33.23 < ♂     | 63.3                | -40.2        |
| Function 9  | BL (mm) ♀ <69.54 < ♂      | 71.5                | -23.0        |
| Function 10 | B1L (mm) ♀ <24.77 < ♂     | 70.0                | -22.4        |
| Function 11 | B2L (mm) ♀ <22.01 < ♂     | 66.8                | -26.4        |
| Function 12 | B3L (mm) ♀ <23.22 < ♂     | 63.8                | -43.7        |
| Function 13 | CL (mm) ♀ <75.28 < ♂      | 73.5                | -19.1        |
| Function 14 | C1L (mm) ♀ <25.34 < ♂     | 70.7                | -23.8        |
| Function 15 | C2L (mm) ♀ <24.63 < ♂     | 68.5                | -36.7        |
| Function 16 | C3L (mm) ♀ <24.90 < ♂     | 61.5                | -46.8        |
| Function 17 | DL (mm) ♀ <69.09 < ♂      | 75.0                | -15.6        |
| Function 18 | D1L (mm) ♀ <25.04 < ♂     | 70.5                | -23.3        |
| Function 19 | D2L (mm) ♀ <22.75 < ♂     | 64.2                | -35.9        |
| Function 20 | D3L (mm) ♀ <21.72 < ♂     | 59.2                | -54.1        |
| Function 21 | EL (mm) ♀ <51.13 < ♂      | 71.5                | -21.7        |
| Function 22 | E1L (mm) ♀ <22.73 < ♂     | 70.0                | -29.1        |
| Function 23 | E2L (mm) ♀ <17.19 < ♂     | 63.7                | -35.6        |
| Function 24 | E3L (mm) ♀ <17.54 < ♂     | 60.5                | -48.9        |

HPL: Handprint length, HBP: Handprint breadth, ♂:Male, ♀:Female

hand and handprint measurements in both genders.<sup>[13,18,22]</sup> In this study, bilateral differences were statistically significant in the measurements of the distal phalanx of the thumb, medial phalanx of the little finger, and proximal phalanx of the little finger in the male gender ( $P = 0.022$ ,  $P = 0.011$ ,  $P = 0.003$ ) [Table 4]. In the female gender, the bilateral difference was statistically significant in the distal phalanx of index finger, distal phalanx of middle finger, medial phalanx of middle finger, and distal phalanx of ring finger ( $P = 0.008$ ,  $P = 0.026$ ,  $P = 0.009$ ,  $P = 0.000$ ).

In the correlation between height and hand and handprint measurements, the SEE was lower in males than in females (SEE for males: 4.21–5.12; SEE for females: 4.64–6.04). In the study conducted by de Souza and Kunkel<sup>[10]</sup> in the Brazilian population, it was reported that the SEE was higher in men than in women (SEE: 5.35–5.41 for men; SEE: 4.72–4.77 for women).

The measurement with the least SEE for height estimation from hand and handprint measurements for males was HL measurement in both right and left hand (SEE: 4.21–4.26), and the measurement with the least SEE for females was HL measurement in both right and left hand (SEE: 4.64–4.90). In previous studies, it has been stated that HL is one of the best measures of height.<sup>[9,11,13,14,17-19,21,23-26]</sup>

In the discrimination analysis performed to determine gender from hand and handprint measurements, it was detected that the most accurate measurements for gender determination were height, HL, and HPL (92.7%, 83%, and 80.2%) [Table 7]. In the literature, hand width and HL are above 90% for gender determination in the Indo-Mauritius population,<sup>[27]</sup> and in the study conducted by Kanchan and Rastogi<sup>[28]</sup> in North and South Indian populations, hand width and HL were above 85%. It has been reported that handprint width and HPL have an accuracy rate of over 85% in gender identification in Croatian population,<sup>[29]</sup> and HPL and handprint width have an accuracy rate of over 90% in gender identification in Western Australian population.<sup>[9]</sup> The results obtained in this study support other community studies available in the literature.

## Conclusion

As a result, it was observed that the accuracy of using hand and handprint measurements in determining height and gender in the Turkish population was satisfactory. Thus, this situation provides support for the use of hand and handprint measurements in the Turkish population both in fire, natural disasters, and terrorist incidents where corpses cannot be identified and in the identification of unidentified criminals involved in forensic crimes.

## Financial support and sponsorship

Nil.

## Conflicts of interest

There are no conflicts of interest.

## References

1. Uzun Ö. Evaluation of Upper Extremity Anthropometric Measurements in Terms of Height and Gender Estimation (PhD Thesis). Karadeniz Technical University, Institute of Health Sciences. Trabzon, (Advisor: Associate Dr. Gülay Yeginoğlu); 2017.
2. Kutun H. Gender Criteria in Arm and Leg Bones: An Investigation on Tepecik Society (Master's Thesis). Ankara University, Institute of Social Sciences. Ankara, (Advisor: Professor Dr. Ayla Sevim Erol); 2008.
3. Kim W, Kim YM, Yun MH. Estimation of stature from hand and foot dimensions in a Korean population. *J Forensic Leg Med* 2018;55:87-92.
4. Steele DG. The estimation of sex on the basis of the talus and calcaneus. *Am J Phys Anthropol* 1976;45:581-8.
5. Case DT, Ross AH. Sex determination from hand and foot bone lengths. *J Forensic Sci* 2007;52:264-70.
6. Metin Tellioglu A, Karakas S. Sex Determination from Humerus by Morphometric Methods. *FU Med J Health Sci* 2013;27:75-9.
7. Ecker A. Some Remarks on a Fluctuating Character in the Hand of Man. Germany: Verlag Nicht Ermittellbar; 1875.
8. Phelps VR. Relative index finger length as a sex-influenced trait in man. *Am J Hum Genet* 1952;4:72-89.
9. Ishak NI, Hemy N, Franklin D. Estimation of sex from hand and handprint dimensions in a Western Australian population. *Forensic Sci Int* 2012;221:6.e1-6.
10. de Souza FG, Kunkel ME. Estimation of stature from hand and

- handprint dimensions in the Brazilian population. *Res Biomed Eng* 2022;38:571-79.
11. Abdel-Malek AK, Ahmed AM, el-Sharkawi SA, el-Hamid NA. Prediction of stature from hand measurements. *Forensic Sci Int* 1990;46:181-7.
  12. Zulkifly NR, Wahab RA, Layang E, Ismail D, Desa WN, Hisham S, *et al.* Estimation of stature from hand and handprint measurements in Iban population in Sarawak, Malaysia and its applications in forensic investigation. *J Forensic Leg Med* 2018;53:35-45.
  13. Supare MS, Bagul AS, Pandit SV, Jadhav JS. Estimation of stature from arm span in medical students of Maharashtra, India. *Ann Med Health Sci Res* 2015;5:218-21.
  14. Rastogi P, Nagesh KR, Yoganarasimha K. Estimation of stature from hand dimensions of North and South Indians. *Leg Med (Tokyo)* 2008;10:185-9.
  15. Kanchan T, Menezes RG, Moudgil R, Kaur R, Kotian MS, Garg RK. Stature estimation from foot dimensions. *Forensic Sci Int* 2008;179:241.e1-5.
  16. Tang J, Chen R, Lai X. Stature estimation from hand dimensions in a Han population of Southern China. *J Forensic Sci* 2012;57:1541-4.
  17. Jee SC, Yun MH. Estimation of stature from diversified hand anthropometric dimensions from Korean population. *J Forensic Leg Med* 2015;35:9-14.
  18. Uhrová P, Beňuš R, Masnicová S, Obertová Z, Kramárová D, Kyselíková K, *et al.* Estimation of stature using hand and foot dimensions in Slovak adults. *Leg Med (Tokyo)* 2015;17:92-7.
  19. Ahmed AA. Estimation of stature from the upper limb measurements of Sudanese adults. *Forensic Sci Int* 2013;228:178.
  20. Paulis MG. Estimation of stature from handprint dimensions in Egyptian population. *J Forensic Leg Med* 2015;34:55-61.
  21. Sanli SG, Kizilkanat ED, Boyan N, Ozsahin ET, Bozkir MG, Soames R, *et al.* Stature estimation based on hand length and foot length. *Clin Anat* 2005;18:589-96.
  22. Bhatnagar DP, Thapar SP, Batish MK. Identification of personal height from the somatometry of the hand in Punjabi males. *Forensic Sci Int* 1984;24:137-41.
  23. Agnihotri AK, Agnihotri S, Jeebun N, Googoolye K. Prediction of stature using hand dimensions. *J Forensic Leg Med* 2008;15:479-82.
  24. Habib SR, Kamal NN. Stature estimation from hand and phalanges lengths of Egyptians. *J Forensic Leg Med* 2010;17:156-60.
  25. Jasuja OP, Singh G. Estimation of stature from hand and phalange length. *J Indian Acad Forensic Med* 2004;26:100-6.
  26. Krishan K, Sharma A. Estimation of stature from dimensions of hands and feet in a North Indian population. *J Forensic Leg Med* 2007;14:327-32.
  27. Jowaheer V, Agnihotri AK. Sex identification on the basis of hand and foot measurements in indo-Mauritian population – A model based approach. *J Forensic Leg Med* 2011;18:173-6.
  28. Kanchan T, Rastogi P. Sex determination from hand dimensions of North and South Indians. *J Forensic Sci* 2009;54:546-50.
  29. Kolić A, Jerković I, Andelinović Š. Sex estimation from handprints in a Croatian population sample: Developing a tool for sex identification in criminal investigations. *ST OPEN* 2020;1:1-11.

# Anatomical Study of Pterygoalar and Pterygospinous Bars/Foramina in West Anatolian Skulls

## Abstract

**Introduction:** Pterygoalar bar (PTAB) is a bony bridge formed by the incomplete or complete ossification of the pterygoalar ligament extending between the lateral pterygoid lamina (LPL) and the greater wing of the sphenoid bone. Complete ossification of the pterygoalar ligament results in the formation of the so-called “pterygoalar foramen” (PTAF) or Hyrtl’s foramen. On the other hand, pterygospinous bar (PTSB) is another bony bridge resulting from incomplete or complete ossification of the pterygospinous ligament, which extends from the pterygospinous process of the LPL to the sphenoidal spine. Complete ossification of this ligament forms the pterygospinous foramen (PTSF) or the Civinini’s foramen. This study was undertaken to examine detailed anatomy and incidence of PTAB, PTSB, and the corresponding foramina, as well as to establish their relationship with foramen ovale (FO). **Materials and Methods:** A total of 152 dry adult human skulls (304 sides) obtained from the collection of the Anatomy Department of Dokuz Eylül University were examined in terms of the presence/absence of PTAB/PTSB, their incidence and side, degree of ossification (complete/incomplete), and their relationship with FO. The distance between the spinous processes was measured in cases with incomplete ossification of PTAB/PTSB, whereas a digital caliper with 0.01 mm sensitivity (Mitutoyo, Japan) was used to measure horizontal and vertical diameters of the foramina in cases with complete ossification (i.e., when PTAF and PTSF were present). SPSS 22.0 statistical software was used for statistical analysis with Student’s *t*-test and Pearson’s correlation analysis. The level of significance was set at  $P < 0.05$ . **Results:** Of the 152 skulls, 11 (7.23%) harbored PTAF and 2 harbored PTSF (1.3%). An incomplete PTAB or incomplete PTSB was present in 110/304 (33.4%) and 21/304 (6.9%) of the sides examined, respectively. PTAB was located medial, lateral, inferior, inferolateral, and inferomedial to FO in 15 (4.93), 29 (9.53%), 77 (25.32%), 28 (9.21%), and 3 (0.98%) of the sides. The distance between PTAB and FO was  $7.43 \pm 2.58$  mm on the right and  $7.51 \pm 2.50$  mm on the left. The distance between two PTABs was  $10.43 \pm 3.65$  mm on the right and  $10.29 \pm 3.30$  mm on the left. The vertical diameter of PTAF was  $3.80 \pm 2.08$  mm, and the horizontal diameter was  $4.96 \pm 2.24$ . In the presence of a foramen, the mean thickness of PTAB was  $2.27 \pm 0.74$  mm, the mean width was  $3.45 \pm 3.40$  mm, and the mean length was  $6.54 \pm 3.64$  mm. No significant differences were identified between right- and left-sided measurements ( $P > 0.05$ ). **Discussion and Conclusion:** Close adjacency of PTAB/PTSB to FO as well as their ability to form foramina may hamper the procedures requiring placement of transcutaneous needles into FO or may present anatomical challenges in surgery involving the base of the cranium. Owing to the possibility of neural compression, they may also have clinical significance for craniofacial neurosurgeons, anesthesiologists, radiologists, and dental surgeons. Our results may provide some anatomical insights for planning infratemporal fossa surgery.

**Keywords:** Foramen ovale, pterygoalar bar, pterygoalar foramen, pterygospinous bar, pterygospinous foramen, trigeminal neuralgia

## Introduction

In the upper part of the infratemporal area, there are two ligaments originating from the interpterygoid aponeuroses that extend from the lateral pterygoid lamina (LPL) of the pterygoid process to the infratemporal surface of the sphenoid bone. The pterygoalar ligament (Hyrtl’s ligament) is

formed by the upper margin of the lateral interpterygoid aponeurosis, which extends from the root of LPL to the infratemporal surface of the greater wing of the sphenoid bone anterolateral to the foramen spinosum. This ligament courses lateral to the foramen ovale (FO) and anterolateral to the sphenoidal spine.<sup>[1]</sup> Pterygospinous ligament (Civinini’s ligament), which represents a thickening of the fascia between lateral and medial pterygoid muscles, extends

This is an open access journal, and articles are distributed under the terms of the Creative Commons Attribution-NonCommercial-ShareAlike 4.0 License, which allows others to remix, tweak, and build upon the work non-commercially, as long as appropriate credit is given and the new creations are licensed under the identical terms.

For reprints contact: WKHLRPMedknow\_reprints@wolterskluwer.com

**How to cite this article:** Aksu F, Karabekir S. Anatomical study of pterygoalar and pterygospinous bars/foramina in west Anatolian skulls. *J Anat Soc India* 2023;72:334-42.

Funda Aksu,  
Selim Karabekir<sup>1</sup>

Departments of Anatomy  
and <sup>1</sup>Neurosurgery, School  
of Medicine, Dokuz Eylül  
University, Izmir, Turkey

## Article Info

Received: 28 October 2022

Revised: 17 August 2023

Accepted: 26 November 2023

Available online: 30 December 2023

## Address for correspondence:

Prof. Dr. Funda Aksu,  
Department of Anatomy, Dokuz  
Eylül University Medical  
Faculty, 35340 Inciralti, Izmir,  
Turkey.  
E-mail: funda.aksu@deu.edu.tr

## Access this article online

Website: <https://journals.lww.com/joai>

DOI:  
10.4103/jasi.jasi\_156\_22

## Quick Response Code:



from the pterygospinous process of LPL to the sphenoidal spine. Therefore, as compared to pterygoalar ligament, pterygospinous ligament follows a course that is more medial, is further away from the base of the skull, attaches more posteriorly, and generally extends by crossing the lumen of FO.<sup>[2-4]</sup>

Partial or complete ossification of pterygoalar ligament leads to the formation of an anatomical structure known as pterygoalar bar (PTAB), which is closely located to FO.<sup>[4-9]</sup> Complete ossification of pterygoalar ligament results in the formation of pterygoalar foramen (PTAF), also known as Hyrtl's foramen, through which motor branches of the mandibular nerve (buccinator, lateral pterygoid, and temporalis muscle) as well as the auriculotemporal nerve, veins of pterygoid venous plexus, and certain arterioles<sup>[7,10-14]</sup> are reported to pass. The presence of PTAB may lead to certain neurological disorders such as difficulty in mastication, neuralgia, loss of taste sensation, paresthesia in the face or tongue, or reduced salivation from the parotid glands, as a result of compression effect on deep temporal, lateral pterygoid, buccal, auriculotemporal, and lingual branches of the mandibular nerve as well as on chorda tympani.<sup>[14-17]</sup> Furthermore, it has considerable clinical significance, since it may lead to nerve compression or trapped nerve during percutaneous anesthetic procedures for trigeminal neuralgia, in addition to the potential risk for interfering with needle access to FO.<sup>[3,6,18-20]</sup> Thus, a sound anatomical knowledge of these bony bridges and their prevalence is important for surgeons, neurologists, and anesthesiologists.<sup>[3,5,7-9,11,18]</sup>

Pterygospinous bar (PTSB) is a bony bridge formed by the incomplete or complete ossification of the pterygospinous ligament. Total ossification of this ligament creates the pterygospinous foramen (PTSF), or the foramen of Civinini, that conveys branches of the mandibular nerve and that may result in a variety of anatomical variations.<sup>[4,7,9,11]</sup> The branches of the medial meningeal artery and nerve supplying the medial pterygoid muscle as well as the masticatory branches of the mandibular nerve pass through PTSF.<sup>[21]</sup> An ossified pterygospinous ligament may cause paresthesia and pain in the presulcal areas of the tongue, base of the oral cavity, and gingival surfaces, impaired speech, anesthetic effect on the mucous glands of the tongue, as well as a loss of taste sense in the anterior two-thirds of the tongue due to compression of the adjacent chorda tympani.<sup>[3,11]</sup> The presence of PTSB may complicate surgery involving the lateral skull base as well as the parapharyngeal and retropharyngeal spaces approached through the infratemporal fossa.<sup>[11,13-15]</sup> Complete ossification of PTSB may also hamper the access of percutaneous needles to the trigeminal ganglion inserted through FO for mandibular nerve block and may complicate transzygomatic surgery.<sup>[3,5,8,10,11,22]</sup>

Ossification of the pterygospinous and pterygoalar ligaments and the resultant nerve compression may also manifest itself

through symptoms such as mandibular neuralgia, nerve palsy, and headache, numbness, or syncope. While these ligaments are in close contact with important anatomical structures such as the mandibular nerve and its branches, otic ganglion, median meningeal artery and vein, tympanic nerve, and medial and lateral pterygoid muscles, they occupy a deep and high position in the infratemporal fossa.<sup>[7]</sup>

This study was undertaken to examine the presence, incidence, and morphology of the ossified ligaments, i.e., PTAB and PTSB and the resultant PTAF and PTSF, as well as to evaluate their topographic relationship with FO.

## Materials and Methods

A total of 152 adult dry skull samples of unknown sex and age from Western Anatolia were obtained from the Anatomy Department, Medical Faculty of Dokuz Eylül University. Ethical approval was not obtained for this study as it did not require participation of any live subjects instead only bony material was used. Skulls with evidence of significant trauma or pathology were excluded. The presence and incidence of PTAB/PTSB and PTAF/PTSF were examined in 304 sides [Figures 1-5].

Based on observations on both bones between which the ligaments extend, PTAB and PTSB were defined as "incomplete" when trabeculae and processes failed to unite, whereas they were designated as "complete" when union was present leading to formation of a foramen.<sup>[7,15]</sup> In case of incomplete ossification of PTAB/PTSB, the distance was measured using a digital sliding caliper (Mitutoyo, Japan) with a sensitivity of 0.01 in vertical and horizontal diameters for samples harboring PTAF/PTSF with two bony processes. In the presence of a complete bony bar, the width, length, and thickness of the bar obliterating the foramen were measured [Figures 1-5]. The relationship between these structures and FO was explored. In addition, the shortest distance from PTAB to FO was recorded.

Statistical analysis was performed using SPSS ver. 22.0 (SPSS Inc., Chicago, IL, USA) statistical software pack with Student's *t*-test and Pearson's correlation test. The level of significance was set at  $P < 0.05$ .

## Results

Among 152 dry skulls overall, PTAF was present in 11 (3.6%; left sided in six and right sided in five) and PTSF was present in 2 (0.6%; one in the right and one in the left). Of these, concurrent PTAF and PTSF on both right and left sides were present in only one (0.3%). Among 304 sides, an incomplete PTAB was present in 110 (33.4%), and an incomplete PTSB was present in 21 (6.9%) [Figures 1-5].

PTAB's location was medial, lateral, inferior, inferolateral, and inferomedial to FO in 15 (4.93%), 29 (9.53%), 77 (25.32%), 28 (9.21%), and 3 (0.98%) cases, respectively. The PTAB-FO distance was  $7.43 \pm 2.58$  mm on the right

and  $7.51 \pm 2.50$  mm on the left; the distance between two incomplete PTABs was  $10.43 \pm 3.65$  mm on the right and  $10.29 \pm 3.30$  mm on the left; the distance between two incomplete PTSBs was  $8.70 \pm 3.15$  mm on the right and  $8.70 \pm 3.52$  mm on the left [Table 1]. The mean vertical and horizontal diameters of PTAF were  $3.80 \pm 2.08$  mm and  $4.96 \pm 2.24$  mm, respectively. In the presence of complete PTAB, the mean thickness, width, and length of the bar were  $2.27 \pm 0.74$  mm,  $3.45 \pm 3.40$  mm, and  $6.54 \pm 3.64$  mm, respectively. The vertical and horizontal diameters of PTSFs were  $3.20 \pm 0.69$  and  $3.70 \pm 0.23$  mm, respectively [Table 2].

### Discussion

The terminology used for the ossified structures under the sphenoid bone that are adjacent to FO is far from being consistent. PTAB and PTAF have been rarely defined in the anatomic literature, and although major anatomy textbooks do not routinely refer to these structures, they are relatively common.<sup>[6,9]</sup> Furthermore, pterygospinous and pterygoalar ligaments exhibit a significant degree of variability in terms of complete or incomplete ossification. As such, the published literature regarding the incidence and morphometric features of PTAB and PTSB lacks consensus and provides variable data.<sup>[11]</sup> Furthermore, mechanisms underlying the formation and development of these structures are poorly understood. Genetic and evolutionary factors have been proposed to be involved in the occurrence of these bony structures, due to the presence of significant differences between ethnic groups in humans.<sup>[6]</sup> Although the occurrence of PTAB has been regarded as a natural secondary process, studies in child skulls showing the presence of ossified PTAB suggest that

this anomaly may represent a genetic variation.<sup>[12]</sup> Even more interesting is the fact that the widespread presence of PTAB has been reported in skulls from herbivores, rodents, and adult monkeys, and some authors have even claimed that PTAB may be an atavistic structure.<sup>[23,24]</sup> Some studies showed a higher prevalence of PTAB among the elderly.<sup>[18]</sup>

### Clinical significance of pterygoalar bar/pterygospinous bar

The presence of PTAB has two major clinical consequences: the potential to produce neurological symptoms and to act as a mechanical barrier for needle entry when approaching FO.<sup>[25]</sup> Until now, no prospective clinical studies have evaluated symptoms associated with the presence of PTAB. Published data on clinically significant PTAB are limited to case reports or case series, hence the lack of accurate data on the incidence of symptomatic patients with PTAB.<sup>[6]</sup> Irrespective of gender, as opposed to more common presence of PTAF on the left, PTSFs are generally right sided.<sup>[13]</sup> PTAF has been considered to have more clinical significance based on higher incidence, lower surface area, proximity to FO, more frequent occurrence of superposition, and more lateral position as compared to PTSF.<sup>[13]</sup> During percutaneous mandibular or trigeminal nerve block, smaller PTAF surface and thicker PTAB closing the foramen increase the likelihood of blood vessel and nerve compression, and superior or lateral position relative to FO renders access to FO difficult or even impossible, causing significant clinical challenges.<sup>[13]</sup>

According to some researchers, complete ossification of pterygoalar ligament may be more dangerous than complete ossification of pterygospinous ligament, since the former

**Table 1: Distance between processes or tubercles in incomplete pterygoalar bar and pterygospinous bar for both sides**

|                                       | Side  | Minimum | Maximum | Median | Mean  | SD   | P    |
|---------------------------------------|-------|---------|---------|--------|-------|------|------|
| PTAB-FO distance (mm)                 | Right | 2.6     | 18.6    | 7.25   | 7.43  | 2.58 | 0.81 |
|                                       | Left  | 2.6     | 16.4    | 7.25   | 7.51  | 2.50 |      |
| Distance between two incomplete PTABs | Right | 2.6     | 19.9    | 10.5   | 10.43 | 3.65 | 0.73 |
|                                       | Left  | 2.7     | 19.5    | 9.9    | 10.29 | 3.30 |      |
| Distance between two incomplete PTSBs | Right | 4.0     | 12.65   | 9.2    | 8.70  | 3.15 | 1.0  |
|                                       | Left  | 4.4     | 17.6    | 8.55   | 8.70  | 3.52 |      |

Diameters of PTAF and PTSF and the dimensions of complete PTAB. PTAB: Pterygoalar bar, PTSB: Pterygospinous bar, FO: Foramen ovale, SD: Standard deviation

**Table 2: Diameters of pterygoalar foramen and pterygospinous foramen**

|                    | Measurement | Minimum | Maximum | Median | Mean | SD   | P    |
|--------------------|-------------|---------|---------|--------|------|------|------|
| PTAF diameter (mm) | Vertical    | 2.3     | 9.5     | 3.1    | 3.80 | 2.08 | 0.22 |
|                    | Horizontal  | 2.8     | 10.7    | 4.5    | 4.96 | 2.24 |      |
| Complete PTAB (mm) | Width       | 1.4     | 13      | 2.4    | 3.45 | 3.40 | 0.06 |
|                    | Length      | 3.1     | 16      | 5.7    | 6.54 | 3.64 |      |
|                    | Thickness   | 0.9     | 3.2     | 2.5    | 2.27 | 0.74 |      |
|                    |             |         |         |        |      |      |      |
| PTSF diameter (mm) | Vertical    | 2.6     | 3.8     | 3.2    | 3.20 | 0.69 | 0.21 |
|                    | Horizontal  | 3.5     | 3.9     | 4.5    | 3.70 | 0.23 |      |

Measured values in the presence of complete PTAB. PTAF: Pterygoalar foramen, PTSF: Pterygospinous foramen, PTAB: Pterygoalar bar, SD: Standard deviation

may totally obstruct FO during thermocoagulation of trigeminal ganglion or mandibular nerve performed to treat trigeminal neuralgia, and these ossified ligaments may lead to inadequate anesthesia as a result of difficulties associated with the advancement of the needle through FO.<sup>[3,4,8,20,26]</sup>

Singh<sup>[20]</sup> in his anatomical study of 730 skull bases proposed a new and detailed classification to account for varying degrees of ossification of PTAB/PTSB. Literature search of that researcher showed a highly variable incidence of PTAF and PTSF reported in different populations, ranging between 1% and 31.2% and between 1.3% and 62.4%, respectively. Thus, morphological and topographical clarifications of these structures carry much significance.<sup>[20]</sup>

### **Pterygoalar bar/pterygoalar foramen prevalence and location**

PTAB prevalence is considerably variable. In Chouke's study<sup>[23]</sup> involving 1544 dry skulls from America, complete PTAB was present in 10.3%, whereas in another study by the same author involving 2745 dry skulls, the prevalence was 5.9%. In Kapur *et al.*'s study,<sup>[13]</sup> incomplete ossification of the pterygoalar ligament was found in 20% of 100 dry skulls. In Pékala *et al.*'s meta-analysis,<sup>[6]</sup> the general prevalence of complete and incomplete PTAB was found to be 4.4% and 8.4%, respectively, with PTAB being more commonly observed unilaterally on the left. According to these authors, incomplete or complete PTAB prevalence was lowest among European populations. In a geographical subgroup analysis of that study, Asian populations were found to have the highest prevalence of PTAB (7.0%), followed by South (5.0%) and North (5.0%) America. A complete PTAB was least common in Europe (2.6%). In the current study of dry skulls from Western Anatolia, the PTAB occurrence rate was 3.6%. The reported prevalence of ossified PTAB exhibits significant variability between 1.3% and 62.4%.<sup>[4,14]</sup> According to Chouke,<sup>[23]</sup> the prevalence of Hyrtl's foramen was almost twice higher in Africans than in Caucasians (12.88% vs. 7.04%). While Kapur *et al.*<sup>[21]</sup> reported complete and incomplete PTAB in 5.9% and 14.4% of the skulls examined, respectively, the corresponding values reported by Peker *et al.*<sup>[15]</sup> in an Anatolian population were 9.7% and 10.2%. On the other hand, lower frequencies were reported in a Turkish population by Pinar *et al.*<sup>[27]</sup> and in an American population by Tubbs *et al.*;<sup>[14]</sup> the frequencies for complete and incomplete PTAB in these two studies were 1.1% and 0.7% and 4.98% and 0.7%, respectively. Interestingly, while Rosa *et al.*<sup>[4]</sup> observed the highest incidence of PTAB in the literature (12.9% for complete and 49.9% for incomplete ossification), Suazo *et al.*<sup>[28]</sup> reported much lower prevalence, again in a Brazilian sample (3.8% and 22.4%, respectively). Shaw<sup>[17]</sup> proposed that PTAB was present in approximately 1 out of 100 adults. A complete unilateral PTAB was present in approximately 5% of skulls from an Anatolian population, whereas bilateral PTAB

was significantly less common (1%).<sup>[9]</sup> A similar incidence was reported for PTAF by Kapur *et al.*<sup>[21]</sup> According to Rossi *et al.*,<sup>[7]</sup> complete and incomplete ossification of the pterygoalar ligament was present in 2.73% and 0.54% of the human skulls, respectively. In contrast with these reports, Skrzat *et al.*<sup>[9]</sup> in a Polish population and Chakravarthi and Bab,<sup>[29]</sup> in an Indian population, observed higher frequencies of complete PTAB (7.1% and 19.7%, respectively) as compared to incomplete PTAB (1.4% and 8.5%, respectively). In a recent meta-analysis of dried human skulls, 4.4% of the samples harbored a completely ossified PTAB, as compared to 8.4% for incompletely ossified PTAB.<sup>[3]</sup> Ossified PTAB was present in 8.4% of the samples (2.8% complete and 5.6% incomplete) in the study by Ryu *et al.*<sup>[8]</sup> In an Indian sample of dry skulls, Harikrishnan<sup>[11]</sup> observed the presence of PTAB in 11% of the cases. In 1951, Chouke and Hodes<sup>[30]</sup> determined the presence of PTAB in a total of 1234 samples (bilateral 0.89%). Lepp and Sandner<sup>[26]</sup> reported that PTAB was present in approximately 8%–10% of the population, and that pterygoalar ligament was more commonly ossified than pterygospinous ligament. In Rosa *et al.*'s study,<sup>[4]</sup> PTAB was found in 62.35% of the radiographic images examined (49.44% incomplete and 12.91% complete ossification). The reported rates of incomplete and complete PTAB by Antonopoulou *et al.*<sup>[25]</sup> were 7% and 1%, respectively. In a cadaveric study of 15 samples by Iwanaga *et al.*,<sup>[31]</sup> 27 of the 30 sides examined had at least one pterygoalar ligament/bar or pterygospinous ligament/bar.

### **Complete pterygoalar foramen**

This was observed in 14.7% of a Croatian population by Kapur *et al.*,<sup>[21]</sup> in 0.65% of an American population by Tubbs *et al.*,<sup>[14]</sup> and in 0.65%, 19.7%, and 0.3% of three separate Indian populations by Chakravarthi and Babu,<sup>[29]</sup> Kavitha Kamath and Vasantha,<sup>[5]</sup> and Singh,<sup>[20]</sup> respectively.

### **Incomplete pterygoalar foramen**

This was reported in 49.4% of a Brazilian population by Rosa *et al.*<sup>[4]</sup> and in 29%, 3.92%, and 3.3% of three different Indian populations by Kavitha Kamath and Vasantha,<sup>[5]</sup> De Villiers,<sup>[32]</sup> and Singh.<sup>[20]</sup>

Kapur *et al.*<sup>[13]</sup> determined the presence of PTAF in 15% of 100 human skulls, with left-sided dominance of this structure; again, complete ossification, i.e., PTAB, was significantly more common on the left (12%) than on the right (3%).

Natsis *et al.*<sup>[18]</sup> found that 31.7% of the 145 dry skull samples from a Greek population harbored PTAB, with 4.1% of these being completely ossified (i.e., foramen) and 27.6% being incompletely ossified. Skrzat *et al.*<sup>[9]</sup> found the presence of PTAB and foramen in 5 of the 70 skulls examined.

The most common type of PTAB is unilateral incomplete type.<sup>[6]</sup> In most of the previous studies, PTAB was more commonly reported on the left.<sup>[5,14,17,23,33]</sup> De Villiers,<sup>[32]</sup>

however, found more common presence of PTAB in an African sample of dry skulls. In Natsis *et al.*'s study,<sup>[18]</sup> no side dominance was observed. In our study, there was only a very small difference in the number of PTAB on the right and left sides of the skulls (one more PTAB on the right), consistent with Natsis *et al.*'s<sup>[18]</sup> observations.

#### **Pterygoalar bar morphometry: The distance between two incomplete pterygoalar bars**

The average distance between two incomplete PTABs reported by Natsis *et al.*<sup>[18]</sup> was  $7.49 \pm 2.76$  mm. In our study, the corresponding values on the right and left were  $10.43 \pm 3.65$  mm and  $10.29 \pm 3.30$  mm, respectively. These differences may reflect geographical and ethnic differences.

#### **Complete pterygoalar bar morphometry**

The mean length of PTAB reported by Skrzat *et al.*<sup>[9]</sup> and Peçkala *et al.*<sup>[6]</sup> was 4–8 mm and 6.27 mm, respectively. The mean PTAB length in our study, i.e.,  $6.54 \pm 3.64$  mm, was consistent with these previous reports. However, in contrast with these studies, PTAB width and thickness were also measured for the first time in our study which were found to be  $2.27 \pm 0.74$  mm and  $3.45 \pm 3.40$  mm, respectively.

#### **Pterygoalar foramen morphometry**

Published literature provides no information regarding the effect of the dimensions of PTAF on structures passing through it.<sup>[6]</sup> The mean diameter of PTAF reported by Kapur *et al.*,<sup>[13]</sup> Galdames *et al.*,<sup>[34]</sup> Skrzat *et al.*,<sup>[9]</sup> and Tubbs *et al.*<sup>[14]</sup> was  $3.46 \pm 1.26$  mm, 5.2 mm,  $8.4 \pm 1.79$  mm, and 9.42 mm, respectively. The horizontal and vertical diameters of this foramen reported by Patnaik *et al.*<sup>[35]</sup> were 4.45 and 4.7 mm, respectively. PTAF diameter ranged between 7 and 11 mm in Skrzat *et al.*'s study.<sup>[9]</sup> The horizontal and vertical diameters of PTAF were found to be  $4.79 \pm 1.39$  mm and  $3.21 \pm 1.70$  mm, respectively, in Natsis *et al.*'s study.<sup>[18]</sup> In a 2017 meta-analysis, the mean horizontal and vertical diameters for PTAF were reported to be 5.31 mm and 3.56 mm, respectively.<sup>[6]</sup> Despite measurements were performed on dry bones in the present study, our observations were consistent with these previous reports: the horizontal diameter of PTAF was  $4.96 \pm 2.24$  mm, the vertical diameter was  $3.80 \pm 2.08$  mm, and the length was 6.54 mm. The fact that comparable results were obtained in our study and Peçkala *et al.*'s study<sup>[6]</sup> may be indicative of lack of significant geographical effects.

#### **Relationship between pterygoalar bar/pterygoalar foramen and FO**

FO is located on the greater wing of the sphenoid bone in the base of the skull, in close adjacency of the posterior margin of LPL, medial to foramen spinosum, and lateral to foramen lacerum. It provides a connection between the cranial fossa and infratemporal fossa, conveying mandibular nerve, accessory meningeal artery, lesser petrosal nerve, and emissary vein. An accurate understanding of the location of FO is of utmost importance for certain diagnostic and

surgical procedures such as electroencephalographic analysis, microvascular decompression with percutaneous trigeminal rhizotomy, and percutaneous biopsy of cavernous sinus tumors.<sup>[8]</sup> Therefore, radiological guidance is required for visualizing FO and related structures.<sup>[15]</sup> Otherwise, higher doses of anesthesia may be required to achieve adequate anesthetic efficacy in the trigeminal nerve or its branches.<sup>[9]</sup>

In Kapur *et al.*'s study<sup>[13]</sup> of 100 dry skulls, PTAF was lateral to, across, or medial to FO in 40%, 40%, and only 20% of the cases, respectively. Skrzat *et al.*<sup>[9]</sup> reported that FO may be positioned medial or lateral to FO, and while it was found to cross FO in one case, PTAB's position may vary according to FO and its dimensions may range from short and narrow bony trabecular structures to wider laminae. According to Henry *et al.*,<sup>[36]</sup> PTAB is generally located lateral to FO or passes underneath FO by dividing it into two parts. Tubbs *et al.*<sup>[14]</sup> also reported that PTAB was generally lateral to PTAB. Natsis *et al.*<sup>[18]</sup> observed that PTAB was generally lateral to or crosses FO. In previous studies, PTAB was reported to lie medially, laterally, or inferior to FO.<sup>[4,9,20,22]</sup> In contrast, PTAB was lateral, inferior, and medial to FO in 17, 15, and 5 of the cases reported by Kavitha Kamath and Vasantha.<sup>[5]</sup> In our study, PTAB was medial, lateral, inferior, inferolateral, and inferomedial to the foramen in 15 (4.93%), 29 (9.53%), 77 (25.32%), 28 (9.21%), and 3 (0.98%) of the cases, respectively.

In Kapur *et al.*'s study,<sup>[13]</sup> the distance between PTAB and FO was  $3.14 \pm 1.82$ . In our study, the same distance was  $7.43 \pm 2.58$  mm and  $7.51 \pm 2.50$  mm on the right and left, respectively. The observed differences may stem from differences in measurement points as well as geographical and ethnic factors.

#### **Pterygospinous bar incidence and location**

In several studies, PTSB was more commonly reported to be present on the left side,<sup>[5,14,17,23]</sup> except for one study reporting mostly bilateral presence of PTSB.<sup>[3]</sup>

The incidence of PTSB observed by Harikrishnan<sup>[11]</sup> in 140 Indian dry skulls was 49%, whereas this figure was 28% in Ryu *et al.*'s<sup>[8]</sup> study examining dry skulls from Korea (complete and incomplete ossification 1.4% and 16.6%, respectively). Kapur *et al.*,<sup>[21]</sup> however, found a lower complete ossification rate of 1.31% for PTSB in a total of 305 skull samples from Croatia. Peker *et al.*<sup>[15]</sup> observed that this bony bridge was present in 8.8% of a sample of dry skulls from Anatolia. This figure for PTSB was 9.61% (5.76% complete and 3.84% incomplete) among 416 dry skull samples from an Indian population in Nayak *et al.*'s study.<sup>[37]</sup> Rosa *et al.*<sup>[4]</sup> examining the radiographies obtained from 93 dry skulls, identified the presence of pterygospinous ligament in 27.97% of the radiographs, 19.36% being incompletely, and 8.61% being completely ossified.

Wood and Jones<sup>[38]</sup> found ossification of pterygospinous ligament in 8% of a sample from Hawaii. Lang and

Hetterich<sup>[39]</sup> reported ossified pterygospinous ligament in 12%–13% of their samples from an African population. According to Shaw,<sup>[17]</sup> approximately 1 out of 10 adults may harbor such a pattern of ossification. Kavitha Kamath and Vasantha<sup>[5]</sup> found PTAB only in 26.83%, PTAF only in 58.54%, and both bony bars in 14.63% of 100 dry skull samples. Antonopoulou *et al.*<sup>[25]</sup> found a PTAB frequency of 25% and a completely ossified PTAB frequency of 2% in 100 dry skulls. The incidence of complete ossification of PTAB in studies by Kapur *et al.*,<sup>[13]</sup> Tubbs *et al.*,<sup>[14]</sup> Civinini,<sup>[2]</sup> Antonopoulou *et al.*,<sup>[25]</sup> Peker *et al.*,<sup>[15]</sup> and Rosa *et al.*<sup>[4]</sup> was 4%, 1.3%, 2.3%, 2%, 8.8%, and 8.61%, respectively. Matys *et al.*<sup>[3]</sup> found that 5.8% and 22% of their samples had complete or incomplete ossification of PTAB, respectively, and that this was more common than PTAF. Henry *et al.*,<sup>[36]</sup> in their meta-analysis, observed a higher rate of PTAB in Caucasians than Africans (10.7% vs. 2.78%). Henry *et al.*,<sup>[36]</sup> in their study, measured the length and width of PTAB as 7.48 mm and 3.06 mm, respectively. In Henry *et al.*'s<sup>[36]</sup> meta-analysis, the authors concluded that the general prevalence of PTAB was quite high. Iwanaga *et al.*<sup>[31]</sup> examined 15 cadaveric samples and found that 50.0% of them harbored PTAB or the ligament. In our study, the rate of complete and incomplete ossification of PTAB was 0.6% and 6.9%, respectively, and these figures were lower than those observed for PTAF. It is interesting to note that the rate of complete ossification of PTAB in this sample of dry skulls from Western Anatolia is lowest as compared to other previous reports.

#### Pterygoalar bar incidence and location

No consensus exists regarding the structures conveyed through PTAF. According to Henry *et al.*,<sup>[36]</sup> branches of the mandibular nerve supplying temporal, masseter, and lateral pterygoid muscles pass through PTAF. While Peker *et al.*<sup>[15]</sup> reported that medial pterygoid nerves and vessels passed through this foramen, Henry *et al.*<sup>[36]</sup> mentioned the



Figure 1: Pterygoalar foramen, complete pterygoalar bar, and incomplete pterygoalar bar in dry skull. LPL: Lateral pterygoid lamina, PTAF: Pterygoalar foramen, PTAB: Pterygoalar bar, PTS: Pterygospinous

passage of the medial pterygoid nerve and some vessels of the pterygoid venous plexus. Harikrishnan<sup>[11]</sup> observed an unusually large PTAF in 140 dry skulls from an Indian population and discussed its potential clinical implications.

#### Complete pterygoalar foramen

The lowest incidence (i.e., 0%) for this structure was reported by Das and Paul,<sup>[40]</sup> whereas Rosa *et al.*<sup>[4]</sup> observed the highest, i.e., 8.61%, in a Brazilian population. The same figure was 5.5% in an Anatolian population, as reported by Peker *et al.*<sup>[15]</sup> Again, this was present in 0.3% of the Indian samples in Singh's study<sup>[20]</sup> and in 1% in Kavitha Kamath and Vasantha's study.<sup>[5]</sup> The highest incidence reported in India was 5.76%, based on Nayak *et al.*'s study.<sup>[37]</sup> Kapur *et al.*<sup>[13]</sup> identified the presence of PTAF in 4% of 100 dry human skulls. De Froe and Wagenaar,<sup>[41]</sup> in their anatomical study of dry skulls from European populations, observed that 5% of the skulls harbored PTAF.

Saran *et al.*<sup>[22]</sup> found a complete ossification of PTAF in 1.2% of 80 skulls, whereas Henry *et al.*,<sup>[36]</sup> in their meta-analysis of 35 studies, found a complete PS bar rate of 4.4%. In Kapur *et al.*'s study<sup>[21]</sup> in a Bosnian population, the rate of PTAF was lower (1.31%). In our study, the incidence of PTAF formed by complete PTAF was 0.6%.

#### Incomplete pterygoalar foramen

The lowest incidence, 1%, was reported by Das and Paul,<sup>[40]</sup> as compared to the highest incidence of 19.36% reported by Rosa *et al.*<sup>[4]</sup> in a Brazilian population. The reported figures from India are 8.5% in Singh's study<sup>[20]</sup> and 16% in Kavitha Kamath and Vasantha's study.<sup>[5]</sup> Saran *et al.*<sup>[22]</sup> found that 7.5% of 80 skulls examined harbored an incomplete pterygoalar ligament. In Henry's *et al.*'s<sup>[36]</sup> meta-analysis of 28 studies, 11.6% of the samples had PS incomplete bar. This figure was 6.9% in the current study.

#### Pterygoalar foramen morphometry

In Henry's *et al.* meta-analysis,<sup>[36]</sup> the average horizontal and vertical diameters of PTAF were reported to be 9.05

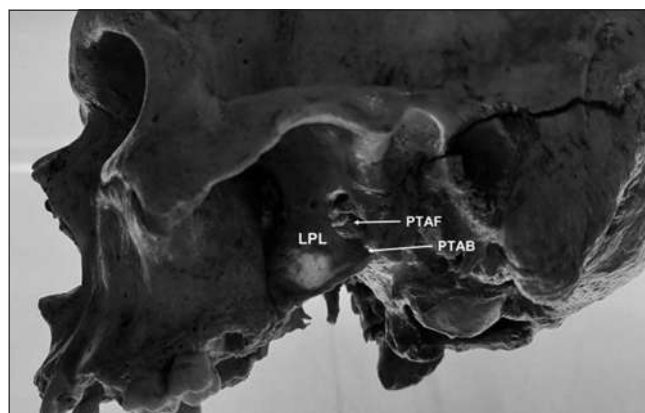


Figure 2: A very large pterygoalar foramen in dry skull and a highly thickened complete pterygoalar bar. LPL: Lateral pterygoid lamina, PTAF: Pterygoalar foramen, PTAB: Pterygoalar bar

and 5.75 mm, respectively. According to that study, dimensions of PTSF may vary, even in the same skull with bilateral presence of this structure. Furthermore, it may emerge as a large foramen (diameter of up to 10 mm) or may be divided into five separate foramens with varying dimensions.<sup>[36]</sup> The mean diameters/dimensions for PTSF reported by Kapur *et al.*,<sup>[13]</sup> Jansirani *et al.*,<sup>[12]</sup> and Galdames

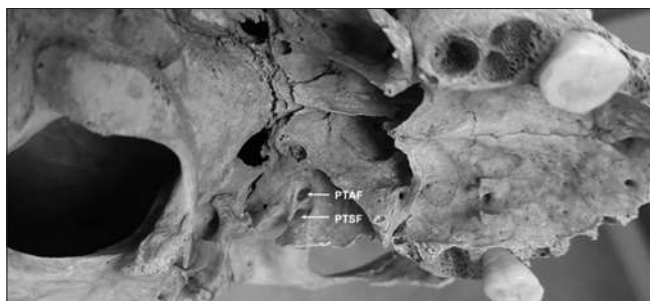


Figure 3: Pterygoalar foramen and pterygospinous foramen occurring concurrently in dry skull. PTAF: Pterygoalar foramen, PTSF: Pterygospinous foramen



Figure 4: Pterygoalar foramen and complete pterygoalar bar in dry skull. LPL: Lateral pterygoid lamina, PTAF: Pterygoalar foramen, PTAB: Pterygoalar bar



Figure 5: Occurrence of incomplete pterygoalar bar in dry skull. LPL: Lateral pterygoid lamina, PTAB: Pterygoalar bar

*et al.*<sup>[34]</sup> were  $8.77 \pm 1.53$  mm,  $7.5$  mm  $\times$   $7$  mm, and  $10.63$  mm  $\times$   $7.37$  mm, respectively. The horizontal diameter of PTSF in the right and left sides was approximately 4 mm in Nayak *et al.*'s study.<sup>[37]</sup> In our study, the vertical diameter of PTSB was  $3.20 \pm 0.69$  mm, and the horizontal diameter was  $3.70 \pm 0.23$  mm [Table 2].

### The relationship between pterygospinous bar/pterygoalar foramen and FO

Previous studies reported that PTSB was located medially or inferiorly relative to FO.<sup>[4,9,20,22]</sup> However, in Kavitha Kamath and Vasantha's study<sup>[5]</sup> of 100 dry skulls, PTSB was found to cross FO and was inferiorly (13 samples) or medially (5 samples) located. In contrast with PTAB, which is located laterally to or passes under FO dividing it into two parts, PTSB is located medially to or underneath FO.<sup>[18,36]</sup>

In the radio-anatomic study of Rosa *et al.*<sup>[4]</sup>, PTSF was found to be located medially to FO in almost all cases, whereas Kapur *et al.*<sup>[13]</sup> found lateral position of PTSF in 50%, medial in 25%, and superimposed in 25%. According to the findings of Kapur *et al.*<sup>[13]</sup> in 100 dry skulls, PTSF was present in 4% of the samples, predominantly on the right side. In 50% of the cases, PTSF was located lateral to FO, whereas it was located medially in 2% and coursed across FO in 25%. In our study of 152 skulls, we observed PTSF in only two cases and on the left side, one of which occurred in conjunction with PTAF [Figure 3].

### Conclusion

Although human populations have a low incidence of PTAB and PTAF, it appears that improving our understanding regarding the morphology and topography of these structures may have some clinical relevance. Better characterization of the variability of human morphology according to geographical and other factors is a prerequisite to improve surgical performance and to achieve further developments in medicine. Information on the ossification status of the ligaments in question is required for improved interpretation of radiological images in patients with trigeminal neuralgia as well as for better surgical planning and management strategies in procedures such as transfacial needle approaches requiring access to infratemporal fossa and parapharyngeal area. Close proximity of PTAB and PTSB to FO and occasional presence of the related foramen may be highly important for neurosurgeons, anesthesiologists, radiologists, craniofacial surgeons, and dental care specialists due to potential nerve compression. As opposed to previous reports, the width and thickness of PTAB were measured for the first time in the current study. We believe that the information provided herein may also prove to be valuable for cranial and maxillofacial surgeons when planning surgery in the skull base through the infratemporal fossa approach.

## Acknowledgments

The authors wish to thank Prof. Nukhet Gocmen Karabekir, MD, and Bayram Aydinlik, MD, for their help and contribution.

## Financial support and sponsorship

Nil.

## Conflicts of interest

There are no conflicts of interest.

## References

- Hyrtil J. Regarding the crotaphitico-buccinatorium foramen in humans. *Sitzungsber Akad Wissensch Math-Naturw Cl, Wien* 1862;46:111.
- Civinini F. Pterygospinous ligament found, described demonstrated by Filippo Civinini from Pistoia in. *Arch sc Med Fis Toscane* 1837;1:381-7.
- Matys T, Ali T, Zaccagna F, Barone DG, Kirolos RW, Massoud TF. Ossification of the pterygoalar and pterygospinous ligaments: A computed tomography analysis of infratemporal fossa anatomical variants relevant to percutaneous trigeminal rhizotomy. *J Neurosurg* 2019;132:1942-51.
- Rosa RR, Faig-Leite H, Faig-Leite FS, Moraes LC, Moraes ME, Filho EM. Radiographic study of ossification of the pterygospinous and pterygoalar ligaments by the hirtz axial technique. *Acta Odontol Latinoam* 2010;23:63-7.
- Kavitha Kamath B, Vasantha K. Anatomical Study of pterygospinous and pterygoalar bar in human skulls with their phylogeny and clinical significance. *J Clin Diagn Res* 2014;8:C10-3.
- Pekala PA, Henry BM, Pekala JR, Frączek PA, Tattera D, Natsis K, *et al.* The pterygoalar bar: A meta-analysis of its prevalence, morphology and morphometry. *J Craniomaxillofac Surg* 2017;45:1535-41.
- Rossi AC, Freire AR, Manoel C, Prado FB, Botacin PR, Caria PH. Incidence of the ossified pterygoalar ligament in Brazilian human skulls and its clinical implications. *J Morphol* 2011;28:69-71.
- Ryu SJ, Park MK, Lee UY, Kwak HH. Incidence of pterygospinous and pterygoalar bridges in dried skulls of Koreans. *Anat Cell Biol* 2016;49:143-50.
- Skrzatek J, Walocha J, Srodek R. An anatomical study of the pterygoalar bar and the pterygoalar foramen. *Folia Morphol (Warsz)* 2005;64:92-6.
- Bergman RA, Afifi AK, Miyachi R. Illustrated encyclopedia of Human Anatomic Variation: opus V: skeletal systems: cranium. *Illustrated Encyclopedia of Human Anatomic Variation*; 1995.
- Harikrishnan P. Analysis of clinical significance of the pterygospinous and pterygoalar bars. *J Craniofac Surg* 2020;31:e449-51.
- Jansirani D, Mugunthan N, Anbalagan J, Sudha R, Shivadeep S. A study on ossified pterygospinous and pterygoalar ligaments in Indian skulls. *Natl J Basic Med Sci* 2012;3:103-7.
- Kapur E, Ciric D, Talovic E. Ossification of the pterygospinous and pterygoalar ligaments and their clinical relevance. *Folia Med Fac Med Univ Saraev* 2017;52:9-15.
- Tubbs RS, May WR Jr, Apaydin N, Shoja MM, Shokouhi G, Loukas M, *et al.* Ossification of ligaments near the foramen ovale: An anatomic study with potential clinical significance regarding transcutaneous approaches to the skull base. *Neurosurgery* 2009;65:60-4.
- Peker T, Karaköse M, Anil A, Turgut HB, Gülekon N. The incidence of basal sphenoid bony bridges in dried crania and cadavers: Their anthropological and clinical relevance. *Eur J Morphol* 2002;40:171-80.
- Peuker ET, Fischer G, Filler TJ. Entrapment of the lingual nerve due to an ossified pterygospinous ligament. *Clin Anat* 2001;14:282-4.
- Shaw JP. Pterygospinous and pterygoalar foramina: A role in the etiology of trigeminal neuralgia? *Clin Anat* 1993;6:173-8.
- Natsis K, Piagkou M, Skotsimara G, Totlis T, Apostolidis S, Panagiotopoulos NA, *et al.* The ossified pterygoalar ligament: An anatomical study with pathological and surgical implications. *J Craniomaxillofac Surg* 2014;42:e266-70.
- Piagkou MN, Demesticha T, Piagkos G, Androutsos G, Skandalakis P. Mandibular nerve entrapment in the infratemporal fossa. *Surg Radiol Anat* 2011;33:291-9.
- Singh R. Ossification of pterygospinous and pterygoalar ligaments and their clinical significance: An anatomic study. *J Craniofac Surg* 2022;33:1603-6.
- Kapur E, Dilberović F, Redžepagić S, Berhamović E. Variation in the lateral plate of the pterygoid process and the lateral subzygomatic approach to the mandibular nerve. *Med Arh* 2000;54:133-7.
- Saran RS, Ananthi KS, Subramaniam A, Balaji MT, Vinaitha D, Vaithianathan G. Foramen of civinini: A new anatomical guide for maxillofacial surgeons. *J Clin Diagn Res* 2013;7:1271-5.
- Chouke KS. On the incidence of the foramen of civinini and the porus crotaphitico-buccinatorius in American whites and negroes; observations on 2745 additional skulls. *Am J Phys Anthropol* 1947;5:79-86.
- Daimi SR, Siddiqui AU, Gill SS. Analysis of foramen ovale with special emphasis on pterygoalar bar and pterygoalar foramen. *Folia Morphol (Warsz)* 2011;70:149-53.
- Antonopoulou M, Piagou M, Anagnostopoulou S. An anatomical study of the pterygospinous and pterygoalar bars and foramina – Their clinical relevance. *J Craniomaxillofac Surg* 2008;36:104-8.
- Lepp FH, Sandner O. Anatomic-radiographic study of ossified pterygospinous and “innominate” ligaments. *Oral Surg Oral Med Oral Pathol* 1968;26:244-60.
- Pinar Y, Arsu G, Aktan-Ikiz ZA. The pterygospinous and the pterygoalar bridges. *Sendrom* 2004;18:66-9.
- Suazo I, Matamala D, Smith R. Anatomical study of the pterygospinous and pterygoalar bony bridges and foramina in dried crania and its clinical relevance. *Int J Morphol* 2010;28:405-8.
- Chakravarthi KK, Babu KS. An anatomical study of the pterygo-alar bar and porus crotaphitico buccinatorius. *Int J Med Health Sci* 2012;1:3-9.
- Chouke KS, Hodes PJ. The pterygoalar bar and its recognition by roentgen methods in trigeminal neuralgia. *Am J Roentgenol Radium Ther* 1951;65:180-2.
- Iwanaga J, Clifton W, Dallapiazza RF, Miyamoto Y, Komune N, Gremillion HA, *et al.* The pterygospinous and pterygoalar ligaments and their relationship to the mandibular nerve: Application to a better understanding of various forms of trigeminal neuralgia. *Ann Anat* 2020;229:151466.
- De Villiers H. The skull of the African Negro: A biometrical and morphological study: (Thesis.... University of the Witwatersrand, 1963) Johannesburg: Witwatersrand University Press; 1968.
- Zakrzewska JM. Medical management of trigeminal neuralgia. *Br Dent J* 1990;168:399-401.

34. Galdames SI, Matamala Z, Smith D. Anatomical Study of the pterygospinous and pterygoalar bony bridges and foramens in dried crania and its clinical relevance. *Int J Morphol* 2010;28:405-8.
35. Patnaik VV, Singla RK, Sanju B. Bilateral pterygoalar bar and porus crotaphitico buccinatorius: A case report. *J Anat Soc India* 2001;50:161-2.
36. Henry BM, Pękala PA, Frączek PA, Pękala JR, Natsis K, Piagkou M, *et al.* Prevalence, morphology, and morphometry of the pterygospinous bar: A meta-analysis. *Surg Radiol Anat* 2020;42:497-507.
37. Nayak SR, Saralaya V, Prabhu LV, Pai MM, Vadgaonkar R, D'Costa S. Pterygospinous bar and foramina in Indian skulls: Incidence and phylogenetic significance. *Surg Radiol Anat* 2007;29:5-7.
38. Wood-Jones F. The non-metrical morphological characters of the skull as criteria for racial diagnosis: Part II: The non-metrical morphological characters of the Hawaiian skull. *J Anat* 1931;65:368-78.
39. Lang J, Hetterich A. Contribution on the postnatal development of the processus pterygoideus. *Anat Anz* 1983;154:1-31.
40. Das S, Paul S. Ossified pterygospinous ligament and its clinical implications. *Bratisl Lek Listy* 2007;108:141-3.
41. De Froe A, Wagenaar JH. Meaning of the porus crotaphiticobuccinatorius and the foramen pterygospinosum for neurology and radiology. *Fortschr Röntgenstr* 1935;52:64-9.

# Study of Neck–Shaft Angle in Plain Radiographs of Adult Kashmiri Population

## Abstract

**Introduction:** The knowledge about different diameters of the head and different dimensions of the neck of the femur is essential in orthopedic surgery, for radiological practice in identifying pathology of bone. **Aim:** The study aimed to determine the mean values of femoral neck–shaft angle. **Materials and Methods:** The present study was conducted in the Department of Anatomy, Government Medical College (GMC), Srinagar, in collaboration with the Department of Radiodiagnosis and Imaging GMC, Srinagar. Two hundred X-rays of males (100) and females (100) of the pelvis with both hips' anteroposterior view in the age group of 20–50 years were used in the present study. **Inclusion criteria:** (a) Patients complaining of pain in the hip, who had no joint pathology defined on the basis of radiological examination. (b) Patients of the age group of 20–50 years. (c) Patients without any deformity of the hip joint. **Exclusion criteria:** (a) Patients having a history of pathologies such as osteoarthritis, tuberculosis, and fractures around the hip joint. (b) Patients having a history of surgical intervention on proximal femur, acetabulum, or pelvis. (c) Patients who did not have the radiographs with appropriate technique. **Femoral neck–shaft angle:** The long axis of the shaft of the femur and long axis of the neck of the femur were marked with the help of marker, and the point of intersection of these two axes gave us the neck–shaft angle. This angle was measured with the help of goniometer. Two-sided *P* values were reported, and  $P < 0.05$  was considered statistically significant. **Observations:** All the 200 X-rays belonged to the adult (20–50 years) population. The overall mean neck shaft angle (NSA) of all the 200 subjects on the right side was  $128.18^\circ \pm 2.92^\circ$  and was statistically insignificant with  $P = 0.841$ . The overall mean NSA of all the 200 subjects on the left side was  $127.37^\circ \pm 3.40^\circ$  and was statistically insignificant with  $P = 0.607$ . **Conclusion:** The results calculated provide important information about gender, age, and side variations of NSA for the anatomists, radiologists, and orthopedic surgeons. Radiological knowledge of NSA will help the orthopedicians in diagnosing and selecting various treatment modalities in fractures around the hip joint, dislocation of the hip joint, and also surgical procedures such as implantation of prosthesis. The data thus obtained can be used as a baseline for future studies in the departments of anatomy, radiodiagnosis, and orthopedics.

**Keywords:** Femur, goniometer, neck–shaft angle

## Introduction

The femur or the thigh bone is the longest and the strongest bone of the body. It has an upper end, a lower bicondylar end, and a long shaft which is convex forward. Proximally, the head is directed medially upward and slightly forward which articulates with the acetabulum to form the hip joint.<sup>[1]</sup>

The femoral neck is about 5 cm long and connects the head with the shaft of the femur. It is directed upward medially and slightly forward. The angle between the long axis of the neck and the long

axis of the shaft of the femur is called as neck–shaft angle or angle of inclination and is about  $125^\circ$ .<sup>[2]</sup> This angle facilitates movement at the hip joint, enabling the limb to swing clear of the pelvis.

The knowledge about different diameters of the head and different dimensions of the neck of the femur is essential in orthopedic surgery, for radiological practice in identifying the pathology of bone.<sup>[3]</sup>

Knowing the normal morphology of the hip joint and proximal femur is highly important for the orthopedicians to repair the geometry of the proximal femur after both trauma and hip arthroplasty. The chief intent is the restoration of normal hip biomechanics.<sup>[4]</sup> One of the major

This is an open access journal, and articles are distributed under the terms of the Creative Commons Attribution-NonCommercial-ShareAlike 4.0 License, which allows others to remix, tweak, and build upon the work non-commercially, as long as appropriate credit is given and the new creations are licensed under the identical terms.

For reprints contact: WKHLRPMedknow\_reprints@wolterskluwer.com

**How to cite this article:** Makdoomi MA, Khan JA, Mohammad BG, Bhat SA, Hamid S. Study of neck–shaft angle in plain radiographs of Adult Kashmiri population. *J Anat Soc India* 2023;72:343-8.

**Mohd Arif Makdoomi, Javed Ahmad Khan, Bhat Gulam Mohammad, Sajad A Bhat<sup>1</sup>, Shahnawaz Hamid<sup>1</sup>**

Department of Anatomy, Government Medical College, Hospital Administration, SKIMS, Srinagar, Jammu and Kashmir, India

## Article Info

Received: 28 October 2022

Accepted: 26 November 2023

Available online: 30 December 2023

## Address for correspondence:

Dr. Sajad A Bhat, Hospital Administration, SKIMS, Srinagar, Jammu and Kashmir, India. E-mail: drsajadk@rediffmail.com

## Access this article online

Website: <https://journals.lww.com/joai>

DOI: 10.4103/jasi.jasi\_155\_22

## Quick Response Code:



problems arising after total hip arthroplasty is limb length discrepancy. The use of templates and radiographs in preoperative planning may minimize this problem, and pre- and intraoperative templating was suggested for this purpose.<sup>[5-7]</sup>

### Aims and objectives

The aim of the study was to determine the mean values of the femoral neck–shaft angle.

### Materials and Methods

The present study was conducted in the Department of Anatomy, Government Medical College (GMC), Srinagar in collaboration with the Department of Radiodiagnosis and Imaging GMC, Srinagar. Two hundred X-rays of males (100) and females (100) of the pelvis with both hips' anteroposterior view in the age group of 20–50 years were used in the present study. The radiographs belonged to patients who had presented with pain in the hip or lower back. Only those radiographs were included in the present study which did not show any pathological condition. The radiographs were obtained from the Department of Radiodiagnosis and Imaging, GMC, Srinagar.

#### Instruments used

1. Goniometer
2. Measuring scale
3. Markers
4. Divider.

#### Inclusion criteria

1. Patients complaining of pain in the hip, who had no joint pathology defined on the basis of radiological examination.
2. Patients of the age group of 20–50 years.
3. Patients without any deformity of the hip joint.

#### Exclusion criteria

1. Patients having a history of pathologies such as osteoarthritis, tuberculosis, and fractures around the hip joint
2. Patients having a history of surgical intervention on the proximal femur, acetabulum, or pelvis
3. Patients who did not have the radiographs with appropriate technique.

#### Methods

Radiological measurements used in the present study were obtained from the standard pelvic radiographs. The anteroposterior view of radiographs was used, whereas the patient was in the supine position and both the lower limbs internally rotated at 15°. The film focal distance of these radiographs was 1.2 m. The midpoint between the two anterior superior iliac spines and the upper boundary of symphysis pubis was used for centralization.

Radiographs having the following features were included in the study:

1. Symmetrical obturator foramen
2. Lateralization of greater trochanter
3. Clarity of the piriform fossa
4. Pubis and coccyx in the same plane
5. Absence of hip joint arthrosis.

#### Femoral neck–shaft angle

Long axis of the shaft of the femur and long axis of the neck of the femur were marked with the help of marker, and the point of intersection of these two axes gave us the neck–shaft angle. This angle was measured with the help of goniometer.

#### Statistical methods

Data were entered into a Microsoft Excel Spreadsheet. Categorical variables were summarized as percentages. Continuous variables were summarized as mean and standard deviation. To test the hypothesis of no difference in measurements between males and females, unpaired *t*-test was used. Measurements were compared across age groups using one-way ANOVA. Paired *t*-test was used to compare the difference in measurements between the right and left sides. Analysis was done using SPSS version 23. Two-sided *P* values were reported, and *P* < 0.05 was considered statistically significant.

### Observations and Results

#### Observation

In the present study, the radiographs were taken in digital format. The data were analyzed both separately and compared with other sides in both hips in both the sexes and summarized in the tables separately.

Table 1 shows the age distribution of the study population. All the 200 X-rays belonged to the adult (20–50 years) population. Of the age ≤30 years, there were 54 X-rays contributing 27% of the total X-rays. Similarly, in the age group of 31–40 years, there were 69 X-rays, making 34.5% of total X-rays. Of the age group of 41–50 years, there were 77 X-rays, making 38.5% of the total X-rays. The mean age of the study underpopulation was 37.3 ± 8.7 years.

Table 2 shows the overall dimensions of neck–shaft angle in the studied population (200 X-rays).

The mean of neck–shaft angle (rt.) was found to be 128.18° ± 2.92°. The mean of neck–shaft angle (lt.) was found to be 127.37° ± 3.40°.

Table 3 shows the neck–shaft angle in the right and left femurs of both the sexes each consisting of 100 males and 100 females. The mean neck–shaft angle in the males on the right side is 128.43°, with the standard deviation of ±2.78° and standard error mean of 0.27. On the left side, it is 127.52° with a standard deviation of ±3.43° and standard error mean of 0.34. Hence, in males, the neck–shaft angle

**Table 1: Age distribution of the study population**

| Age (years)     | Frequency (%) |
|-----------------|---------------|
| ≤30.0           | 54 (27.0)     |
| 31.0–40.0       | 69 (34.5)     |
| 41.0+           | 77 (38.5)     |
| Total           | 200 (100.0)   |
| Mean±SD (years) | 37.3±8.47     |

SD: Standard deviation

**Table 2: Distribution of overall dimensions of neck shaft angle in the study population**

|             | Angle_rt    | Angle_lt    |
|-------------|-------------|-------------|
| Valid (n)   | 200         | 200         |
| Missing (n) | 0           | 0           |
| Mean±SD     | 128.18±2.92 | 127.37±3.40 |
| Minimum     | 121.0       | 120.0       |
| Maximum     |             | 135.0       |

SD: Standard deviation

**Table 3: Association of neck–shaft angle with gender**

|        | Sex    | n   | Mean   | SD   | SEM  | P     |
|--------|--------|-----|--------|------|------|-------|
| NSA_rt | Female | 100 | 127.94 | 3.05 | 0.30 | 0.237 |
|        | Male   | 100 | 128.43 | 2.78 | 0.27 | 0.237 |
| NSA_lt | Female | 100 | 127.22 | 3.38 | 0.33 | 0.535 |
|        | Male   | 100 | 127.52 | 3.43 | 0.34 | 0.535 |

NSA: Neck–shaft angle, SD: Standard deviation, SEM: Standard error of mean

on the right side is higher as compared to that on the left side. In females, a slight difference in the neck–shaft angle on the right and left sides was observed with the mean value of 127.94° on the right side and the standard deviation of ±3.05° and standard error mean of 0.30. On the left side, the mean value observed was 127.22° with a standard deviation of ±3.38° and standard error mean of 0.33.

The association of females and males in NSA on the right side was insignificant with  $P = 0.237$ , and on the left side, the association of females and males in NSA was also insignificant with  $P = 0.535$ .

Table 4 shows the association of neck–shaft angle with age:

The mean NSA on the right side in the age group of 20–30 years in 54 subjects was 128.37° ± 3.03° with 95% confidence interval (127.54°–129.19°), and on the left side, it was 127.68° ± 3.65° with 95% confidence interval (126.68°–128.68°).

The mean NSA on the right side in the age group of 31–40 years in 69 subjects was 128.05° ± 2.61° with 95% confidence interval (127.42°–128.68°), and on the left side, it was 127.43° ± 3.29° with 95% confidence interval (126.64°–128.22°).

The mean NSA on the right side in the age group of 41–50 years in 77 subjects was 128.16° ± 3.13° with

95% confidence interval (127.45°–128.87°), and on the left side, it was 127.09° ± 3.34° with 95% confidence interval (126.33°–127.85°).

The overall mean NSA of all the 200 subjects on the right side was 128.18° ± 2.92° and was statistically insignificant with  $P = 0.841$ . The overall mean NSA of all the 200 subjects on the left side was 127.37° ± 3.40° and was statistically insignificant with  $P = 0.607$ .

Table 5 shows the comparison of NSA in bilateral hips in all 200 subjects of both genders. The values of NSA on two sides show  $P = 0.001$  which is significant.

In case of females, the mean NSA on the right side of 100 subjects was 127.94° ± 3.05°, whereas on the left side, it was 127.22° ± 3.38°. The mean difference of 95% confidence interval was 0.72, and this association of the right and left sides was statistically significant with  $P = 0.041$  [Table 6].

In case of males, the mean NSA on the right side of 100 subjects was 128.43° ± 2.78°, whereas on the left side, it was 127.52° ± 3.43°. The mean difference of 95% confidence interval was 0.91, and this association of the right and left sides was statistically significant with  $P = 0.015$  [Table 6].

Table 8 depicts the paired sample statistics in the age group of 20–30 years of the subjects under study: The mean NSA on the right side in the age group of 20–30 years in 54 subjects was 128.37° ± 3.03° with the mean difference of 95% of confidence interval 0.69, and on the left side, it was 127.68° ± 3.65° with the mean difference of confidence interval of 0.69. This association of the right and left sides was statistically insignificant in this age group with  $P = 0.137$ .

Table 9 depicts the paired sample statistics in the age group of 31–40 years of the subjects under study: The mean NSA on the right side in the age group of 31–40 years in 69 subjects was 128.05° ± 2.61° with the mean difference 95% of confidence interval 0.62, and on the left side, it was 127.43° ± 3.29° with the mean difference of confidence interval of 0.62. This association of the right and left sides was statistically insignificant in this age group with  $P = 0.159$ .

Table 10 depicts the paired sample statistics in the age group of 41–50 years of the subjects under study: The mean NSA on the right side in the age group of 41–50 years in 77 subjects was 128.16° ± 3.13° with the mean difference 95% of confidence interval 1.08, and on the left side, it was 127.09° ± 3.34° with the mean difference of confidence interval of 1.08. This association of the right and left sides was statistically significant in this age group with  $P = 0.012$ .

## Discussion

In the present study, 200 subjects (100 males and 100 females) in the age group of 20–50 years were selected.

**Table 4: The association of neck–shaft angle with age**

| NSA     | n   | Mean   | SD   | SE   | 95% CI for mean |             | Minimum | Maximum | P     |
|---------|-----|--------|------|------|-----------------|-------------|---------|---------|-------|
|         |     |        |      |      | Lower bound     | Upper bound |         |         |       |
| NSA_rt  |     |        |      |      |                 |             |         |         |       |
| ≤30.0   | 54  | 128.37 | 3.03 | 0.41 | 127.54          | 129.19      | 121.0   | 134.0   | 0.841 |
| 31.0–40 | 69  | 128.05 | 2.61 | 0.31 | 127.42          | 128.68      | 124.0   | 133.0   |       |
| 41.0+   | 77  | 128.16 | 3.13 | 0.35 | 127.45          | 128.87      | 121.0   | 134.0   |       |
| Total   | 200 | 128.18 | 2.92 | 0.20 | 127.77          | 128.59      | 121.0   | 134.0   |       |
| NSA_lt  |     |        |      |      |                 |             |         |         |       |
| ≤30.0   | 54  | 127.68 | 3.65 | 0.49 | 126.68          | 128.68      | 120.0   | 135.0   | 0.607 |
| 31.0–40 | 69  | 127.43 | 3.29 | 0.39 | 126.64          | 128.22      | 121.0   | 134.0   |       |
| 41.0+   | 77  | 127.09 | 3.34 | 0.38 | 126.33          | 127.85      | 120.0   | 135.0   |       |
| Total   | 200 | 127.37 | 3.40 | 0.24 | 126.89          | 127.84      | 120.0   | 135.0   |       |

CI: Confidence interval, NSA: Neck–shaft angle, SD: Standard deviation, SE: Standard error

**Table 5: Paired sample statistics comparison of two sides in all 200 subjects**

| Pair 1   | Mean   | n   | SD   | SEM  | Mean difference* (95% of CI) | P      |
|----------|--------|-----|------|------|------------------------------|--------|
| Angle_rt | 128.18 | 200 | 2.92 | 0.20 | 0.82 (0.32–1.31)             | <0.001 |
| Angle_lt | 127.37 | 200 | 3.40 | 0.24 |                              |        |

SD: Standard deviation, SEM: Standard error of mean, CI: Confidence interval

**Table 6: Paired sample statistics according to gender in females**

| Sex      | Mean   | n   | SD   | SEM  | Mean difference* (95% of CI) | P     |
|----------|--------|-----|------|------|------------------------------|-------|
| Angle_rt | 127.94 | 100 | 3.05 | 0.30 | 0.72 (0.31–1.41)             | 0.041 |
| Angle_lt | 127.22 | 100 | 3.38 | 0.33 |                              |       |

SD: Standard deviation, SEM: Standard error of mean, CI: Confidence interval

**Table 7: Paired sample statistics according to gender in males**

| Sex      | Mean   | n   | SD   | SEM  | Mean difference* (95% of CI) | P     |
|----------|--------|-----|------|------|------------------------------|-------|
| Angle_rt | 128.43 | 100 | 2.78 | 0.27 | 0.91 (0.18–1.64)             | 0.015 |
| Angle_lt | 127.52 | 100 | 3.43 | 0.34 |                              |       |

SD: Standard deviation, SEM: Standard error of mean, CI: Confidence interval

Measurements were done separately on the radiographs on both sides of each gender [Figure 1]. The mean value was calculated, a comparison was done between the measurements of neck–shaft angle on two sides in each gender, and each side was also compared with the neck–shaft angle of the corresponding side in the other sex. In the study, the mean neck–shaft angle on the right side in males was found to be  $128.43^\circ \pm 2.78^\circ$ , and on the left side, it was  $127.52^\circ \pm 3.43^\circ$ . Thus, we observed a difference of  $0.91^\circ$  in the mean values of neck shaft angle on the two sides in males [Table 7]. In females, the mean neck–shaft angle values on the right side were found to be  $127.94^\circ \pm 3.05^\circ$ , and on the left side, it was  $127.22^\circ \pm 3.38^\circ$ . Thus, we



Figure 1: Instruments used

observed a difference of  $0.72^\circ$  in the mean values of neck–shaft angle on the two sides in females [Table 6]. However, the mean neck–shaft angle on the right side in males was higher than those in females. The mean neck–shaft angle on the left side of the two sexes was close to each other.

Silva *et al.*, in 2003,<sup>[8]</sup> while conducting morphometric study in 66 femurs (33 right and 33 left) and found no significant difference in the neck–shaft angle values on the two sides which is contradictory to our study.

Atkinson *et al.*, in 2010,<sup>[9]</sup> used 100 consecutive Caucasian patients (61 males and 39 females) to study the differences in hip morphology between the genders in patients undergoing hip resurfacing; in the study, they compared the neck–shaft angle. The males had a mean neck–shaft angle of  $129^\circ$  (range: 119–138), and the females had a mean neck–shaft angle of  $128^\circ$  (range: 121–138). The present study is consistent with our study with respect to gender.

Our study findings were consistent with a study conducted by Kour *et al.*, in 2013<sup>[10]</sup> who found the average NSA in males on the right side to be  $121.63^\circ \pm 2.41^\circ$ , and on the left side, it was  $121.33^\circ \pm 2.36^\circ$ , whereas in females, the mean NSA on the right side was found to be  $121.16^\circ \pm 2.50^\circ$ , whereas on the left side, it was found to be  $120.94^\circ \pm 2.51^\circ$ .

Ma *et al.*, in 2014,<sup>[11]</sup> in a Chinese study analyzed neck–shaft angle with computed tomography and found no

**Table 8: Paired sample statistics according to age between 20 and 30 years**

|          | Mean   | n  | SD   | SEM  | Mean difference*<br>(95% of CI) | P     |
|----------|--------|----|------|------|---------------------------------|-------|
| Angle_rt | 128.37 | 54 | 3.03 | 0.41 | 0.69 (0.22–1.59)                | 0.137 |
| Angle_lt | 127.68 | 54 | 3.65 | 0.49 |                                 |       |

SD: Standard deviation, SEM: Standard error of mean, CI: Confidence interval

**Table 9: Paired sample statistics according to age between 31 and 40 years**

|          | Mean   | n  | SD   | SEM  | Mean difference*<br>(95% of CI) | P     |
|----------|--------|----|------|------|---------------------------------|-------|
| Angle_rt | 128.05 | 69 | 2.61 | 0.31 | 0.62 (0.25–1.49)                | 0.159 |
| Angle_lt | 127.43 | 69 | 3.29 | 0.39 |                                 |       |

SD: Standard deviation, SEM: Standard error of mean, CI: Confidence interval

**Table 10: Paired sample statistics according to age between 41 and 50 years**

|          | Mean   | n  | SD   | SEM  | Mean difference*<br>(95% of CI) | P     |
|----------|--------|----|------|------|---------------------------------|-------|
| Angle_rt | 128.16 | 77 | 3.13 | 0.35 | 1.08 (0.24–1.91)                | 0.012 |
| Angle_lt | 127.09 | 77 | 3.34 | 0.38 |                                 |       |

SD: Standard deviation, SEM: Standard error of mean, CI: Confidence interval

significant difference in the neck–shaft angle on the two sides in males which is contradictory to present study, but the same parameter in females on the two sides was close to each other which is contradictory with the present study. Moreover, the neck–shaft angle values when compared in the two sexes were also close to each other which is consistent with present study.

Boese *et al.*, 2016,<sup>[12]</sup> while measuring femoral neck–shaft angle on plain radiographs observed that the mean neck–shaft angle of healthy adults was 128.8° (98–180°), and in patients of osteoarthritis, it was 131.5. For rotation corrected, the mean NSA was 128.5, and for nonrotation corrected, it was 129.5° [Figure 2].

Yet, another study conducted by Pathak *et al.*, in 2016,<sup>[13]</sup> showed the mean value of NSA for males to be 129.26° and in females the mean value of NSA to be 126.62°, thus is in concinnity with our study.

Adekoya-Cole *et al.*, 2016,<sup>[14]</sup> studied femoral neck–shaft angle in 264 hip joints of 132 subjects, 68 males and 64 females in adult Nigerian population. The average neck–shaft angle for an adult Nigerian was 130.77° ± 6.03° with a mean neck–shaft angle of 131.28 ± 6.56 on the right side and 130.22 ± 5.18 for the left side. In males, mean neck–shaft angle was 131.57° ± 5.66°, whereas the mean value for the adult female was 129.97 ± 6.33. The above findings were consistent with our study; as in our study also, the mean value of male NSA was more than that of females and

**Figure 2: The femoral neck–shaft angle**

also the values on the right side are higher as compared to the left. Another radiological study conducted by Parashar *et al.*, in 2017,<sup>[15]</sup> for femoral NSA found the mean NSA on the right side was 130.22° and on the left side was 129.81° which was consistent with our study with respect to the side variation. Shrestha *et al.*, in 2018,<sup>[16]</sup> in their radiological study of NSA in the Nepalese population found that in males, average right NSA was 132.96° ± 6.05° and left NSA was 131.54° ± 13.66°, whereas in females, the average right NSA was 134° ± 6.57° and on left side 132.98° ± 6.23°. The above findings according to gender were not consistent with our study but right–left variation corroborated with our study.

Yin *et al.*, in 2018,<sup>[17]</sup> observed that neck–shaft angle was higher on the right side in males which is consistent with our present study, but in females also, it was higher on the right side which is consistent with present study.

Ates *et al.*, 2019,<sup>[18]</sup> while doing radiological measurement of neck–shaft angle in 200 subjects (100 males and 100 females) observed that the mean neck–shaft angle in males was 128.19° ± 5.08°, and in females, it was 128.4° ± 5.18°. No significant difference in the mean value of neck–shaft angle in the males on two sides was observed which is contradictory to the present study. However, the values on the two sides in female subjects and also the mean values of neck–shaft angle in both the sexes were close to each other which is inconsistent with the present study.

## Conclusion

The results calculated provide important information about gender, age, and side variations of NSA for the anatomists, radiologists, and orthopedic surgeons. Radiological knowledge of NSA will help the orthopedicians in diagnosing and selecting various treatment modalities for fractures around the hip joint, dislocation of the hip joint, and also surgical procedures such as implantation of prosthesis.

The data thus obtained can be used as a baseline for future studies in the departments of anatomy, radiodiagnosis, and orthopedics.

### Financial support and sponsorship

Nil.

### Conflicts of interest

There are no conflicts of interest.

### References

1. Chaurasia's BD. Human anatomy. Regional and Applied. Dissection and Clinical: textbook. 2003;1.
2. Singh V. Textbook of Anatomy; Femur Volume II: Abdomen and Lower Limb. 3<sup>rd</sup> ed. Vol 1. Reed Elsevier India Private Limited; 2020.
3. Chowdhury MS, Naushaba H, Mahbul Mawla Chowdhury AH, Khan LF, Ara JG. Morphometric study of full ossified head and neck of human left femur. *J Dhaka Natl Med Coll Hos* 2012;18:9-13.
4. Tipton SC, Sutherland JK, Schwarzkopf R. The assessment of limb length discrepancy before total hip arthroplasty. *J Arthroplasty* 2016;31:888-92.
5. Deorio JK. Intraoperative evaluation of limb length in hip arthroplasty using a single AP radiograph. *Hip Int* 2005;15:199-205.
6. Desai AS, Dramis A, Board TN. Leg length discrepancy after total hip arthroplasty: A review of literature. *Curr Rev Musculoskelet Med* 2013;6:336-41.
7. Kayani B, Pietrzak J, Hossain FS, Konan S, Haddad FS. Prevention of limb length discrepancy in total hip arthroplasty. *Br J Hosp Med (Lond)* 2017;78:385-90.
8. Silva VJ, Oda JY, Santana DM. Anatomical aspects of the proximal femur of adults Brazilians. *Int J Morphol* 2003;21:303-8.
9. Atkinson HD, Johal KS, Willis-Owen C, Zadow S, Oakeshott RD. Differences in hip morphology between the sexes in patients undergoing hip resurfacing. *J Orthop Surg Res* 2010;5:76.
10. Kaur P, Mathew S, George U. A study of neck shaft angle in the North-West Indian population on radiographs. *Int J Basic Appl Med Sci* 2013;3:9-15.
11. Ma H, Han Y, Yang Q, Gong Y, Hao S, Li Y, *et al.* Three-dimensional computed tomography reconstruction measurements of acetabulum in Chinese adults. *Anat Rec (Hoboken)* 2014;297:643-9.
12. Boese CK, Dargel J, Oppermann J, Eysel P, Scheyerer MJ, Bredow J, *et al.* The femoral neck-shaft angle on plain radiographs: A systematic review. *Skeletal Radiol* 2016;45:19-28.
13. Pathak SK, Maheshwari P, Ughareja P, Gadi D, Raj PM, Gour SK. Evaluation of femoral neck shaft angle on plain radiographs and its clinical implications. *Int J Res Orthop* 2016;2:383-6.
14. Adekoya-Cole TO, Akinmokin OI, Soyebi KO, Oguche OE. Femoral neck shaft angles: A radiological anthropometry study. *Niger Postgrad Med J* 2016;23:17-20.
15. Parashar R, Sharma A, Gupta UK. Correlation of neck shaft angle with age. A radiographic study. *Int J Res Med* 2017;6:93-6.
16. Shrestha R, Gupta HK, Hamal RR, Pandit R. radiographic anatomy of the neck-shaft angle of femur in Nepalese people: Correlation with its clinical implication. *Kathmandu Univ Med J (KUMJ)* 2018;16:124-8.
17. Yin Y, Zhang R, Jin L, Li S, Hou Z, Zhang Y. The hip morphology changes with ageing in Asian population. *BioMed Research International* 2018;2018.
18. Ates A, Aydin E, Maralcan G. Proximal femur morphology and radiological measurement of femuroacetabular distance. *Glob J Res Anal* 2019;8:52.

## Determination of the Foot Deformities that May Occur during the Coronavirus Disease 2019 Lockdown Process in Ballet Students

### Abstract

**Aim:** This study aimed to compare foot injury prevalence, causes, and risk factors before and after the coronavirus disease 2019 (COVID-19) lockdown in ballet dancers. In this study, it is also aimed to determine the foot deformities that may occur during the pandemic process and to obtain results that will enable the necessary measures to be taken. **Subjects and Methods:** Our study includes students between the ages of 13 and 21 years who study full time at the Dokuz Eylül University State Conservatory Ballet Department, which provides professional ballet education. This study used a cross-sectional measurements design to evaluate foot morphometry during two distinct periods of time: the first was before to COVID-19 lockdown, and the second was after end of the lockdown. Measurements were made on the photographs taken for the right and left sides. Our study includes anatomical and morphometric measurements of foot digit length, foot length, foot width, and foot angles (intermetatarsal angle, hindfoot varus angle, and hallux valgus angle). **Results:** Forty-one ballet students with a mean age of  $15.81 \pm 2.28$  years and who had been taking ballet training for an average of  $6.93 \pm 2.32$  years were included in our study. When the foot angles (intermetatarsal angle, hindfoot varus angle, and hallux valgus angle) were examined, a significant difference was found except for the hallux valgus angles before and after lockdown. There was no significant relationship between the lengths of digits, foot length, foot width, age and body mass index parameters, and foot angles (intermetatarsal angle, hindfoot varus angle, and hallux valgus angle). However, a relationship was found between the foot angles before and after the lockdown. **Conclusion:** We can say that this result shows us that the COVID-19 lockdown process increases the tend to foot injury in ballet students. We think that this is due to continuing their ballet training on their own or online without ballet instructors in ballet studios.

**Keywords:** Ballet, foot injury, hallux valgus angle, morphometry

### Introduction

The coronavirus disease 2019 (COVID-19) lockdown has led to a large reduction in physical activity for many children and young people across the country and has increased mental health and general well-being issues. Recent studies that have incorporated the lockdown period have focused on how dance can help the general population stay fit and healthy or how lockdown has changed preprofessional dancers' training and life.<sup>[1,2]</sup> Lockdown itself has meant that preprofessional training institutions alter their face-to-face dance classes to online delivery, which has been an exceptional challenge for both students and teachers as neither had any experience of such conditions. Although these online activities could never replace traditional dance classes, which did provide

This is an open access journal, and articles are distributed under the terms of the Creative Commons Attribution-NonCommercial-ShareAlike 4.0 License, which allows others to remix, tweak, and build upon the work non-commercially, as long as appropriate credit is given and the new creations are licensed under the identical terms.

For reprints contact: WKHLRPMedknow\_reprints@wolterskluwer.com

a stimulus to innovate the dance curriculum and education. Accompanied with unstable internet connections, which led to low image quality, their usual detailed movement feedback was made particularly challenging. Normally, face-to-face ballet education can cause many deformities by exposing the lower extremity to heavy stresses. Anatomical suitability and training technique are very important to minimize these deformities. There is a strong relationship between the development of deformities and disabilities and anatomical features and training technique. In this study, it was conducted to examine the effect of the pandemic process during COVID-19 on foot morphometry, which is important for ballet dancers. Currently, there are no published data on how the lockdown due to the pandemic has affected the foot morphometry in ballet students. This study aimed to compare foot injury

**How to cite this article:** Kabakci AG, Ayvazoglu S, Bozkir MG. Determination of the foot deformities that may occur during the coronavirus disease 2019 lockdown process in ballet students. *J Anat Soc India* 2023;72:349-54.

**Ayşe Gul Kabakci,  
Seda Ayvazoglu<sup>1</sup>,  
Memduha Gulhal  
Bozkir**

*Department of Anatomy,  
Faculty of Medicine, Cukurova  
University, Adana, <sup>1</sup>Department  
of Performing Arts, Ballet State  
Conservatory, Dokuz Eylül  
University, İzmir, Turkey*

### Article Info

**Received:** 03 October 2022

**Accepted:** 24 November 2023

**Available online:** 30 December 2023

### Address for correspondence:

*Dr. Ayşe Gul Kabakci,  
Department of Anatomy,  
Faculty of Medicine, Cukurova  
University, Sarıçam, Adana,  
Turkey.  
E-mail: aysegulll-88@hotmail.  
com*

### Access this article online

**Website:** <https://journals.lww.com/joai>

**DOI:**  
10.4103/jasi.jasi\_137\_22

### Quick Response Code:



prevalence, causes, and risk factors before and after the COVID-19 lockdown in ballet dancers. This study also aimed to determine the foot deformities that may occur during the pandemic process and to obtain results that will enable the necessary measures to be taken.

## Subjects and Methods

To explore how the COVID-19 pandemic might impact ballet education, we present our own measurements that we wrote in the 1<sup>st</sup> weeks following university campus shutdowns, city lockdowns, and border closures. Our study includes students between the ages of 13 and 21 years who study full time at the Dokuz Eylül University State Conservatory Ballet Department, which provides professional ballet education. This study used a cross-sectional measurements design to evaluate foot morphometry during two distinct periods: the first was before the COVID-19 lockdown, and the second was after the end of the lockdown. The experimental procedures were conducted in conformity with the Declaration of Helsinki. The relevant guidelines and regulations were strictly followed when conducting the study. The study protocol was approved by the Ethics Committee of Cukurova University. Ethical approval was granted by the University of Cukurova (200/15). Each participant and their parents signed an informed consent form before participation and using their photo in our study. Inclusion criteria include the ballet students who are receiving full-time dance training at least 2 years at Dokuz Eylül University. The ballet students who have graduated or are at the master's or a higher level were omitted.

### Photography design

All profile photographs were acquired using a Digital SLR Camera with fixed shooting values.(Canon EOS 80D; ISO 100 f/4.5). The students were taken to a meter-high platform, and they were allowed to take positions in the marked area. The photographic setup consisted of a tripod 1 m away from the student. The tripod height was adapted to each subject's knee level. This plane is described as a reference plane. In a standing position, each subject was asked to relax and was anatomic positioned. The photographs of the students were taken from the knee level down to the dorsum of the foot. In addition, foot photographs were taken from the lateral and posterior positions. Acquired images were then transferred to a computer. The measurement scale was divided into degree and was made on the computer screen as digital and estimations were expressed as degree. Measurements were made using Image J 1.52a with 1/100 mm sensitivity. Using the measurement feature of the software (image J 1.52a with 1/100 mm sensitivity), first the distal point of the angle is chosen, and a line is drawn to the mid position of the angle measurement where the mouse button is hold. The second line is drawn by moving the mouse to the third point, and the angle measurement results are recorded. All measurements were made three times by the same person.

Measurements were made on the photographs taken for the right and left sides. Our study includes anatomical and morphometric measurements of foot digit length, foot length, foot width, and foot angles (intermetatarsal angle, hindfoot varus angle, and hallux valgus angle).

### Statistical analysis

SPSS 21.0 was used for statistical analysis of the measurement results. From these measurements, means, standard deviations, and minimum and maximum values were calculated;  $P < 0.001$ ,  $P < 0.01$ , and  $P < 0.05$  were considered statistically significant. Skewness and kurtosis statistics were used to determine the normality of the data distribution. Values between +1.5 and -1.5 were considered to be in accordance with the normal distribution. Pearson analyses were used for correlation analyses with data showing a normal distribution, and Spearman analyses were used for data that did not fit a normal distribution. In addition, data with a normal distribution were evaluated using ANOVA, and data not without a normal distribution were evaluated using the Mann-Whitney *U*-test.

## Results

Forty-one ballet students with a mean age of  $15.81 \pm 2.28$  years and who had been taking ballet training for an average of  $6.93 \pm 2.32$  years were included in our study. The lengths of the foot digits, the foot lengths, and the foot widths were measured on the right and left sides in Table 1. When the foot angles (intermetatarsal angle, hindfoot varus angle, and hallux valgus angle) were examined, a significant difference was found except for the hallux valgus angles before and after lockdown. There was no significant relationship between the lengths of digits, foot length, foot width, age and body mass index (BMI) parameters, and foot angles (intermetatarsal angle, hindfoot varus angle, and hallux valgus angle) in Table 3. However, a relationship was found between the foot angles before and after lockdown in Table 4.

## Discussion

Professional ballet dancers are dance artists, and due to the high-intensity training required and the technical discipline and difficulty needed for dance performance, "dance injury" is common in ballet dancers.<sup>[3]</sup> When the literature is examined, lower extremity injuries are among 65%–80% of all ballet injuries. If the most common damages are examined in detail, since they are located in the lower extremities; 7%–14% hip, 14%–20% knee, 5%–8% leg, 15%–22% wrist, and 13%–15% foot injuries are due to injuries. Studies have shown that 50% of injuries are due to overuse. The overuse percentages are: it was found to be 20% lower extremity, 15% wrist, and 15% foot.<sup>[4]</sup> Studies are lacking on the intense physical demands of dancing that exposes dancers' feet to a high risk of injuries such as hallux valgus, metatarsal injury, and subsequent ankle pain. We examined foot morphometry and foot

**Table 1: Length measurements of ballet students**

| Parameters               | Mean±SD (minimum–maximum) |                          |
|--------------------------|---------------------------|--------------------------|
|                          | Right                     | Left                     |
| First digit length (cm)  | 5.06±0.53 (3.99–6.38)     | 5.04±0.48 (4.10–6.38)    |
| Second digit length (cm) | 4.35±0.58 (3.03–5.50)     | 4.26±0.81 (3.90–5.31)    |
| Third digit length (cm)  | 3.73±0.48 (2.63–4.68)     | 3.85±0.50 (2.68–4.95)    |
| Fourth digit length (cm) | 3.46±0.51 (2.34–4.63)     | 3.55±0.45 (2.40–4.63)    |
| Fifth digit length (cm)  | 2.92±0.48 (2.14–3.99)     | 3.01±0.44 (2.17–3.88)    |
| Foot length (cm)         | 22.90±1.90 (19.36–26.85)  | 22.79±1.83 (19.63–26.85) |
| Foot width (cm)          | 9.10±0.69 (7.39–10.34)    | 9.13±0.69 (7.41–10.91)   |

SD: Standard deviation

**Table 2: Angle measurements of ballet students before and after lockdown**

| Parameters                    | Mean±SD (minimum–maximum) |                          | P     |
|-------------------------------|---------------------------|--------------------------|-------|
|                               | Before lockdown           | After lockdown           |       |
| Body mass index               | 19.56±0.77 (18.50–21.80)  | 20.80±1.39 (19.30–24.00) | 0.000 |
| Intermetatarsal angle (right) | 18.18±0.21 (15.19–22.00)  | 19.77±0.23 (16.19–24.94) | 0.002 |
| Intermetatarsal angle (left)  | 17.60±0.19 (14.19–2.25)   | 19.12±0.22 (15.23–23.51) | 0.001 |
| Hindfoot varus angle (right)  | 8.18±0.23 (4.38–12.21)    | 9.89±0.25 (4.98–14.21)   | 0.002 |
| Hindfoot varus angle (left)   | 8.32±0.20 (4.13–12.58)    | 9.05±0.23 (5.13–13.58)   | 0.001 |
| Hallux valgus angle (right)   | 24.21±0.71 (12.34–42.39)  | 26.23±0.75 (13.34–44.39) | 0.213 |
| Hallux valgus angle (left)    | 23.73±0.59 (12.38–35.57)  | 25.58±0.61 (13.38–38.57) | 0.166 |

P significance value (ANOVA). SD: Standard deviation

angles (intermetatarsal angle, hindfoot angle, and hallux valgus angle) in our study. The weight should be in the center of the foot. Otherwise, since only one side of the leg muscles are used, imbalance will occur. Wrist sprains are facilitated as weight is placed on the lateral ligaments in inward sickling and medial ligaments in outward sickling. Hallux valgus deformity may occur as the thumb will be pushed to the valgus position in outward sickling. Another factor of injury is making wrong practices without the supervision of the instructor. The arrival of the COVID-19 forced nearly all preprofessional dancers to train and study from home due to the lockdown. Before this, the reported injury prevalence for dancers was between 3% and 95%.<sup>[5]</sup> Injuries were mainly in the muscles of the lower limb and chronic in nature. Perceived causes of these injuries were overwork, fatigue, and the recurrence of an old injury.<sup>[6]</sup> Furthermore, the anatomical, biomechanical, and hormonal gender differences might have contributed to these results.

Globally, the outbreak of COVID-19 has forced different countries to implement strict social distancing measures and sanitary regimens. People were under the lockdown, working remotely, homeschooling children, and facing quarantine challenges related to eating habits, sleeping time, physical inactivity, and stress. A small-scale study in Italy during lockdown hypothesized based on previous evidence, that children and young people typically gain weight during Summer holidays, that the same would happen during the lockdown. This study concluded that activity decreased while sleep increased.<sup>[7]</sup> In our study, the mean BMI values of ballet students were  $19.56 \pm 0.77$  before lockdown and  $20.80 \pm 1.39$  after lockdown. We determined that there was

a significant increase in BMI values after the lockdown period. Outcomes were stratified by three BMI levels: healthy weight (BMI: 18.5–24.9 kg/m<sup>2</sup>), overweight (BMI: 25.0–29.9 kg/m<sup>2</sup>), and obesity (BMI: 30.0 kg/m<sup>2</sup> or above).<sup>[8]</sup> Even though there was an increase in BMI during the lockdown period, ballet students' BMI values remained within a healthy weight.

Hallux valgus was first proposed by Carl Hueter in 1871 and is one of the common diseases in the forefoot characterized by the outward deviation of the hallux beyond the normal physiological angle and first metatarsal adduction. It is a common deformity of the forefoot that usually exists on both feet.<sup>[1]</sup> It is generally believed that when the outward deviation of the hallux is more than 15°.<sup>[9]</sup> The normal value of the angle between the longitudinal axis of the first toe and the extended line of the longitudinal axis of the second toe is 8°–12°. For patients with metatarsal adduction, the normal value is 8°–10°. The hallux valgus can be classified according to the hallux valgus angle and the first/second intermetatarsal angle. Moderate intensity: the medial part of the first metatarsal head protrudes with pain, hallux valgus angle <30°, and intermetatarsal angle <13°. Moderate: the thumb has lateral deviation to compress the second toe, the sesamoid bone is dislocated, the hallux valgus angle is 30°–40°, and the intermetatarsal angle is 13°–16°. High intensity: the thumb has lateral deviation to ride across the second toe, the hallux has pronation, the dislocation of the sesamoid bone is located at the fibular margin of the metatarsal head (7°), hallux valgus angle >40°, and intermetatarsal angle >14°.<sup>[10]</sup> In our study, the hallux valgus angle on the right side was found to be  $24.21 \pm 0.71$  before the lockdown and  $26.23 \pm 0.75$

**Table 3: Correlation analysis between anatomical parameters**

|      | <i>r</i> ( <i>P</i> ) |              |              |              |              |              |              |              |              |              |              |              |  |  |
|------|-----------------------|--------------|--------------|--------------|--------------|--------------|--------------|--------------|--------------|--------------|--------------|--------------|--|--|
|      | IA1R                  | IA1L         | HA1R         | HA1L         | HVA1R        | HVA1L        | IA2R         | IA2L         | HA2R         | HA2L         | HVA2R        | HVA2L        |  |  |
| Age  | 0.05 (0.73)           | -0.15 (0.92) | 0.05 (0.75)  | 0.02 (0.90)  | 0.14 (0.37)  | 0.03 (0.84)  | 0.03 (0.84)  | -0.07 (0.68) | 0.04 (0.80)  | 0.08 (0.61)  | 0.13 (0.44)  | 0.01 (0.93)  |  |  |
| BMI1 | -0.05 (0.76)          | 0.05 (0.78)  | -0.01 (0.97) | 0.08 (0.64)  | -0.07 (0.65) | -0.15 (0.36) | -0.05 (0.78) | -0.03 (0.84) | -0.08 (0.63) | 0.06 (0.70)  | -0.05 (0.76) | -0.13 (0.42) |  |  |
| BMI2 | 0.01 (0.95)           | 0.14 (0.39)  | -0.01 (0.99) | 0.08 (0.63)  | -0.01 (0.93) | -0.09 (0.59) | 0.02 (0.99)  | 0.03 (0.88)  | -0.03 (0.83) | 0.10 (0.52)  | -0.01 (0.96) | -0.08 (0.60) |  |  |
| Year | 0.19 (0.23)           | 0.08 (0.64)  | 0.15 (0.36)  | 0.09 (0.56)  | 0.19 (0.23)  | 0.14 (0.40)  | 0.18 (0.27)  | 0.04 (0.82)  | 0.14 (0.39)  | 0.15 (0.36)  | 0.18 (0.26)  | 0.11 (0.50)  |  |  |
| DL1R | 0.09 (0.57)           | 0.06 (0.71)  | 0.02 (0.90)  | 0.12 (0.47)  | -0.08 (0.60) | 0.03 (0.85)  | 0.02 (0.91)  | 0.04 (0.80)  | 0.11 (0.51)  | 0.22 (0.17)  | -0.11 (0.49) | 0.02 (0.92)  |  |  |
| DL2R | 0.11 (0.49)           | 0.22 (0.16)  | -0.01 (0.93) | 0.13 (0.42)  | 0.07 (0.68)  | 0.11 (0.51)  | 0.03 (0.87)  | 0.14 (0.37)  | 0.09 (0.57)  | 0.23 (0.15)  | 0.02 (0.88)  | 0.08 (0.62)  |  |  |
| DL3R | 0.04 (0.81)           | 0.15 (0.36)  | 0.01 (0.94)  | 0.02 (0.90)  | 0.03 (0.84)  | 0.07 (0.68)  | -0.03 (0.84) | 0.07 (0.65)  | 0.09 (0.60)  | 0.09 (0.58)  | -0.02 (0.93) | 0.03 (0.84)  |  |  |
| DL4R | 0.16 (0.32)           | 0.21 (0.18)  | 0.18 (0.25)  | 0.31 (0.05)  | -0.04 (0.81) | -0.02 (0.90) | 0.07 (0.66)  | 0.17 (0.30)  | 0.25 (0.11)  | 0.33 (0.04)  | -0.06 (0.71) | -0.02 (0.93) |  |  |
| DL5R | 0.08 (0.60)           | 0.22 (0.17)  | -0.10 (0.55) | 0.11 (0.50)  | 0.08 (0.60)  | 0.10 (0.54)  | 0.01 (0.94)  | 0.11 (0.51)  | -0.01 (0.94) | 0.19 (0.24)  | 0.05 (0.75)  | 0.10 (0.55)  |  |  |
| FLR  | 0.01 (0.95)           | 0.01 (0.99)  | -0.16 (0.32) | -0.03 (0.87) | -0.03 (0.84) | -0.03 (0.87) | -0.03 (0.87) | -0.03 (0.85) | 0.08 (0.63)  | -0.08 (0.63) | -0.08 (0.63) | -0.09 (0.59) |  |  |
| FWR  | 0.27 (0.09)           | 0.11 (0.49)  | 0.08 (0.62)  | 0.15 (0.36)  | 0.13 (0.41)  | 0.01 (0.95)  | 0.16 (0.31)  | -0.03 (0.88) | 0.24 (0.13)  | 0.32 (0.04)  | 0.11 (0.48)  | 0.03 (0.87)  |  |  |
| DL1L | 0.09 (0.57)           | 0.05 (0.78)  | -0.02 (0.88) | 0.04 (0.82)  | 0.10 (0.52)  | 0.04 (0.82)  | 0.02 (0.93)  | 0.07 (0.67)  | 0.07 (0.59)  | 0.09 (0.59)  | 0.01 (0.99)  | 0.08 (0.63)  |  |  |
| DL2L | 0.09 (0.56)           | 0.08 (0.63)  | -0.15 (0.34) | -0.02 (0.91) | 0.02 (0.92)  | 0.20 (0.22)  | 0.02 (0.93)  | -0.02 (0.94) | 0.03 (0.86)  | 0.13 (0.42)  | 0.01 (0.95)  | 0.13 (0.42)  |  |  |
| DL3L | -0.08 (0.61)          | 0.18 (0.27)  | -0.19 (0.23) | -0.06 (0.69) | 0.05 (0.75)  | 0.16 (0.33)  | -0.20 (0.21) | 0.04 (0.80)  | -0.14 (0.40) | 0.01 (0.99)  | 0.01 (0.97)  | 0.13 (0.44)  |  |  |
| DL4L | 0.03 (0.86)           | 0.12 (0.47)  | 0.01 (0.96)  | 0.09 (0.57)  | -0.01 (0.98) | 0.04 (0.81)  | -0.11 (0.49) | 0.03 (0.88)  | 0.08 (0.63)  | 0.14 (0.38)  | 0.04 (0.80)  | 0.03 (0.85)  |  |  |
| DL5L | -0.03 (0.84)          | 0.20 (0.20)  | -0.16 (0.33) | 0.08 (0.64)  | 0.03 (0.84)  | 0.03 (0.84)  | -0.10 (0.52) | 0.08 (0.62)  | -0.13 (0.44) | 0.12 (0.46)  | -0.01 (0.94) | 0.04 (0.79)  |  |  |
| FLL  | 0.02 (0.90)           | 0.03 (0.84)  | -0.16 (0.33) | -0.07 (0.65) | -0.03 (0.83) | -0.01 (0.99) | -0.03 (0.87) | -0.07 (0.65) | -0.03 (0.85) | 0.04 (0.82)  | -0.07 (0.65) | -0.06 (0.71) |  |  |
| FWL  | 0.17 (0.29)           | 0.13 (0.44)  | -0.06 (0.69) | 0.17 (0.30)  | 0.03 (0.87)  | -0.06 (0.69) | 0.06 (0.71)  | -0.08 (0.63) | 0.11 (0.48)  | 0.33 (0.03)  | 0.01 (0.94)  | -0.04 (0.79) |  |  |

IA1R: Intermetatarsal angle right before lockdown, IA1L: Intermetatarsal angle left before lockdown, HA1R: Hindfoot varus angle right before lockdown, HA1L: Hindfoot varus angle left before lockdown, HVA1R: Hallux valgus angle right after lockdown, HVA1L: Hallux valgus angle left after lockdown, IA2R: Intermetatarsal angle right after lockdown, IA2L: Intermetatarsal angle left after lockdown, HA2R: Hindfoot varus angle right after lockdown, HA2L: Hindfoot varus angle left after lockdown, HVA2R: Hallux valgus angle right after lockdown, HVA2L: Hallux valgus angle left after lockdown, BMI1: Body mass index before lockdown, BMI2: Body mass index after lockdown, Year: The year she studied ballet, DL1R: Digit 1 length right, DL2R: Digit 2 length right, DL3R: Digit 3 length right, DL4R: Digit 4 length right, DL5R: Digit 5 length right, FLR: Foot length right, FWR: Foot width right, DL1L: Digit 1 length left, DL2L: Digit 2 length left, DL3L: Digit 3 length left, DL4L: Digit 4 length left, DL5L: Digit 5 length left, FLL: Foot length left, FWL: Foot width left, *r*: Pearson correlation analysis value, *P*: Degree of significance

Table 4: Correlation analysis between foot angles

|       | <i>r</i> ( <i>P</i> ) |             |             |              |              |              |             |             |             |              |              |              |  |  |
|-------|-----------------------|-------------|-------------|--------------|--------------|--------------|-------------|-------------|-------------|--------------|--------------|--------------|--|--|
|       | IAIR                  | IAIL        | HAIR        | HAIL         | HVAIR        | HVA1L        | IA2R        | IA2L        | HA2R        | HA2L         | HVA2R        | HVA2L        |  |  |
| IAIR  | -                     | 0.58 (0.00) | 0.71 (0.00) | 0.33 (0.03)  | 0.43 (0.01)  | 0.38 (0.02)  | 0.95 (0.00) | 0.64 (0.00) | 0.76 (0.00) | 0.40 (0.01)  | 0.45 (0.00)  | 0.41 (0.01)  |  |  |
| IAIL  | 0.58 (0.00)           | -           | 0.24 (0.13) | 0.37 (0.02)  | 0.38 (0.02)  | 0.13 (0.41)  | 0.04 (0.83) | 0.61 (0.00) | 0.93 (0.00) | 0.27 (0.09)  | 0.39 (0.01)  | 0.48 (0.00)  |  |  |
| HAIR  | 0.71 (0.00)           | 0.24 (0.13) | -           | 0.38 (0.01)  | 0.13 (0.41)  | 0.04 (0.83)  | 0.61 (0.00) | 0.35 (0.03) | 0.95 (0.00) | 0.40 (0.01)  | 0.15 (0.35)  | 0.08 (0.60)  |  |  |
| HAIL  | 0.33 (0.03)           | 0.37 (0.02) | 0.38 (0.01) | -            | -0.23 (0.15) | -0.29 (0.07) | 0.33 (0.03) | 0.36 (0.02) | 0.38 (0.01) | 0.94 (0.00)  | -0.22 (0.17) | -0.23 (0.16) |  |  |
| HVAIR | 0.43 (0.01)           | 0.38 (0.01) | 0.13 (0.41) | -0.23 (0.15) | -            | 0.83 (0.00)  | 0.42 (0.01) | 0.39 (0.01) | 0.16 (0.31) | -0.13 (0.43) | 0.99 (0.00)  | 0.85 (0.00)  |  |  |
| HVA1L | 0.38 (0.01)           | 0.46 (0.00) | 0.04 (0.83) | -0.29 (0.07) | 0.83 (0.00)  | -            | 0.40 (0.01) | 0.51 (0.01) | 0.06 (0.69) | -0.19 (0.25) | 0.83 (0.00)  | 0.99 (0.00)  |  |  |
| IA2R  | 0.95 (0.00)           | 0.62 (0.00) | 0.61 (0.00) | 0.33 (0.03)  | 0.42 (0.01)  | 0.39 (0.01)  | -           | 0.72 (0.00) | 0.65 (0.00) | 0.38 (0.02)  | 0.45 (0.00)  | 0.43 (0.01)  |  |  |
| IA2L  | 0.64 (0.00)           | 0.93 (0.00) | 0.36 (0.02) | 0.35 (0.03)  | 0.39 (0.01)  | 0.51 (0.00)  | 0.72 (0.00) | -           | 0.32 (0.04) | 0.32 (0.04)  | 0.41 (0.01)  | 0.53 (0.00)  |  |  |
| HA2R  | 0.76 (0.00)           | 0.27 (0.09) | 0.95 (0.00) | 0.38 (0.01)  | 0.16 (0.31)  | 0.06 (0.69)  | 0.65 (0.00) | 0.32 (0.04) | -           | 0.46 (0.00)  | 0.17 (0.28)  | 0.10 (0.55)  |  |  |
| HA2L  | 0.40 (0.01)           | 0.38 (0.02) | 0.40 (0.01) | 0.94 (0.00)  | -0.13 (0.43) | -0.19 (0.25) | 0.38 (0.02) | 0.32 (0.04) | 0.46 (0.00) | -            | -0.12 (0.45) | -0.14 (0.39) |  |  |
| HVA2R | 0.45 (0.00)           | 0.39 (0.01) | 0.15 (0.35) | -0.22 (0.17) | 0.99 (0.00)  | 0.83 (0.00)  | 0.45 (0.00) | 0.41 (0.01) | 0.17 (0.28) | -0.12 (0.45) | -            | 0.86 (0.00)  |  |  |
| HVA2L | 0.41 (0.01)           | 0.48 (0.00) | 0.08 (0.60) | -0.22 (0.16) | 0.85 (0.00)  | 0.99 (0.00)  | 0.43 (0.01) | 0.53 (0.00) | 0.10 (0.55) | -0.14 (0.39) | 0.86 (0.00)  | -            |  |  |

IAIR: Intermetatarsal angle right before lockdown, IAIL: Intermetatarsal angle left before lockdown, HAIR: Hindfoot varus angle right before lockdown, HA1L: Hindfoot varus angle left before lockdown, HVA1R: Hallux valgus angle left before lockdown, IA2R: Intermetatarsal angle right after lockdown,

IA2L: Intermetatarsal angle left after lockdown, HA2R: Hindfoot varus angle right after lockdown, HA2L: Hindfoot varus angle left after lockdown, HVA2R: Hallux valgus angle right after lockdown, HVA2L: Hallux valgus angle left after lockdown, *r*: Pearson correlation analysis value, *P*: Degree of significance

after the lockdown. We evaluated the hallux valgus angle on the left side before and after lockdown as  $23.73 \pm 0.59$  and  $25.58 \pm 0.61$ , respectively. We observed an increase in the values on the right and left sides after lockdown. However, it was not statistically significant. We also noticed that the right side has more tendency to be hallux valgus deformity. The results of our study were found to be higher than the normal values in the literature. We think that this result is due to the fact that the individuals in our study have been doing ballet for an average of  $6.93 \pm 2.32$  years. Hallux valgus degrees of ballet students in our study were found to be low. Hallux valgus deformity is usually accompanied by an increase in the intermetatarsal angle. In the ballet students in our study, the intermetatarsal angle values on the right side were found to be  $18.18 \pm 0.21$  before lockdown,  $19.77 \pm 0.23$  after lockdown,  $17.60 \pm 0.19$  before lockdown, and  $19.12 \pm 0.22$  after lockdown on the left side. A significant increase was observed after lockdown on both sides (right  $P = 0.002$  and left  $P = 0.001$ ). The increase in the intermetatarsal angle was also seen more on the right side. The increase in intermetatarsal angle values after lockdown in ballet students supports the increase in hallux valgus angle values [Table 2]. In our correlation analysis results, a strong positive correlation was found between the intermetatarsal angle and the hallux valgus angle on both the right and left sides before and after the lockdown. Another angle in our study that is positively correlated with the intermetatarsal angle on both sides and before and after lockdown is the hindfoot varus angle. In the ballet students in our study, the hindfoot varus angle on the right side was  $8.18 \pm 0.23$  before lockdown and  $9.89-0.25$  after lockdown,  $8.32 \pm 0.20$  before lockdown, and  $9.05 \pm 0.23$  after lockdown on the left side. It was found that there was a significant increase in hindfoot varus angle values on both sides (right  $P = 0.002$  and left  $P = 0.001$ ) after lockdown. It occurs as a result of an imbalance in hindfoot varus muscle strength. During the lockdown process, we thought that there might be changes in muscle strength due to the disruption of the ballet training in the ballet studio. Therefore, we included the hindfoot varus angle, which will reflect the change in muscle strength, in our measurements. The back of the foot is in varus, the lateral part of the foot overloading and thus ankle instability, peroneal tendinitis, and stress fracture. Hindfoot movements were examined and showed within normal ( $5^{\circ}$ – $10^{\circ}$ ) inversion values and eversion values ( $10^{\circ}$ – $20^{\circ}$ ) at the subtalar joint.<sup>[11]</sup> The hindfoot varus degree values in our study showed a significant increase after lockdown on both the right and left sides. The hindfoot varus degrees of ballet students in our study before and after lockdown were within the normal range in both inversion and eversion. Moreover, in our study, we also included ballet students' morphometric measurements such as digit lengths, foot lengths, and foot widths. No relationship was found between the foot angles and these length and width measurements. Hallux valgus angle, intermetatarsal angle, and hindfoot varus angles increased after the lockdown period. We can say that this result shows us that the COVID-19 lockdown process

increases the tend to foot injury in ballet students. We think that this is due to continuing their ballet training on their own or online without ballet instructors in ballet studios. Most ballets are absolutely and completely committed to ballet, making great sacrifices during their training from a young age onward, with the aim of becoming professional ballet dancers. In the everyday schedule of training and rehearsals, discipline is a fundamental prerequisite for a career as a professional ballet dancer. Ballet students must work with perseverance, purpose, and concentration. They are used to accepting and swiftly reacting to criticism and constructively taking instructions.<sup>[12,13]</sup> Therefore, during the lockdown due to COVID-19, ballet students stayed away from ballet studios with mirrors, one-on-one guidance from their instructors, and training with their group mates. We think that this situation will increase the susceptibility to injuries. For example, during every relevé, pay attention to the optimal weight distribution in the foot. The main load should lie between the first and second metatarsals. Especially if the mobility of the metatarsophalangeal joint of the big toe is limited, it cannot compensate for this lacking range of motion by “sickling” the foot when rising to relevé. Otherwise, the first and second metatarsals will be overloaded; injuries and deformities may occur with the increase of the hallux valgus angle and the intermetatarsal angle.

## Conclusion

With this study, we wanted to emphasize the importance of training with teamwork in ballet studios and training with a ballet trainer during the lockdown process. In addition, we think that we will guide orthopedists and physical therapists with measurement values that will affect foot deformities and tend to injury in ballet students. To prevent such injuries, we recommend performing supportive practices such as mobilizing the tarsus, strengthening the transverse arch respectively and the intrinsic foot muscles, strengthening the long peroneal muscle, contract-relax stretching of the calf muscles.<sup>[14]</sup> We also think that the following points will prevent injuries in daily life:

- Watch out when walking – and especially when jogging – to put down your feet as parallel as possible and push off from the transverse arch
- Let your feet have a rest sometimes. A footbath in the evening will relax the foot muscles. Massage the painful spots and pay particular attention to the inner side and the sole as well as to the insertion of the Achilles tendon
- Take your time when buying shoes. All of your shoes should fit properly, not only dance ones. Especially after long training days, your walking shoes should not put additional strain on your feet.

Since the COVID-19 is a pandemic process, measurements with instruments could not be made by direct physical contact. Evaluations were made quickly

and safely with the photographing method. However, the flexibility factor, which we think will be affected by lockdown, could not be evaluated. This is one of the limitations of the study. We suggest that similar studies in which the flexibility factor is evaluated be produced with more ballet students.

## Financial support and sponsorship

Nil.

## Conflicts of interest

There are no conflicts of interest.

## References

1. Tariao FC, Yang JM. Delivering face-to-face dance classes in Singapore during the COVID-19 pandemic. *Journal of Dance Education* 2022;22:233-44.
2. Bird JM, Karageorghis CI, Hamer M. Relationships among behavioural regulations, physical activity, and mental health pre- and during COVID-19 UK lockdown. *Psychol Sport Exerc* 2021;55:101945.
3. Li F, Adrien N, He Y. Biomechanical risks associated with foot and ankle injuries in ballet dancers: A systematic review. *Int J Environ Res Public Health* 2022;19:4916.
4. Kabakci AG, Yücel AH. Basic Five Foot Positions and Anatomical Structure in Classical Ballet. *Journal of Archive Literature Review* 2018;27:414-25.
5. Stephens N, Nevill AM, Wyon MA. Injury incidence and severity in musical theatre dance students: 5-year prospective study. *Int J Sports Med* 2021;42:1222-7.
6. Dang Y, Koutedakis Y, Wyon M. Fit to dance survey: Elements of lifestyle and injury incidence in Chinese dancers. *Med Probl Perform Art* 2020;35:10-8.
7. Pietrobelli A, Pecoraro L, Ferruzzi A, Heo M, Faith M, Zoller T, *et al.* Effects of COVID-19 lockdown on lifestyle behaviors in children with obesity living in Verona, Italy: A longitudinal study. *Obesity (Silver Spring)* 2020;28:1382-5.
8. de Boer W, Corpeleijn E, Dekker L, Mierau J, Koning R. How is sport participation related to mortality, diabetes and prediabetes for different body mass index levels? *Scand J Med Sci Sports* 2021;31:1342-51.
9. Ying J, Xu Y, István B, Ren F. Adjusted indirect and mixed comparisons of conservative treatments for hallux valgus: A systematic review and network meta-analysis. *Int J Environ Res Public Health* 2021;18:3841.
10. Li HT, Bao BX, Zhang JZ. Effects of single-foot centered and double-foot centered x-ray projection on hallux valgus measurement. *Orthop Surg* 2020;12:94-9.
11. El-Sayed MM, Seleem OA. Hind-foot correction and stabilization by pins in plaster after surgical release of talipes equino varus feet in older children. *J Orthop Surg Res* 2010;5:42.
12. Huang PY, Lin CW, Jankaew A, Lin CF. Relationship of extrinsic risk factors to lower extremity injury in collegiate ballet dancers. *Front Bioeng Biotechnol* 2022;10:878448.
13. Novosel B, Sekulic D, Peric M, Kondric M, Zaletel P. Injury occurrence and return to dance in professional ballet: Prospective analysis of specific correlates. *Int J Environ Res Public Health* 2019;16:765.
14. Skwiot M, Śliwiński Z, Żurawski A, Śliwiński G. Effectiveness of physiotherapy interventions for injury in ballet dancers: A systematic review. *PLoS One* 2021;16:e0253437.

# Pneumatized Crista Galli and its Correlation with Intraethmoidal Location of the Anterior Ethmoidal Artery

## Abstract

**Background/Aim:** Crista galli (CG) is an essential anatomical formation located in the midline on the cribriform plate. In the presence of pneumatized CG (PCG) variations, changes will occur in the anatomy of the anterior skull base. Anterior ethmoidal artery (AEA) crosses the medial wall of the orbit and progresses intraethmoidally; in case it is damaged during endoscopic procedures, it may cause severe epistaxis or intraorbital hematoma. This study aims to examine the CG morphometric features in the Turkish population and to investigate the changes in the distance of the AEA from the nasion and sphenoidal sinus (SS) according to CG morphometry. **Materials and Methods:** In the study, computerized tomography images of 200 cases were used, CG height-in the coronal plane, PCG ratio, and the distances of the AEA from the nasion line to the anterior wall of the SS were measured in the horizontal plane. In the presence of PCG, the changes in AEA according to their distance from the mentioned formations were examined. **Results:** The mean CG height was  $12.8 \pm 2.4$  mm; partial or total pneumatization was observed in 31.5% of the cases. The average distance from the anterior border of the AEA to the Nasion during its intraethmoidal course was  $28.3 \pm 3.6$  mm, with males having a greater distance than females. Additionally, the average distance to the anterior wall of SS was  $17.5 \pm 2.9$  mm. **Conclusion:** This study determined that the distance of the AEA to the nasion was greater in cases with PCG than in cases without pneumatization on both sides.

**Keywords:** Anterior ethmoidal artery, computed tomography, crista galli, pneumatized crista galli, variation

## Introduction

The anatomical structure known as the crista galli (CG) is located above the cribriform plate in the midline. It has a thin, curved shape that extends to the vertical line and serves as the falx cerebri's attachment point.<sup>[1]</sup> An important marker for transcribriiform and extradural endoscopic interventions is the determination of the midline. As a result, numerous studies on its localization, variations in its morphometry, and its relationship with neighboring structures have been published in the literature.<sup>[2]</sup> Studies have also suggested that CG morphometric characteristics can be used to determine sex.<sup>[3]</sup>

In most cases, the CG is a compact bone; however, pneumatized CG (PCG) refers to separating the bone lamellae and air filling. Rates of PCG in the general population range from 2.4% to 66.6%.<sup>[1,4]</sup> It has been demonstrated that PCG is connected to air chambers in the frontal sinus and/

This is an open access journal, and articles are distributed under the terms of the Creative Commons Attribution-NonCommercial-ShareAlike 4.0 License, which allows others to remix, tweak, and build upon the work non-commercially, as long as appropriate credit is given and the new creations are licensed under the identical terms.

For reprints contact: WKHLRPMedknow\_reprints@wolterskluwer.com

or anterior ethmoidal cells.<sup>[5]</sup> Because it contributes to the etiology of recurrent headaches, pneumatization of the CG may be impacted by chronic sinusitis and results in complications. It has been suggested in the literature that patients with chronic headaches who evacuate their PCG content may have more success treating their chronic sinusitis and that there may be a connection between PCG and mucocele.<sup>[6,7]</sup>

Nasion is a popular anthropometric point for determining the midline of the skull in addition to CG. The deepest point of the nasofrontal groove is the nasion, which is where the frontal bone and nasal bones converge.<sup>[8]</sup> Different ethnic groups have different depths and morphometric traits.<sup>[9]</sup> This anthropometric point serves as an important landmark in endoscopic approaches to the frontal region and anterior skull base, including the modified Lothrop procedure.<sup>[8]</sup>

The term "sphenoidal sinus (SS)" refers to the numerous air chambers found within the body of the sphenoid bone.

**How to cite this article:** Yaprak F, Coban I, Ozer MA, Govsa F. Pneumatized crista galli and its correlation with intraethmoidal location of the anterior ethmoidal artery. *J Anat Soc India* 2023;72:355-9.

Fulya Yaprak,  
Istemihan Coban,  
Mehmet Asim Ozer<sup>1</sup>,  
Figen Govsa<sup>1</sup>

Department of Anatomy, Faculty of Medicine, Izmir Democracy University, <sup>1</sup>Department of Anatomy, Faculty of Medicine, Ege University, Izmir, Turkey

## Article Info

Received: 02 February 2023

Revised: 09 November 2023

Accepted: 10 November 2023

Available online: 30 December 2023

## Address for correspondence:

Dr. Fulya Yaprak,  
Department of Anatomy, Faculty of Medicine, Izmir Democracy University, Izmir, Turkey.  
E-mail: fulyayaprak@hotmail.com

## Access this article online

Website: <https://journals.lww.com/joai>

DOI:  
10.4103/jasi.jasi\_12\_23

## Quick Response Code:



In transsphenoidal approaches to skull base lesions and interventions to the pituitary, optic chiasm, and cavernous sinus, the anterior wall of this sinus serves as a crucial anatomical barrier.<sup>[10]</sup> The anterior ethmoidal artery (AEA) is the most dangerous artery that could result in severe intra- and postoperative complications during endoscopic procedures approaching the skull base from the anterior and posterior directions.<sup>[11]</sup> After passing through the optic canal, the AEA becomes a branch of the ophthalmic artery. The ethmoidal labyrinth, the orbit, and the anterior cranial fossa are where the AEA is located throughout its path. It travels to the intraethmoidal/intranasal region after exiting the orbit through the same-named foramen. This section of the artery travels anteriorly either freely or in a bony canal. Numerous studies have demonstrated that changes or subsequent anomalies in the sinonasal region have an impact on the AEA either directly or indirectly.<sup>[12,13]</sup> This interaction will inevitably be clinically reflected. Surgery in the paranasal region, which experiences high variation rates, carries a high risk of AEA injury. Due to its elastic structure, it may retract into the orbit and cause hemorrhage into the orbit and hematoma if it is traumatized, which may also result in nosebleeds. If the orbital hemorrhage is not treated, the pressure in this compartment will increase, which could compress the optic nerve and have severe consequences such as blindness.<sup>[14]</sup>

This study sought to determine the distance between the anterior wall of the SS and the AEA during its intraethmoidal course, as well as the relationship between these measurements and the presence of CG height and PCG.

## Materials and Methods

### Study design

This descriptive study retrospectively examined multiplanar thin-section computerized tomography (CT) images obtained at the hospital archive, between 2018 and 2020. The images were captured using a “6-Slice Multidetector CT scanner” (Philips Brilliance 6, Philips Medical Systems, Amsterdam, The Netherlands), and the cases for the study were chosen from those with images containing at least 150–400 slices of 0.6–1 mm thickness and an acquisition dose of 120 kV to 220 mA. Coronal, sagittal, and horizontal CT slices from the images examined through the Sectra IDS7 version 21.2.15.6346©2019 program were evaluated together by two separate observers.

### Study group

Two hundred patients (100 men and 100 women) aged between 18 and 70 were included in the research. Exclusion criteria were history of the previous skull base or paranasal sinus surgery, congenital facial anomaly, history of disease or trauma causing erosion of the ethmoid roof, presence of chromosomal anomaly, being younger than 18 years and older than 70 years at the time of image acquisition, and poor image quality in imaging methods.

## Methods

The distance from the most anterior border of the intranasal part of AEA to the level of nasion was measured. The localization of the nasion was determined by comparison with the sagittal plane image at the same level [Figure 1a].

The anteroposterior distance of the AEA from the most anterior level of the anterior wall of the SS during its course in the ethmoidal labyrinth was measured. This measurement was performed by determining the level of the anterior wall of the SS in the sagittal plane and marking it in the horizontal plane [Figure 1b]. The values were compared between gender, age group, and the right and left sides. Statistical analyses were performed in the evaluations, and significance was investigated.

CG height was measured in the section where the CG was the highest in the coronal plane on computed tomography images. In the current study, cases with PCG were identified, and the presence of this variation was investigated regardless of partial or total ventilation [Figure 2]. In addition, in cases with PCG, the relationship between the distance of the posterior border to the anterior wall of SS and the distance of the anterior border to the nasion during the intraethmoidal course of the AEA was examined.

### Statistical analysis

Statistical analyses were carried out using Stata, version 13.0, web-based R software (R Foundation for Statistical Computing, version 3.5.2, package: nparLD), and IBM SPSS Statistics 25.0 (IBM SPSS Statistics for Windows, version 25.0. Armonk, NY, USA: IBM Corp.) (StataCorp LLC, 4905 Lakeway Drive, College Station, Texas 77,845, USA). The Shapiro–Wilk test was used to determine whether the numerical variables fit the “Normal Distribution.” In the study, categorical data

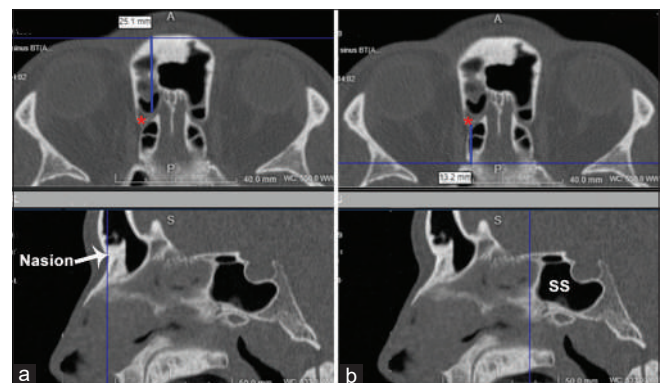


**Figure 1:** (a) In the sagittal section in the lower image, the line passing through the nasion is seen as a horizontal blue line in the upper image. The distance from the anterior border of the arteria ethmoidalis anterior (\*) to this line was measured during its intraethmoidal course. (b) In the sagittal section in the lower image, the line passing through the anterior bony border of the sinus sphenoidalis is traced as a horizontal blue line in the upper image. The distance from the posterior border of the arteria ethmoidalis anterior (\*) to this line was measured during its intraethmoidal course. SS: Sphenoidal sinus, \*: Anterior ethmoidal artery where it leaves the orbit

were summarized using frequency and ratio values, while numerical data were summarized using mean, standard deviation, median, and range values. In all analyses, the significance level was set at  $P < 0.05$ . The Mann–Whitney  $U$ -test was used for two independent group comparisons for all quantitative variables. The relationship between qualitative variables was examined using either Fisher’s exact probability testing or Pearson’s Chi-square testing. The relationship between quantitative variables was evaluated using Spearman correlation analysis.

**Ethics committee**

This radioanatomical, descriptive study was evaluated by the Medical Research Ethics Committee and approved with protocol number 20-7.1T/12.

**Results**

The ages of the patients included in the study ranged from 18 to 70 years, with a mean of  $46 \pm 14$  years (47 in women and 45 in men); 49% of the patients were in Group 1 and 51% were in Group 2, when we divided the patients into two groups according to their ages as Group 1: 18–45 and Group 2: 46–70.

The distance of the anterior border of the AEA during the intraethmoidal course of the AEA to the nasion in the

horizontal plane was measured as  $28.3 \pm 3.6$  mm (16.1–40.0) on average in 400 arteries. This value was close to the mean and standard deviation on the right ( $28.4 \pm 3.6$  mm) and left ( $28.2 \pm 3.5$  mm) ( $P = 0.202$ ). It was  $28.4 \pm 3.6$  mm between 18 and 45 years and  $28.2 \pm 3.5$  mm between 45 and 70 years ( $P = 0.891$ ). The mean values were  $29.3 \pm 3.6$  mm (17.6–40.0) in males and  $27.3 \pm 3.3$  mm (16.1–37.0) in females, and there was a statistically significant difference with gender [ $P < 0.001$ , Table 1].

The distance perpendicular to the anterior wall of the SS during the progression of the AEA in the ethmoidal labyrinth until it leaves the orbit and enters the skull base (AEA-SS) averaged  $17.5 \pm 2.9$  mm (8.6–26.2) in 400 arteries. When the right side was specifically evaluated, this value was  $17.6 \pm 2.8$  mm, whereas  $17.4 \pm 3.0$  mm on the left side ( $P = 0.143$ ). In women, this value was  $17.5 \pm 3.2$  and  $17.4 \pm 2.6$  mm in men ( $P = 0.492$ ). The distance was  $17.5 \pm 3.27$  mm between 18 and 45 years and  $17.5 \pm 3.04$  mm between 45 and 70 years; however, this difference was not statistically significant [ $P = 0.806$ , Table 1].

The mean CG height was  $12.8 \pm 2.4$  mm (7.1–19.7). It was  $12.9 \pm 2.5$  mm between 18 and 45 and  $12.8 \pm 2.2$  mm between 46 and 70 years of age. This value was  $12.9 \pm 2.2$  mm in women and  $12.8 \pm 2.6$  mm in men. No significant difference was found in our data according to gender and age group variables [ $P = 0.664$  and  $P = 0.696$ , respectively, Table 1].

CG pneumatization was found in 35% of men and 28% of women; 28% between 18 and 45 years and 35% between 46 and 70 years, but these differences were not statistically significant [ $P = 0.149$  for gender and  $P = 0.238$  for age groups, Table 1]. The current study group found PCG at an average rate of 31.5%.

The mean CG height was  $12.9 \pm 2.4$  mm in patients with PCG. The mean distance of the AEA to the nasion was 29.2 mm on the left and 29.3 mm on the right, whereas the mean distance to the anterior wall of the SS was 17.4 mm on the left and 17.6 mm on the right in cases with PCG. It is statistically significant that the distance from the anterior border of the AEA to the nasion tends to increase in the presence of PCG ( $P = 0.039$  on the right and  $P = 0.022$  on the left).

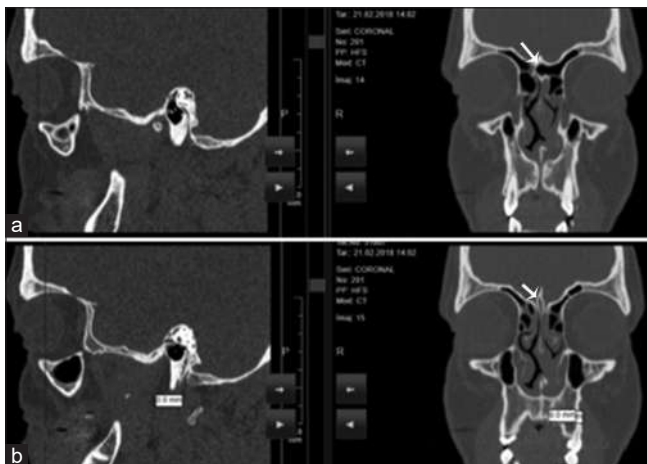


Figure 2: (a) A coronal section taken more anteriorly than in image b shows a pneumatized crista galli (PCG) associated with the sinus frontalis in the right image (white arrow). (b) A coronal section was taken more posteriorly than in image a, showing a normal crista galli in the right image (white arrow). This case can be given as an example of partial PCG

**Table 1: Comparison of the data related to the anterior ethmoidal artery, nasion, sphenoidal sinus, and crista galli according to age group and gender**

| Measurements;<br>mean±SD (range) (mm) | Gender    |           | Age groups |           | Total                |
|---------------------------------------|-----------|-----------|------------|-----------|----------------------|
|                                       | Female    | Male      | 18–45      | 46–70     |                      |
| AEA-Nasion                            | 27.3±3.3* | 29.3±3.6* | 28.4±3.6   | 28.2±3.5  | 28.3±3.6 (16.1–40.0) |
| AEA-SS                                | 17.5±3.2  | 17.4±2.6  | 17.6±2.8   | 17.4±3.0  | 17.5±2.9 (8.6–26.2)  |
| CG height                             | 12.9±2.2  | 12.8±2.6  | 12.9±2.5   | 12.8±2.2  | 12.8±2.4 (7.1–19.7)  |
| PCG, n (%)                            | 28 (28.0) | 35 (35.0) | 28 (28.0)  | 35 (35.0) | 63 (31.5)            |

\* $P < 0.001$ . PCG: Pneumatized crista galli, SD: Standard deviation, AEA: Anterior ethmoidal artery, CG: Crista galli, AEA-SS: AEA-sphenoidal sinus

## Discussion

Studies investigating PCG found frequency of PCG between 2.4% and 66.6%. The average study group age, the study group's ethnicity, and methodological differences could all be contributing factors to the wide range. For instance, this rate was only 4.6% in histopathologic studies,<sup>[15]</sup> whereas 66.6% in a study using CT scans of adult human skulls.<sup>[4]</sup> In a radiologic study on children, this rate was 12.2%, but Al Quadah discovered a PCG rate of 28% in a radiologic study on adults.<sup>[16]</sup> This rate was 30.1% in a CT study on 196 patients admitted to the otorhinolaryngology clinic due to chronic sinusitis.<sup>[17]</sup> The frequency of PCG in our study was found to be 31.5%, which is consistent with that of another study in Turkey, with a rate of 29.8% with 402 asymptomatic patients.<sup>[18]</sup> The fact that we included nontotal PCGs may be why our value, which was higher than studies done in the general population, like the study by Al-Quadah,<sup>[16]</sup> is higher. Even though the presence of PCG was higher in women than in men and in the age group of 46–70 years compared to the age group of 18–45 years, this difference was not statistically significant. Similar to this outcome, no correlation between the presence of PCG and age was discovered in a study carried out in Turkey in 2021.<sup>[2]</sup>

CG is a crest-shaped structure extending into the anterior skull base cavity, and the falx cerebri and dura mater are attached to this bony protrusion. During the endoscopic intervention of some tumors located in the anterior skull base, the falx cerebri must be separated from its attachment to the CG. Throughout this surgical procedure, part of the upper end of the CG is removed by drilling. Therefore, the vertical height of the CG is as essential clinically as its morphologic type or anteroposterior length. In a radiological study by Lee *et al.* in Canada, the CG vertical height was  $12.9 \pm 2.5$  mm.<sup>[19]</sup> In a study in Japan in 2020 on patients with brain tumors, the mean CG height was  $15.9\text{--}3.2$  mm ( $7.3\text{--}26.0$  mm).<sup>[20]</sup> In studies conducted in Turkey on CG height, the results were close. While in the study by Uçar *et al.* on CT images, CG height was  $14.0 \pm 2.9$  mm ( $6.0\text{--}23.4$  mm),<sup>[2]</sup> in another study conducted in Turkey in 2021, CG height was  $14.1 \pm 3.1$  mm ( $6.6\text{--}22.6$  mm); in the most mentioned study, the likelihood of male gender in patients with a CG height above 15.15 mm was approximately 12 times higher than in patients with a CG height  $< 15.5$  mm.<sup>[3]</sup> In the current study, the mean CG height was  $12.8 \pm 2.4$  mm, which was minimally lower than other studies conducted in the same country and close to the study of Lee *et al.*<sup>[19]</sup> Although this value was 1 cm higher in males, this difference between genders was not statistically significant. The mean CG height was  $12.9 \pm 2.4$  mm in patients with PCG. In a 2017 study conducted in Croatia on CT images of 102 skulls, the mean CG height was found to be  $10.1 \pm 3.0$  mm ( $3.6\text{--}17.1$  mm), and it was found to

be statistically significant that CG height was higher in women (mean 14.2 in women and 9.5 in men) in cases with PCG.<sup>[4]</sup> According to the findings in our study, it cannot be said that there is a significant correlation between the presence of PCG and CG elevation independent of gender and age group.

In endoscopic interventions in the sinonasal region, the nasion and the anterior wall of the SS can be determined, and the potential distance of the AEA to these structures can be estimated. In cases where an anterior approach to the frontonasal region is required, such as the modified Lothrop procedure, the relationship between the nasion and the AEA is important. In our study, the distance from the point where the AEA was closest to the nasion during its intraethmoidal course to the vertical line passing through the nasion was found  $28.3 \pm 3.6$  mm and longer in men. The difference in this distance between genders should be taken into consideration. The distance of the AEA from the vertical line passing through the anterior wall of the SS, which may also be important in approaching the posterior skull base in endoscopic interventions, was  $17.5 \pm 2.9$  mm, although there was no significant difference between genders. Considering this information in cases where the artery should be approached posteriorly may help clinicians prevent possible intraoperative and postoperative complications.

The cases were not classified in this study, although various classification studies had been carried out based on the location and extent of PCG.<sup>[4,20,21]</sup> This study did not address the connection between the size of the PCG and the correlation with the distance between the AEA and the nasion and SS. Future research should examine the morphometry of CG and AEA in patients with chronic sinusitis and mucocele in addition to the general population, considering that symptomatic patients may require more frequent endoscopic intervention.

## Conclusion

Our study determined that the distance of the AEA to the nasion was greater in patients with PCG compared to those without pneumatization on both sides. Therefore, it can be suggested that the presence of PCG is not riskier in arterial injury during interventional procedures.

## Ethics approval

Approval was obtained from the institutional review board of Faculty of Medicine (approval number: 20-7.1T/12. H.). The procedures used in this study adhere to the tenets of the Declaration of Helsinki.

## Financial support and sponsorship

Nil.

## Conflicts of interest

There are no conflicts of interest.

## References

1. Basić N, Basić V, Jukić T, Basić M, Jelić M, Hat J. Computed tomographic imaging to determine the frequency of anatomical variations in pneumatization of the ethmoid bone. *Eur Arch Otorhinolaryngol* 1999;256:69-71.
2. Uçar H, Bahşi I, Orhan M, Yalçın ED. The radiological evaluation of the crista galli and its clinical implications for anterior skull base surgery. *J Craniofac Surg* 2021;32:1928-30.
3. Komut E, Golpinar M. A comprehensive morphometric analysis of crista galli for sex determination with a novel morphological classification on computed tomography images. *Surg Radiol Anat* 2021;43:1989-98.
4. Mladina R, Antunović R, Cingi C, Muluk NB, Skitarelić N, Malić M. An anatomical study of pneumatized crista galli. *Neurosurg Rev* 2017;40:671-8.
5. Alsaied AS. *Paranasal Sinus Anatomy: What the Surgeon Needs to Know*. London: IntechOpen; 2017. p. 3-36. Available from: <https://www.intechopen.com/chapters/55472>. [Last accessed on 2023 Jan 30].
6. Socher JA, Santos PG, Correa VC, Silva LC. Endoscopic surgery in the treatment of crista galli pneumatization evolving with localized frontal headaches. *Int Arch Otorhinolaryngol* 2014;17:246-50.
7. Ghanei M, Harandi AA, Rezaei F, Vasei A. Sinus CT scan findings in patients with chronic cough following sulfur mustard inhalation: A case-control study. *Inhal Toxicol* 2006;18:1135-8.
8. Zhao Y, Liu J, Yang D, Han J, Zhao J, Wang Y. Trans-nasion-complex approach for endoscopic modified Lothrop procedure: Conception, anatomy, and technique. *Front Surg* 2022;9:871635.
9. Liang X, Sun S, Ma H, Gu T, Guo H, Zhao Z, *et al.* The ideal nasion in Chinese: A preference analysis of the general population. *J Craniofac Surg* 2022;33:2486-92.
10. Safarian M, Sadeghi M, Saedi B. Endoscopic sphenoid sinus anatomic considerations: A study on 60 cadavers. *Iran J Otorhinolaryngol* 2021;33:237-42.
11. Asanau A, Timoshenko AP, Vercherin P, Martin C, Prades JM. Sphenopalatine and anterior ethmoidal artery ligation for severe epistaxis. *Ann Otol Rhinol Laryngol* 2009;118:639-44.
12. Jang D, Lachanas V, White LC, Kountakis SE. Supraorbital ethmoid cell: A consistent landmark for endoscopic identification of the anterior ethmoidal artery. *Allergy Rhinol* 2014;151:1073-7.
13. Wong DK, Shao A, Campbell R, Douglas R. Anterior ethmoidal artery emerging anterior to bulla ethmoidalis: An abnormal anatomical variation in Waardenburg's syndrome. *Allergy Rhinol (Providence)* 2014;5:168-71.
14. Sargi ZB, Casiano RR. Surgical anatomy of the paranasal sinuses. In: Kountakis SE, Önerci M, editors. *Rhinologic and Sleep Apnea Surgical Techniques*. Berlin, Heidelberg: Springer; 2007.
15. Marjanovic Kavanagh M, Tokic T, Jakovcevic A, Smiljanic R, Bumber B, Prstacic R. Pneumatized crista galli: A histopathologic study. *Otolaryngol Head Neck Surg* 2020;163:517-21.
16. Al-Qudah MA. Anatomical variations in sino-nasal region: A computer tomography (CT) study. *J Med J* 2010;44:290-7.
17. Manea C, Mladina R. Crista galli sinusitis – A radiological impression or a real clinical entity. *J Rhinol* 2016;6:167-71.
18. Acar G, Cicekcibasi AE, Koplay M, Kelesoglu KS. The relationship between the pneumatization patterns of the frontal sinus, crista galli and nasal septum: A tomography study. *Turk Neurosurg* 2020;30:532-41.
19. Lee JM, Ransom E, Lee JY, Palmer JN, Chiu AG. Endoscopic anterior skull base surgery: Intraoperative considerations of the crista galli. *Skull Base* 2011;21:83-6.
20. Akiyama O, Kondo A. Classification of crista galli pneumatization and clinical considerations for anterior skull base surgery. *J Clin Neurosci* 2020;82:225-30.
21. Haggiannou J, Owens D, Whittet HB. Evaluation of anatomical variation of the crista galli using computed tomography. *Clin Anat* 2010;23:370-3.

## Middle Mesenteric Artery: A Rare Vascular Anomaly

### Abstract

**Background:** Normally, branches of superior mesenteric and inferior mesenteric arteries (IMA) supply the parts of intestine derived from midgut and hindgut and their variations are uncommon. One of the rarest variations is the presence of a middle mesenteric artery (MMA), an anomalous ventral branch of abdominal aorta originating in between the origins of superior and IMA supplying variable portions of the colon, sporadically reported mainly as case reports. **Materials and Methods:** While retrospectively examining multi-detector computed tomography angiographic abdominal scans of 500 subjects for analyzing the variations of branches of abdominal aorta, an anomalous artery supplying variable parts of colon was observed in one male patient. **Observations:** We report here an incidentally detected presence of MMA supplying large portions of colon in a male patient with nonrotation of gut, cholelithiasis, and portal hypertension. Computed tomography angiography of this patient also revealed variant celiac artery branching with hepatosplenic trunk and direct aortic origin of left gastric artery. Thus, there were five ventral branches of abdominal aorta supplying the gut which is a very rare presentation. Hepatic flexure of the colon was present between diaphragm and right lobe of the liver (Chilaiditi syndrome). **Discussion and Conclusion:** Our literature search has yielded 26 such cases reported globally, and to the best of our knowledge, this is the first report from India. Associated anomalies reported include abdominal aortic aneurysm, nonrotation of gut, and presence of other vascular anomalies. Failure to identify such an anomalous artery may result in its damage with subsequent bowel ischemia and other complications during surgery.

**Keywords:** Anomalous mesenteric arteries, aortic origin of left gastric artery, hepato-splenic trunk, middle mesenteric artery, nonrotation of gut

### Introduction

Normally, three ventral branches of abdominal aorta (AbA), namely the celiac (CA), superior mesenteric (SMA), and inferior mesenteric arteries (IMA) supply derivatives of embryonic foregut, midgut, and hindgut, respectively. Jejunal and ileal branches of SMA supply the loops of the small bowel. Ileocolic (ICA), right colic (RCA), and middle colic (MCA) branches from superior mesenteric and left colic and sigmoid branches from inferior mesenteric supply the colon and form an anastomotic marginal artery critical for nourishment of the colon. Detailed anatomical knowledge of colonic arterial supply is crucial for successful outcome of hemicolectomy and prevention of life-threatening mesenteric ischemia. Although variations in the branching pattern of CA are more frequently encountered, variant branching pattern of SMA and IMA are less common. One of the rarest variant is the middle

mesenteric artery (MMA) arising from the ventral aspect of abdominal aorta, between the origins of SMA and IMA and supplying variable portions of small and large intestines. Benton and Cotter were the first to report in the English literature, the presence of an artery arising directly from aorta and supplying entire transverse colon and proximal descending colon which was designated as duplicated IMA. There was a common trunk from SMA dividing into RCA and ICA and there was no MCA.<sup>[1]</sup> Reported prevalence of the MMA varies between 0.05% and 0.1%.<sup>[2,3]</sup> This anomalous artery has variously been reported as duplicated IMA, second SMA, accessory MCA, aortic origin of MCA, aortic origin of RCA, aortic origin of ICA, in previous reports. Lawdahl and Keller in 1987 coined the term “MMA” to denote an artery arising from aorta in between the origins of SMA and IMA.<sup>[4]</sup> In this report, we present an incidentally detected case of MMA supplying parts of intestine from terminal ileum to proximal descending colon.

This is an open access journal, and articles are distributed under the terms of the Creative Commons Attribution-NonCommercial-ShareAlike 4.0 License, which allows others to remix, tweak, and build upon the work non-commercially, as long as appropriate credit is given and the new creations are licensed under the identical terms.

For reprints contact: WKHLRPMedknow\_reprints@wolterskluwer.com

**How to cite this article:** Babu CSR, Kumar A, Sharma Y, Gupta OP. Middle mesenteric artery: A rare vascular anomaly. *J Anat Soc India* 2023;72:360-6.

**C. S. Ramesh Babu,**  
**Arjun Kumar<sup>1</sup>,**  
**Yashika Sharma<sup>2</sup>,**  
**O. P. Gupta<sup>2</sup>**

*Department of Anatomy,*  
*Muzaffarnagar Medical College,*  
*Muzaffarnagar; <sup>1</sup>Department*  
*of Anatomy, Subharti Medical*  
*College, <sup>2</sup>Dr. O. P. Gupta*  
*Imaging Center, Meerut,*  
*Uttar Pradesh, India*

### Article Info

**Received:** 29 October 2023

**Revised:** 04 November 2023

**Accepted:** 23 November 2023

**Available online:** 30 December 2023

### Address for correspondence:

*Prof. C. S. Ramesh Babu,*  
*Department of Anatomy,*  
*Muzaffarnagar Medical*  
*College, N. H. 58, Opposite*  
*Begrajpur Industrial Area,*  
*Muzaffarnagar - 251 203,*  
*Uttar Pradesh, India.*  
*E-mail: csrameshb@gmail.com*

### Access this article online

**Website:** <https://journals.lww.com/joai>

**DOI:**  
10.4103/jasi.jasi\_113\_23

### Quick Response Code:



## Materials and Methods

Contrast-enhanced multi-detector computed tomographic abdominal scans of 500 subjects were retrospectively assessed for branching variations of the AbA. The radiology center routinely obtains written informed consent from all patients before contrast injection.

## Results

We present here a case of MMA detected incidentally in a male aged 63 years with a clinical diagnosis of cholelithiasis and portal hypertension and subjected to contrast-enhanced CT angiography for further evaluation (1/500; 0.2% prevalence). The MMA was arising from the ventral aspect of abdominal aorta at the level of lower border of L2 vertebra, 5.46 cm distal to origin of SMA, and 1.86 cm proximal to origin of IMA [Figure 1]. The diameter of MMA at its origin was 5.1 mm and that of SMA was 5.4 mm and IMA was 3.5 mm. After turning sharply to the right anterior to aorta and SMA, the MMA bifurcated into branches running horizontally in opposite directions. The right branch further divided into ascending and descending branches to supply transverse colon, ascending colon, cecum and terminal ileum, and the left branch supplied splenic flexure and proximal descending colon [Figure 2a and b]. Normal colic branches of SMA,

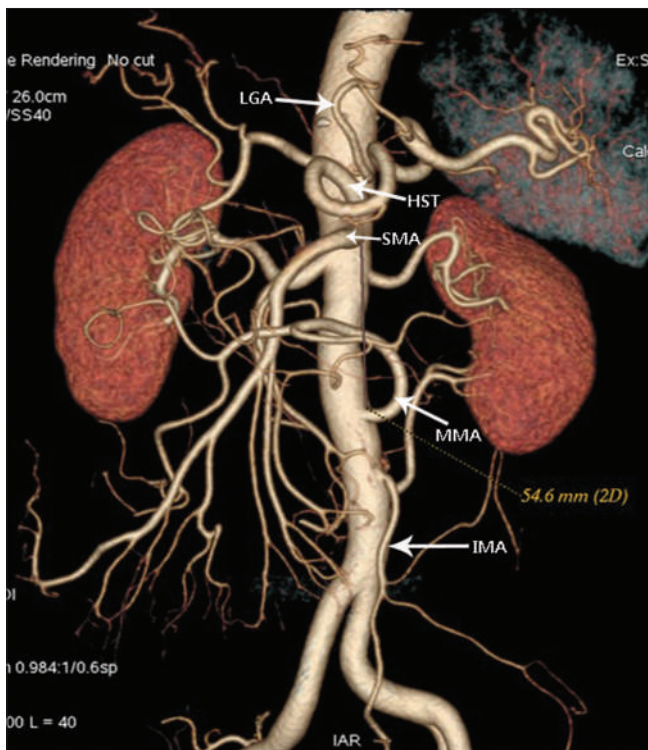


Figure 1: Volume rendered MDCT image showing origin of Middle Mesenteric Artery (MMA) from ventral aspect of abdominal aorta in between the origins of Superior Mesenteric (SMA) and Inferior Mesenteric arteries (IMA). Note the left gastric artery (LGA) arising directly from the aorta and presence of hepatosplenic trunk (HST). Observe the presence two left renal arteries one main and the other inferior polar. There is a single right renal artery

namely MCA, RCA, and ICA, arising from its right side were not present. Nonrotation gut was also noted with small bowel loops on the right and large bowel loops on the left side [Figure 3c]. The transverse colon extended obliquely downward from hepatic flexure which intervened between the right lobe of the liver and diaphragm. The patient exhibited Chilaiditi syndrome as a segment of the colon was seen intervening between the right lobe of the liver and diaphragm [Figure 3a]. Partial thrombosis of superior mesenteric and portal veins was seen. The presence of cholelithiasis was confirmed [Figure 3b]. Anomaly of celiac trunk was also observed in the form of hepatosplenic trunk and direct aortic origin of left gastric artery. Thus, there were five ventral branches arising from the abdominal aorta, left gastric artery, hepatosplenic trunk, SMA, MMA, and IMA [Figure 4].

## Discussion

Infra-diaphragmatic parts of the gut derived from embryonic foregut, midgut, and hindgut are supplied by three ventral branches of AbA, namely the CA, SMA, and IMA, respectively. Of these three branches, the SMA is generally considered as an indispensable branch supplying loops of small intestine and major part of large intestine. Three colic branches, the middle, right and ileocolic from SMA supply midgut derived parts of the large intestine. In a recent meta-analysis involving 45 studies and 6090 specimens, Negoi *et al.* reported pooled prevalence of 94.6%, 60.1%, and 99.8% for MCA, RCA, and ICA, respectively, suggesting the rarity of their variations.<sup>[5]</sup> One of the rarest variation of colonic arterial supply is the presence of MMA, arising from the ventral aspect of AbA in between the origins of SMA and IMA, replacing one or all colic branches of SMA and IMA.

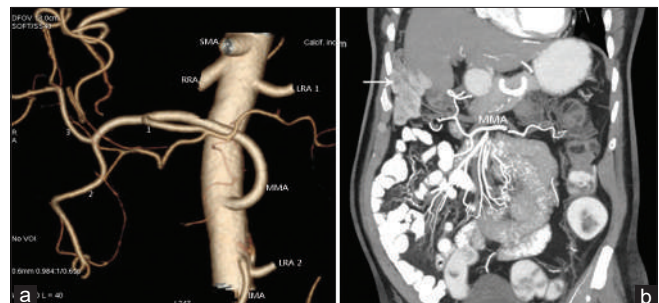


Figure 2: (a) VR image showing the branching pattern of middle mesenteric artery (MMA). For clarity other arteries and their branches were cropped. MMA is turning sharply to the right anterior to aorta and SMA and divides into left (1) and right branches. Right branch further divides into descending (2) and ascending (1) branches. MMA – Middle Mesenteric Artery; IMA- Inferior Mesenteric Artery; SMA- Superior Mesenteric Artery; LRA- Left Renal Artery; RRA- Right Renal Artery. (b) Coronal section showing Middle Mesenteric artery (MMA) branches. Note the presence of small bowel loops on the right and large bowel loops on the left. Also note the intervention of colon between the right lobe of liver and diaphragm (arrow) – Chilaiditi sign



Figure 3: (a) Axial sections showing a loop of large bowel (arrow) between right lobe of liver and the diaphragm. (b) Cholelithiasis is noted in gall bladder (GB). (c) Coronal section showing non-rotation of gut



Figure 4: Sagittal scan showing 5 ventral branches arising from the abdominal aorta. 1 - Direct aortic origin of left gastric artery. 2- Hepatosplenic trunk -common origin of splenic and common hepatic arteries; 3- Superior mesenteric artery; 4- Middle mesenteric artery; 5- Inferior mesenteric artery

Our literature search has yielded 26 cases of MMA reported globally and ours is the 27<sup>th</sup> case and to the best of our knowledge, the first case to be reported from India. The general features of the MMA, the area of its distribution and associated abnormalities of the published cases are summarized in Table 1. Only the articles published in English and other language articles with English abstract were included in the table. There is a male preponderance (male 20: female 6) in the occurrence of this anomalous artery and gender was not mentioned in one report. Six cases were associated with abdominal aortic aneurysm, five cases with nonrotation of gut and three cases with the presence of celiaco-mesenteric trunk. In one case, the MMA gave origin to left testicular artery. In the present case, celiac trunk variant in the form of hepatosplenic trunk and direct aortic origin of left gastric was also observed.

Although Benton and Cotter<sup>[1]</sup> were the first to report this anomalous artery as duplicated IMA in 1963, a French article by Delannoy in 1923, describing a case of double SMA, one supplying jejunum and ileum and the second supplying right and transverse colon was quoted by Lawdahl and Keller, Kachlik *et al.*, Vandoni *et al.* and Dirrigl *et al.* as the first report.<sup>[4,6,18,19]</sup> In addition, Kachlik *et al.*<sup>[6]</sup> quoted three more French articles, Sato *et al.*<sup>[17]</sup> quoted two Japanese articles and Abe *et al.*<sup>[28]</sup> quoted one Japanese article, all reporting the presence of this anomalous artery.

**Table 1: Reported cases of middle mesenteric artery**

| Author, year                                 | Modality                 | Gender, age (years) | Nomenclature used                                  | Distance from SMA (cm) | Distance from IMA (cm) | Structures supplied  | Associated anomalies/remarks   |
|--|--------------------------|---------------------|--|------------------------|------------------------|--|--|
| Benton and Cotter, 1963 <sup>[1]</sup>       | Cadaver                  | Male, 71            | Duplication of inferior mesenteric                 |                        |                        | Transverse and proximal descending colon   |  |
| Lawdahl and Keller, 1987 <sup>[4]</sup>      | Angiography              | Male, 70            | Middle mesenteric artery                           |                        |                        | Splenic flexure  |  |
| LeQuire et al., 1991 <sup>[7]</sup>          | Aortography              | Male, 62            | Middle mesenteric artery                           | 11.0                   | 4.0                    | Cecum, ascending and transverse colon  | Splenic flexure hemorrhage   |
| Yoshida et al., 1993 <sup>[8]</sup>          | Arterio-graphy           | Male, 49            | Middle mesenteric (anomalous middle colic)         | 4.8                    | 2.7                    | Transverse colon   | Left renal tumor   |
| Vahl et al., 1997 <sup>[9]</sup>             | CT angio                 | Male, 75            | Ileocolic artery from abdominal aorta              |                        |                        | Ascending and transverse colon   | Abdominal aortic aneurysm  |
| Higashi and Hirai, 1998 <sup>[10]</sup>      | Cadaver                  | Female, 74          | Second superior mesenteric artery                  |                        |                        | Cecum, ascending, transverse, proximal descending colon                                    | Nonrotation of gut, Celiaco-mesenteric trunk                             |
| Koizumi et al., 1999 <sup>[11]</sup>         | MDCT angio               | Female, 55          | Middle mesenteric artery                           | 5.3                    | 2.9                    | Cecum, ascending and transverse colon  |  |
| Uchida et al., 2004 <sup>[12]</sup>          | Angiography CT           | Male, 57            | Middle mesenteric artery                           |                        |                        |  | Intestinal nonrotation, colon cancer                                     |
| Skoulikaris et al., 2005 <sup>[13]</sup>     | Angiography              | Male, 70            | Middle mesenteric artery                           |                        |                        | Proximal descending colon  |  |
| Woodfield and Torigian, 2006 <sup>[14]</sup> | MDCT angio               | Male, 72            | Middle mesenteric artery                           | 4.6                    | 11.6                   | Distal small bowel, cecum, ascending colon, transverse colon, hepatic and splenic flexures | Abdominal aortic aneurysm, bowel nonrotation, three right renal arteries |
| Kawai et al., 2006 <sup>[15]</sup>           | Cadaver                  | Female, 73          | Middle mesenteric artery                           | 4.7                    | 3.3                    | Ascending colon, transverse colon  | Nonrotation of gut   |
| Falkensammer et al., 2006 <sup>[16]</sup>    | CT angio angiography     | Male, 81            | Middle mesenteric artery                           |                        |                        | Cecum, ascending, transverse and descending colon  | Abdominal aortic aneurysm, origin of IMA occluded                        |
| Sato et al., 2007 <sup>[17]</sup>            | CT angio                 | Male, 66            | Middle mesenteric artery                           |                        | 2.0                    | Transverse colon   | Aortic aneurysm, celiacomesenteric trunk. Mobile cecum                   |
| Vandoni et al., 2007 <sup>[18]</sup>         | Angiography              | Male, 74            | Middle mesenteric artery                           |                        |                        | Transverse colon, descending and sigmoid colon   | Abdominal aortic aneurysm, occlusion of IMA                              |
| Kachlik et al., 2009 <sup>[6]</sup>          | Cadaver                  | -                   | Middle mesenteric artery                           | 5.0                    | 2.0                    | Splenic flexure and descending colon   | 149 cadavers studied   |
| Dirrigl et al., 2009 <sup>[19]</sup>         | CT angio USG             | Male, 69            | Middle mesenteric artery                           | 6.0                    | 1.2                    | Distal jejunum, ileum, cecum, ascending, transverse and descending colon                   | Abdominal aortic aneurysm  |
| Ulucam et al., 2009 <sup>[20]</sup>          | Cadaver                  | Female, 32          | Middle mesenteric artery (middle colic from aorta) | 5.25                   | 4.25                   | Transverse colon   |  |
| Naito et al., 2011 <sup>[21]</sup>           | Cadaver                  | Male, 67            | Middle mesenteric artery                           | 3.0                    |                        | Transverse and proximal descending colon   | Gave origin to left testicular artery                                    |
| Milnerowicz et al., 2012 <sup>[2]</sup>      | Cadaveric arterio-graphy | Male, 55            | Middle mesenteric (aberrant middle colic)          |                        |                        | Transverse colon   | Isolated transverse colon from 114 cadavers                              |
| Bryce et al., 2013 <sup>[22]</sup>           | MDCT angio               | Female, 30          | Mesenteric anomaly                                 |                        |                        | Ileum, cecum, ascending and transverse colon   |  |
| Abdel-Aal and Moustafa, 2015 <sup>[23]</sup> | CT angio                 | Male, 51            | Middle mesenteric artery                           | 4.8                    | 5.5                    | Ileum, cecum, ascending colon  | Renal donor  |

Contd...

Table 1: Contd...

| Author, year                             | Modality           | Gender, age (years) | Nomenclature used                       | Distance from SMA (cm) | Distance from IMA (cm) | Structures supplied  | Associated anomalies/remarks                               |
|--|--------------------|---------------------|---|------------------------|------------------------|--|--|
| Ponti and Gailloud, 2016 <sup>[24]</sup> | Spinal angiography | Male, 71            | Right colic artery from abdominal aorta |                        |                        | Ascending colon, hepatic flexure   |  |
| Venieratos et al., 2018 <sup>[3]</sup>   | Cadaver            | Male, 66            | Middle mesenteric                       | 3.3                    | 3.8                    | Transverse colon, head of pancreas   |  |
| Manyama et al., 2019 <sup>[25]</sup>     | Cadaver            | Female, 85          |   |                        | 2.0                    | Ascending, transverse and descending colon                                 |  |
| Sheridan et al., 2022 <sup>[26]</sup>    | Cadaver            | Male, 68            | Middle mesenteric                       | 1.0                    | 0.5                    | Transverse colon, splenic flexure  | Hepatogastrophrenic and celiacomesenteric trunks           |
| Muraki et al., 2022 <sup>[27]</sup>      | Angiography 3-D CT | Male, 87            | Middle mesenteric artery                | 7.2                    | 1.2                    | Transverse colon and proximal descending colon                             | Hematoma, colonic ischemia and resection colon             |
| Present study 2023                       | MDCT angio         | Male, 63            | Middle mesenteric artery                | 5.46                   | 1.86                   | Terminal ileum, cecum, ascending, transverse and proximal descending colon | LGA from aorta and hepatosplenic trunk, nonrotation of gut |

Abdominal aortic aneurysm: 6 cases, Nonrotation of gut: 5 cases, Celiacomesenteric trunk: 3, Variant celiac trunk: 1, Male: female: 20:6. Only articles published in English language and other language articles with English abstracts were included. CT: Computed tomography, MDCT: Multidetector CT, LGA: Left gastric artery, IMA: Inferior mesenteric artery, SMA: Superior mesenteric, USG: Ultrasound sonography

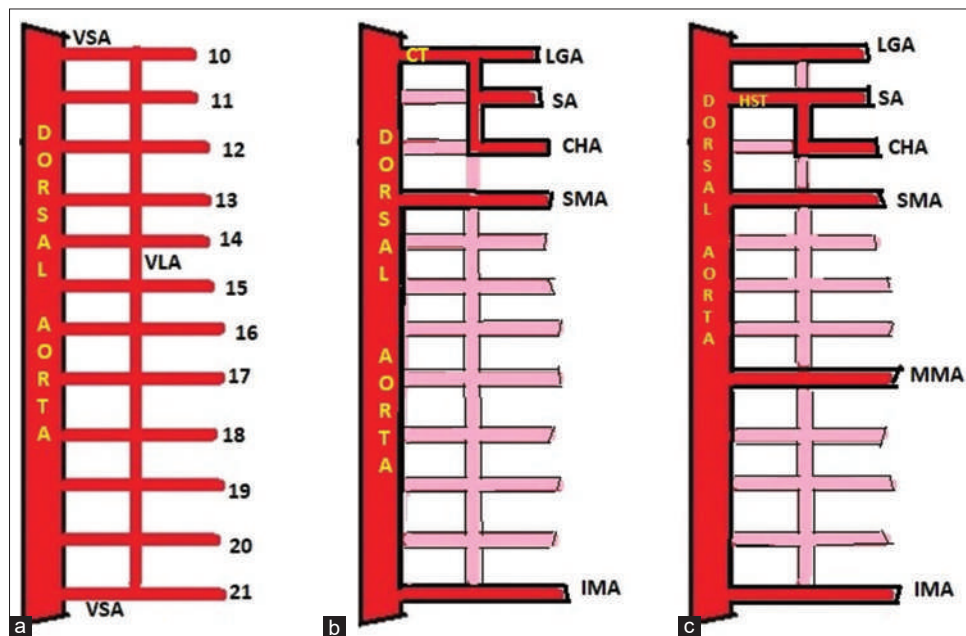


Figure 5: Development of celiac and mesenteric arteries from ventral splanchnic arteries (VSA). (a) A series of ventral splanchnic arteries (numbered 10-22) arise from dorsal aorta to supply the developing gut. These arteries are connected to each other by a Ventral longitudinal anastomosis (VLA). (b) Shows normal development. The 10<sup>th</sup>, 11<sup>th</sup> and 12<sup>th</sup> arteries with the regression of proximal parts of 11<sup>th</sup> and 12<sup>th</sup> contribute to the development of celiac trunk (CT) and its three branches left gastric (LGA), Splenic (SA) and Common hepatic (CHA). The 13<sup>th</sup> VSA develops into superior mesenteric (SMA) and 21<sup>st</sup> into inferior mesenteric artery (IMA). Normally the 14<sup>th</sup> to 20<sup>th</sup> VSA and VLA regress along with regression of VLA between 12<sup>th</sup> and 13<sup>th</sup> VSA. Parts which will undergo regression are shown in pink color. (c) Persistence of any one of the VSAs between 14<sup>th</sup> to 20<sup>th</sup> gives rise to Middle Mesenteric artery (MMA). Regression of VLA between 10<sup>th</sup> and 11<sup>th</sup> VSAs gives rise to direct aortic origin of left gastric artery (LGA). Persistence of proximal part of 11<sup>th</sup> VSA forms the Hepatosplenic trunk (HST)

In a study of colonic arterial supply involving 149 cadavers, one case of MMA was observed supplying splenic flexure and proximal descending colon.<sup>[6]</sup> In another study of colonic arteriography of 114 cadaveric transverse colons, Milnerowicz et al. observed the presence of MMA supplying transverse colon.<sup>[2]</sup> Because of its infrarenal

aortic origin, MMA is at a greater risk of occlusion and liable to damage during endovascular repair of abdominal aortic aneurysm. Wu et al. reporting an extremely rare variation of absence of SMA in an adult proposed a novel classification system for superior - IMA variations and suggested the existence of an aberrant MMA as Type IV.<sup>[29]</sup>

## Embryology

During the early stages of the development, a series of ventral splanchnic arteries (VSA) originate from the dorsal aorta to supply the developing gut. Initially, dorsal aorta and the VSAs were paired vessels but later fuse to form unpaired vessels. These VSAs are interconnected to each other by a ventral longitudinal anastomosis (VLA) lying in front of dorsal aorta [Figure 5a]. The 10<sup>th</sup>, 11<sup>th</sup>, and 12<sup>th</sup>, ventral segmental arteries together with part of VLA develop into celiac trunk and its three branches [Figure 5b]. The proximal part of 11<sup>th</sup> and 12<sup>th</sup> VSAs from the dorsal aorta undergoes regression. The VLA between 12<sup>th</sup> and 13<sup>th</sup> VSAs regress and the 13<sup>th</sup>, VSA becomes the SMA. The 21<sup>st</sup> VSA becomes the IMA after the regression of VLA and 14<sup>th</sup> to 20<sup>th</sup> VSAs [Figure 5b]. Persistence of any one of the VSAs between the 14<sup>th</sup> and 20<sup>th</sup> leads to the development of a MMA [Figure 5c].

Normally, during the development, the U-shaped midgut loop herniates into umbilical coelom and remains as a physiological umbilical hernia outside the fetal body between 6<sup>th</sup> and 10<sup>th</sup> week undergoing first a 90° anticlockwise rotation and then a 180° anticlockwise rotation. Reduction of the hernia and return of the midgut loop into abdominal cavity occurs during the 11<sup>th</sup> week in an orderly manner such that caecum and colon are last to return. Nonrotation of the gut occurs due to failure of the second 180° rotation and return of colon first and small intestinal loops last resulting in colon occupying the left and the small bowel loops the right side of the abdomen.

## Clinical importance and Conclusion

Thorough knowledge and complete familiarity of the occurrence of such rare vascular anomaly of presence of MMA will prevent its accidental ligation and subsequent infraction of the target organ. Because of its association with the abdominal aortic aneurysm, endovascular aneurysmal repair may result in occlusion of this anomalous vessel with a significant risk of bowel ischemia. Since lymphatic vessels draining a target organ generally follow the arteries and veins supplying that organ, precise presurgical mapping of the anomalous vessels will greatly help the oncosurgeon planning a locoregional lymph node clearance in cases of colonic cancer. Knowledge of possibility of presence of such anomalous vessel is important for anatomists, surgeons, surgical oncologists, radiologists, and interventional radiologists.

## Financial support and sponsorship

Nil.

## Conflicts of interest

There are no conflicts of interest.

## References

- Benton RS, Cotter WB. A hitherto undocumented variation of the inferior mesenteric artery in man. *Anat Rec* 1963;145:171-3.
- Milnerowicz S, Milnerowicz A, Taboła R. A middle mesenteric artery. *Surg Radiol Anat* 2012;34:973-5.
- Venieratos D, Tsoucalas G, Panagouli E. A rare branching pattern of a middle mesenteric artery supplying the head of the pancreas and the transverse colon. *Acta Med Acad* 2018;47:199-203.
- Lawdahl RB, Keller FS. The middle mesenteric artery. *Radiology* 1987;165:371-2.
- Negoi I, Beuran M, Hostiuc S, Negoi RI, Inoue Y. Surgical anatomy of the superior mesenteric vessels related to colon and pancreatic surgery: A systematic review and meta-analysis. *Sci Rep* 2018;8:4184.
- Kachlik D, Laco J, Turyna R, Baca V. A very rare variant in the colon supply – Arteria mesenterica media. *Biomed Pap Med Fac Univ Palacky Olomouc Czech Repub* 2009;153:79-82.
- LeQuire MH, Sorge DG, Brantley SD. The middle mesenteric artery: An unusual source for colonic hemorrhage. *J Vasc Interv Radiol* 1991;2:141-5.
- Yoshida T, Suzuki S, Sato T. Middle mesenteric artery: An anomalous origin of a middle colic artery. *Surg Radiol Anat* 1993;15:361-3.
- Vahl AC, van den Berg FG, Rauwerda JA. The ileocolic artery as a separate aortic branch in a patient with an aortic aneurysm. *Eur J Vasc Endovasc Surg* 1997;13:417-8.
- Higashi N, Hirai K. Nonrotation of the midgut with abnormality of the superior mesenteric artery. *Kaibogaku Zasshi* 1998;73:529-32.
- Koizumi J, d'Othée BJ, Otal P, Rousseau H, Joffre F, Kohda E, et al. Middle mesenteric artery visualized by computed tomographic angiography. *Abdom Imaging* 1999;24:556-8.
- Uchida H, Kawamura YJ, Takegami K, Matsuda K, Watanabe T, Masaki T, et al. Colon cancer complicated by vascular and intestinal anomaly. *Hepatogastroenterology* 2004;51:156-8.
- Skoulikaris N, Argyriou P, Chatoupis K, Christopoulos D, Tsocanas D. Middle mesenteric artery: A rare variant. *Eurorad* 2005. [doi: 10.1594/eurorad/case3405].
- Woodfield CA, Torigian DA. MDCT angiography of middle mesenteric artery with associated bowel nonrotation complicating management of abdominal aortic aneurysm. *AJR Am J Roentgenol* 2006;187:W524-7.
- Kawai K, Koizumi M, Honma S, Tokiyoshi A, Kodama K. A case of nonrotation of the midgut with a middle mesenteric artery. *Ann Anat* 2006;188:13-7.
- Falkensammer J, Hakaim AG, Paz-Fumagalli R, Oldenburg WA. Endovascular repair of an infrarenal abdominal aortic aneurysm with a dominant middle mesenteric artery: A case report. *Vasc Endovascular Surg* 2006;40:338-41.
- Sato O, Matsumoto H, Kondoh K. Middle mesenteric artery encountered during abdominal aortic aneurysm surgery. *J Vasc Surg* 2007;16:799-801.
- Vandoni RE, Alerci M, Froment P, Braghetti A, Bogen M, Gertsch P. Middle mesenteric artery: Contraindication to endovascular repair of an abdominal aortic aneurysm? *Vasa* 2007;36:41-3.
- Dirrigl AM, Zimmermann A, Ockert S, Eckstein HH. Middle mesenteric artery arising from an inflammatory infrarenal aortic aneurysm. *J Vasc Surg* 2009;49:474-7.
- Ulucam E, Yilmaz A, Cigali BS, Bozer C, Elevli L. Middle colic artery arising directly from aorta as a middle mesenteric artery. *Trakya Univ Tip Fak Derg* 2009;26:87-9.
- Naito M, Yi SQ, Terayama H, Hirai S, Qu N, Itoh M. A left testicular artery arising from a middle mesenteric artery. *Clin*

- Anat 2011;24:266-7.
22. Bryce Y, Heffess A, Schiller J. CT angiogram of mesenteric anomaly. *J Vasc Interv Radiol* 2013;24:1367.
  23. Abdel-Aal AK, Moustafa AS. Incidentally discovered middle mesenteric artery in a renal donor. *J Radiol Case Rep* 2015;9:15-20.
  24. Ponti A, Gailloud P. Direct origin of the right colic artery from the abdominal aorta. *Ital J Anat Embryol* 2016;121:100-4.
  25. Manyama M, Malyango A, Raoof A, Mligiliche NL, Msuya C, Nassir N, *et al.* A variant source of arterial supply to the ascending, transverse and descending colon. *Surg Radiol Anat* 2019;41:1383-6.
  26. Sheridan A, Reynolds E, Maynes E, Wind G, Leighton MX, Granite G. A hepatogastrophrenic trunk, celiacomesenteric trunk, and a middle mesenteric artery in a 68-year-old white male donor. *Diagnostics (Basel)* 2022;12:1597.
  27. Muraki M, Moriya T, Katada Y, Masuno R, Suzuki S, Sugahara S, *et al.* Middle mesenteric artery: Angiographic and three-dimensional computed tomography findings. *Radiol Case Rep* 2022;17:2484-7.
  28. Abe T, Ujiie A, Taguchi Y, Satoh S, Shibuya T, Jun Y, *et al.* Anomalous inferior mesenteric artery supplying the ascending, transverse, descending and sigmoid colons. *Anat Sci Int* 2019;93:144-8.
  29. Wu Y, Peng W, Wu H, Chen G, Zhu J, Xing C. Absence of the superior mesenteric artery in an adult and a new classification method for superior-inferior mesenteric arterial variations. *Surg Radiol Anat* 2014;36:511-5.

### The Editorial Process

A manuscript will be reviewed for possible publication with the understanding that it is being submitted to Journal of the Anatomical Society of India alone at that point in time and has not been published anywhere, simultaneously submitted, or already accepted for publication elsewhere. The journal expects that authors would authorize one of them to correspond with the Journal for all matters related to the manuscript. All manuscripts received are duly acknowledged. On submission, editors review all submitted manuscripts initially for suitability for formal review. Manuscripts with insufficient originality, serious scientific or technical flaws, or lack of a significant message are rejected before proceeding for formal peer-review. Manuscripts that are unlikely to be of interest to the Journal of the Anatomical Society of India readers are also liable to be rejected at this stage itself.

Manuscripts that are found suitable for publication in Journal of the Anatomical Society of India are sent to two or more expert reviewers. During submission, the contributor is requested to provide names of two or three qualified reviewers who have had experience in the subject of the submitted manuscript, but this is not mandatory. The reviewers should not be affiliated with the same institutes as the contributor/s. However, the selection of these reviewers is at the sole discretion of the editor. The journal follows a double-blind review process, wherein the reviewers and authors are unaware of each other's identity. Every manuscript is also assigned to a member of the editorial team, who based on the comments from the reviewers takes a final decision on the manuscript. The comments and suggestions (acceptance/ rejection/ amendments in manuscript) received from reviewers are conveyed to the corresponding author. If required, the author is requested to provide a point by point response to reviewers' comments and submit a revised version of the manuscript. This process is repeated till reviewers and editors are satisfied with the manuscript.

Manuscripts accepted for publication are copy edited for grammar, punctuation, print style, and format. Page proofs are sent to the corresponding author. The corresponding author is expected to return the corrected proofs within three days. It may not be possible to incorporate corrections received after that period. The whole process of submission of the manuscript to final decision and sending and receiving proofs is completed online. To achieve faster and greater dissemination of knowledge and information, the journal publishes articles online as 'Ahead of Print' immediately on acceptance.

### Clinical trial registry

Journal of the Anatomical Society of India favors registration of clinical trials and is a signatory to the Statement on publishing clinical trials in Indian biomedical

journals. Journal of the Anatomical Society of India would publish clinical trials that have been registered with a clinical trial registry that allows free online access to public. Registration in the following trial registers is acceptable: <http://www.ctri.in/>; <http://www.actr.org.au/>; <http://www.clinicaltrials.gov/>; <http://isrctn.org/>; <http://www.trialregister.nl/trialreg/index.asp>; and <http://www.umin.ac.jp/ctr>. This is applicable to clinical trials that have begun enrollment of subjects in or after June 2008. Clinical trials that have commenced enrollment of subjects prior to June 2008 would be considered for publication in Journal of the Anatomical Society of India only if they have been registered retrospectively with clinical trial registry that allows unhindered online access to public without charging any fees.

### Authorship Criteria

Authorship credit should be based only on substantial contributions to each of the three components mentioned below:

1. Concept and design of study or acquisition of data or analysis and interpretation of data;
2. Drafting the article or revising it critically for important intellectual content; and
3. Final approval of the version to be published.

Participation solely in the acquisition of funding or the collection of data does not justify authorship. General supervision of the research group is not sufficient for authorship. Each contributor should have participated sufficiently in the work to take public responsibility for appropriate portions of the content of the manuscript. The order of naming the contributors should be based on the relative contribution of the contributor towards the study and writing the manuscript. Once submitted the order cannot be changed without written consent of all the contributors. The journal prescribes a maximum number of authors for manuscripts depending upon the type of manuscript, its scope and number of institutions involved (vide infra). The authors should provide a justification, if the number of authors exceeds these limits.

### Contribution Details

Contributors should provide a description of contributions made by each of them towards the manuscript. Description should be divided in following categories, as applicable: concept, design, definition of intellectual content, literature search, clinical studies, experimental studies, data acquisition, data analysis, statistical analysis, manuscript preparation, manuscript editing and manuscript review. Authors' contributions will be printed along with the article. One or more author should take responsibility for the integrity of the work as a whole from inception to published article and should be designated as 'guarantor'.

## Conflicts of Interest/ Competing Interests

All authors of must disclose any and all conflicts of interest they may have with publication of the manuscript or an institution or product that is mentioned in the manuscript and/or is important to the outcome of the study presented. Authors should also disclose conflict of interest with products that compete with those mentioned in their manuscript.

## Submission of Manuscripts

All manuscripts must be submitted on-line through the website <https://review.jow.medknow.com/jasi>. First time users will have to register at this site. Registration is free but mandatory. Registered authors can keep track of their articles after logging into the site using their user name and password.

- If you experience any problems, please contact the editorial office by e-mail at [editor@jasi.org.in](mailto:editor@jasi.org.in)

The submitted manuscripts that are not as per the "Instructions to Authors" would be returned to the authors for technical correction, before they undergo editorial/peer-review. Generally, the manuscript should be submitted in the form of two separate files:

### [1] Title Page/First Page File/covering letter:

This file should provide

1. The type of manuscript (original article, case report, review article, Letter to editor, Images, etc.) title of the manuscript, running title, names of all authors/ contributors (with their highest academic degrees, designation and affiliations) and name(s) of department(s) and/ or institution(s) to which the work should be credited, . All information which can reveal your identity should be here. Use text/rtf/doc files. Do not zip the files.
2. The total number of pages, total number of photographs and word counts separately for abstract and for the text (excluding the references, tables and abstract), word counts for introduction + discussion in case of an original article;
3. Source(s) of support in the form of grants, equipment, drugs, or all of these;
4. Acknowledgement, if any. One or more statements should specify 1) contributions that need acknowledging but do not justify authorship, such as general support by a departmental chair; 2) acknowledgments of technical help; and 3) acknowledgments of financial and material support, which should specify the nature of the support. This should be included in the title page of the manuscript and not in the main article file.
5. If the manuscript was presented as part at a meeting, the organization, place, and exact date on which it was read. A full statement to the editor about all submissions and previous reports that might be regarded as

redundant publication of the same or very similar work. Any such work should be referred to specifically, and referenced in the new paper. Copies of such material should be included with the submitted paper, to help the editor decide how to handle the matter.

6. Registration number in case of a clinical trial and where it is registered (name of the registry and its URL)
7. Conflicts of Interest of each author/ contributor. A statement of financial or other relationships that might lead to a conflict of interest, if that information is not included in the manuscript itself or in an authors' form
8. Criteria for inclusion in the authors'/ contributors' list
9. A statement that the manuscript has been read and approved by all the authors, that the requirements for authorship as stated earlier in this document have been met, and that each author believes that the manuscript represents honest work, if that information is not provided in another form (see below); and
10. The name, address, e-mail, and telephone number of the corresponding author, who is responsible for communicating with the other authors about revisions and final approval of the proofs, if that information is not included on the manuscript itself.

**[2] Blinded Article file:** The main text of the article, beginning from Abstract till References (including tables) should be in this file. The file must not contain any mention of the authors' names or initials or the institution at which the study was done or acknowledgements. Page headers/ running title can include the title but not the authors' names. Manuscripts not in compliance with the Journal's blinding policy will be returned to the corresponding author. Use rtf/doc files. Do not zip the files. **Limit the file size to 1 MB.** Do not incorporate images in the file. If file size is large, graphs can be submitted as images separately without incorporating them in the article file to reduce the size of the file. The pages should be numbered consecutively, beginning with the first page of the blinded article file.

**[3] Images:** Submit good quality color images. **Each image should be less than 2 MB in size.** Size of the image can be reduced by decreasing the actual height and width of the images (keep up to 1600 x 1200 pixels or 5-6 inches). Images can be submitted as jpeg files. Do not zip the files. Legends for the figures/images should be included at the end of the article file.

**[4] The contributors' / copyright transfer form** (template provided below) has to be submitted in original with the signatures of all the contributors within two weeks of submission via courier, fax or email as a scanned image. Print ready hard copies of the images (one set) or digital images should be sent to the journal office at the time of submitting revised manuscript. High resolution images (up to 5 MB each) can be sent by email.

Contributors' form / copyright transfer form can be submitted online from the authors' area on <https://review.jow.medknow.com/jasi>.

## Preparation of Manuscripts

Manuscripts must be prepared in accordance with "Uniform requirements for Manuscripts submitted to Biomedical Journals" developed by the International Committee of Medical Journal Editors (October 2008). The uniform requirements and specific requirement of Journal of the Anatomical Society of India are summarized below. Before submitting a manuscript, contributors are requested to check for the latest instructions available. Instructions are also available from the website of the journal ([www.jasi.org.in](http://www.jasi.org.in)) and from the manuscript submission site <https://review.jow.medknow.com/jasi>.

Journal of the Anatomical Society of India accepts manuscripts written in American English.

## Copies of any permission(s)

It is the responsibility of authors/ contributors to obtain permissions for reproducing any copyrighted material. A copy of the permission obtained must accompany the manuscript. Copies of any and all published articles or other manuscripts in preparation or submitted elsewhere that are related to the manuscript must also accompany the manuscript.

## Types of Manuscripts

### Original articles:

These include randomized controlled trials, intervention studies, studies of screening and diagnostic test, outcome studies, cost effectiveness analyses, case-control series, and surveys with high response rate. The text of original articles amounting to up to 3000 words (excluding Abstract, references and Tables) should be divided into sections with the headings Abstract, Keywords, Introduction, Material and Methods, Results, Discussion and Conclusion, References, Tables and Figure legends.

An abstract should be in a structured format under following heads: **Introduction, Material and Methods, Results, and Discussion and Conclusion.**

**Introduction:** State the purpose and summarize the rationale for the study or observation.

**Material and Methods:** It should include and describe the following aspects:

**Ethics:** When reporting studies on human beings, indicate whether the procedures followed were in accordance with the ethical standards of the responsible committee on human experimentation (institutional or regional) and with the Helsinki Declaration of 1975, as revised in 2000

(available at [http://www.wma.net/e/policy/17-c\\_e.html](http://www.wma.net/e/policy/17-c_e.html)). For prospective studies involving human participants, authors are expected to mention about approval of (regional/ national/ institutional or independent Ethics Committee or Review Board, obtaining informed consent from adult research participants and obtaining assent for children aged over 7 years participating in the trial. The age beyond which assent would be required could vary as per regional and/ or national guidelines. Ensure confidentiality of subjects by desisting from mentioning participants' names, initials or hospital numbers, especially in illustrative material. When reporting experiments on animals, indicate whether the institution's or a national research council's guide for, or any national law on the care and use of laboratory animals was followed. Evidence for approval by a local Ethics Committee (for both human as well as animal studies) must be supplied by the authors on demand. Animal experimental procedures should be as humane as possible and the details of anesthetics and analgesics used should be clearly stated. The ethical standards of experiments must be in accordance with the guidelines provided by the CPCSEA and World Medical Association Declaration of Helsinki on Ethical Principles for Medical Research Involving Humans for studies involving experimental animals and human beings, respectively). The journal will not consider any paper which is ethically unacceptable. A statement on ethics committee permission and ethical practices must be included in all research articles under the 'Materials and Methods' section.

### Study design:

**Selection and Description of Participants:** Describe your selection of the observational or experimental participants (patients or laboratory animals, including controls) clearly, including eligibility and exclusion criteria and a description of the source population. *Technical information:* Identify the methods, apparatus (give the manufacturer's name and address in parentheses), and procedures in sufficient detail to allow other workers to reproduce the results. Give references to established methods, including statistical methods (see below); provide references and brief descriptions for methods that have been published but are not well known; describe new or substantially modified methods, give reasons for using them, and evaluate their limitations. Identify precisely all drugs and chemicals used, including generic name(s), dose(s), and route(s) of administration.

Reports of randomized clinical trials should present information on all major study elements, including the protocol, assignment of interventions (methods of randomization, concealment of allocation to treatment groups), and the method of masking (blinding), based on the CONSORT Statement (<http://www.consort-statement.org>).

## Reporting Guidelines for Specific Study Designs

| Initiative | Type of Study  | Source  |
|------------|--|---|
| CONSORT    | Randomized controlled trials                           | <a href="http://www.consort-statement.org">http://www.consort-statement.org</a>   |
| STARD      | Studies of diagnostic accuracy                         | <a href="http://www.consort-statement.org/stardstatement.htm">http://www.consort-statement.org/stardstatement.htm</a>                   |
| QUOROM     | Systematic reviews and meta-analyses                   | <a href="http://www.consort-statement.org/Initiatives/MOOSE/moose.pdf">http://www.consort-statement.org/Initiatives/MOOSE/moose.pdf</a> |
| STROBE     | Observational studies in epidemiology                  | <a href="http://www.strobe-statement.org">http://www.strobe-statement.org</a>   |
| MOOSE      | Meta-analyses of observational studies in epidemiology | <a href="http://www.consort-statement.org/Initiatives/MOOSE/moose.pdf">http://www.consort-statement.org/Initiatives/MOOSE/moose.pdf</a> |

**Statistics:** Whenever possible quantify findings and present them with appropriate indicators of measurement error or uncertainty (such as confidence intervals). Authors should report losses to observation (such as, dropouts from a clinical trial). When data are summarized in the Results section, specify the statistical methods used to analyze them. Avoid non-technical uses of technical terms in statistics, such as ‘random’ (which implies a randomizing device), ‘normal’, ‘significant’, ‘correlations’, and ‘sample’. Define statistical terms, abbreviations, and most symbols. Specify the computer software used. Use upper italics ( $P$  0.048). For all  $P$  values include the exact value and not less than 0.05 or 0.001. Mean differences in continuous variables, proportions in categorical variables and relative risks including odds ratios and hazard ratios should be accompanied by their confidence intervals.

**Results:** Present your results in a logical sequence in the text, tables, and illustrations, giving the main or most important findings first. Do not repeat in the text all the data in the tables or illustrations; emphasize or summarize only important observations. Extra- or supplementary materials and technical detail can be placed in an appendix where it will be accessible but will not interrupt the flow of the text; alternatively, it can be published only in the electronic version of the journal.

When data are summarized in the Results section, give numeric results not only as derivatives (for example, percentages) but also as the absolute numbers from which the derivatives were calculated, and specify the statistical methods used to analyze them. Restrict tables and figures to those needed to explain the argument of the paper and to assess its support. Use graphs as an alternative to tables with many entries; do not duplicate data in graphs and tables. Where scientifically appropriate, analyses of the data by variables such as age and sex should be included.

**Discussion:** Include summary of *key findings* (primary outcome measures, secondary outcome measures, results

as they relate to a prior hypothesis); *Strengths and limitations* of the study (study question, study design, data collection, analysis and interpretation); *Interpretation and implications* in the context of the totality of evidence (is there a systematic review to refer to, if not, could one be reasonably done here and now?, what this study adds to the available evidence, effects on patient care and health policy, possible mechanisms); *Controversies* raised by this study; and *Future research directions* (for this particular research collaboration, underlying mechanisms, clinical research).

Do not repeat in detail data or other material given in the Introduction or the Results section. In particular, contributors should avoid making statements on economic benefits and costs unless their manuscript includes economic data and analyses. Avoid claiming priority and alluding to work that has not been completed. New hypotheses may be stated if needed, however they should be clearly labeled as such. About 30 references can be included. These articles generally should not have more than six authors.

### Review Articles:

These are comprehensive review articles on topics related to various fields of Anatomy. The entire manuscript should not exceed 7000 words with no more than 50 references and two authors. Following types of articles can be submitted under this category:

- Newer techniques of dissection and histology
- New methodology in Medical Education
- Review of a current concept

Please note that generally review articles are by invitation only. But unsolicited review articles will be considered for publication on merit basis.

### Case reports:

New, interesting and rare cases can be reported. They should be unique, describing a great diagnostic or therapeutic challenge and providing a learning point for the readers. Cases with clinical significance or implications will be given priority. These communications could be of up to 1000 words (excluding Abstract and references) and should have the following headings: Abstract (unstructured), Key-words, Introduction, Case report, Discussion and Conclusion, Reference, Tables and Legends in that order.

The manuscript could be of up to 1000 words (excluding references and abstract) and could be supported with up to 10 references. Case Reports could be authored by up to four authors.

### Letter to the Editor:

These should be short and decisive observations. They should preferably be related to articles previously published in the Journal or views expressed in the journal. They should not be preliminary observations that need a later

paper for validation. The letter could have up to 500 words and 5 references. It could be generally authored by not more than four authors.

**Book Review:** This consists of a critical appraisal of selected books on Anatomy. Potential authors or publishers may submit books, as well as a list of suggested reviewers, to the editorial office. The author/publisher has to pay INR 10,000 per book review.

#### Other:

Editorial, Guest Editorial, Commentary and Opinion are solicited by the editorial board.

#### References

References should be *numbered* consecutively in the order in which they are first mentioned in the text (not in alphabetic order). Identify references *in text*, tables, and legends by Arabic numerals in superscript with square bracket after the punctuation marks. *References cited only* in tables or figure legends should be numbered in accordance with the sequence established by the first identification in the text of the particular table or figure. Use the style of the examples below, which are based on the formats used by the NLM *in Index Medicus*. The titles of journals *should be abbreviated* according to the style used in Index Medicus. Use complete name of the journal for non-indexed journals. Avoid using abstracts as references. Information from manuscripts submitted but not accepted should be cited in the text as “unpublished observations” with written permission from the source. Avoid citing a “personal communication” unless it provides essential information not available from a public source, in which case the name of the person and date of communication should be cited in parentheses in the text. The commonly cited types of references are shown here, for other types of references such as newspaper items please refer to ICMJE Guidelines (<http://www.icmje.org> or [http://www.nlm.nih.gov/bsd/uniform\\_requirements.html](http://www.nlm.nih.gov/bsd/uniform_requirements.html)).

#### Articles in Journals

1. Standard journal article (for up to six authors): Parija S C, Ravinder PT, Shariff M. Detection of hydatid antigen in the fluid samples from hydatid cysts by co-agglutination. *Trans. R.Soc. Trop. Med. Hyg.*1996; 90:255–256.
2. Standard journal article (for more than six authors): List the first six contributors followed by *et al.*

Roddy P, Goiri J, Flevaud L, Palma PP, Morote S, Lima N. *et al.*, Field Evaluation of a Rapid Immunochromatographic Assay for Detection of *Trypanosoma cruzi* Infection by Use of Whole Blood. *J. Clin. Microbiol.* 2008; 46: 2022-2027.

3. Volume with supplement: Otranto D, Capelli G, Genchi C: Changing distribution patterns of canine vector borne diseases in Italy: leishmaniosis vs. dirofilariosis.

*Parasites & Vectors* 2009; Suppl 1:S2.

#### Books and Other Monographs

1. Personal author(s): Parija SC. Textbook of Medical Parasitology. 3rd ed. All India Publishers and Distributors. 2008.
2. Editor(s), compiler(s) as author: Garcia LS, Filarial Nematodes In: Garcia LS (editor) Diagnostic Medical Parasitology ASM press Washington DC 2007: pp 319-356.
3. Chapter in a book: Nesheim M C. Ascariasis and human nutrition. In Ascariasis and its prevention and control, D. W. T. Crompton, M. C. Nesbemi, and Z. S. Pawlowski (eds.). Taylor and Francis, London, U.K.1989, pp. 87–100.

#### Electronic Sources as reference

Journal article on the Internet: Parija SC, Khairnar K. Detection of excretory *Entamoeba histolytica* DNA in the urine, and detection of *E. histolytica* DNA and lectin antigen in the liver abscess pus for the diagnosis of amoebic liver abscess. *BMC Microbiology* 2007, 7:41. doi:10.1186/1471-2180-7-41. <http://www.biomedcentral.com/1471-2180/7/41>

#### Tables

- Tables should be self-explanatory and should not duplicate textual material.
- Tables with more than 10 columns and 25 rows are not acceptable.
- Number tables, in Arabic numerals, consecutively in the order of their first citation in the text and supply a brief title for each.
- Place explanatory matter in footnotes, not in the heading.
- Explain in footnotes all non-standard abbreviations that are used in each table.
- Obtain permission for all fully borrowed, adapted, and modified tables and provide a credit line in the footnote.
- For footnotes use the following symbols, in this sequence: \*, †, ‡, §, ||, ¶, \*\*, ††, ‡‡
- Tables with their legends should be provided at the end of the text after the references. The tables along with their number should be cited at the relevant place in the text

#### Illustrations (Figures)

- Upload the images in JPEG format. The file size should be within 1024 kb in size while uploading.
- Figures should be numbered consecutively according to the order in which they have been first cited in the text.
- Labels, numbers, and symbols should be clear and of uniform size. The lettering for figures should be large enough to be legible after reduction to fit the width of a printed column.
- Symbols, arrows, or letters used in photomicrographs

should contrast with the background and should be marked neatly with transfer type or by tissue overlay and not by pen.

- Titles and detailed explanations belong in the legends for illustrations not on the illustrations themselves.
- When graphs, scatter-grams or histograms are submitted the numerical data on which they are based should also be supplied.
- The photographs and figures should be trimmed to remove all the unwanted areas.
- If photographs of individuals are used, their pictures must be accompanied by written permission to use the photograph.
- If a figure has been published elsewhere, acknowledge the original source and submit written permission from the copyright holder to reproduce the material. A credit line should appear in the legend for such figures.
- Legends for illustrations: Type or print out legends (maximum 40 words, excluding the credit line) for illustrations using double spacing, with Arabic numerals corresponding to the illustrations. When symbols, arrows, numbers, or letters are used to identify parts of the illustrations, identify and explain each one in the legend. Explain the internal scale (magnification) and identify the method of staining in photomicrographs.
- Final figures for print production: Send sharp, glossy, un-mounted, color photographic prints, with height of 4 inches and width of 6 inches at the time of submitting the revised manuscript. Print outs of digital photographs are not acceptable. If digital images are the only source of images, ensure that the image has minimum resolution of 300 dpi or 1800 x 1600 pixels in TIFF format. Send the images on a CD. Each figure should have a label pasted (avoid use of liquid gum for pasting) on its back indicating the number of the figure, the running title, top of the figure and the legends of the figure. Do not write the contributor/s' name/s. Do not write on the back of figures, scratch, or mark them by using paper clips.
- The Journal reserves the right to crop, rotate, reduce, or enlarge the photographs to an acceptable size.

### Protection of Patients' Rights to Privacy

Identifying information should not be published in written descriptions, photographs, sonograms, CT scans, etc., and pedigrees unless the information is essential for scientific purposes and the patient (or parent or guardian, wherever applicable) gives informed consent for publication. Authors should remove patients' names from figures unless they have obtained informed consent from the patients. The journal abides by ICMJE guidelines:

1. Authors, not the journals nor the publisher, need to obtain the patient consent form before the publication and have the form properly archived. The consent

forms are not to be uploaded with the cover letter or sent through email to editorial or publisher offices.

2. If the manuscript contains patient images that preclude anonymity, or a description that has obvious indication to the identity of the patient, a statement about obtaining informed patient consent should be indicated in the manuscript.

### Sending a revised manuscript

The revised version of the manuscript should be submitted online in a manner similar to that used for submission of the manuscript for the first time. However, there is no need to submit the "First Page" or "Covering Letter" file while submitting a revised version. When submitting a revised manuscript, contributors are requested to include, the 'referees' remarks along with point to point clarification at the beginning in the revised file itself. In addition, they are expected to mark the changes as underlined or colored text in the article.

### Reprints and proofs

Journal provides no free printed reprints. Authors can purchase reprints, payment for which should be done at the time of submitting the proofs.

### Publication schedule

The journal publishes articles on its website immediately on acceptance and follows a 'continuous publication' schedule. Articles are compiled in issues for 'print on demand' quarterly.

### Copyrights

The entire contents of the Journal of the Anatomical Society of India are protected under Indian and international copyrights. The Journal, however, grants to all users a free, irrevocable, worldwide, perpetual right of access to, and a license to copy, use, distribute, perform and display the work publicly and to make and distribute derivative works in any digital medium for any reasonable non-commercial purpose, subject to proper attribution of authorship and ownership of the rights. The journal also grants the right to make small numbers of printed copies for their personal non-commercial use under Creative Commons Attribution-Noncommercial-Share Alike 4.0 Unported License.

### Checklist

#### Covering letter

- Signed by all contributors
- Previous publication / presentations mentioned
- Source of funding mentioned
- Conflicts of interest disclosed

## Authors

- Last name and given name provided along with Middle name initials (where applicable)
- Author for correspondence, with e-mail address provided
- Number of contributors restricted as per the instructions
- Identity not revealed in paper except title page (e.g. name of the institute in Methods, citing previous study as ‘our study’, names on figure labels, name of institute in photographs, etc.)

## Presentation and format

- Double spacing
- Margins 2.5 cm from all four sides
- Page numbers included at bottom
- Title page contains all the desired information
- Running title provided (not more than 50 characters)
- Abstract page contains the full title of the manuscript
- Abstract provided (structured abstract of 250 words for original articles, unstructured abstracts of about 150 words for all other manuscripts excluding letters to the Editor)
- Key words provided (three or more)
- Introduction of 75-100 words
- Headings in title case (not ALL CAPITALS)
- The references cited in the text should be after punctuation marks, in superscript with square bracket.
- References according to the journal’s instructions, punctuation marks checked

- Send the article file without ‘Track Changes’

## Language and grammar

- Uniformly American English
- Write the full term for each abbreviation at its first use in the title, abstract, keywords and text separately unless it is a standard unit of measure. Numerals from 1 to 10 spelt out
- Numerals at the beginning of the sentence spelt out
- Check the manuscript for spelling, grammar and punctuation errors
- If a brand name is cited, supply the manufacturer’s name and address (city and state/country).
- Species names should be in italics

## Tables and figures

- No repetition of data in tables and graphs and in text
- Actual numbers from which graphs drawn, provided
- Figures necessary and of good quality (colour)
- Table and figure numbers in Arabic letters (not Roman)
- Labels pasted on back of the photographs (no names written)
- Figure legends provided (not more than 40 words)
- Patients’ privacy maintained (if not permission taken)
- Credit note for borrowed figures/tables provided
- Write the full term for each abbreviation used in the table as a footnote

# Journal of the Anatomical Society of India on Web

<https://review.jow.medknow.com/jasi>

The Journal of the Anatomical Society of India now accepts articles electronically. It is easy, convenient and fast. Check following steps:

## 1 Registration

- Register from <https://review.jow.medknow.com/jasi> as a new author (Signup as author)
- Two-step self-explanatory process

## 2 New article submission

- Read instructions on the journal website or download the same from manuscript management site
- Prepare your files (Article file, First page file and Images, Copyright form & Other forms, if any)
- Login as an author
- Click on 'Submit new article' under 'Submissions'
- Follow the steps (guidelines provided while submitting the article)
- On successful submission you will receive an acknowledgement quoting the manuscript ID

## 3 Tracking the progress

- Login as an author
- The report on the main page gives status of the articles and its due date to move to next phase
- More details can be obtained by clicking on the ManuscriptID
- Comments sent by the editor and reviewer will be available from these pages

## 4 Submitting a revised article

- Login as an author
- On the main page click on 'Articles for Revision'
- Click on the link "Click here to revise your article" against the required manuscript ID
- Follow the steps (guidelines provided while revising the article)
- Include the reviewers' comments along with the point to point clarifications at the beginning of the revised article file.
- Do not include authors' name in the article file.
- Upload the revised article file against New Article File - Browse, choose your file and then click "Upload" OR Click "Finish"
- On completion of revision process you will be able to check the latest file uploaded from Article Cycle (In Review Articles-> Click on manuscript id -> Latest file will have a number with 'R', for example XXXX\_100\_15R3.docx)

## Facilities

- Submission of new articles with images
- Submission of revised articles
- Checking of proofs
- Track the progress of article until published

## Advantages

- Any-time, any-where access
- Faster review
- Cost saving on postage
- No need for hard-copy submission
- Ability to track the progress
- Ease of contacting the journal

## Requirements for usage

- Computer and internet connection
- Web-browser (Latest versions - IE, Chrome, Safari, FireFox, Opera)
- Cookies and javascript to be enabled in web-browser

## Online submission checklist

- First Page File (rtf/doc/docx file) with title page, covering letter, acknowledgement, etc.
- Article File (rtf/doc/docx file) - text of the article, beginning from Title, Abstract till References (including tables). File size limit 4 MB. Do not include images in this file.
- Images (jpg/jpeg/png/gif/tif/tiff): Submit good quality colour images. Each image should be less than 10 MB) in size
- Upload copyright form in .doc / .docx / .pdf / .jpg / .png / .gif format, duly signed by all authors, during the time mentioned in the instructions.

## Help

- Check Frequently Asked Questions (FAQs) on the site
- In case of any difficulty contact the editor





# Journal of The Anatomical Society of India

---

## Salient Features:

- Publishes research articles related to all aspects of Anatomy and Allied medical/surgical sciences.
- Pre-Publication Peer Review and Post-Publication Peer Review
- Online Manuscript Submission System
- Selection of articles on the basis of MRS system
- Eminent academicians across the globe as the Editorial board members
- Electronic Table of Contents alerts
- Available in both online and print form.

## **The journal is registered with the following abstracting partners:**

Baidu Scholar, CNKI (China National Knowledge Infrastructure), EBSCO Publishing's Electronic Databases, Ex Libris – Primo Central, Google Scholar, Hinari, Infotrieve, Netherlands ISSN center, ProQuest, TdNet, Wanfang Data

## **The journal is indexed with, or included in, the following:**

SCOPUS, Science Citation Index Expanded, IndMed, MedInd, Scimago Journal Ranking, Emerging Sources Citation Index.

Impact Factor® as reported in the 2022 Journal Citation Reports® (Clarivate Analytics, 2023): 0.4

---

## Editorial Office:

**Dr. Vishram Singh**, Editor-in-Chief, JASI  
B5/3 Hahnemann Enclave, Plot No. 40, Sector 6,  
Dwarka Phase – 2, New Delhi - 110 075, India.  
Email: editorjasi@gmail.com  
(O) | Website: www.asiindia.in

---

The journal is owned and run by The Anatomical Society of India